

Dicarboxylic acids transport, metabolism and roduction in aerobic Saccharomyces cerevisia

Shah, Mihir

DOI

[10.4233/uuid:0f74bf4d-8919-4b5f-b1f1-75b731230468](https://doi.org/10.4233/uuid:0f74bf4d-8919-4b5f-b1f1-75b731230468)

Publication date

2016

Document Version

Final published version

Citation (APA)

Shah, M. (2016). *Dicarboxylic acids transport, metabolism and roduction in aerobic Saccharomyces cerevisia*. [Dissertation (TU Delft), Delft University of Technology]. <https://doi.org/10.4233/uuid:0f74bf4d-8919-4b5f-b1f1-75b731230468>

Important note

To cite this publication, please use the final published version (if applicable). Please check the document version above.

Copyright

Other than for strictly personal use, it is not permitted to download, forward or distribute the text or part of it, without the consent of the author(s) and/or copyright holder(s), unless the work is under an open content license such as Creative Commons.

Takedown policy

Please contact us and provide details if you believe this document breaches copyrights. We will remove access to the work immediately and investigate your claim.

Dicarboxylic acids transport, metabolism and production in aerobic *Saccharomyces cerevisiae*

Proefschrift

ter verkrijging van de graad van doctor
aan de Technische Universiteit Delft,
op gezag van de Rector Magnificus prof. ir. K.C.A.M. Luyben
voorzitter van het College voor Promoties,
in het openbaar te verdedigen op
woensdag 26 oktober 2016 om 12.30 uur

Door

Mihir Vidyut SHAH
Master of Science, Indian Institute of Technology, Madras
geboren te Gujarat, India

This dissertation has been approved by the

promotor: Prof. dr. ir. J. J. Heijnen

copromotor: Dr. W. M. van Gulik

Composition of the doctoral committee:

Rector Magnificus	Chairperson
Prof. J. J. Heijnen	Promotor, TU Delft
Dr. W. M. van Gulik	Copromotor, TU Delft

Onafhankelijke leden:

Prof. F. Bruggeman	Vrije Universiteit Amsterdam, The Netherlands
Prof. G. Eggink	Wageningen University, The Netherlands
Prof. M. Casal	University of Minho, Portugal
Prof. G. J. Witkamp	3mE Faculty, TU Delft
Prof. W.R. Hagen	TU Delft, Reserve-lid

Overige leden:

Dr. S. Hartmans	DSM N.V., The Netherlands
-----------------	---------------------------

The research work was carried out in the Cell Systems Engineering Group, Department of Biotechnology, Faculty of Applied Sciences, Delft University of Technology, The Netherlands.

The research project was funded by the BE BASIC Foundation, The Netherlands

Summary

The production process of chemicals derived from petroleum needs to be replaced as it is not feasible in the long run, due to depleting crude oil reserves and ever increasing emissions of greenhouse gases. With the progress and potential in the field of metabolic engineering, the focus has been on the production of industrially relevant chemicals from renewable resources using fermentation processes with engineered microorganisms. However, the production of these chemicals from the fermentative route poses some challenges such as achieving high yield, titer and productivity, inhibition of the produced chemicals on microorganisms and economic feasibility of the process.

This thesis focusses on *Saccharomyces cerevisiae* to produce dicarboxylic acids (malic, fumaric and succinic acid; with main interest in fumaric acid) and to understand the physiology of *S. cerevisiae* at low pH in the presence of extracellular fumaric acid. *S. cerevisiae* is chosen for dicarboxylic acids production as it can be cultivated at low pH ($\text{pH} < \text{pK}$) which leads to cost effective downstream processing of organic acids and it can be easily genetically engineered. *S. cerevisiae* is not a natural producer of fumaric acid, and most likely lacks the transporter needed for its export, therefore engineering of the metabolic pathway and the transport will be needed. Another aspect to consider in the large scale production process of fumaric acid is the response of *S. cerevisiae* towards the presence of a high extracellular fumaric acid concentration. Also at low pH, passive diffusion of fumaric acid could be expected, leading to futile cycling and lower yields. Table 1 shows the list of strains studied in this thesis.

Initially the transport and metabolism of fumaric acid with glucose as co-substrate in aerobic *S. cerevisiae* and the implications of high extracellular fumaric acid levels on its large scale production process were studied. The experiments (Chapter 2) were done in glucose limited chemostats in aerobic conditions with different amounts of fumaric acid added in the chemostat feed (from 1mM to 120 mM of fumaric acid) at a constant pH of 3.0 ($\text{pH} < \text{pK}_a$ of fumaric acid which is 3.09). Strains cultivated were CEN.PK 113-7D (wild type)

and ADIS 244 expressing the heterologous dicarboxylic acid transporter DCT-02. The DCT-02 transporter was studied for its ability to transport fumaric acid.

Table 1. *S. cerevisiae* strains used in this thesis.

Strain	Genotype	Comment
CEN.PK 113-7D	<i>MATa, MAL2-8^c SUC2</i>	Wild type strain to understand the fumaric acid transport and metabolism (Chapter 2 and 3). Also used as a control strain.
ADIS 244	<i>CEN.PK 113-7D, sit2::[ENO1p-DCT_02-ENO1t]</i>	Expresses heterologous DCT-02 transporter. Strain studied to examine the ability of DCT-02 to transport dicarboxylic acids (Chapter 2).
Suc 501	<i>(MATa ura3-52 HIS3 LEU2 TRP1 MAL2-8^c SUC2), sit2::[TDH3p-FRDg-TDH3t;TPI1p-PCKa-PMA1t] sit4::[TDH3p-MDH3 TDH3t; ENO1p-DCT_02-ENO1t; lox72; TPI1p-FUMR-PMA1t] adh1::[PGK1p-PYC2-PGK1t;URA3p-URA3-URA3t]</i>	Engineered to produce succinic acid via the reductive route and expressing the DCT-02 transporter. Results obtained with this strain were compared with Suc 958 results, both the strains were cultivated under same conditions (Chapter 4).
Suc 958	<i>Derived from Suc 501 with the knock-out of heterologous fumarate reductase</i>	Engineered to produce fumaric acid via the reductive route and expressing the DCT-02 transporter. Strain was characterized in high CO ₂ environment for C4 acids production (Chapter 4).
Fum 114	<i>(MATa; ura3-52; trp1-289; leu2-3,112; his3 D1; MAL2-8^c; SUC2) fum1::loxp zwf1::loxp</i>	Engineered to produce fumaric acid as a catabolic product. Strain was evolved to improve fumaric acid production (Chapter 5).
Fum 116	<i>(MATa; ura3-52; trp1-289; leu2-3,112; his3 D1; MAL2-8^c; SUC2) fum1::loxp zwf1::loxp, sit2::[ENO1p-DCT_02-ENO1t]</i>	Engineered to produce fumaric acid as a catabolic product and expressing heterologous DCT-02 transport. Strain was evolved to improve fumaric acid production (Chapter 5).

A linear relation was found between the uptake rate of fumaric acid and its residual extracellular un-dissociated concentration which clearly indicates diffusion as the uptake mechanism of fumaric acid. The calculated permeability coefficient of fumaric acid (8.6×10^{-9} m/s) was approximately 8 fold higher than succinic acid which agrees with the higher hydrophobicity of fumaric acid. However, at a high residual concentration of fumaric acid (~65 mM) with CEN.PK 113-7D, a significantly lower net uptake rate of fumaric acid was observed than predicted from its permeability coefficient. Under these conditions also a higher maintenance requirement was observed indicating futile cycling of fumaric acid. This explains the lower net uptake rate of fumaric acid than expected via passive diffusion. This futile cycling was most likely due to the expression (induced by a high intracellular fumaric acid concentration) of transporters (for e.g. ABC transporters) by *S. cerevisiae* to export fumaric acid in order to avoid a too high intracellular accumulation due to membrane diffusion. ADIS 244 expressing DCT-02 produced higher amounts of malate and succinate compared to CEN.PK 113-7D, but DCT-02 was not able to contribute towards the import or export of fumaric acid. From the total acid out/in ratio calculated for malate and succinate in ADIS 244, the export mechanism of DCT-02 was most likely uniport for totally dissociated species of malic and succinic acid.

After entering the cell via diffusion, fumaric acid was metabolized as observed from the increase in steady state biomass concentration and RQ. The metabolic route of fumaric acid (gluconeogenesis) was surmised using the intracellular concentration of the central carbon pathway metabolites and intracellular fluxes obtained from the metabolic network (Chapter 2).

To further investigate the transport of fumaric acid (Chapter 3), a glucose limited chemostat experiment was done with stepwise change in the fermenter pH from 3.0 to 6.0 and back with 60 mM of fumaric acid in the chemostat glucose based feed. pH was varied in order to have different fractions of the species of fumaric acid (F^{2-} , HF^- and H_2F) in the extracellular space. The experiment was designed to differentiate between the possible uptake of the charged forms (F^{2-} and HF^-) and the uncharged form (H_2F) of fumaric acid. Results show that only H_2F was transported across the cell membrane via diffusion and further metabolized. The permeability of the cells

for fumaric acid increased with increasing pH, which is most likely due to a change in membrane composition.

At low pH of 3.0, fumaric acid diffusion into the cell is significant which contributes towards its futile cycling in a fumaric acid producing strain, thus reducing its yield and productivity considerably. Also at pH 3.0 the maintenance requirement of *S. cerevisiae* was higher compared to the maintenance observed at pH 4.0, even without the presence of extracellular fumaric acid. This higher maintenance requirement at pH 3.0 was most probably due to the futile cycling of H⁺, and based on the extra maintenance observed the permeability of H⁺ was estimated to be 2.71×10^{-7} m/s. To overcome this problem of fumaric acid and H⁺ futile cycling at pH 3.0, either fumaric acid production should be considered at higher pH or *S. cerevisiae* should be evolved in order to reduce its membrane permeability towards fumaric acid and H⁺.

In chapter 4, two *S. cerevisiae* strains (Suc 501 and Suc 958, Table 1) engineered to produce C4 acids were studied in an aerobic glucose limited chemostat, at low pH of 3.0 and under high CO₂ environment in order to stimulate the reductive part of the TCA cycle and promote C4 acids formation. Both strains overexpressed the reductive part of the TCA cycle (PEPCK, MDH, FUMR and PYC) in the cytosol and the DCT-02 transporter. The only difference between these two strains was that Suc 501 also overexpressed heterologous fumarate reductase. Therefore, succinic and fumaric acid were the expected end products of the reductive part of the TCA cycle in Suc 501 and Suc 958 respectively. In high CO₂ environment succinic acid productivity increased significantly in both strains (from 0.10 mmol/Cmol.h (air) to 7.46 mmol/Cmol.h (50% CO₂) in Suc 501 and from 2.3 mmol/Cmol.h (air) to 18.7 mmol/Cmol.h (50% CO₂) in Suc 958). At increased CO₂ levels no improvements in the already low malate and fumarate productivities were observed. The observed increase in succinic acid productivity was expected in Suc 501 as the route of its formation was via the reductive part of the TCA cycle which was stimulated by high CO₂. But succinic acid formation was not expected in Suc 958 instead fumaric acid production was expected. Calculated intracellular fluxes indicate that the high secretion rate of succinate in Suc 958 was most likely due to the exchange between mitochondrial succinate formed via the oxidative part of

the TCA cycle and the high concentration of cytosolic fumarate formed via the reductive part. The cytosolic fumarate formed apparently could not be exported. This mitochondrial exchange of fumarate and succinate restricts the maximum q_{suc} to 25 mmol/Cmol h at near zero growth rate. Total succinic acid out/in ratios suggested a uniport mechanism to export Suc^{2-} facilitated by the DCT-02 transporter. From the stoichiometry and the transport mechanism of succinic acid, an additional ATP consumption was observed which was due to the futile cycling of succinic acid. From futile cycling rate, permeability coefficient of succinic acid was calculated, in Suc 501 (1.1×10^{-9} m/s) and Suc 958 (4.3×10^{-9} m/s). The stoichiometry of succinic acid formation in Suc 958 suggested a combination of the reductive and oxidative part of the TCA cycle to form succinic acid.

The succinic acid production rate increased with the increased availability of the cytosolic HCO_3^- at high CO_2 concentration. The productivity of succinic acid in Suc 958 was 2 fold higher compared to Suc 501 at 50% CO_2 in the inlet gas. One of the reasons for this significant difference in succinic acid productivity between Suc 501 and Suc 958 might be due to the difference in the cytosolic availability of HCO_3^- (pK of H_2CO_3 is 6.4) which is influenced greatly by an expected lower cytosolic pH in Suc 958, because Suc 958 was cultivated at higher μ (0.10 h^{-1}) than Suc 501 ($\mu = 0.05 \text{ h}^{-1}$).

In chapter 5 *S. cerevisiae* (Table 1) was engineered to make fumaric acid as a catabolic product and couple its production to ATP and thus biomass formation. This was done by knocking out the fumarase (FUM1) and glucose 6-phosphate dehydrogenase (ZWF1) genes. Strains used in this study were Fum 114 (ΔFUM1 , ΔZWF1 , Table 1) and Fum 116 (ΔFUM1 , ΔZWF1 , $\uparrow\text{DCT-02}$) which also expressed the heterologous dicarboxylic acid transporter.

Fum 114 and Fum 116 were evolved in a glucose limited, aerobic chemostat, with the dilution rate of 0.10 h^{-1} and at a pH of 5.0. With evolution there was the expected improvement in the biomass yield and ATP production. Fum 114 achieved this improvement in ATP yield (mol ATP per mol glucose consumed) by switching from ethanol to acetate formation. Fum 116 improved ATP yield by switching from ethanol formation to secretion of acetate, malate and pyruvate. Fum 116 produced very high concentration of malic acid with its

export facilitated by the DCT-02 transporter. The yield of malic acid in Fum 116 increased from 0.28 mol/mol glucose to 0.43 mol/mol glucose at a very high biomass specific secretion rate of 30-37 mmol/Cmol h. Total malic acid out/in ratios again points towards uniport mechanism of Mal²⁻ transport with DCT-02 transporter.

However, the route of malic acid formation in Fum 116 was via the energy consuming reductive part of the TCA cycle. In both Fum 114 and Fum 116, the intracellular concentration of fumarate was 40 to 100 fold higher compared to CEN.PK 113-7D, again indicating export of fumaric acid as a bottleneck. Chemostat data and metabolic network analysis indicated the conversion of fumarate to malate even though the homologous fumarase reaction was knocked out. There was an increase in flux with time from fumarate to malate, but the reaction remained highly irreversible. The flux increase was directly proportional to the increase in intracellular fumaric acid concentration; this suggests the evolution of a hydratase enzyme with low affinity towards fumaric acid.

Maintenance requirements of Fum 114 and Fum 116 were significantly higher during the evolution experiment due to the high extracellular concentration of acetic acid and its futile cycling. Acetic acid permeability coefficient was estimated from the extra maintenance observed, the permeability values agreed with published data and the values decreased with evolution which was most likely due to a change in membrane composition.

Genes involved in the reductive part of the TCA cycle were overexpressed (PYC, PEPCK, MDH, FUM) in *S. cerevisiae* in order to divert the carbon flux towards dicarboxylic acids via the reductive route (Chapter 6). Overexpression of the genes indeed improved the yields of succinic and malic acid but no significant improvement in the fumaric acid yield was observed.

Samenvatting

Omdat de olievoorraden op de lange termijn uitgeput zullen raken en om de uitstoot van broeikasgassen te verminderen is het van belang om te zoeken naar alternatieve, meer milieuvriendelijke, processen voor de productie van brandstoffen en chemicaliën. De huidige technieken voor het genetisch aanpassen van micro organismen (metabolic engineering) maken het in principe mogelijk om chemicaliën te produceren uit hernieuwbare grondstoffen middels grootschalige fermentatie processen. Hierbij moet men realiseren dat dergelijke processen alleen levensvatbaar zijn als ze economisch kunnen concurreren met de traditionele processen gebaseerd op aardolie. De belangrijkste uitdagingen om dergelijke fermentatie processen succesvol te maken zijn het maximaliseren van de geproduceerde hoeveelheid product per hoeveelheid verbruikt substraat (de yield), de productconcentratie aan het einde van het proces (de titer) en de hoeveelheid geproduceerd product per eenheid van reactorvolume per tijd (de productiviteit).

Dit proefschrift richt zich op onderzoek aan de fermentatieve productie van dicarbonsuren (fumaarzuur, appelzuur en barnsteenzuur) door bakkergist (*Saccharomyces cerevisiae*). Het uitgevoerde onderzoek richtte zich voornamelijk op het beter begrijpen van de fysiologie van de gist onder grootschalige fermentatie condities, namelijk lage pH en hoge zuur concentraties. Het uitvoeren van de productie fermentaties bij een lage pH ($\text{pH} < \text{pK}$) is essentieel om de vorming van bijproduct (gips) tijdens de opwerking van het geproduceerde zuur, wat tot extra kosten leidt, te vermijden.

De reden waarom gekozen is voor *S. cerevisiae* als productie organisme is de tolerantie voor lage pH en het feit dat de technieken voor genetische modificatie van dit micro organisme ver ontwikkeld zijn. Dit laatste is essentieel omdat *S. cerevisiae* niet van nature dicarbonsuren produceert en waarschijnlijk ook geen export systemen heeft voor de uitscheiding van dicarbonsuren in het medium. Een ander belangrijk aspect is dat bij lage pH de uitgescheiden dicarbonsuren voornamelijk aanwezig zijn in de ongedissocieerde lipofiele vorm, welke via passieve diffusie de cellen in kan

diffunderen. In combinatie met actieve uitscheiding van het naar binnen gediffundeerde zuur kan dit leiden tot een futiele cyclus, die leidt tot een netto dissipatie van cellulaire energie (ATP) en daarmee tot een verlaging van de product opbrengst.

Tabel 1. Gebruikte *S. cerevisiae* stammen.

Stam	Genotype	Opmerkingen
CEN.PK 113-7D	<i>MATa, MAL2-8^c SUC2</i>	Wild type/controle stam.
ADIS 244	<i>CEN.PK 113-7D, sit2::[ENO1p-DCT_02-ENO1t]</i>	Betuigt heterologe DCT-02 transporter. Stam onderzocht om het vermogen van DCT-02 carbonzuren (hoofdstuk 2) transportereren onderzoeken.
Suc 501	<i>(MATa ura3-52 HIS3 LEU2 TRP1 MAL2-8^c SUC2), sit2::[TDH3p-FRDg-TDH3t;TPI1p-PCKa-PMA1t] sit4::[TDH3p-MDH3 TDH3t; ENO1p-DCT_02-ENO1t; lox72; TPI1p-FUMR-PMA1t] adh1::[PGK1p-PYC2-PGK1t;URA3p-URA3-URA3t]</i>	Ontworpen om barnsteenzuur te produceren via de reductieve route en het uiten van DCT-02 transporter. De resultaten van deze stam werden vergeleken met resultaten Suc 958, beide stammen werden onder dezelfde omstandigheden (hoofdstuk 4) gekweekt.
Suc 958	<i>Afgeleid van Suc 501 door knock out van heteroloog fumaraat reductase</i>	Ontworpen om fumaarzuur te produceren via de reductieve route en het uiten van DCT-02 transporter. Stam werd gekenmerkt hoge CO ₂ omgeving voor C4 zuren productie (Hoofdstuk 4).
Fum 114	<i>(MATa; ura3-52; trp1-289; leu2-3,112; his3 D1; MAL2-8^c; SUC2) fum1::loxp zwf1::loxp</i>	Ontworpen om fumaarzuur produceren als een katabole product. Stam werd geëvolueerd om fumaarzuur productie (hoofdstuk 5) verbeteren.
Fum 116	<i>(MATa; ura3-52; trp1-289; leu2-3,112; his3 D1; MAL2-8^c; SUC2) fum1::loxp zwf1::loxp, sit2::[ENO1p-DCT_02-ENO1t]</i>	Ontworpen om fumaarzuur produceren als een katabole product en het uiten van heterologe DCT-02 transport. Stam werd geëvolueerd om fumaarzuur productie (hoofdstuk 5) verbeteren.

In eerste instantie werd het transport en metabolisme van fumaarzuur bestudeerd in aerobe culturen met glucose als cosubstraat (Hoofdstuk 2). Deze experimenten werden uitgevoerd in glucose gelimiteerde chemostaten bij pH 3, waarbij fumaarzuur werd toegevoegd aan het chemostaat medium in verschillende concentraties (1 tot 120 mmol/L). De chemostaat cultivaties werden uitgevoerd met het wild type (CEN.PK 113-7D) en een mutant waarbij een dicarbonsuur transporterend eiwit (DCT-02) uit *Aspergillus niger* tot expressie was gebracht (ADIS 244). Voor beide stammen bleek de opnamesnelheid van fumaarzuur door de cellen lineair toe te nemen met de concentratie van het ongedissocieerde zuur, tot een extracellulaire concentratie van ongeveer 20 mmol/L, wat duidt op passieve diffusie als import mechanisme. De berekende doorlaatbaarheidscoëfficiënt voor fumaarzuur (8.6×10^{-9} m/s) bleek ongeveer acht keer groter dan de doorlaatbaarheidscoëfficiënt voor barnsteen zuur, wat te verwachten viel gezien de grotere hydrofobiciteit van fumaarzuur vergeleken met barnsteen zuur.

Echter, bij een hogere extracellulaire fumaarzuur concentratie van ongeveer 65 mmol/L bleek de opnamesnelheid van het zuur veel lager te zijn dan wat op grond van de berekende doorlaatbaarheidscoëfficiënt kon worden verwacht. Dit experiment werd echter alleen met het wild type (CEN.PK 113-7D) uitgevoerd. Onder deze condities bleek ook de onderhoudscoëfficiënt hoger te zijn, wat kan duiden op een futiele cyclus van passief fumaarzuur import en actief export. Dit zou tevens de lagere netto opname van fumaarzuur door de celen kunnen verklaren. Als een dergelijke futiele cyclus optreedt bij een hoge extracellulaire fumaarzuur concentratie dan zou dit betekenen dat dit leidt tot de expressie van een actief export mechanisme, zoals een ATP Binding Cassette (ABC) transport eiwit, om te voorkomen dat de intracellulaire fumaarzuur concentratie te hoog wordt.

Het bleek dat de stam waarbij de DCT-02 transport eiwit tot expressie was gebracht (ADIS 244) grotere hoeveelheden appel en barnsteen zuur produceerde vergeleken met de wild type stam CEN.PK 113-7D, wat aangeeft dat dit transport eiwit beide zuren exporteert. Fumaarzuur bleek echter niet getransporteerd te worden door DCT-02. Afgaande op de gemeten verhouding tussen de totale extra en extracellulaire zuurconcentraties is het meest

waarschijnlijke transportmechanisme van DCT-02 voor appel en barnsteen zuur transport via uniport van het ongedissocieerde molecuul.

Uit de experimentele resultaten bleek voorts dat consumptie van fumaarzuur door *S. cerevisiae* in chemostaat culturen leidde tot een toename van de steady state biomassa concentratie alsmede de ademhalingscoefficient RQ, waaruit blijkt dat fumaarzuur kan worden gemetaboliseerd. De metabole route voor fumaarzuur metabolisme (gluconeogenese) kon worden afgeleid op basis van metabole flux analyse en metingen van de intracellulaire concentraties van de intermediären van het centraal metabolisme (hoofdstuk 2).

Het transport van fumaarzuur over de celmembraan werd verder onderzocht (hoofdstuk 3) aan de hand van glucose gelimiteerde chemostaat experimenten met een fumaarzuur concentratie van 60 mmol/L in het voedingsmedium. Hierbij werd de pH van de fermentatie stapsgewijs opgevoerd van 3.0 naar 6.0 en terug naar 3.0, zodanig dat bij elke pH waarde een (pseudo)steady state werd bereikt met verschillende extracellulaire fracties van het di- en mono-anion en het ongedissocieerde zuur (F^{2-} , HF^- and H_2F). Het experiment was zo ontworpen om onderscheid te kunnen maken tussen de opname van de geladen (F^{2-} and HF^-) en ongeladen (H_2F) vormen. Uit de resultaten van deze experimenten bleek dat alleen de ongedissocieerde vorm (H_2F) werd opgenomen via passieve diffusie over het celmembraan. De permeabiliteit van het celmembraan voor fumaarzuur bleek toe te nemen met toenemende pH, waarschijnlijk door een verandering van de membraan samenstelling.

Bij lage pH (3.0) is de diffusie van ongedissocieerd fumaarzuur over de celmembraan significant en zal in een productiestam leiden tot een futiele cyclus van passieve diffusie van het zuur de cel in en actief transport naar buiten. Dit leidt tot energie dissipatie en dus tot een aanzienlijke verlaging van de product opbrengst en de productvormingssnelheid. Tevens werd gevonden dat ook in de afwezigheid van fumaarzuur de onderhoudsenergie behoefte van *S. cerevisiae* bij pH 3.0 hoger was dan bij pH 4.0, wat zou kunnen wijzen op het naar binnen lekken van protonen, gevolgd door export via het proton ATP-ase. Op basis van deze extra onderhouds energie behoefte kon berekend worden dat de permeabiliteit van de celmembraan voor protonen gelijk is aan 2.71×10^{-7} m/s bij pH 3.0.

Het optreden van dergelijke futiele cycli kan voorkomen worden door de productie fermentaties uit te voeren bij hogere pH of door de permeabiliteit van de celmembraan van *S. cerevisiae* voor protonen en fumaarzuur te verlagen, bijvoorbeeld middels in vitro evolutie.

Hoofdstuk 4 beschrijft het onderzoek aan twee genetisch gemodificeerde, C4-dicarbonzuur producerende *S. cerevisiae* stammen (Suc 501 and Suc 958, zie Tabel 1). In beide stammen werd het reductieve deel van de TCA route (PEPCK, MDH, FUMR and PYC) tot overexpressie gebracht in het cytosol. Het enige verschil tussen deze twee stammen was dat SUC501 tevens een heteroloog fumaraat reductase bevatte, wat zou moeten leiden tot overproductie van barnsteenzuur, terwijl werd verwacht dat stam SUC958 voornamelijk fumaarzuur zou produceren. De stammen werden gekweekt bij lage pH (3.0) en hoge concentratie opgelost CO₂ teneinde de flux door het reductieve deel van de TCA route te verhogen en daarmee de productie snelheid van C4 zuren. Uit de resultaten bleek dat het verhogen van de opgeloste CO₂ concentratie (door toevoeging van CO₂ aan het beluchtingsgas) in beide stammen leidde tot een significante verhoging van de productiesnelheid van barnsteenzuur (van 0.10 mmol/Cmol.h (0.04% CO₂) tot 7.46 mmol/Cmol.h (50% CO₂) in Suc 501; en van 2.3 mmol/Cmol.h (0.04% CO₂) tot 18.7 mmol/Cmol.h (50% CO₂) in Suc 958). Verhoging van de opgeloste CO₂ concentratie leidde echter niet tot verhoging van de (geringe) productiesnelheden van appelzuur en fumaarzuur in deze stammen. Voor wat betreft stam SUC501 was het geen verassing dat verhoging van de opgeloste CO₂ concentratie leidde tot verhoging van de productiesnelheid van barnsteenzuur, omdat deze stam was ontworpen voor de overproductie van dit zuur. Dit gold echter niet voor SUC958, omdat door afwezigheid van fumaraat reductase fumaarzuur het belangrijkste eindproduct van de reductieve TCA route zou moeten zijn. Uit een metabole flux analyse werd geconcludeerd dat de hoge productiesnelheid van barnsteenzuur in stam SUC958 waarschijnlijk wordt veroorzaakt door uitwisseling van in het mitochondrion geproduceerd barnsteenzuur met in het cytosol (via de tot overexpressie gebrachte reductieve tak van de TCA route) geproduceerd fumaarzuur. Dat de productie van fumaarzuur laag bleef is waarschijnlijk te wijten aan de afwezigheid van een effectief export mechanisme voor dit zuur. De veronderstelde metabole route zou leiden tot een maximale specifieke

barnsteenzuur productiesnelheid van 25 mmol/Cmol h bij een groeisnelheid van vrijwel 0.

Zoals hierboven al werd geconcludeerd is het meest waarschijnlijke mechanisme voor de export van barnsteenzuur door het DCT-02 transport eiwit, uniport van het volledig ongedissocieerde molecuul. Uitgaande van dit transport mechanisme en de via metabole flux analyse berekende additionele ATP consumptie voor de futiele cyclus van passieve diffusie de cel in en actief transport de cel uit voor beide stammen onder barnsteenzuur producerende condities, kon de permeabiliteit van de celmembraan voor barnsteenzuur berekend worden. De berekende waarden waren 1.1×10^{-9} m/s voor SUC501 en 4.3×10^{-9} m/s voor SUC958.

Zoals boven beschreven leidde een verhoging van de opgeloste CO_2 concentratie tot een verhoging van de barnsteenzuur productie in beide stammen. Opmerkelijk was dat de productiesnelheid gemeten voor stam SUC958 meer dan 2 maal hoger was dan voor stam SUC501 bij 50% CO_2 in het beluchtingsgas. Echter, de productie van barnsteenzuur werd voor stam SUC501 bepaald in een chemostaat cultuur bij een hogere groeisnelheid (0.1 h^{-1}) dan voor stam SUC958 (0.05 h^{-1}). Wat de precieze invloed van de groeisnelheid is op de barnsteenzuur productie is niet bekend. Een van de mogelijkheden zou de cytosolaire pH kunnen zijn en daarmee de concentratie opgelost HCO_3^- (pK van H_2CO_3 is 6.4).

Hoofdstuk 5 beschrijft het onderzoek wat werd uitgevoerd aan een *S. cerevisiae* stam die fumaarzuur als catabool product produceert, waarbij de omzetting van glucose naar fumaarzuur leidt tot de productie van cellulaire energie in de vorm van ATP. Dit werd gerealiseerd door het uitschakelen van de genen coderend voor fumarase (FUM1) en glucose 6-phosphate dehydrogenase (ZWF1). De geconstrueerde stammen waren (zie Tabel 1) Fum 114 (ΔFUM1 , ΔZWF1) en Fum 116 (ΔFUM1 , ΔZWF1 , $\uparrow\text{DCT-02}$), in deze laatste stam werd ook de heterologe transporter DCT-02 tot expressie gebracht. Met beide stammen werden evolutie experimenten uitgevoerd in aerobe, glucose gelimiteerde chemostaten bij een verdunningssnelheid van 0.10 h^{-1} en een pH van 5.0. De evolutie experimenten leidden tot een stijging van de steady state biomassa concentratie en dus een stijging van de ATP productie. In stam

FUM114 gebeurde dit door daling van de ethanol en toename van de acetaat productie. In stam FUM116 gebeurde hetzelfde maar werd behalve een stijging van de acetaat productie tevens een stijging van appelzuur en pyrodruivenzuur productie waargenomen. Vooral de appelzuur productie was hoog in deze stam, veroorzaakt doordat de uitscheiding van dit zuur werd vergemakkelijkt in aanwezigheid van het DCT-02 transport eiwit. De opbrengst van appelzuur steeg gedurende dit evolutie experiment van 0.28 mol/mol glucose tot 0.43 mol/mol glucose bij een zeer hoge biomassa specifieke productie snelheid van 30-37 mmol/Cmol h. Uit de gemeten verhouding van de totale appelzuur concentraties buiten en binnen de cellen bleek dat ook voor appelzuur het meest waarschijnlijke export mechanisme van DCT-02 uniport is van het ongedissocieerde zuur. De intracellulaire appelzuur concentratie in zowel Fum114 als FUM116 bleek 40 tot 100 maal hoger te zijn vergeleken met de niet producerende wild type stam CEN.PK 113-7D, wat nogmaals aangeeft dat export van fumaarzuur een flessenhals is.

Chemostaat experimenten en metabole netwerk analyse toonde de omzetting van fumaarzuur naar appelzuur aan, ondanks het feit dat de homologe fumarase reactie uitgeklopt was. Er was een toename van de flux van fumaarzuur naar appelzuur, maar de reactie bleef sterk onomkeerbaar. De flux stijging bleek recht evenredig met de toename van de intracellulaire concentratie fumaarzuur, wat de ontwikkeling van een hydratase enzym met lage affiniteit voor fumaarzuur suggereert.

De onderhoudsenergie behoefte tijdens het evolutie experiment van stammen Fum 114 en Fum 116 bleek significant verhoogt te zijn wat waarschijnlijk veroorzaakt werd door de hoge azijnzuur concentratie en de daarmee samenhangende energie consumerende futiele cyclus van azijnzuur import via passieve diffusie en actieve export. De doorlaatbaarheidscoëfficiënt voor azijnzuur werd geschat uit de waargenomen extra onderhoudsenergie. De gevonden waarde kwam overeen met gepubliceerde gegevens en de waarde daalde tijdens het evolutie experiment wat waarschijnlijk te wijten is aan een verandering van de membraansamenstelling.

De genen betrokken bij het reductieve deel van de TCA cyclus (PYC, PEPCK, MDH, FUM) werden in het cytosol tot overexpressie gebracht in *S. cerevisiae*

om de koolstofflux richting dicarbonzuren te leiden via de reductieve route (hoofdstuk 6). Overexpressie van deze genen leidde inderdaad tot verhoogde productie van barnsteenzuur en appelzuur, maar er werd geen significante verbetering in de productie van fumaarzuur waargenomen.

Table of contents

Chapter 1.	Introduction	1
Chapter 2.	Transport and metabolism of fumaric acid in <i>Saccharomyces cerevisiae</i> in aerobic glucose limited chemostat culture	21
Chapter 3.	Effect of pH on fumaric acid permeability, its uptake and futile cycling in <i>Saccharomyces cerevisiae</i>	57
Chapter 4.	Metabolic response of engineered C4- acids producing <i>Saccharomyces cerevisiae</i> in high CO ₂ environments	89
Chapter 5.	Evolution of engineered <i>Saccharomyces cerevisiae</i> for the aerobic production of dicarboxylic acids	139
Chapter 6.	Metabolic engineering of <i>Saccharomyces cerevisiae</i> for the production of dicarboxylic acids	189
Chapter 7.	Outlook	203
References		210
Publications		225
Curriculum Vitae		226
Acknowledgements		227

Chapter 1

Introduction

Fumaric acid is an unsaturated dicarboxylic acid which, due to its structure, is used mainly in polymerization and esterification processes (1). Due to its weak acid property it can also be used as a food acidulate. The current production of fumaric acid is from maleic acid which is obtained from the oxidation of butane (2, 3), so the process is dependent on the availability of crude oil. Fumaric acid is an industrially important chemical, as is also mentioned in the report by the U.S Department of Energy, which has the potential to be produced from biomass (4). It is therefore, from an environmental point of view, highly relevant to develop more sustainable production processes for fumaric acid.

Fumaric acid is present in nature as an intermediate of the TCA cycle. Before the advent of crude oil as feedstock, fumaric acid was produced in a fermentation process using natural producer fungi *Rhizopus* spp. (5). The fermentative production of fumaric acid using *Rhizopus* spp. was carried out in batch cultures under aerobic conditions and using calcium carbonate as a neutralizing agent (6). *Rhizopus* spp. produces fumaric acid mainly from pyruvate which, through carboxylation, is converted to oxaloacetate and subsequently to malate via malate dehydrogenase and finally to fumarate through fumarase. Most of the fumarate is produced via the reductive branch of the TCA cycle, of which all the enzymes are present in the cytosol (7). During the fermentation process calcium carbonate is supplied to control the pH and at the same time maintain the dissolved CO₂ concentration at a sufficiently high level to increase the driving force for fumaric acid biosynthesis via the reductive branch of TCA cycle. The yield of fumaric acid reported in *Rhizopus* spp. is higher than 1 mol/ mol of glucose, due to incorporation of CO₂ in the reductive route of the TCA cycle (7). The high fumaric acid production by *Rhizopus* spp. is attributed to i) the kinetic properties of the fumarase enzyme which favors the conversion of malate to fumarate, but is inhibited by a high concentration of fumarate (8, 9); ii) a high capacity of the reductive route (7, 10) and iii) nitrogen limited cultivation conditions (11, 12). As *Rhizopus* spp. effectively excretes the produced fumaric acid, it should contain an efficient fumaric acid exporter which, however, has not been identified yet.

Rhizopus spp. is not favored for the industrial scale production of fumaric acid due to its morphology and difficulty to genetically engineer. The yeast *Saccharomyces cerevisiae* could be a potential organism for the industrial scale

Table 1.1. Yield of fumaric acid per mol of glucose consumed for different metabolic routes. The energy required for fumaric acid export is not taken into account.

Route	Stoichiometry to produce fumarate	Yield (mol/ mol glucose consumed)
Oxidative	-1 Glucose -3O ₂ + 1 Fumarate + 2H ⁺ + 2 CO ₂ + 9.13 ATP*	1.0
Reductive	-0.5 Glucose + 1 Fumarate + 2H ⁺ - 1 CO ₂ + 0 ATP	2.0
Glyoxylate	-1 Glucose - 3 O ₂ + 1 Fumarate + 2 H ⁺ + 2 CO ₂ + 9.13 ATP	1.0
Urea cycle	-1.5 Glucose - 3.0 O ₂ + 2 Fumarate + 4 H ⁺ + 1 CO ₂ + 5.9 ATP + 5H ₂ O	1.33

*P/NADH ratio of 1.23 and P/FADH₂ ratio of 0.98

Current status of C4 dicarboxylic acid production from engineered *S. cerevisiae*

Although for *S. cerevisiae* the interest is in fumaric acid production, it is useful to have an overview of other C4 dicarboxylic acids (malic and succinic acid) produced. Wild type *S. cerevisiae* strains produce only very low amounts of the C4 dicarboxylic acids involved in the TCA cycle (malate, fumarate and succinate). Several attempts have been undertaken to improve the yield and productivity of dicarboxylic acids in *S. cerevisiae* and other microorganisms. In the section below an overview is given of published studies aimed at engineering *S. cerevisiae* for the production of dicarboxylic acids.

Malic acid production

The strains used, applied genetic modifications and cultivation conditions are summarized in table 1.2. Sake yeast strain no. 28 without any modifications in the pathway produced malic acid, though with a very low yield of 0.004 mol/ mol glucose, the malic acid secreted by this strain was attributed to the lower

activity of the mitochondrial enzymes involved in the oxidative part of the TCA cycle compared to other wild type *S. cerevisiae* strains (13). Malic acid yield of $0.095 \text{ mol.}(\text{mol glucose})^{-1}$ has been reported when only a fumarase enzyme with a higher affinity towards fumarate compared to malate was overexpressed in *S. cerevisiae* (14, 15). Both the studies did not target the production of malic acid from any particular route (Oxidative or the reductive TCA cycle).

The route to obtain malic acid with highest yield is the reductive part of the TCA cycle which also consumes CO_2 . A malic acid yield of $0.42 \text{ mol.}(\text{mol glucose})^{-1}$ was achieved in aerobic shake flasks with an engineered *S. cerevisiae* strain wherein the reductive route was targeted by overexpressing pyruvate carboxylase (PYC2), malate dehydrogenase (MDH3) and a heterologous dicarboxylic acid transporter (SpMAE1) and the pyruvate decarboxylase genes were knocked out (16, 17). Calcium carbonate was used as a buffer in the shake flasks study and also to increase the availability of CO_2 for the reductive part of the TCA cycle. The yield of malic acid was further improved in this strain to $0.48 \text{ mol.}(\text{mol glucose})^{-1}$ in aerobic batch fermentations by increasing the partial pressure of CO_2 in the aeration gas to 0.15 bar at a controlled pH of 6.8 (18). Though the yield was improved in the batch bioreactor study, a higher productivity of $1.41 \text{ mmol/ g DCW/h}$ was obtained in the shake flask study (see Table 1.2). The reason for the lower biomass specific productivity of malic acid in the bioreactor maintaining high partial pressure of CO_2 (0.15 bar) is not clear, but it might be due to the presence of calcium in the shake flasks which could impact genes expression levels (19) and can also influence the activity of pyruvate carboxylase enzyme (20). Also the dissolved oxygen level is probably lower or even limiting in shake flasks than in bioreactor, which leads to a more reduced cytosol which stimulates the reductive route.

Table 1.2. Malic acid production in *S. cerevisiae*

	Pines <i>et al.</i> , 1996 (14)	Zelle <i>et al.</i> , 2008 (17)	Zelle <i>et al.</i> , 2010 (18)	Nakayama <i>et al.</i> , 2012 (13)
<i>S. cerevisiae</i> host strain	DMM1-15A	CEN.PK 113-7D	CEN.PK 113-7D	Sake yeast strain no. 28
Modifications in pathway	↑FUM1	ΔPDC1, ΔPDC5, ΔPDC6, ↑PYC2, ↑MDH3	ΔPDC1, ΔPDC5, ΔPDC6, ↑PYC2, ↑MDH3	None, but the strain has low mitochondrial enzyme activity
Production route intended through modifications	Via the reductive and the oxidative TCA cycle	Via the reductive TCA cycle	Via the reductive TCA cycle	Via the reductive and the oxidative TCA cycle
Overexpression of a transporter	No	↑SpMAE1	↑SpMAE1	No
Cultivation	Aerobic, shake flask	Aerobic, shake flasks	Aerobic, Batch cultivation in a bioreactor	Aerobic, Shake flask
Temperature	30°C	30°C	30°C	25°C
Dissolved oxygen	N.A	N.A	~0%	N.A
pH	N.A*	Between 6 to 7.5 (with CaCO ₃)	6.8	N.A
Media	Defined, CaCO ₃ as a buffer	Defined, CaCO ₃ as a buffer	Defined	Complex
P _{CO2} (Bar)	N.A	N.A	0.15	N.A
Initial Glucose (mM)	555.55	1050	555.55	555.55
	(Galactose)			
Average dry biomass concentration (g/L)	N.A	1.0	6.0	N.A
Final malate concentration (mM)	43.25	440	266.66	2.46
Yield (mol malate/mol glucose)	0.095	0.42	0.48	0.004

Cultivation time (h)	33	312	82	95
Malic acid productivity (mol/m ³ /h)	1.30	1.41	3.25	0.025
Biomass specific malic acid production (mmol/ g DCW/h)	N.A	1.41	0.54	N.A
Other organic acids produced	Pyruvate (9 mM), Citrate (156 mM) were also produced, no fumarate was detected	Pyruvate (34 mM), Succinate (68 mM) Fumarate (17 mM)	Pyruvate (347 mM) , Succinate (86 mM) and Fumarate (18 mM) were also produced	N.A

*N.A= not available

Succinic acid production

Table 1.3 shows an overview of the reported studies. Succinic acid production in different studies was targeted via different routes (oxidative TCA, reductive TCA and glyoxylate route), primarily by making succinic acid as the end product of that particular route.

In the study by Ito *et al.* (21), succinic acid formation was targeted only via the oxidative route of the TCA cycle, by knocking out succinate dehydrogenase (SDH1 and SDH2), alcohol dehydrogenase (ADH1-5) and expressing SpMAE1 transporter. After these modifications, a succinic acid yield of 0.032 mol.(mol glucose)⁻¹ was obtained (21). The SpMAE1 transporter was expressed to facilitate the export of succinic acid, which indeed decreased the intracellular concentration of succinic acid from 22 μmol.gDCW⁻¹ observed without SpMAE1 to 6 μmol.gDCW⁻¹ with SpMAE1 transporter, which indicates that export is a potential metabolic bottleneck in its production (21). Otero *et al.* (22) made succinic acid as the end product of the oxidative and the glyoxylate route by disrupting the succinate dehydrogenase (SDH3) and 3-phosphoglycerate dehydrogenase (SER3, SER33) genes and overexpressing isocitrate lyase (ICL1).

In this strain the succinic acid concentration improved from 0.25 mM to 7.6 mM with a final yield of $0.08 \text{ mol.}(\text{mol glucose})^{-1}$ through evolution (22). Raab *et al.* (23) achieved a succinic acid yield of $0.11 \text{ mol.}(\text{mol glucose})^{-1}$, which was 4.8 fold higher than the wild type strain, was achieved by the knock-out of SDH1, SDH2 and isocitrate dehydrogenase (IDH1, IDP1), thereby the succinic acid production in this strain was only via the glyoxylate pathway (23). Contrary to the previous study, in this study no intracellular accumulation of succinic acid was observed and no heterologous transporter was expressed to facilitate succinic acid export.

A higher yield of succinic acid could be obtained via the CO_2 assimilating reductive route of the TCA cycle, which was targeted in the study by Yan *et al.* (24). A succinic acid yield of $0.21 \text{ mol.}(\text{mol glucose})^{-1}$ was achieved at a low pH of 3.8 by overexpressing the reductive TCA cycle enzymes and knocking out glycerol 3-phosphate dehydrogenase (GPD1) and cultivating the engineered strain aerobically with 10% CO_2 in the inlet gas to push the carbon flux through the reductive route (24).

S. cerevisiae was engineered by DSM B.V. to produce succinic acid via the reductive route, by overexpressing the reductive TCA cycle genes (PYC2, PEPCK, MDH3, RoFUM and FRDg) and a heterologous dicarboxylic acid transporter (DCT-02). The strain was cultivated at a low pH of 3.0 in an aerobic, glucose limited chemostat with a dilution rate controlled at 0.05 h^{-1} and partial pressure of CO_2 set at 0.65 bar, the strain produced 30 mM of succinic acid during the steady state with a glucose (75.75 mM) and ethanol (21 mM) mix in the chemostat feed (91% glucose + 9% ethanol) (25). This represents a yield of 0.36 mol succinic acid per mol hexose equivalent. At least five times higher biomass specific productivity of succinic acid was reported in this study compared to other studies in Table 1.3, which was most likely due to the presence of the DCT-02 transporter and high partial pressure of CO_2 . It should however be noted that the biomass specific productivity for succinic acid is about 5 times lower than the malic acid in the studies mentioned in Table 1.2.

Succinic acid production at low pH with an engineered *S. cerevisiae* is already in operation at an industrial scale with a joint venture of DSM B.V. and Roquette Frères. A high yield and productivity of succinic acid has been

achieved by the overexpression of the enzymes in the reductive branch of the TCA cycle in order to assimilate carbon dioxide and of a heterologous dicarboxylic acid transporter DCT-02 from *Aspergillus niger* as described in the patents by DSM B.V., The Netherlands (26–28).

Table 1.3. Succinic acid production in *S. cerevisiae*

	Raab <i>et al.</i> , 2010 (23)	Jamalzadeh <i>et al.</i> , 2012 (25)	Otero <i>et al.</i> , 2013 (22)	Ito <i>et al.</i> , 2014 (21)	Yan <i>et al.</i> , 2014(24)
<i>S. cerevisiae</i> host strain	AH22	CEN.PK 113-5D	CEN.PK 113-5D	S149	CEN.PK 113-7D
Modifications in pathway	Δ SDH1, Δ SDH2, Δ IDH1, Δ IDP2	\uparrow PYC2, \uparrow PEPCK, \uparrow MDH3, \uparrow RoFU M, \uparrow FRDg	Δ SDH3, Δ SER3, Δ SER33, \uparrow ICL1 evolution engineerin g	Δ ADH1- 5, Δ SDH1, Δ SDH2	Δ PDC1, Δ PDC5, Δ PDC6, Δ GPD1, Δ FUM1, \uparrow PYC2, \uparrow MDH3, \uparrow FUMC, \uparrow FRDS1
Production route intended through modifications	Via glyoxylate route	Via the reductive route	Via oxidative TCA cycle and via glyoxylate cycle	Via oxidative TCA cycle	Via reductive TCA cycle
Overexpressi on of a transporter	No	\uparrow DCT-02	No	\uparrow SpMAE 1	No
Cultivation	Aerobic shake flasks	Aerobic, glucose limited chemostat	Aerobic, batch cultivation in a bioreactor	Aerobic shake flasks	Aerobic batch fermentatio n in a bioreactor
Temperature	30°C	30°C	30°C	30°C	30°C
Dissolved oxygen	N.A	40%	N.A	N.A	>30%
pH	N.A	3.0	5.0	N.A*	3.8
Media	Defined	Defined	Defined	Defined	Defined
P _{CO2} (Bar)	N.A	0.65	N.A	N.A	0.10
Initial Glucose (mM)	279	75.75 (+ 21 mM ethanol) in chemostat feed	100	111	555.55
Average dry	6	5	2	~10	~35 (O.D)

biomass concentration (g/L)	(O.D. [*])				
Final succinate concentration (mM)	30.6	30	7.6	3.6	110.1
Yield (mol succinate/mol glucose)	0.11	0.36	0.08	0.032	0.21
Cultivation time (h)	168	Continuous production in chemostat, D=0.05 h ⁻¹	N.A	120	120
Succinic acid productivity (mol/m ³ /h)	0.18	1.5	N.A	0.03	0.92
Biomass specific succinic acid production rate (mmol/g DCW/h)	0.06	0.3	N.A	0.006	0.05
Other organic acids produced	Pyruvate (1.1 mM), α-Ketoglutarate (0.8 mM)	Acetate (1 mM), Malate (2 mM)	N.A	Fumarate (0.12 mM)	Pyruvate (245.7 mM)

N.A = not available, O.D = Optical Density (1 O.D =0.50 g/L)

Fumaric acid production

Table 1.4 shows the studies done in *S. cerevisiae* to produce fumaric acid. All were done in aerobic shake flasks using calcium carbonate as a buffer. The pH was not mentioned in these studies, but must have most likely been around 6.0 due to the presence of calcium carbonate. Biotin was added to the growth media when pyruvate carboxylase enzyme was overexpressed in order to obtain its higher activity.

Pines *et al.* (29) studied the impact of overexpressing MDH2 in *S. cerevisiae* on the organic acids production, the study was not done with the intention to produce fumaric acid. Expressing only MDH2, did produce fumaric acid though with a very low yield and productivity as shown in Table 1.4. Apart from fumarate, significant amounts of malate and citrate were produced.

S. cerevisiae was engineered to produce fumaric acid by overexpressing heterologous enzymes of the TCA cycle taken from the natural fumaric acid producer *Rhizopus* spp.. *S. cerevisiae* produced fumaric acid with a yield of $0.05 \text{ mol.}(\text{mol glucose})^{-1}$ with the knock-out of fumarase (FUM1), overexpression of pyruvate carboxylase from *Rhizopus* spp. (RoPYC) and overexpression of the homologous mitochondrial succinate fumarate carrier (SFC1) (30). The fumaric acid yield was further improved to $0.10 \text{ mol/ mol glucose}$ with the overexpression of homologous pyruvate carboxylase (PYC2) and malate dehydrogenase from *Rhizopus* spp.(RoMDH) (31). *S. cerevisiae* was engineered further with the knock-out of fumarase (FUM1), thiamine diphosphate (THI2), and overexpression of RoPYC, RoMDH and fumarase from *Rhizopus* spp. (RoFUM) resulting in a fumaric acid yield of $0.20 \text{ mol.}(\text{mol glucose})^{-1}$ (32). The rationale behind deletion of THI2 is that this leads to a higher production of pyruvate (33), which can be diverted to fumarate by overexpressing the TCA cycle enzymes of the reductive part. The highest yield of fumaric acid $0.51 \text{ mol.}(\text{mol glucose})^{-1}$ was reported with a module based optimization of the pathways consisting of a reductive module (RoPYC, RoMDH, RoFUM1 and plasma membrane dicarboxylic acid transporter SpMAE1), an oxidative module (KGD2, SUCLG2, SDH1 and SFC1) and a module to control the expression levels of glycerol 3-phosphate and pyruvate decarboxylase in order to control the formation of glycerol and ethanol (34). The biomass specific productivity of fumaric acid is comparable to that of succinic acid.

Table 1.4. Fumaric acid production in *S. cerevisiae*

	Pines <i>et al.</i> , 1997 (29)	Xu <i>et al.</i> , 2012 (30)	Xu <i>et al.</i> , 2012 (31)	Xu <i>et al.</i> , 2013 (32)	Chen <i>et al.</i> , 2015 (34)
<i>S. cerevisiae</i> strain	DMM1-15A	CEN.PK2_1C	BMA64	CEN.PK2_1C	CEN.PK2_1C (most likely)
Modifications in pathway	↑MDH	ΔFUM1, ↑RoPYC, ↑SFC1	↑PYC2, ↑RoMDH	ΔTHI2, ΔFUM1, ↑RoPYC, ↑RoMDH, ↑RoFUM	ΔTHI2, ΔFUM1, ↑RoPYC, ↑RoMDH, ↑RoFUM1, ↑KGD2, ↑SDH1, ↑SFC1,
Production route intended through modification	Study to check the effect of overexpressing MDH	Via oxidative TCA cycle	Via reductive TCA cycle	Via oxidative and reductive TCA cycle	Via oxidative and reductive TCA cycle
Overexpression of a transporter	No	No	No	No	↑SpMAE1
Cultivation	Aerobic, shake flask	Aerobic shake flasks	Aerobic shake flasks	Aerobic shake flasks	Aerobic shake flasks
Temperature	30°C	30°C	30°C	30°C	30°C
Dissolved oxygen	N.A	N.A	N.A	N.A	N.A
pH	N.A*	N.A	N.A	N.A	N.A
Media	Defined, CaCO ₃ as a buffer	Defined, CaCO ₃ as a buffer	Defined, CaCO ₃ as a buffer	Defined, CaCO ₃ as a buffer	Defined, CaCO ₃ as a buffer
P _{CO2} (Bar)	N.A	N.A	N.A	N.A	N.A
Initial Glucose (mM)	555.55 (Galactose)	277.80	333.30	277.80	555.55
Average dry biomass concentration (O.D*)	40	5	3.7	3.3	N.A
Final fumarate concentration (mM)	3.2	14.4	27.4	48.6	285.6
Yield (mol fumarate/m)	0.005	0.05	0.10	0.20	0.51

ol glucose)					
Cultivation time (h)	45	96	108 (most likely)	96	N.A
Fumaric acid productivity (mol/m ³ /h)	0.07	0.15	0.25	0.50	N.A
Biomass specific fumaric acid production (mmol/g DCW/h)	0.003	0.06	0.135	0.30	N.A
Other organic acids produced	Malate (88.05 mM), Citrate (212 mM)	N.A	Pyruvate (2.9 mM), Malate (4.9 mM), Succinate (0.5 mM)	Pyruvate (23.5 mM), α -Ketoglutarate (3.6 mM)	N.A

N.A = not available, O.D = Optical Density (1 O.D = 0.50 g/L)

Summary of C4 acids production studies

Remarkably, in most of the published studies on C4 dicarboxylic acid production the cultivations were carried out in shake flasks with the addition of calcium carbonate, which functions as pH buffer and results in an increased CO₂ concentration to thermodynamically push the flux towards the reductive part of the TCA cycle. Also most likely the O₂ limitation increases the driving force of the reductive route, though the dissolve oxygen was not mentioned in most of the studies. It has indeed been shown from bioreactor studies that a high partial pressure of CO₂ results in improved succinate and malate production (Table 1.2, 1.3), most likely via the reductive TCA cycle. We also noticed that in some studies a heterologous dicarboxylic acid transporter was expressed in the plasma membrane, while in other studies this was not done. Surprisingly, even without expressing such a transporter and thus with only pathway modifications, also significant improvements in the yield and final concentrations of dicarboxylic acids were obtained. From table 1.3 in which the studies related to succinic acid production are summarized, it can be seen

that with a *S. cerevisiae* not expressing any transporter also achieved a high yield of succinic acid. It can therefore not be excluded that wild type *S. cerevisiae* already contains transporter proteins with capacities to export dicarboxylic acids. Remarkably the influence of the cultivation pH and O₂ limitation on the production of dicarboxylic acids in *S. cerevisiae* has not been studied systematically, and often the information on dissolved O₂ and the cultivation pH is not given.

For malate and fumarate the obtained maximum yields are close to 0.50 mol/mol glucose, which is still far from the theoretical yield of 2 mol/mol glucose. A maximum biomass specific productivity of 1.41 mmol/g DCW/h was obtained for malate using a heterologous dicarboxylic acid transporter, while significantly lower biomass specific productivities were obtained for succinate and fumarate. The most probable explanation for this could be that the heterologous SpMAE1 transporter, also termed as “malate transporter”, used in these studies has a higher affinity for malate compared to succinate and fumarate (35).

Energetics of dicarboxylic acid transport

To achieve a high extracellular concentration of dicarboxylic acids at industrial scale, the presence of an efficient dicarboxylic acid transporter is as important as the optimization of the metabolic pathway for biosynthesis of the desired acid. Inefficient export will lead to intracellular accumulation of the produced acid and will interfere with cellular metabolism, leading to reduced production at increased acid titers.

In contrast to alcohols, which are lipophilic and can easily diffuse through the cell membrane, dicarboxylic acids are charged molecules which cannot pass the membrane as such. Depending on the pH, an equilibrium exists between three different forms of dicarboxylic acids (H₂A, HA⁻ and A²⁻, see Figure 1.2) where only the lipophilic uncharged form, H₂A, can diffuse into the cell through passive diffusion. However, in the cytosol, where the pH is near neutral, more than 99% of the species are either HA⁻ or A²⁻ which can be exported only via a specific transport protein (Figure 1.4)

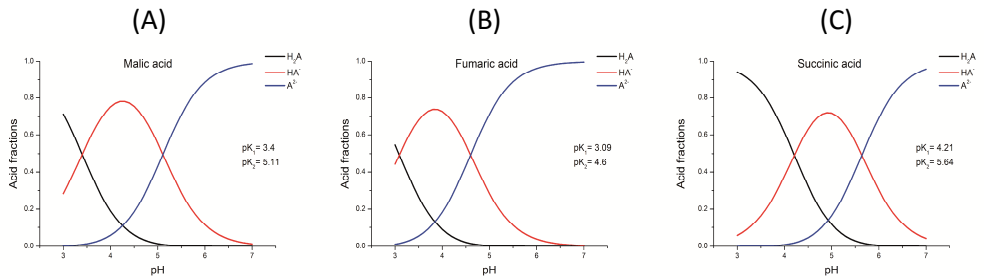


Figure 1.2. Fractions of three different forms of dicarboxylic acids (H_2A , HA^- , A^{2-}) over a pH range of 3.0 to 7.0 at 30° C and zero ionic strength. A) Malic B) Fumaric and C) Succinic acid.

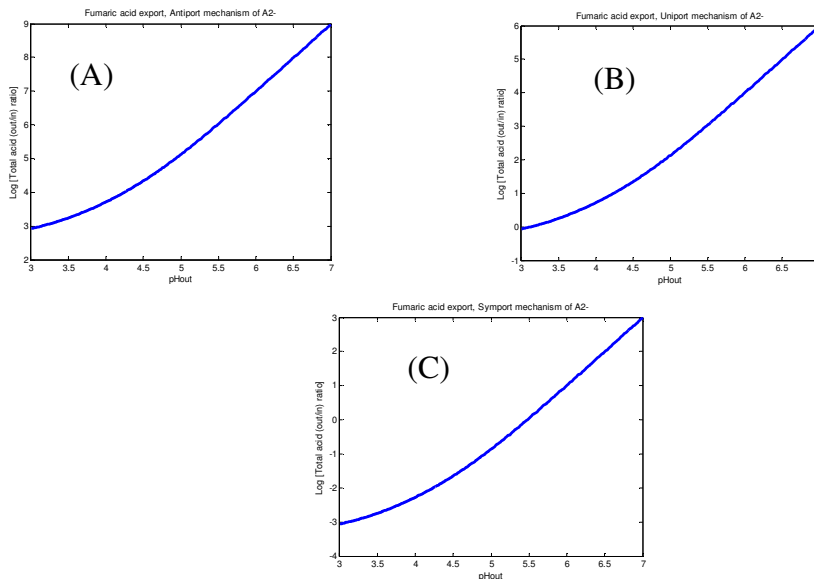


Figure 1.3. Fumaric acid export: Maximal total fumaric acid out/in ratio (in Log10 scale) as a function of the extracellular pH with A) Antiport B) Uniport and C) Symport mechanism of A^{2-} ($pH_{in} = 7.0$, $pmf = 180$ mV, $pK_1 = 3.09$, $pK_2 = 4.6$, $T = 30$ °C).

S. cerevisiae lacks specific transporters for dicarboxylic acids (36). However, *S. cerevisiae* does have the capability to export charged species of succinate and malate to prevent accumulation of these acids in the cytoplasm, but the export system has a very low affinity (37). Therefore the expression of a heterologous

transporter is required to turn *S. cerevisiae* into an efficient dicarboxylic acid producer. The thermodynamic aspects of dicarboxylic acids transport are described in detail by Tayamaz-Nikerel *et al.*(38). From calculations on the thermodynamics of dicarboxylic acid biosynthesis and export it was found that it is not feasible to produce fumaric acid under anaerobic conditions at low pH. The reason is that the pathway of fumarate, is ATP neutral and thus under anaerobic conditions, there is no energy available to export fumarate and the produced 2H^+ (38). Therefore a fumaric acid production process at low pH has to be carried out under aerobic conditions.

The maximal total acid out/in ratio which can be achieved by an exporter depends on the export mechanism, the cytosolic and extracellular pH and the proton motive force. For example Figure 1.3 shows that for an extracellular pH of 3.0 (required to eliminate the salt problem) the transport mechanism of A^{2-} has to be a proton antiport to provide sufficient thermodynamic driving force to achieve export against a high extracellular concentration of fumaric acid (total acid out/in ratio ~ 1000).

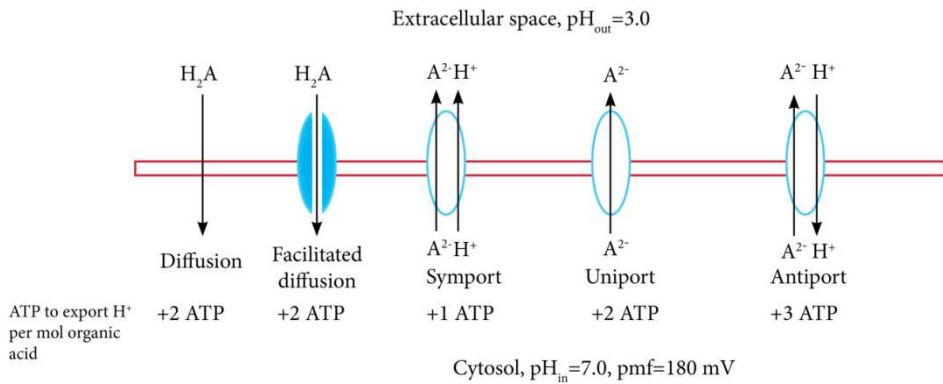


Figure 1.4. Different possible export mechanisms for dicarboxylic acids for extracellular pH of 3.0. At this pH there might be passive diffusion of the un-dissociated acid (H_2A) into the cells. Shown are the active export (antiport, uniport and symport) of A^{2-} , but HA^- could also be exported in a similar way, although its concentration inside the cell is very low (Figure 1.2). Also shown is the ATP required to export H^+ and organic acid.

The energy requirement to export one molecule of fumaric acid will then be 3 ATP to export 3 protons (assuming a H^+ /ATP stoichiometry of 1) via the plasma membrane H^+ ATP-ase (Figure 1.4). But if the cultivation is performed at pH 7.0, then a symport mechanism will be sufficient to achieve out/in ratio of 1000. Because in this case only one proton has to be exported for each molecule of fumaric acid excreted, the energy requirement for this mechanism will be one ATP (Figure 1.4). Assuming that fumaric acid production occurs via the reductive pathway and thus the ATP consuming pyruvate carboxylase reaction is used, then even at pH 7.0 fumaric acid production requires 1 ATP/mol acid, which makes the process not feasible under anaerobic conditions. Therefore, with the current pathways, the fermentation process for the production of fumaric acid has to be carried out under aerobic conditions to provide sufficient ATP for fumaric acid export and cell maintenance, irrespective of the cultivation pH.

Futile cycling

Fermentative production of organic acids is preferred at low pH to avoid waste salt formation and to achieve a cheaper product recovery. However, producing organic acids at a low pH can have one major disadvantage, which is the futile cycling of the produced organic acid. At for example pH 3.0, a significant part of the produced organic acid is present in the lipophilic un-dissociated (H_2A) form in the extracellular space (Figure 1.2), which can permeate into the cells by passive diffusion across the plasma membrane. After entering into the cells the acid will dissociate and subsequent export of the dissociated form(s) and the associated protons will require metabolic energy in the form of ATP. This passive diffusion into and active export from the cells will create an ATP dissipating futile cycle. The rate of diffusion of the un-dissociated form of a certain acid into the cells will determine the rate of ATP dissipation in this futile cycle. How fast an acid can diffuse into a living cell depends on the membrane composition and the membrane solubility properties of the un-dissociated acid. Some insight can be obtained from the octanol/water partition coefficient (K_{ow}) which is a measure of the lipophilicity of a compound. For fumaric, succinic and malic acid the values of Log K_{ow} are 2.88, 0.29 and 0.021 respectively (Log K_{ow} database, Sangster research laboratories, Montreal, Quebec, Canada). From these values it can be inferred that the

lipophilicity, and therewith permeability, of fumaric acid would be approximately 140 times higher than that of malic acid. This makes it very likely that fumaric acid would have a high futile cycling rate at low pH which leads to additional ATP dissipation and will result in a lower fumaric acid yield on the supplied substrate. A way to reduce this could be adaptation of the yeast to high levels of the un-dissociated acid, resulting in a changed membrane composition with reduced permeability for organic acids (39) and thus reduced energy costs due to futile cycling.

Growth of *S. cerevisiae* on dicarboxylic acids

It is indisputable that the organic acid producer should not be able to grow on the organic acid produced. *S. cerevisiae* is classified as a Krebs negative yeast (36), which means that it does not have the ability to utilize dicarboxylic acids of the TCA cycle as the sole carbon source. The reason for this was presumed to be the inability of this yeast to import dicarboxylic acids (40). However, it has been shown that through evolution in a carbon limited chemostat, with controlled pH of 4.0, and at increasing concentrations of succinic acid in feed medium, *S. cerevisiae* appeared to be capable of using succinic acid as the sole carbon source (41). However, so far no information is available whether *S. cerevisiae* can be evolved to grow on malic or fumaric acid as sole carbon sources and whether this yeast has transport systems for these acids.

Scope of the thesis

This thesis focusses on the aerobic metabolism and transport of fumaric acid in *S. cerevisiae* mostly at pH 3.0, but malic and succinic acid were also studied. All experiments were carried out under well controlled steady state conditions in glucose limited, aerobic chemostats, sometimes co-fed with fumaric acid. We also engineered the central metabolism and the cell membrane transport of dicarboxylic acids in *S. cerevisiae* and studied the effects of these modifications on the production and transport of fumaric, malic and succinic acid.

In **Chapter 2** we have investigated the uptake and metabolism of fumaric acid by *S. cerevisiae* in an aerobic glucose limited chemostat at a controlled pH of

3.0 ($\text{pH} < \text{pK}$ of fumaric acid) with increasing fumaric acid levels in the feed. The contribution of a heterologous DCT-02 transporter to the transport of fumaric acid was also examined in this study. From the obtained steady state chemostat data, metabolic flux analysis and measurement of intracellular and extracellular metabolite levels, we quantified the rate of fumaric acid uptake and the fate of the fumaric acid imported into the cells.

In **Chapter 3** we focused specifically on the uptake mechanism of fumaric acid in *S. cerevisiae* and looked for indications whether any homologous membrane protein is involved in the transport of fumaric acid and the role of passive diffusion in fumaric acid uptake. In this study *S. cerevisiae* was aerobically cultivated at a pH range of 3.0 to 6.0 with 60 mM of fumaric acid in the chemostat glucose based feed media to achieve different concentrations of H_2F , HF^- and F^{2-} in the extracellular space. This allowed us to relate the absolute uptake rate to one of the three forms of fumaric acid and discuss possible uptake mechanisms (passive diffusion or via a protein).

Wherein Chapter 2 and 3 fumaric acid uptake was studied, in **Chapter 4** the secretion of dicarboxylic acids (succinic, fumaric and malic acid) was investigated. An engineered *S. cerevisiae* strain overexpressing the enzymes involved in the reductive route of the TCA cycle and a heterologous DCT-02 transporter to facilitate dicarboxylic acids export was cultivated in a glucose limited chemostat, under aerobic conditions and at pH 3.0. Cultivations were performed at CO_2 concentrations in the aeration gas of 0%, 25% and 50% to push the carbon flux through the reductive branch of the TCA cycle leading to a high succinic acid production rate. This allowed us to study the stoichiometry and kinetics of metabolism and export of succinic acid and the role of futile cycling.

Chapter 5 explores the evolution based improvement of an engineered strain towards aerobic fumaric acid production. In this study *S. cerevisiae* was engineered such that fumaric acid was the metabolite of which the production resulted in the highest aerobic ATP production. In this strain the genes coding for glucose 6-phosphate dehydrogenase (in PPP pathway) (*zwf1*) and fumarase (in TCA cycle) (*fum1*) were disrupted where after the only envisaged route of fumaric acid synthesis was via the oxidative part of the TCA cycle.

In **Chapter 6** we present our work on the overexpression of heterologous and homologous enzymes involved in the reductive branch of the TCA cycle and studied the effects on the production of dicarboxylic acids. Heterologous reductive enzymes from *Rhizopus delemar* (which is the natural producer of fumaric acid) were used. Two heterologous dicarboxylic acid transporters DCT-02 and SpMAE1 were expressed to check their ability to export fumaric acid. The engineered strains were studied in aerobic shake flasks at glucose excess and nitrogen starvation with calcium carbonate as buffer and also as a source of CO₂ to push dicarboxylic acid production.

Chapter 2

**Transport and metabolism of fumaric acid in
Saccharomyces cerevisiae in aerobic glucose
limited chemostat culture**

Abstract

Currently, research is being focused on the industrial scale production of fumaric acid and other relevant organic acids from renewable feedstocks via fermentation, preferably at low pH for better product recovery. However, at low pH a large fraction of the extracellular acid is present in the un-dissociated form, which is lipophilic and can diffuse into the cell. There are no studies done on the impact of high extracellular concentration of fumaric acid in aerobic conditions on *S. cerevisiae*, which is a relevant issue to study for industrial scale production. In this work we studied the uptake and metabolism of fumaric acid in *S. cerevisiae* in glucose limited chemostat cultures at a cultivation pH of 3.0 (pH < pK). Steady states were achieved with different extracellular levels of fumaric acid obtained by adding different amounts of fumaric acid to the feed media. The experiments were carried out with the wild type *S. cerevisiae* CEN.PK 113-7D and an engineered *S. cerevisiae* ADIS 244 expressing a heterologous dicarboxylic acid transporter (DCT-02) from *Aspergillus niger*, to examine whether it would be capable of exporting fumaric acid. We observed that fumaric acid entered the cells most likely via passive diffusion of the un-dissociated form. Approximately two-third of the fumaric acid in the feed was metabolized together with glucose. From metabolic flux analysis, an increased ATP dissipation was observed only at high intracellular concentrations of fumarate, possibly due to the export of fumarate via an ABC transporter. The implications of our results for industrial scale production of fumaric acid are discussed.

Introduction

Fumaric acid, an intermediate of the citric acid cycle, is a dicarboxylic acid commonly found in nature. Due to its acidic properties it is used as an acidulant in food and beverages and as antibacterial agent in the feed industry (42). With the presence of a double bond and two carboxylic acid groups, fumaric acid can also be used to produce resins and biodegradable polymers (43). Fumaric acid is therefore one of the top twelve building block chemicals listed by the US Department of energy (4).

In the past, fumaric acid production was accomplished via fermentation using *Rhizopus* strains (44), but was gradually replaced by a cheaper alternative, that is, through chemical synthesis from petrochemicals. However, aiming at sustainable production of industrially relevant chemicals, research has again focused on the development of a fermentative process for production from renewable feedstocks. *Rhizopus* spp. are able to produce fumaric acid with yields close to 0.5 g acid/g of glucose (5). However, due to its filamentous morphology this fungus is less suited for large scale fermentative production of fumaric acid. An alternative host could be the yeast *S. cerevisiae* which grows as a unicellular organism and has the additional advantage that it can be cultivated at low pH, which makes downstream processing more cost effective. Furthermore, the array of available genetic tools for *S. cerevisiae* greatly facilitates metabolic engineering efforts aimed at obtaining high rates and yields of fumaric acid production. It should be realized, however, that at a low pH of e.g. 3.0, approximately 50% of the extracellular fumaric acid is present in its completely un-dissociated, lipophilic form. In case of an engineered strain with an efficient, energy driven, export mechanism for fumaric acid, the un-dissociated species could diffuse back into the cell while being simultaneously exported, resulting in an ATP dissipating futile cycle which would greatly reduce the yield of fumaric acid and increase oxygen consumption. Therefore, before developing a *S. cerevisiae* strain for the highly efficient production of fumaric acid, it is relevant to study the significance of fumaric acid uptake by the cells, especially at high extracellular concentrations of the un-dissociated form and at low pH.

Apart from the possible import of fumaric acid through passive diffusion of the un-dissociated form, it is also relevant to study the possible presence of other transport systems, as well as the fate of the imported fumaric acid, that is, whether it is (partly) metabolized and/or excreted by the cells after being taken up. It has been published that *S. cerevisiae* is not able to grow on dicarboxylic acids as the sole carbon source (36). Nevertheless, it was shown in another publication that, after *in-vitro* evolution, *S. cerevisiae* was able to grow on succinic acid as the sole carbon source (41). However, to our knowledge no information is available on whether fumaric acid can be co-metabolized in combination with other substrates such as glucose.

An important aspect towards the overproduction of fumaric acid is to efficiently export the acid. As *S. cerevisiae* is not a natural producer of dicarboxylic acids, it most probably does not possess efficient transport systems to secrete these acids. Nevertheless Xu *et al.* (2013) reported the construction of a *S. cerevisiae* strain capable of producing fumaric acid up to a titer of 5.6 g.L⁻¹ without introducing a specific transporter for excretion of the acid. However, to further increase the production capacity an efficient exporter will be indispensable for the engineering of *S. cerevisiae* as observed by Zelle *et al.*, (2008) for malic acid production.

In the current study we focus on the effects of large scale production conditions of organic acids, which are preferably carried out at low pH in a fed batch mode at low extracellular substrate and high extracellular acid concentrations. To mimic these conditions we carried out glucose limited aerobic chemostat cultures with different concentrations of fumaric acid in the feed medium at pH 3.0. Aerobic conditions were chosen because a thermodynamic analysis revealed that fumaric acid production at low pH under anaerobic conditions is not feasible (38). Uptake and metabolism of fumaric acid was quantified for the CEN.PK 113-7D and ADIS 244, containing a heterologous dicarboxylic acid transporter (DCT-02) from *Aspergillus niger*, to study its possible role in fumaric acid transport.

Materials and methods

Strain and cultivation condition

The study was done using *Saccharomyces cerevisiae* CEN.PK 113-7D and ADIS 244. ADIS 244 was also derived from CEN.PK 113-7D expressing a heterologous dicarboxylic acid transporter DCT-02 from *Aspergillus niger*, the strain was kindly provided by Royal DSM B.V (Delft, The Netherlands) . DCT-02 gene integration procedure is same as described in the patent by DSM IP Assets B.V (26). In the ADIS 244 strain the DCT-02 gene was integrated into the SIT2 locus of CEN.PK 113-7D. Strain is prototrophic and contains the KanMX marker. Strain stocks were kept at -80°C in 30% glycerol. Pre-cultures were grown in 250 ml Erlenmeyer flasks with 100 ml of defined medium containing: $20\text{ g}\cdot\text{L}^{-1}$ glucose monohydrate, $5\text{ g}\cdot\text{L}^{-1}$ $(\text{NH}_4)_2\text{SO}_4$, $3\text{ g}\cdot\text{L}^{-1}$ KH_2PO_4 , $0.5\text{ g}\cdot\text{L}^{-1}$ $\text{MgSO}_4\cdot 7\text{H}_2\text{O}$, $1\text{ mL}\cdot\text{L}^{-1}$ trace mineral solution and $1\text{ mL}\cdot\text{L}^{-1}$ vitamin solution. The pre culture medium was filter sterilized using PVDF membrane filters with $0.2\ \mu\text{m}$ pore size (Millipore, Massachusetts, USA). Shake flask cultures were incubated at 30°C on a gyratory shaker at 200 rpm.

Chemostat cultivations were carried out on a low salt minimal medium as described by Canelas *et al.* (45). The composition of this medium was: $8.25\text{ g}\cdot\text{L}^{-1}$ (41.67 mM) Glucose. H_2O , $0.30\text{ g}\cdot\text{L}^{-1}$ $(\text{NH}_4)_2\text{SO}_4$, $3.0\text{ g}\cdot\text{L}^{-1}$ $\text{NH}_4\text{H}_2\text{PO}_4$, $0.30\text{ g}\cdot\text{L}^{-1}$ KH_2PO_4 , $0.50\text{ g}\cdot\text{L}^{-1}$ $\text{MgSO}_4\cdot 7\text{H}_2\text{O}$, $1\text{ mL}\cdot\text{L}^{-1}$ trace mineral solution, $1\text{ mL}\cdot\text{L}^{-1}$ vitamin solution, and $0.50\text{ g}\cdot\text{L}^{-1}$ (10.85 mM) ethanol. Ethanol was added to the feed medium to avoid oscillations. The composition of the trace element and vitamin solutions were the same as described by Verduyn *et al.* (46). The media was filter sterilized using Sartopore 150 filters (Sartorius, Gottingen, Germany) into a previously heat sterilized vessel (20 min at 121°C) containing an amount of Basildon silicone anti-foam (Basildon Chemicals Ltd, UK) such that the final concentration of antifoam in the medium was $0.10\text{ g}\cdot\text{L}^{-1}$. The medium composition used for the increase in extracellular fumaric acid was the same as the composition described above, except that it contained either 1, 10, 20, 40, 60 or 120 mM of fumaric acid.

To avoid solubility problems, the two highest fumaric acid concentrations in the feed of 60 and 120 mM were realized by adding 35 mM of fumaric acid combined respectively with 25 and 85 mM of dipotassium fumarate. For the

highest concentration of 120 mM of fumaric acid in the feed, the $\text{NH}_4\text{H}_2\text{PO}_4$ concentration was increased to $5 \text{ g}\cdot\text{L}^{-1}$ to avoid nitrogen limitation in case a significant amount of fumaric acid would be consumed as a carbon source in addition to glucose.

Chemostat cultivation

Glucose limited chemostat cultivations were carried out in bench scale bioreactors (Applikon, The Netherlands) with a working volume of 1 L. The reactor was inoculated with an overnight grown pre-culture and was first operated in a batch mode. After the end of the batch phase the reactor was switched to chemostat mode with a dilution rate of 0.10 h^{-1} . The culture temperature was maintained at 30°C and the pH was measured using a pH sensor (type 465-50-S7, Mettler-Toledo, Urdorf, Switzerland) and controlled at pH 3.0 by titration with 2M KOH and 2M H_2SO_4 using a Biostat Bplus controller (Sartorius BBI Systems, Melsungen, Germany). The dissolved oxygen concentration was measured with a DO sensor (Mettler-Toledo GmbH, Greinfensee, Switzerland). Chemostat cultivations were performed at a stirrer speed of 800 rpm. Feed medium was supplied continuously by means of a peristaltic pump (Cole-Parmer Masterflex Peristaltic Pump, Model 77521-50). The culture volume was maintained at $1000 \pm 50 \text{ mL}$ through a peristaltic effluent pump controlled by a level sensor. Air was sparged at a flow rate of 0.30 L min^{-1} using a mass flow controller (Brooks 5850 TR, Hatfield, PA, USA) and an overpressure of 0.30 bar was maintained in the bioreactor. The exhaust gas was cooled with a condenser connected to the cryostat set at 4°C and the part of the exhaust gas directed to the exhaust gas analyses was dried by passing it through a Permapure drying column (Inacom Instruments, Overberg, The Netherlands). The CO_2 and O_2 concentrations in the exhaust gas were monitored through a combined paramagnetic/infrared off-gas analyzer (NGA 2000, Rosemount, USA). Data acquisition during the course of the experiments was done using MCFS/win 2.1 software (Sartorius BBI Systems, Melsungen, Germany). Chemostat cultivations were assumed to have reached steady state after a period of five volume changes, if stable readings of the CO_2 and O_2 levels in the exhaust gas and the dissolved oxygen concentration were obtained.

Stepwise increase in the extracellular fumaric acid concentration

After achieving a steady state in glucose limited chemostat culture in the absence of fumaric acid, the feed vessel was exchanged by a vessel with the same medium, containing a specified amount of fumaric acid. In this way the fumaric acid concentration in the feed was increased stepwise from 0 to 1, 10, 20, 40 and 60 and finally 120 mM of fumaric acid. Each time the medium vessel was replaced by a vessel with a higher concentration of fumaric acid, simultaneously a concentrated solution of fumaric acid was injected in the chemostat. This was done to reduce the wash-in time of the fumaric acid and thus to shorten the time required to reach a new steady state. Each steady state was maintained for approximately 2 days, during which samples were taken for intra- and extracellular metabolite quantification.

Rapid sampling for intracellular metabolite quantification

For the quantification of intracellular metabolites, rapid sampling of broth from the chemostat was performed using a custom built rapid sampling setup (47). With this setup approximately 1.2 g of broth sample was withdrawn within 0.8 s into 6 mL of quenching solution (100% methanol at -40°C) and immediately mixed by vortexing. Each tube was weighed after sampling to determine the exact amount of sample taken. The quenched sample was then rapidly poured onto a 0.45 µm (PES, Pall, USA) filter containing 40 ml of 100% methanol at -40°C. After removal of the liquid by vacuum filtration, the remaining cell cake was washed with 40 ml of 100% precooled methanol (-40 °C) to remove the extracellular fumaric acid and other extracellular compounds. Effective removal of all extracellular fumaric acid is required for proper quantification of the intracellular level. The above described washing procedure appeared sufficient to avoid interference of extracellular fumaric acid with the quantification of the intracellular level (see Appendix 2.C). Metabolite extraction was carried out as follows: the filter containing the cell cake was immersed in 30 ml of 75% preheated ethanol (75°C) in a 50 ml Falcon tube, while at the same time 120 µl of 13C labelled internal standard solution was added. Thereafter the tube was placed in a 95°C water bath for 3 min and then stored at -80°C until further processing. Subsequently the samples were evaporated to dryness using a Rapid-Vap (Labconco, USA) (48), thereafter the

residue was re-dissolved in 600 μl of Milli-Q water and centrifuged at 10000g for 5 min to remove cell debris. After a second centrifugation step at 10000 g for 10 min, the cell extracts were stored at -80°C until metabolite quantification with GC-MS and LC-MS.

Dry weight and total organic carbon determination

Approximately 5 ml of broth was filtered using a pre-dried and pre-weighed 0.45 μm (PES, Pall, USA) filter. The filter with the biomass was dried in an oven at 70°C until constant weight (approximately 24 h). Thereafter the filters were cooled down in a desiccator for 15 min before weighing them to determine the biomass concentration.

Extracellular metabolite analysis

Samples of culture filtrate were taken by rapidly withdrawing approximately 2 mL of broth into a syringe containing steel beads at -18°C to cool the sample rapidly to 0°C . Immediately thereafter the medium was separated from the cells through filtration using 0.45 μm syringe filters (49). This method allows accurate determination of residual glucose and other extracellular metabolites. In case of 40, 60 and 120 mM of fumaric acid in the feed, steel beads were not used in order to prevent crystallization of fumaric acid at low temperature.

Extracellular concentrations of ethanol, glucose, acetate and glycerol were quantified through HPLC analysis using a Bio-Rad HPX-87H 300 column (7.8 mm). The column was eluted with phosphoric acid (1.5 mM in Milli-Q water) at a flow rate of 0.6 mL min^{-1} . The injection volume was 10 μl and the auto sampler temperature was 15°C . The detection was accomplished by a refractometer (Waters 2414) and a UV detector (Waters 484; 210 nm). Succinate, malate and fumarate were also quantified with HPLC, using a Bio-Rad HPX-87H 300 column (7.8 mm). The column was eluted with phosphoric acid (45 mM in milli Q water). The reason for using more concentrated eluent was to have a better resolution of the peaks.

Calculation of biomass specific rates and metabolic flux analysis

For each steady state, the biomass specific net conversion rates were calculated from steady state compound balances. Using the constraint that the elemental conservation relations should be satisfied, standard data reconciliation techniques were used to obtain better estimates of the biomass specific rates with reduced standard errors (50).

Steady state metabolic flux analysis was performed using a metabolic network model for *S. cerevisiae* as described by Daran-Lapujade *et al.* (2004). In the metabolic network model the uptake of fumaric acid was considered to occur via passive diffusion, and the export of succinic and malic acid via uniport mechanism of the fully dissociated. Pyruvate decarboxylase was not required in the model as the medium contained a mixture of glucose and ethanol as carbon source (on carbon basis: 92 % glucose and 8% ethanol). The P/O ratio used for the calculations was 1.23 as obtained by Lange *et al.* (2002) . Further modifications of the stoichiometric model to incorporate fumaric acid metabolism are described in the results section. The stoichiometric model contains 148 reactions, 165 metabolites and 3 compartments (cytosol, mitochondria and extracellular).

The stoichiometric model was also applied for *a priori* calculations of steady state biomass specific conversion rates in glucose limited chemostat cultivations with co-consumption of fumaric acid. The maintenance energy requirement used in the model was 80 mmol ATP /Cmol biomass/h, which was the value estimated by Jamalzadeh *et. al.* (2013) obtained from glucose limited, aerobic chemostat culture experiments with *S. cerevisiae* at pH 3.0 and a dilution rate of 0.10 h⁻¹.

Results

S. cerevisiae strains CEN.PK 113-7D and ADIS 244 (expressing the DCT-02 transporter), were grown in aerobic glucose limited chemostat cultures at pH 3.0 and at a dilution rate of 0.10 h⁻¹. Steady states were assumed to be achieved after reaching stable concentrations of O₂ and CO₂ in the offgas of the chemostats, as well as stable dissolved oxygen levels. At steady state in

the absence of fumaric acid, the only difference in the biomass specific rates of both the CEN.PK 113-7D and ADIS 244 strains (Supplementary data, Table 2.S2) was the secretion of small amounts of succinic and malic acid by ADIS 244. The excretion of these acids was most probably caused by the presence of the DCT-02 transporter (26). Notably, fumaric acid was not secreted by the ADIS 244 strain. Except for the excretion of small amounts of succinic and malic acid, the biomass specific rates were not significantly different in both the strains, therefore the introduction of the DCT-02 transporter did not have a severe impact on the physiology of *S. cerevisiae* in aerobic glucose limited chemostats.

***S. cerevisiae* can use fumaric acid as a co-substrate along with glucose**

After attaining a steady state in the absence of fumaric acid, the chemostat cultures were subjected to a stepwise increase in the extracellular fumaric acid concentration, by replacing the feeding media with media containing increasing fumaric acid concentrations (see materials and methods section). After each increase in the fumaric acid concentration in the feed, the cultivation was run until a new steady state was obtained, before proceeding to the next increase in fumaric acid concentration. During each steady state the intracellular and extracellular concentrations of fumaric acid, biomass dry weight and the O₂ and CO₂ levels in the off gas were quantified to get insight into the transport and possible metabolism of fumaric acid. It was observed that during the steady states the concentration of fumaric acid in the effluent of the chemostat cultures of both the strains was significantly lower than in the influent (Fig 1A), indicating the uptake and conversion of fumaric acid in both the CEN.PK 113-7D and ADIS 244. The biomass specific conversion rate of fumaric acid increased with increasing extracellular fumaric acid concentration (Figure 2.1B) and was higher for ADIS 244 for extracellular concentrations above 5 mM.

In the stoichiometric model we assumed the use of fumaric acid as carbon source and incorporated the most likely route of fumaric acid metabolism, that is, via fumarase and malate dehydrogenase to oxaloacetate, and from oxaloacetate to PEP through PEP carboxykinase (gluconeogenesis). Using this stoichiometric model, we estimated the increase in biomass, respiratory

quotient and oxygen uptake rate with the consumption of fumaric acid and compared it with the experimental results.

It was observed that the steady state biomass concentration increased with increased amounts of fumaric acid consumed (Figure 2.1C), indicating that the fumaric acid taken up by the cells was used as a carbon source for growth. This was again confirmed by the observed increase of the respiratory quotient with increase in biomass specific fumaric acid uptake rate (Figure 2.1D), which also matched well with the estimated respiratory quotient (RQ) using the flux model. As fumarate is a more oxidized substrate compared to glucose, the metabolism of fumaric acid should indeed result in an increased RQ.

For CEN.PK 113-7D, the fumaric acid concentration in the feed was increased further from 60 to 120 mM. This resulted in a doubling of the specific fumaric acid consumption rate from 15 to 31 mmol.Cmol⁻¹.h⁻¹ (Figure 2.1B). Nevertheless, the steady state biomass concentration increased only slightly, from 5.34 to 5.59 g.L⁻¹ (Figure 2.1C), compared to the increase from 4.11 to 5.34 g.L⁻¹ when the specific fumaric acid consumption rate increased from 0 to 15 mmol.Cmol⁻¹.h⁻¹. For fumaric acid consumption rates between 0 and 15 mmol/Cmol.h the steady state biomass concentrations for CEN.PK 113-7D observed experimentally were only slightly lower than estimated via the flux model (Figure 2.1C). The biomass yields for the ADIS 244 strain were somewhat lower compared to CEN.PK 113-7D, which is most likely caused by the excretion of malic and succinic acid by the ADIS 244 strain, which was not observed for CEN.PK 113-7D (Figure 2.2).

Using the flux model, we also calculated the oxygen uptake rate in correlation with the rate of fumaric acid metabolism (Figure 2.1E). According to the calculations carried out with the flux model, the biomass specific oxygen uptake rate of *S. cerevisiae* slowly increases with increasing metabolism of fumaric acid. However, at the highest residual fumaric acid concentration of 67 mM, and corresponding biomass specific uptake rate of 31 mmol.Cmol⁻¹.h⁻¹, the experimental oxygen uptake rate was significantly higher than estimated through the flux model, indicative of an increased rate of ATP dissipation at increased extracellular fumaric acid concentrations, which points to futile cycling of fumaric acid.

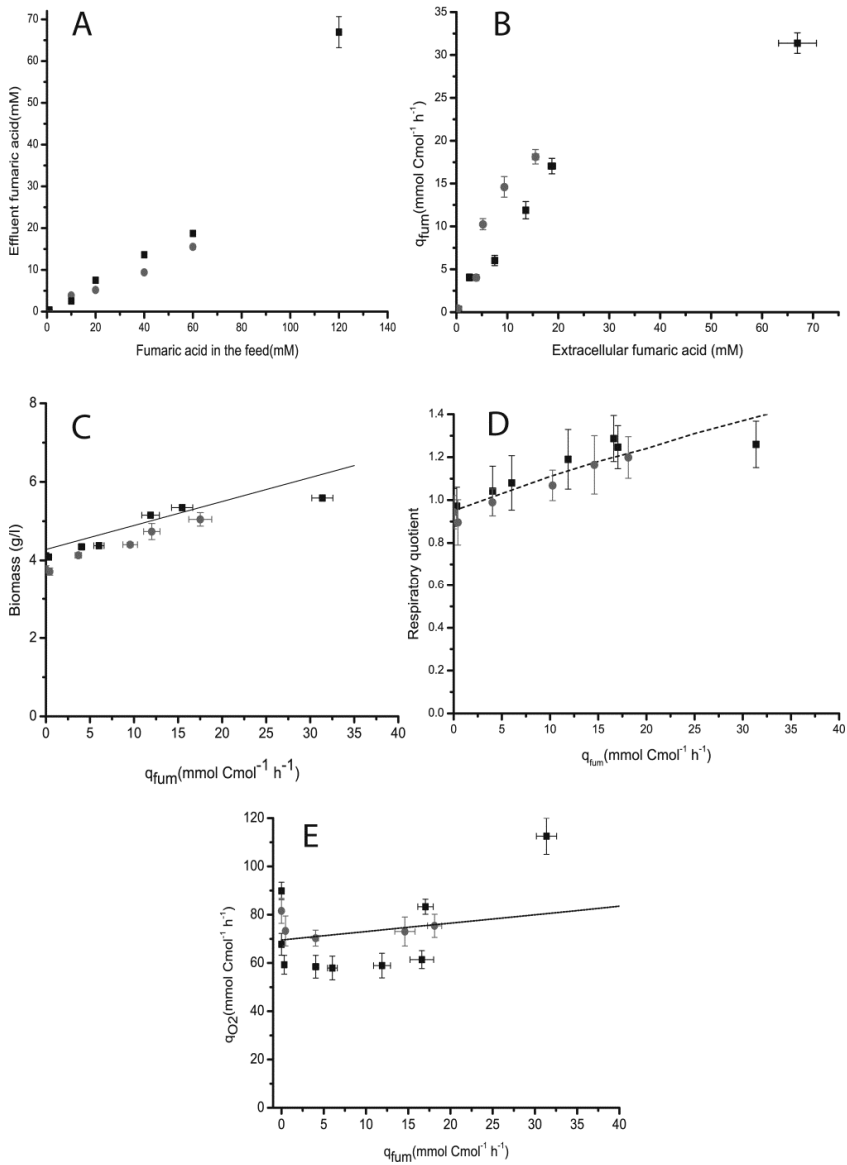


Figure 2.1. A) Steady state extracellular concentration of fumaric acid at different fumaric acid concentrations in the chemostat feed B) Steady state biomass specific fumaric acid uptake rates plotted against the measured extracellular concentration of fumaric acid. C) Steady state biomass concentration vs steady state biomass specific fumaric acid uptake rate D) Steady state respiratory quotient vs steady state biomass specific fumaric acid uptake rate. E) Experimentally obtained steady state biomass specific oxygen

uptake rate vs steady state biomass specific fumaric acid uptake rate. (●: ADIS 244, ■: CEN.PK 113-7D) and estimates using the flux model (--)

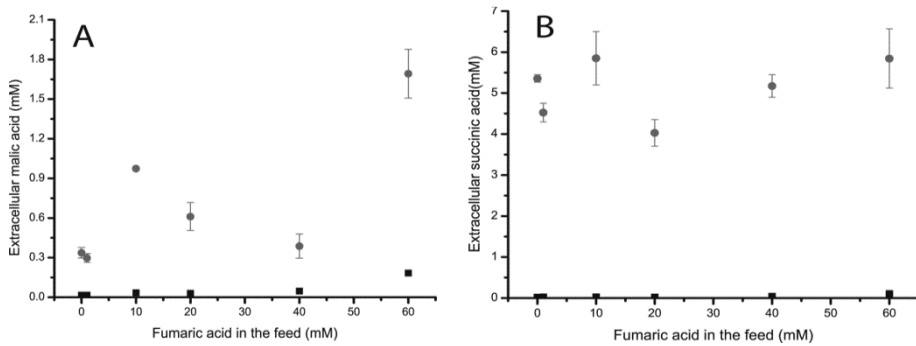


Figure 2.2. Extracellular concentrations of malic (A) and succinic (B) acid in steady state glucose limited chemostat cultivations of ADIS 244 and CEN.PK 113-7D strains at different levels of fumaric acid in the feed.

Metabolic flux analysis

Metabolic flux analysis was carried out for the steady states achieved with different concentrations of fumaric acid in the feed. The aim of performing the flux analysis was twofold; first to verify, based on calculated fluxes combined with measured intracellular concentrations of associated metabolites, whether our assumptions on how fumaric acid was metabolized by *S. cerevisiae* were justified and second to estimate the rate of ATP dissipation of the cells in the presence of increasing levels of extracellular fumaric acid. It has been previously reported that futile cycling of weak acids, due to passive influx via diffusion of the un-dissociated form and subsequent active export, results in increased ATP dissipation, for example in case of benzoic (53) and acetic acid (54), leading to reduced biomass yields and increase in biomass specific oxygen uptake rates.

A metabolic map with the calculated flux distributions for the chemostat steady states with 0, 60 and 120 mM of fumaric acid in the feed with CEN.PK 113-7D is shown in Figure 2.3. Due to the additional consumption of fumaric acid as carbon source together with glucose, there was a significant decrease in the glycolytic flux for the cultivations with 60 and 120 mM of fumaric acid in the feed and also a significant decrease in the intracellular concentration of

upper glycolytic metabolites (Supplementary, Table 2.S1). Nevertheless the mass action ratios of the glycolytic reactions PGI, PGM and ENO did not change with an increasing consumption of fumaric acid (Table 2.1) and their values remained close to equilibrium. This is in accordance with the findings of Canelas *et al.* (2011) and shows that the capacities of the glycolytic enzymes are high and therefore they operate close to equilibrium.

It was observed that with increased consumption of fumaric acid, and calculated increase of the flux through fumarase (Bold arrow, Figure 2.3), the ratio of intracellular malate/fumarate decreased steeply from a value close to the apparent in-vivo equilibrium ratio of around 5.0 (55) to values between 1 and 2 (Figure 2.4). Also the PEP/OAA ratio decreased significantly (Table 2.1). These changes clearly points at an increasing thermodynamic driving force needed to push the fumarase and PEP carboxykinase reactions towards the formation of malate and PEP respectively in order to process fumaric acid via gluconeogenesis (Bold arrows, Figure 2.3).

To verify whether futile cycling occurred, the ATP dissipation rates were calculated for different extracellular fumaric acid levels. Up to a total extracellular fumaric acid concentration of 19 mM, no increase in ATP dissipation was observed (Supplementary, Table 2.S1). However, at the highest residual concentration of 67 mM a significant increase in the biomass specific oxygen uptake rate and a subsequent increase in ATP dissipation was observed for CEN.PK 113-7D (ADIS 244 was not cultivated at this concentration). The maintenance energy requirements of CEN.PK 113-7D increased from 93 mmol ATP.Cmol⁻¹.h⁻¹ with 19 mM of residual fumaric acid to 166 mmol ATP.Cmol⁻¹.h⁻¹ with 67 mM of residual fumaric acid, which is most likely due to the futile cycling of fumaric acid. With 67 mM of residual fumaric acid the intracellular level was 24 μmol.gDCW⁻¹, which is fifty times higher than the intracellular level observed in the absence of extracellular fumaric acid. Such an increase of the intracellular fumaric acid level could lead to the expression of a transport protein involved in the active export of fumaric acid, most likely the mono- and/or di-anion form, as the intracellular concentration of un-dissociated fumaric acid is negligible at the near neutral pH of the cytosol. For example Pdr12 is an ABC transporter which is expressed in the

presence of weak acids (56). The active export of fumaric acid in combination with the continuous influx by passive diffusion creates a futile cycle.

Table 2.1. Experimental mass action ratios of relevant reactions at different concentrations of fumaric acid in the feed.

Reaction	Mass action ratio (Product/ Substrate)	0 mM ADIS	60 mM ADIS	0 mM CEN.PK 113- 7D	60 mM CEN.PK 113- 7D	120 mM CEN.PK 113- 7D
PGI	F6P/G6P	0.28 ± 0.01	0.29 ± 0.05	0.27 ± 0.02	0.28 ± 0.03	0.25 ± 0.0
PGM	2PG/3PG	0.10 ± 0.00	0.11 ± 0.03	0.10 ± 0.0	0.10 ± 0.00	0.10 ± 0.0
ENO	PEP/2PG	4.10 ± 0.60	4.05 ± 0.11	3.08 ± 0.15	3.85 ± 0.43	3.33 ± 0.08
FUMR	MAL/FUM	7.27 ± 2.25	0.64 ± 0.09	3.63 ± 0.22	1.17 ± 0.23	2.15 ± 0.03
PEPCK	PEP/OAA	74 ± 10	22 ± 0.57	300 ± 12.50	23.40 ± 3.17	9.33 ± 1.24

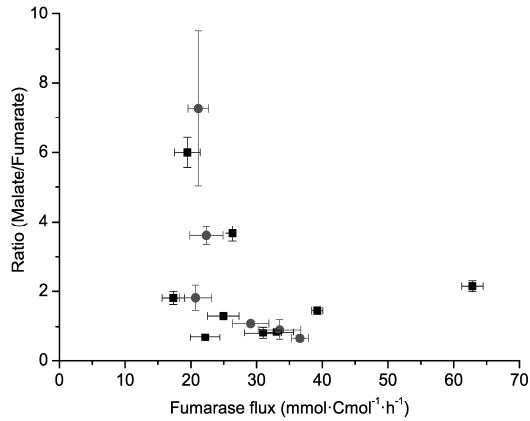


Figure 2.4. Malate/fumarate ratio versus flux through fumarase reaction

Uptake of fumaric acid

As discussed above, significant uptake and metabolism of fumaric acid occurred in both the strains during glucose limited chemostat growth. At 120 mM of fumaric acid in the feed, the amount of carbon consumed in the form of fumaric acid was 50% of the total (glucose + fumaric acid). The question is now via which transport mechanism the acid is taken up by the cells.

Because the cultivations were carried out at a pH of 3.0, approximately 50% of the acid was in un-dissociated form (appendix 2.B, Figure 2.B1). A plausible transport mechanism is therefore passive diffusion of the un-dissociated lipophilic acid across the plasma membrane. As the intracellular pH of *S. cerevisiae* is known to be well controlled at a value close to neutral (57), the concentration of un-dissociated fumaric acid inside the cells can be assumed negligible. Therefore the driving force for diffusion of the un-dissociated form into the cells is determined only by its extracellular concentration and this uptake can be considered irreversible.

From a plot of the specific fumaric acid consumption rate against its extracellular concentration of un-dissociated form in the chemostat (Appendix

2.A, Figure 2.A1), there appears to be a linear relation upto 10 mM for both the strains, which indicates that passive diffusion is indeed the main uptake mechanism.

Assuming irreversible passive diffusion of un-dissociated acid as uptake mechanism, the fumaric acid uptake rate can be described by the following equation:

$$q_{H_2F} = k \frac{6V_x}{d_x} C_{H_2F_{ex}} \quad (1)$$

wherein q_{H_2F} is the biomass specific uptake rate of un-dissociated fumaric acid in $\text{mol Cmol}^{-1} \text{ s}^{-1}$, k is the permeability coefficient in m.s^{-1} , $C_{H_2F_{ex}}$ is the extracellular concentration of un-dissociated fumaric acid in mM, V_x is the cell volume in $\text{m}^3 \cdot \text{Cmol}^{-1}$ ($52.8 \times 10^{-6} \text{ m}^3 \cdot \text{Cmol}^{-1}$, Kresnowati *et al.* (2008a)) and d_x is the cell diameter in m ($5 \times 10^{-6} \text{ m}$, Kresnowati *et al.* (2008a)).

The concentrations of un-dissociated fumaric acid for the different steady states were calculated from the measured total concentrations, the culture pH and dissociation constants, which were corrected for the ionic strength of the medium (Appendix 2.B, table 2.B2). The obtained values of the permeability coefficients were $12.90 \pm 0.96 \times 10^{-9} \text{ m.s}^{-1}$ and $8.64 \pm 0.31 \times 10^{-9} \text{ m.s}^{-1}$ for ADIS 244 and CEN.PK 113-7D respectively (see Appendix 2.B).

The obtained values of the membrane permeability coefficients for fumaric acid were compared with the literature values for other weak acids by plotting them against their octanol water partition coefficients (Figure 2.5). The octanol water partition coefficient ($\text{Log } K_{ow}$) determines the lipophilicity of a compound. A weak acid with a high octanol water partition coefficient is more lipophilic and is expected to have a higher membrane permeability coefficient. Using the $\text{log } K_{ow}$ of fumaric acid, its permeability coefficient was calculated from equation (2). Escher *et al.* (2008) estimated the correlation between permeability and octanol water partition coefficient by compiling the data of the permeability (P_o in cm.s^{-1}) for 165 common drug molecules across an artificial lipid membrane, obtaining the following correlation:

$$\text{Log } P_o \text{ (cm/s)} = 1.18 \text{ log } K_{ow} - 5.68 \quad (2)$$

The value of the fumaric acid permeability coefficient obtained from equation (2) is $72.9 \times 10^{-9} \text{ m}\cdot\text{s}^{-1}$. Fumaric acid permeability was also compared with the water octanol partition coefficient along with other weak acids in Figure 2.5. These comparisons indicate that our experimentally calculated value is 9 times lower than what would be expected based on the known water octanol partition coefficient using equation (2). However, it can also be seen from Figure 2.5 that the monocarboxylic acids have a higher, and the dicarboxylic acids fumarate and succinate have a lower permeability coefficient than estimated from equation (2). Equation (2) provides an average relation between octanol water partition and membrane permeability as it is derived using artificial lipid membranes. Still we can conclude that fumaric acid has higher water octanol partition coefficient than succinic which is also reflected in its experimentally calculated higher permeability coefficient than succinic acid.

At 120 mM of fumaric acid in the feed an increase in ATP dissipation was observed (see in metabolic flux analysis) which points towards the futile cycling of fumaric acid as the most likely reason. This is possible only with the expression of a membrane transporter involved in the export of fumaric acid. To evaluate the export of fumaric acid we compared the experimental out/in ratios of total fumaric acid with the theoretically expected out/in ratios (see Table 2.2) for different transport mechanisms. The out/in ratio of total fumaric acid with 120 mM of fumaric acid in the feed was 5.50, which corresponds best with the export via uniport of Fum^{2-} or antiport of HFum^- .

Table 2.2. Theoretically calculated equilibrium ratios (out/in) of total fumaric acid at pH_{out} of 3.0, pmf 180 mV and cytosolic pH of 7.0 (pH_{in})

Transported molecule	Symport	Uniport	Antiport	ABC transporter	CEN.PK 113-7D	ADIS 244
Fum²⁻	8.1E-04	0.86	855	10^7	5.5 (67 mM fumaric acid outside)	2.08 (17.5 mM fumaric acid outside)
HFum⁻	8.9E-07	8.1E-04	0.86	10^{10}		
H₂Fum		9.07E-10 (Passive diffusion)				

Thermodynamically the experimental ratios must be smaller than the theoretically expected out/in ratios. Therefore, as seen from Table 2.2, thermodynamically feasible transport mechanisms to export fumaric acid are antiport of Fum²⁻ or ABC export of Fum²⁻ or HFum⁻. This export of fumaric acid together with its diffusive influx constitutes a futile cycle which dissipates energy. Note that not only Fum²⁻ or HFum⁻ but also 2H⁺ or H⁺ must be exported using H⁺/ATP ase at the expense of 1 mol ATP/mol H⁺. Assuming ABC transport as an export mechanism then the total ATP spent per mol of fumaric acid exported must therefore lie between 2 ATP (ABC export of HFum⁻ and export of 1 proton (H⁺) by H⁺/ATPase) and 3ATP (ABC export of Fum²⁻ and export of 2 protons or antiport of Fum²⁻ and export of 3 protons by H⁺/ATPase).

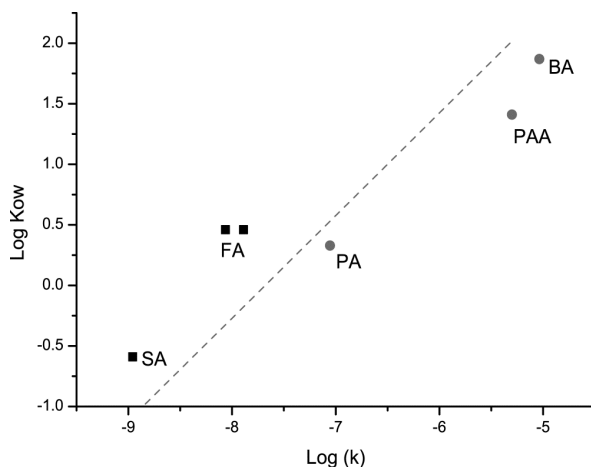


Figure 2.5. Comparison of the permeability coefficient (Log k , k is in m/s) with water octanol partition coefficient (Log K_{ow}) for weak acid Benzoic acid (BA, (60)), Phenylacetic acid (PAA, (61)), Fumaric acid (FA, this study), Propanoic acid (PA, (25)) and Succinic acid (SA, (25)). (---) estimated slope between log K_{ow} and log k using equation (2). Monocarboxylic acids (●); Dicarboxylic acids (■).

Role of the DCT-02 transporter in the transport of dicarboxylic acids

In the chemostat cultivations carried out with the ADIS 244 in the presence or absence of fumaric acid, secretion of succinic and malic acid was observed, showing the role of the DCT-02 transporter in the export of these acids. However, no fumaric acid was secreted in the steady state achieved in the absence of fumaric acid in the feed, indicating the inefficiency of DCT-02 transporter to export fumaric acid. The experimental total acid out-to-in ratios calculated for these cultivations were 2.61 ± 0.46 for succinic acid and 0.29 ± 0.09 for malic acid. For the CEN.PK 113-7D the extracellular concentrations of succinic and malic acid were lower and the out/in ratios were close to 0.01 for both the acids, hence the efficient export of dicarboxylic acids was lacking.

We compared the experimentally obtained out/in ratios with the calculated equilibrium ratios shown in table 2.3, to identify the thermodynamically feasible transport mechanism of these acids. From the obtained data we inferred that the export of these acids by DCT-02 transporter occurs most likely via uniport mechanism of the totally dissociated form or through a proton antiport mechanism of the mono-dissociated form, which are

thermodynamically equivalent. The data clearly indicates that DCT-02 transporter facilitates the export of malate and succinate, but not fumarate.

As the DCT-02 transporter could not export fumaric acid, we did not carry out the chemostat experiment with ADIS 244 in the presence of 120 mM of fumaric acid in the feed as done with CEN.PK 113-7D. The main reason for testing CEN.PK 113-7D with high fumaric acid concentration was to check the metabolic capacity of *S. cerevisiae* to process incoming fumaric acid and to check whether this high influx rate of fumaric acid would induce an export mechanism or not.

Table 2.3. Calculated equilibrium (out/in) ratios of total malate and succinate for different transport mechanisms and obtained experimental values for the ADIS 244 strain at a pH_{out} of 3.0.

Transported molecule (Ratio: out/in)	Symport	Uniport	Antiport	ABC transporter	ADIS244 (experimentally obtained ratios)
Mal²⁻	0.0044	4.34	4300	10^7	0.29 ± 0.09
HMal⁻	4.5E-06	0.0044	4.34	10^{10}	
Suc²⁻	0.07	69	68900	10^7	2.61 ± 0.46
HSuc⁻	7.2E-05	0.07	69	10^{10}	

* Equilibrium ratios were calculated assuming a cytosolic pH of 7.0 and a proton motive force of 180 mV

Discussion

Aerobic, glucose limited chemostat cultivations of *S. cerevisiae* in the presence of fumaric acid were carried out to study the uptake and possible metabolism of the acid under conditions expected for an industrial fermentation process, that is, at a high extracellular concentration of fumaric acid, low residual glucose concentration and low cultivation pH. The results of the experiments clearly showed that under these conditions fumaric acid was used as a carbon and energy source by *S. cerevisiae* with co-metabolism of glucose.

Metabolic flux analysis, combined with the measured intracellular levels of central carbon metabolites suggests that after entering the cytosol, fumaric acid was converted to PEP via malate and oxaloacetate using the gluconeogenic reaction PEP carboxykinase. This was clearly indicated by a significant decrease of the intracellular malate/fumarate and PEP/oxaloacetate ratios at increasing rates of fumarate metabolism, thus providing an increased thermodynamic driving force towards the gluconeogenesis pathway. The consequence of the increased rate of fumarate metabolism was an increased conversion of fumaric acid into PEP, resulting in a decreased conversion of glucose into PEP and thus a reduced glycolytic flux. The consumption of incoming fumaric acid, increased the flux through fumarase up to 39 mmol.Cmol⁻¹.h⁻¹ and above. Simultaneously the ratio of intracellular malate/fumarate decreased steeply from a value close to the apparent in-vivo equilibrium ratio of around 5.0 (55) to values between 1 and 2 (Figure 2.4). This indicates that in our experiments the fumarase reaction operated far from equilibrium. In another study done by Canelas *et al.* (2011) the fumarase flux was increased to a similar value of 45 mmol.Cmol⁻¹.h⁻¹ achieved by increasing the glucose uptake rate. However, they reported that the fumarase reaction remained close to equilibrium under these conditions. This strongly suggests that the kinetic capacity of fumarase in our experiments was much lower than observed by Canelas *et al.* (2011). A possible explanation could be that in our study the residual glucose level increased 9 fold from 0.10 mM to 0.85 mM (Supplementary, Table 2.S3), which may lead to repression of TCA cycle enzymes such as fumarase (62). However, in the experiments reported by Canelas *et al.* (2011) the residual glucose level was approximately 3mM, therefore the decrease of the capacity of fumarase by glucose repression is not likely. In our cultivations the intracellular fumaric acid level was 60 times higher than in the cultivations carried out by Canelas *et al.* (2011)(24 µmol/ g DCW compared to 0.40 µmol/ gDCW in their study) This high intracellular fumarate level in our experiments was a result of the continuous influx of fumaric acid by passive diffusion of the un-dissociated form. It has indeed been reported that fumarase is inhibited by high levels of fumarate (63) which could limit its capacity.

Up to an extracellular un-dissociated fumaric acid concentration of 10 mM, the biomass specific fumaric acid uptake rate increased linearly with its concentration, pointing towards passive diffusion of the lipophilic un-dissociated species into the cytosol. Within this range an increasing extracellular fumaric acid concentration did not result in additional ATP dissipation, as the specific oxygen uptake rate of the culture did not significantly increase (Figure 2.1E). These observations indicate that at moderate fumaric acid levels, genetically based changes in the properties of the plasma membrane and/or the cell wall, and/or induction of active export mechanisms, e.g. multidrug ABC exporters like *pdr12p*, did not occur.

At a significantly higher extracellular un-dissociated acid concentration of 29.4 mM, the measured uptake rate ($31.4 \text{ mmol.Cmol}^{-1}.\text{h}^{-1}$) was significantly lower than the uptake rate calculated from the estimated membrane permeability coefficient, i.e. $58 \text{ mmol.Cmol}^{-1}.\text{h}^{-1}$. At this high extracellular fumaric acid level, the biomass concentration was significantly lower than expected from the amount of carbon intake. Also the biomass specific oxygen uptake rate was significantly higher than calculated from the growth stoichiometry (Figure 2.1C and 2.1E), indicating an additional energy requirement at high extracellular concentrations of un-dissociated fumaric acid. Metabolic flux analysis indeed revealed that the maintenance ATP requirements was $93 \text{ mmol.Cmol}^{-1}.\text{h}^{-1}$ at extracellular un-dissociated fumaric acid concentration of 10 mM and $166 \text{ mmol ATP.Cmol}^{-1}.\text{h}^{-1}$ at an un-dissociated fumaric acid concentration of 29.4 mM. This increase could have been caused by the futile cycling of fumaric acid, resulting in extra ATP dissipating. With 120 mM of fumaric acid in the feed, assuming the futile cycling rate of fumaric acid of $26.6 \text{ mmol.Cmol}^{-1}.\text{h}^{-1}$ ($26.6+31.4=58 \text{ mmol.Cmol}^{-1}.\text{h}^{-1}$) as it would give the net uptake of fumaric acid to $58 \text{ mmol.Cmol}^{-1}.\text{h}^{-1}$ which is expected using the permeability coefficient. Extra ATP dissipation of $73 \text{ mmol.Cmol}^{-1}.\text{h}^{-1}$ was observed with 120 mM compared to 60 mM of fumaric acid in the feed, than it shows that the export of 1 mol of fumaric acid costs 2.75 mol of ATP (extra ATP dissipation of $73 \text{ mmol.Cmol}^{-1}.\text{h}^{-1}$ for the export of $26.6 \text{ mmol.Cmol}^{-1}.\text{h}^{-1}$ of fumaric acid).

It is known that the multidrug exporter *pdr12p* is induced in *S. cerevisiae* by weak monocarboxylic acids such as sorbate, benzoate and propionate and exports the anionic form (39, 56, 64). Furthermore, it has been reported that

an extracellular succinic acid concentration of 50 mM at a cultivation pH of 4.0 (65) and pH 4.5 (66), also results in induction of *pdr12p* in *S. cerevisiae*. It can therefore not be excluded that also high extracellular levels of fumaric acid could result in the induction of *pdr12p* or another export system. Considering the near neutral pH of the yeast cytosol such a transporter could either export the mono- and/or di-anionic species of fumaric acid. Depending on the exported species one or two protons have to be expelled by the plasma membrane proton ATPase as well. This implies that the ATP requirement for fumaric acid export would be 2 or 3 mol ATP per mol of fumaric acid exported, which agrees well with our observed value of 2.75 mol ATP/ mol of fumaric acid.

Information on the permeability of the plasma membrane for fumaric acid is relevant for the development of industrial scale fermentation processes. From the membrane permeability for the acid determined in this study, it can be calculated that the passive influx of un-dissociated fumaric acid could be as high as $4 \text{ mmol.gDCW}^{-1}.\text{h}^{-1}$ at saturating acid concentration and at a cultivation pH of 3.0. Futile cycling (passive influx and active export) of the acid would then result in an ATP dissipation rate of $12 \text{ mmol ATP.gDCW}^{-1}.\text{h}^{-1}$, if it is assumed that for each mol of fumaric acid exported 3 mol of ATP is required. In terms of glucose requirement this would be equivalent to a consumption rate of approximately $0.7 \text{ mmol glucose.gDCW}^{-1}.\text{h}^{-1}$. If this is compared with the published values of the maintenance coefficient of *S. cerevisiae* of $0.07 \text{ mmol glucose.gDCW}^{-1}.\text{h}^{-1}$ (67), futile cycling of fumaric acid at high extracellular levels and low pH could result in a tenfold increase in the maintenance energy requirements and consequently a significant reduction of the aerobic yield of fumaric acid on glucose in industrial fermentation processes for the production of this acid. It is therefore relevant to study the possibility to achieve lower membrane permeability through *in-vitro* evolution. Another, more costly alternative could be continuous removal of extracellular fumaric acid during the fermentation or carrying out the fermentation process at a higher pH.

Acknowledgements

The research project is financed by BE-Basic foundation. We thank Angela ten Pierick, Cor Ras, Patricia van Dam and Reza Maleki Seifar for analytical support. We would also like to thank Dr. Rene Verwaal and Dr. Sybe Hartmans from Royal DSM B. V (Delft, The Netherlands) for providing ADIS 244 strain and for helpful discussions.

Appendix 2.A. Calculation of the permeability coefficient of fumaric acid

For calculating the permeability coefficient, the biomass specific uptake rate of fumaric acid was plotted against the concentration of un-dissociated fumaric acid. The concentration of un-dissociated fumaric acid was calculated from the dissociation constants, corrected for the ionic strength of the medium, and the cultivation pH. The slope of the plot was calculated using weighted least squares regression (Figure 2.A1). The thus calculated permeability coefficients were $12.90 \pm 0.96 \times 10^{-9} \text{ m.s}^{-1}$ and $8.64 \pm 0.31 \times 10^{-9} \text{ m.s}^{-1}$ for the ADIS 244 and CEN.PK 113-7D strains respectively, whereby the membrane surface area was assumed to be $63.36 \text{ m}^2.\text{Cmol}^{-1}$ (68).

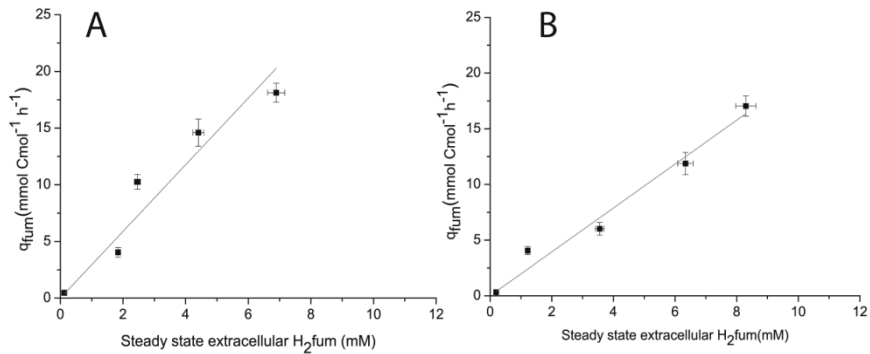
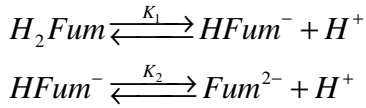


Figure 2.A1. Plots of the specific fumaric acid uptake rate, measured in steady state glucose limited chemostat cultivations, whereby fumaric acid was added to the feed media, against the concentration of un-dissociated fumaric acid. (a) ADIS 244 and (b) CEN.PK 113-7D strain

Appendix 2.B. Transport of dicarboxylic acids over the cell membrane

To understand the mechanism of the transport of dicarboxylic acids over the cell membrane, it is important to know which species of acid is being transported. Dicarboxylic acids attain a pH dependent equilibrium between the un-dissociated, mono-dissociated and totally dissociated species as shown in the following equations:



With dissociation constant $K_1 = [(HA^-)(H^+)/(H_2A)]$ and $K_2 = [(A^{2-})(H^+)/(HA^-)]$. Table 2.B1 shows the values of the dissociation constant for fumaric, malic and succinic acid.

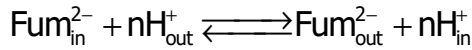
The dissociation constants of fumaric acid were corrected for the ionic strength of the media (Table 2.B2). The ionic strengths of the media increased at increasing fumaric acid concentration, due to the addition of increasing amounts of dipotassium fumarate. The correction was performed according to Alberty (69), using the Gibbs energies of formation of the different acid species of fumaric acid at standard conditions and the Debye-Hückel equation. The pK_1 and pK_2 values at standard conditions (25°C and zero ionic strength) are 3.09 and 4.6 respectively.

At a pH of 3.0 approximately half of the extracellular fumaric acid is present in the un-dissociated form (see Figure 2.B1). It has been reported that the cytosolic pH of *S. cerevisiae* varies between 6.8 to 7.5 depending on the environmental conditions (70). For this pH range fumaric, malic and succinic acid will almost exclusively be present in the fully dissociated form.

Experimental measurements of intracellular and extracellular acid concentrations yields the sum of the concentrations of the three species ($H_2A +$

$\text{HA}^- + \text{A}^{2-}$). Therefore transport mechanisms of dicarboxylic acids can only be deduced on the basis of the measured and calculated intracellular and extracellular total dicarboxylic acid in/out or out/in ratios. Therefore the equilibrium ratios were calculated for the total acids as shown in the equations below:

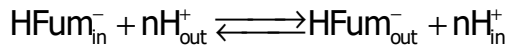
For the export of Fum^{2-} (totally dissociated species, Fum^{2-}):



$$\left(\frac{\text{TA}_o}{\text{TA}_i} \right)_{\text{eq}} = \left[\frac{10^{\text{pK}_1 + \text{pK}_2 - 2\text{pH}_o} + 10^{\text{pK}_2 - \text{pH}_o} + 1}{10^{\text{pK}_1 + \text{pK}_2 - 2\text{pH}_i} + 10^{\text{pK}_2 - \text{pH}_i} + 1} \right] \times 10^{2(\text{pH}_o - \text{pH}_i) + \frac{(n-2)(-pmf)F}{2.303RT}}$$

(eq.2.B.1)

For the export of HFum^- (mono-dissociated species, HFum^-):



$$\left(\frac{\text{TA}_o}{\text{TA}_i} \right)_{\text{eq}} = \left[\frac{10^{\text{pK}_1 - \text{pH}_o} + 10^{\text{pH}_o - \text{pK}_2} + 1}{10^{\text{pK}_1 - \text{pH}_i} + 10^{\text{pH}_i - \text{pK}_2} + 1} \right] \times 10^{(\text{pH}_o - \text{pH}_i) + \frac{(n-1)(-pmf)F}{2.303RT}} \quad (\text{eq.2.B.2})$$

Where pK_1 and pK_2 are the acid dissociation constants, pH_o and pH_i are extracellular and intracellular pH respectively, n is the number of protons transported ($n\text{H}^+$, $n=0$ for uniport, $n=-1$ for antiport, $n=1$ for symport), pmf is the proton motive force, TA_o and TA_i are the total acid concentration in the extracellular and intracellular spaces respectively, F is the faraday constant ($96.5 \text{ kJ.V}^{-1}.\text{mol}^{-1}$), R is the universal gas constant ($0.008314 \text{ kJ.K}^{-1}.\text{mol}^{-1}$) and T is the temperature (303.15 K) at which the experiment was done.

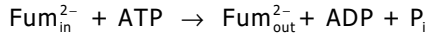
Table 2.B1. Dissociation constant values of fumaric, malic and succinic acid

	pK1	pK2	Source
Fumaric	3.09	4.60	(69)
Malic	3.40	5.11	(17)
Succinic	4.21	5.64	(71)

At pH 3.0, approximately half of the fumaric acid species is in un-dissociated form which is lipophilic and can diffuse through the cell membrane. Therefore assuming passive diffusion as the uptake mechanism, the theoretical thermodynamic equilibrium ratio can be calculated from the following equation:

$$\left(\frac{TA_o}{TA_i} \right)_{eq} = \left[\frac{10^{pH_o - pK_1 - pK_2} + 10^{pH_o - pK_1} + 1}{10^{pH_i - pK_1 - pK_2} + 10^{pH_i - pK_1} + 1} \right] \quad (\text{eq.2.B.3})$$

For the export of fumaric acid using an ABC transporter:



Equilibrium out/in ratio of total fumaric acid :

$$\log \left(\frac{TA_o}{TA_i} \right)_{eq} = \frac{\Delta G_{ATP}}{2.303RT} + \frac{Z F \psi}{2.303RT} \quad (\text{eq.2.B.4})$$

Where ΔG_{ATP} is the amount of Gibbs energy released (57 KJ), ψ is the intracellular potential at pH_{out} of 3.0 (0.015 V) and Z is charge of the species (-1 for HFum⁻ and -2 for Fum²⁻).

From eq 2.B.1, 2.B.2, 2.B.3 and 2.B.4 theoretical equilibrium ratios of total acid over the cell membrane were calculated for all the three species of dicarboxylic acids and the ratios were compared with the experimentally

obtained ratios to discuss the possible transport mechanism for a particular acid.

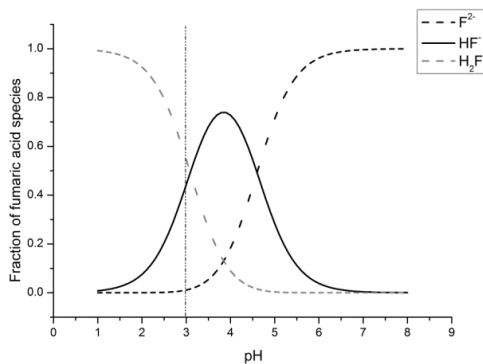


Figure 2.B1. Fraction of fumaric acid species at different pH

Table 2.B2. Dissociation constants of fumaric acid corrected for the ionic strength of the media.

Extracellular fumaric acid (mM)	pK1	pK2
1	2.98	4.40
10	2.98	4.40
20	2.98	4.40
40	2.97	4.37
60	2.93	4.30
120	2.87	4.17

Appendix 2.C. Washing efficiency of 100% methanol to remove extracellular fumaric acid

In order to accurately quantify the intracellular concentration of fumaric acid in the presence of a high extracellular concentration, cold filtration based washing was applied to remove all extracellular fumaric acid (see materials and methods). To check the efficiency of this procedure, broth samples were taken at different time points during steady state chemostat cultivation of the CEN.PK 113-7D strain at a pH of 3.0, of which the feed medium contained 60 mM of fumaric acid. Approximately 1.2 ml of sample was quenched in 6 ml of 100% methanol. The quenched sample was then rapidly poured onto a 0.45 μm (PES, Pall, USA) filter containing 40 ml of 100% methanol at -40°C . After removal of the liquid by vacuum filtration, the remaining cell cake was either washed once, twice or three times with 40 ml of 100% precooled methanol (-40°C) to verify how many washing steps would be required to completely remove the extracellular fumaric acid. From the results shown in Table 2.C1, Appendix 2.C it can be seen that two times washing with 40 mL 100% precooled methanol (-40°C) appeared to be sufficient to remove all extracellular fumaric acid, as the measured intracellular level did not decrease further after more additional washing steps. Also the measured intracellular malic acid level did not decrease. Even after further increasing the number of washing steps (up to 6 x 40 mL no significant decrease of fumaric and malic acid and other intracellular metabolites (e.g. glycolytic intermediates) was observed (results not shown) indicating that metabolite leakage was negligible.

Table 2.C1: Intracellular concentration of fumarate (Fum) and malate (Mal) in $\mu\text{mol/g}$ DCW with different amount of washing

Chemostat 1			Chemostat 2		
Washing with	Fumaric acid	Malic acid	Washing with	Fumaric acid	Malic acid
1 x 40 mL	41.12	14.34	1 x 40 mL	26.58	14.94
2 x 40 mL	11.90	13.02	2 x 40 mL	9.25	9.68
3 x 40 mL	14.68	5.11	3 x 40 mL	8.75	10.28
4 x 40 mL	10.24	15.42	4 x 40 mL	9.55	13.11

Supplementary material

Table 2.S1 Intracellular metabolite concentrations during the steady states with glucose limited chemostat cultivations with different concentrations of fumaric acid (FA) in the feed.

Metabolite ($\mu\text{mol/gDW}$)	0 mM FA		60 mM FA		0 mM FA		60 mM FA		120 mM FA	
	ADIS 244	ADIS 244	ADIS 244	CEN.PK 113-7D	CEN.PK 113-7D	CEN.PK 113-7D	CEN.PK 113-7D	CEN.PK 113-7D	CEN.PK 113-7D	CEN.PK 113-7D
G6P	6.22 ± 0.11	3.43 ± 0.41	8.73 ± 0.30	6.82 ± 0.10	3.65 ± 0.01					
F6P	1.73 ± 0.08	0.98 ± 0.11	2.38 ± 0.14	1.72 ± 0.01	0.90 ± 0.01					
DHAP	0.40 ± 0.13	0.30 ± 0.01	0.60 ± 0.04	0.46 ± 0.02	0.27 ± 0.01					
G3P	0.03 ± 0.01	0.06 ± 0.01	0.06 ± 0.01	0.08 ± 0.01	0.10 ± 0.00					
2PG	0.49 ± 0.02	0.38 ± 0.00	0.39 ± 0.01	0.69 ± 0.01	0.42 ± 0.01					
3PG	4.97 ± 0.03	3.53 ± 0.01	3.99 ± 0.11	6.84 ± 0.07	4.08 ± 0.05					
PEP	2.01 ± 0.28	1.54 ± 0.04	1.20 ± 0.05	2.52 ± 0.02	1.40 ± 0.00					
Pyruvate	1.09 ± 0.03	0.81 ± 0.01	0.66 ± 0.03	0.70 ± 0.02	1.35 ± 0.03					
Succinate	11.60 ± --	4.33 ± 0.38	0.82 ± 0.10	3.11 ± 0.59	7.41 ± 0.24					
Fumarate	0.48 ± 0.07	15.15 ± 1.83	0.49 ± 0.01	9.10 ± 0.37	24.01 ± --					
Malate	3.49 ± 0.95	9.74 ± 0.75	1.78 ± 0.10	13.23 ± 0.05	51.68 ± 0.74					
Oxaloacetate	0.02 ± 0.00	0.07 ± 0.00	0.004 ± 0.0	0.03 ± 0.002	0.15 ± 0.02					
AMP	0.25 ± 0.05	0.37 ± 0.02	N.M ± N.M	N.M ± N.M	N.M ± N.M					
ADP	0.40 ± 0.05	0.60 ± 0.03	N.M ± N.M	N.M ± N.M	N.M ± N.M					
ATP	11.02 ± 0.68	11.70 ± 0.04	N.M ± N.M	N.M ± N.M	N.M ± N.M					

Table 2.S2 Steady state biomass specific rates in the absence of fumaric acid

Rates ($\text{mmol} \cdot \text{Cmol}^{-1} \cdot \text{h}^{-1}$)	0 mM CEN.PK 113-7D		0 mM ADIS 244	
	Unbalanced	Balanced	Unbalanced	Balanced
Glucose	-27.93 ± 1.6	-28.92 ± 0.56	-28.48 ± 1.80	-29.05 ± 1.40
CO ₂	84.47 ± 4.5	86.95 ± 3.40	76.01 ± 4.40	77.06 ± 4.00
O ₂	-104.67 ± 20	-89.94 ± 3.60	-83.93 ± 20.00	-81.67 ± 5.20
Biomass	101.52 ± 1.1	101.53 ± 1.10	99.09 ± 2.20	99.13 ± 2.20
Fumarate	0.00 ± 0.0	0.00 ± 0.00	0 ± 0	0 ± 0
Succinate	0.02 ± 0.0	0.02 ± 0.0	3.71 ± 0.28	3.76 ± 0.27
Malate	0.01 ± 0.0	0.01 ± 0.0	0.33 ± 0.12	0.33 ± 0.13
Ethanol	-7.28 ± 0.41	-7.48 ± 0.31	-7.45 ± 0.46	-7.56 ± 0.42

Table 2.S3 Steady state residual glucose concentration in ADIS 244 and CEN.PK 113-7D strain at different concentration of fumaric acid in the feed (mM)

Fumaric acid step (mM)	ADIS 244 (mM)	CENPK 113-7D (mM)
0	0.10 ± 0.00	0.08 ± 0.00
1	0.08 ± 0.02	0.13 ± 0.02
10	0.07 ± 0.01	0.04 ± 0.00
20	0.07 ± 0.01	0.04 ± 0.00
40	0.04 ± 0.00	0.04 ± 0.00
60	0.05 ± 0.00	0.10 ± 0.01
120		0.84 ± 0.01

Chapter 3

Effect of pH on fumaric acid permeability, its uptake and futile cycling in *Saccharomyces cerevisiae*

Abstract

In this study we examined the uptake and metabolism of fumaric acid in *Saccharomyces cerevisiae*. The aim was to determine whether fumaric acid import occurred through the uptake of the un-dissociated (H_2F) or charged species (HF^- , F^{2-}). Therefore *S. cerevisiae* was cultivated in glucose limited chemostats with fumaric acid as a co-substrate in the feed, under aerobic conditions and at a dilution rate of 0.10 h^{-1} with either ammonium or urea as nitrogen source. Steady states were achieved in the pH range of 3.0 to 6.0, to obtain different fractions of fumaric acid species. Our results suggest that *S. cerevisiae* is able to import only un-dissociated fumaric acid (H_2F) by diffusion over the membrane. The permeability of the *S. cerevisiae* membrane for the un-dissociated form of fumaric acid decreased from $(3.50 \pm 0.99) \times 10^{-8} \text{ m/s}$ at pH 4.0 and 4.5 to $(0.89 \pm 0.13) \times 10^{-8} \text{ m/s}$ at pH 3.0, which has also been observed in other microorganisms exposed to weak organic acids. The H_2F which diffuses into the cytosol was metabolized together with glucose. Metabolic flux analysis was applied to evaluate the occurrence of additional ATP dissipation due to H^+ and/or H_2F futile cycling. At pH 3.0 futile cycling occurred due to diffusive proton influx (with an estimated H^+ permeability of $2.71 \times 10^{-7} \text{ m s}^{-1}$) and subsequent export by H^+ -ATPase. Futile cycling of H_2F did not occur because the observed ATP dissipation at pH 3.0 was not influenced by the absence or presence of 20 mM of extracellular fumaric acid, which shows that for futile cycling the required active fumarate exporter was absent in these experiments. It can be anticipated from our results that in the presence of the necessary active export mechanism for fumaric acid, proton and fumaric acid futile cycling will lead to a lower product yield and higher O_2 consumption in the aerobic fumaric acid production process at pH 3.0.

Introduction

Sustainable production of industrially relevant chemicals, e.g. dicarboxylic acids, through fermentation has recently gained interest in order to eventually replace the current chemical production from fossils. The yeast *Saccharomyces cerevisiae* has the potential to synthesize dicarboxylic acids including fumaric acid (FA) through a sustainable route using renewable feedstocks (72). FA has main applications in the development of biodegradable polymers and as a food additive (42). Production of FA on industrial scale is preferred at low pH ($\text{pH} < \text{pK}$) as it cuts down the titrant and downstream processing costs. Another advantage of *S. cerevisiae* is that it tolerates acidic conditions and grows well at pH 3.0. Recently, there have been some reports describing the engineering of the metabolic pathway of *S. cerevisiae* for the production of FA at pH 5.0 or higher (30–32). However, no attention has been given to the mechanism of the transport of FA in *S. cerevisiae*. Previously we studied FA uptake and metabolism in *S. cerevisiae* in a carbon limited chemostat cultures on mixtures of glucose and FA at pH of 3.0 (± 0.05) where approximately 55% of the extracellular FA is present in the un-dissociated form (H_2F) which is lipophilic and thus can diffuse through the plasma membrane. We observed that *S. cerevisiae* consumed FA as a carbon and energy source together with glucose. The possible uptake mechanism of FA at pH 3.0 could be either active or facilitated transport of the charged species (F^{2-} and/or HF^-) or diffusion of the lipophilic non charged H_2F species. In this previous study we could not satisfactorily determine the transported species. The purpose of this work was to determine whether fumaric acid import occurred through the uptake of the un-dissociated (H_2F) or charged species (HF^- , F^{2-}). The cytosolic pH is near neutral, so if FA enters through passive diffusion of the un-dissociated acid it dissociates into the totally dissociated species (F^{2-}) whereby 2 protons are released.

If the imported FA is metabolized these protons are consumed (Figure 3.1) which leads to H^+ balanced metabolism. If, on the other hand, the mono- (HF^-) or totally dissociated (F^{2-}) species is imported, e.g. through a uniport mechanism, the metabolism of the acid requires the import of protons as well. However, no proton uptake mechanism has been reported in *S. cerevisiae*.

The choice of the nitrogen source can indirectly influence the availability of the protons in the cytosol. The metabolism of ammonium releases one proton per ammonium ion in the cytoplasm (73) which could be used for the metabolism of the charged species of fumaric acid. Mono- and totally dissociated species of fumaric acid can then be metabolized with the coupled uptake of 1 or 2 mol of ammonium ions respectively (Figure 3.1). Roos *et al.* (74) also observed that the metabolism of tartrate anions was coupled to the uptake of ammonium ions in *Penicillium cyclopium*. If urea is used as N-source instead of ammonia there will be no release of protons in the cytoplasm (75) (73). In case only the charged species of FA is imported it cannot be metabolized due to the lack of cytosolic protons (Figure 3.1). At the used dilution rate of 0.10 h^{-1} the ammonium consumption rate is approximately $16 \text{ mmol Cmol}^{-1} \text{ h}^{-1}$. This results in a proton production rate of $16 \text{ mmol H}^+ \text{ Cmol}^{-1} \text{ h}^{-1}$ which would allow a maximum rate of fumaric acid metabolism of $16 \text{ mmol Cmol}^{-1} \text{ h}^{-1}$ if HF^- is the imported species and $8 \text{ mmol Cmol}^{-1} \text{ h}^{-1}$ if F^{2-} is the imported species. Therefore comparing the uptake and metabolism of FA with ammonium and urea as nitrogen source can give insight into the transported species (H_2F , HF^- or F^{2-}). The change in pH will change the fraction of the 3 species of FA (Figure 3.2A) and its effect on fumarate uptake rate will yield additional information about the transported species.

Therefore we carried out well controlled aerobic, glucose limited, chemostat cultivations at different pH (3.0 to 6.0) with 60 mM of FA in the feed, using two different N-sources, ammonium and urea. The uptake and metabolism of FA was quantified from measurements of the biomass concentration, the FA concentration in the effluent, and the rates of oxygen consumption and carbon dioxide production under the different conditions applied (pH and N-source).

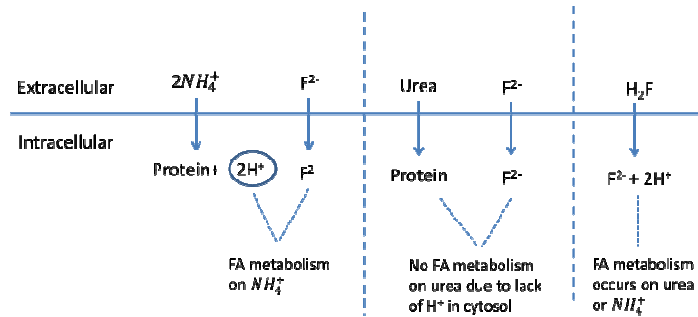


Figure 3.1. Schematic representation of the possible dependency of metabolism of totally dissociated (F^{2-}) and un-dissociated (H_2F) form of fumaric acid (FA) on the available nitrogen source (ammonium or urea).

Materials and methods

Strain and pre-culture growth conditions

Saccharomyces cerevisiae CEN PK 113-7D was used for this study. The pre-culture was grown in 250 ml Erlenmeyer flasks with 100 ml of defined medium containing: 20 g l⁻¹ glucose.H₂O, 5 g l⁻¹ (NH₄)₂SO₄, 3 g l⁻¹ KH₂PO₄, 0.5 g l⁻¹ MgSO₄.7H₂O, 1ml l⁻¹ trace elements solution and 1ml l⁻¹ vitamin solution as described by Verduyn *et al.* (46). The pre-culture medium was filter sterilised using PVDF membrane filters with 0.20 µm pore size (Millipore, Massachusetts, USA). Pre-cultures were incubated at 30°C on a gyratory shaker at 200 rpm.

Chemostat cultivation

Chemostat cultivation was carried out under aerobic conditions in a 2L bioreactor (Applikon, The Netherlands) with a working volume of 1L. The bioreactor was inoculated with 100 ml of overnight grown pre-culture. Chemostat cultivations were carried out on minimal media with composition: 8.25 g l⁻¹ Glucose.H₂O, 0.3 g l⁻¹ (NH₄)₂SO₄, 5.0 g l⁻¹ NH₄H₂PO₄, 0.3 g l⁻¹ KH₂PO₄, 0.5 g l⁻¹ MgSO₄.7H₂O, and 1ml l⁻¹ trace elements solution, 1ml l⁻¹ vitamin solution as described by Canelas *et al.* (45). Also 0.50 g l⁻¹ of ethanol was added to the feed medium to prevent oscillations. To achieve a final concentration of 60 mM of FA in the feed media, a combination of 40 mM

(4.64 g L⁻¹) of fumaric acid and 20 mM (3.84 g L⁻¹) of dipotassium fumarate was added. The medium was filter sterilized using Sartopore 150 filters (Sartorius, Goettingen, Germany) into a previously heat sterilized vessel (20 min at 121 °C) containing an amount of basildon antifoam (KCC Basildon, UK) such that its final concentration in the medium was 100 mg/L. The chemostat cultivation was carried out at a dilution rate of 0.10 h⁻¹, at 30 °C, with a stirrer speed of 800 rpm and at an initial pH of 3.0. The pH was controlled by adding 2M KOH and 2M H₂SO₄ using a Biostat Bplus controller (Sartorius BBI Systems, Melsungen, Germany). Air was sparged at a flow rate of 0.30 vvm using a mass flow controller (Brooks 5850 TR, Hatfield, PA, USA) and an overpressure of 0.30 Bar was maintained. The CO₂ and O₂ concentrations in the exhaust gas were monitored through a combined paramagnetic/infrared offgas analyzer (NGA 2000, Rosemount, USA). MCF5/win 2.1 software (Sartorius BBI Systems, Melsungen, Germany) was used for data acquisition. A steady state was considered to be achieved when stable off gas CO₂ and O₂ readings were obtained.

Steady states were achieved with either urea or ammonium as nitrogen source. The nitrogen content of both the ammonium and the urea containing feed media was the same (47 mM N). The composition of the medium containing urea as nitrogen source was 8.25 gL⁻¹ Glucose.H₂O, 1.44 gL⁻¹ urea, 6.2 gL⁻¹ KH₂PO₄, 1.05 gL⁻¹ MgSO₄.7H₂O, 1mL⁻¹ trace mineral solution, 1mL⁻¹ vitamin solution, 0.5 gL⁻¹ ethanol, 60 mM of fumaric acid and 100 mg L⁻¹ of basildon antifoam. The sequence of steady states obtained is outlined in detail in the next section.

Experimental set-up

As the aim of the experiment was to differentiate between the uptakes of un-dissociated or charged species of fumaric acid in *S. cerevisiae*, we used urea or NH₄⁺ as N-source (see Figure 3.1 for explanation). Moreover we studied the uptake of FA over a range of cultivation pH from 3.0 to 6.0 in order to achieve different concentrations of un-dissociated (H₂Fum), mono-dissociated (Hfum⁻) and totally dissociated (Fum²⁻) species of FA in the extracellular environment as shown in Figure 3.2a.

Figure 3.2B shows the sequence of steady states achieved with ammonium or urea as nitrogen source at different cultivation pH. Steady state no. 0 was obtained without fumaric acid in the feed, afterwards the other steady states (1 to 11) were achieved with 60 mM of fumaric acid in the feed medium. Steady states 1 to 4 were obtained after stepwise increase in the extracellular pH from 3.0 (pH < pK) to 6.0 (pH > pK) using ammonium as the sole nitrogen source. During this stepwise pH increase the dominant species changed from H₂F to F²⁻. Thereafter, the chemostat was switched to a feed medium containing urea as nitrogen source and steady states 5 to 9 were obtained after stepwise decrease in the extracellular pH from 6.0 to 3.0 (Figure 3.2B). The last two steady states 10 and 11 were again achieved with ammonium as nitrogen source at a cultivation pH of 3.0 and 4.5 respectively. The biomass specific rates obtained at steady states 1 and 10, which were carried out under identical conditions were compared in order to check whether adaptation of the CEN.PK 113-7D strain had occurred during the 350 hours of chemostat cultivation, which is a phenomenon which has been described previously (76).

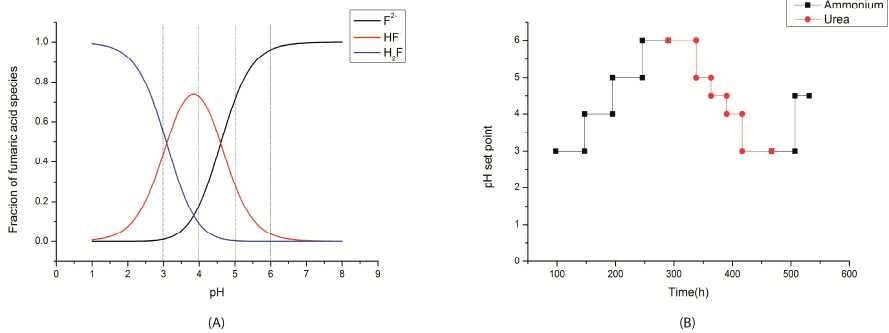


Figure 3.2 (A) Fractions of different species of fumaric acid at different pH (B) Time profile of the 12 steady states obtained at different extracellular pH using either urea (●) or ammonium (■) as the nitrogen source. Steady state no. 0 was achieved without fumaric acid in the feed, and steady states from 1 to 11 were achieved with 60 mM of fumaric acid in the feed.

Measurement of extracellular metabolites

Extracellular metabolites were measured during the steady states using the cold broth filtration method as described by Mashego *et al.* (49). This method allows accurate determination of the residual glucose and other extracellular metabolites. For measuring extracellular fumaric acid, the broth sample was directly filtered through a syringe filter instead of using the cold filtration method in order to avoid FA crystallisation which is facilitated at low temperature.

Concentrations of ethanol, glucose, acetate and glycerol were quantified through HPLC analysis using a Bio-Rad HPX-87H 300 column (7.8 mm). The column was eluted with phosphoric acid (1.5 mM in Milli-Q water) at a flow rate of 0.6 ml min⁻¹. The injection volume was 10 µl and the autosampler temperature was 15°C. The detection was accomplished by a refractometer (Waters 2414) and a UV detector (Waters 484; 210 nm). Succinate, malate and fumarate were also quantified with HPLC, using a Bio-Rad HPX-87H 300 column (7.8 mm). The column was eluted with phosphoric acid (45 mM in milli Q water). The higher phosphoric acid concentration was needed to obtain a better separation of succinate and fumarate.

Intracellular metabolite measurements

A rapid sampling setup as described by Lange *et al.* (47) was used for broth sampling. Approximately 1.2 g of broth sample was withdrawn into 6 mL of quenching solution (100% methanol at -40°C) and was immediately mixed and weighed. The quenched sample was then filtered through a 0.45 µm filter (PES, Pall, USA). The filter cake was washed twice with 40 ml of 100% methanol stored at -40°C (whereby aliquots of 40 ml methanol were kept in 50ml falcon tubes) in order to remove extracellular metabolites and media components (77). After washing, the filter containing the cell cake was immersed in 30 ml of 75% preheated ethanol (75°C) in a 50 ml falcon tube, and at the same time 120 µl of 13C labelled internal standard solution was added. Thereafter the tube was placed in a 95°C water bath for 3 min and then stored at -80°C until further processing. Subsequently the samples were evaporated to dryness using a Rapid-vap (Labconco, USA) (48), and the residue was re-dissolved in

600 μl of milli-Q water and centrifuged twice at 10000g for 5 min to remove cell debris. The obtained cell extracts were stored at -80°C until metabolites were quantified with GC-MS and LC-MS. In all the steady states the supernatant contained high concentrations of FA which can compromise the quantification of the intracellular FA. Therefore additional washing experiments were performed where the number of washing steps was increased from 2 to 4 (Appendix 3.A).

Ammonium measurement assay

Broth samples were taken from the chemostat and filtered through $0.45\ \mu\text{m}$ syringe filters (PES, Pall, USA) to remove biomass. Ammonium was quantified in the supernatant using the enzymatic kit (R-Biopharm, Roche) based on glutamate dehydrogenase reaction which requires NADH as a cofactor. We measured the conversion of NADH to NAD by following the decrease in adsorption at 340 nm which was directly related to the ammonium concentration in the samples. Ammonium concentration as low as $4\ \text{mg L}^{-1}$ (0.23 mM) can be measured accurately using this enzymatic assay.

Data reconciliation

The biomass specific rates in the chemostat were calculated from the steady state broth balances of glucose, ethanol, malic, fumaric, succinic acid, biomass and the gas phase balances for CO_2 and O_2 leading to “unbalanced” rates. The unbalanced rates were reconciled following the approach described by Verheijen (50), which used elemental conservation and the least square method to obtain better estimates of the “unbalanced rates”, leading to the “balanced” biomass specific rates and reduced errors. Balanced means that the rates agree with the conservation constraints (C, H, O, N, charge balances).

Flux analysis

Steady state intracellular fluxes were calculated using the stoichiometric model as described by Lapujade *et al.* (51). In this model the uptake mechanism of ammonium was via uniport mechanism (78, 79) and the uptake of urea was via diffusion (75) as reported in the literature. For the hydrolysis of

urea, the reactions included in the stoichiometric model are urea carboxylase and allophanate hydrolase which together uses 1 mol of urea and 1 mol of ATP to produce 2 mol of ammonium ions and 1 mol of CO₂. In the model it was assumed that the extracellular FA entered by passive diffusion into the cytoplasm and is metabolised via fumarase and malate dehydrogenase to form oxaloacetate which is converted to PEP through PEP carboxykinase. This route was incorporated based on the results obtained by Shah *et al.* (80).

Results

General observations

Saccharomyces cerevisiae was grown in an aerobic glucose limited chemostat at a dilution rate of 0.10 h⁻¹ at different cultivation pH and with either ammonium or urea as nitrogen source. Figure 3.2B shows the sequence in which the steady states were obtained in the chemostat experiment. Steady states no. 1 and 10 are duplicates, achieved at pH 3.0 using ammonium as nitrogen source, to check if there was evolution of the culture during the cultivation period of more than 500 hours. In glucose limited chemostat cultivations a strong decrease in the residual glucose concentration, due to an increase of the affinity of the glucose transport system, is one of the indicators of evolution in the culture (76). This was, however, not observed in our cultivations, as the residual glucose concentration was 0.18 mM and 0.17 mM respectively, for steady states 1 and 10 (Supplementary material, Table 3.1S). Also the yields of biomass, CO₂ production and O₂ consumption per mol of glucose consumed were not significantly different (Supplementary material, Table 3.4S), indicating absence of evolution.

When urea is used as nitrogen source there is a possibility of extracellular urea hydrolysis to ammonium ions. Therefore we measured the extracellular ammonium concentration in the steady states achieved with urea as nitrogen source. We observed that the extracellular ammonium was below the sensitivity of the enzymatic assay used (< 0.23 mM). In the ammonium cultures, the residual ammonium concentration was always higher than 24 mM.

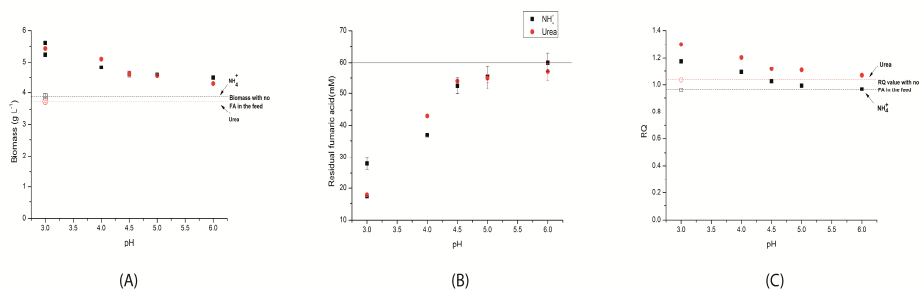


Figure 3.3 Results of the chemostat steady states obtained at different pH with either ammonium or urea as nitrogen source [ammonium (■), urea (●) and with 60 mM of FA in the chemostat feed. Open symbols and dashed lines (---, for NH₄⁺ and ---, for urea) represents the data obtained without FA in the feed] (A) Biomass concentration (B) Residual FA concentration and (C) Respiratory quotient.

Effect of the cultivation pH and nitrogen source on fumaric acid uptake

In all the steady states, the residual glucose concentration (Supplementary material, Table 3.3S) remained very low, so nearly all the glucose was always consumed. Initially the steady state at pH 3.0 (SS:0) was obtained without FA in the feed. Thereafter, the feed medium was replaced with a otherwise identical medium containing 60 mM of FA. This feed replacement at pH 3.0 resulted in a significant increase in the steady state biomass concentration (Figure 3.3A), indicating that the supplied FA was used as carbon source, which was also observed previously (80). The subsequent stepwise increase of the cultivation pH from 3 to 6 resulted in a decrease of the steady state biomass concentration (Figure 3.3A). After reaching a steady state at pH 6 the feed medium of the chemostat was replaced by a medium containing urea as sole nitrogen source which was otherwise identical to the previous medium. After reaching a steady state at pH 6 the cultivation pH was stepwise decreased to 3, resulting in an increase of the biomass concentration due to increased FA consumption (Figure 3.3B). The relation between the steady state biomass concentration and the cultivation pH was the same irrespective of the nitrogen source used: with decreasing pH the biomass concentration increased. This increased biomass concentration correlated directly with the decrease in the residual FA concentration and therefore an increase in FA consumption (Figure

3.3B). Because there was no significant secretion of FA derived metabolites (malate, OAA), FA was fully metabolized into biomass, which was also reflected in an increased respiratory quotient (RQ) (Figure 3.3C) which was expected because FA is more oxidized (per carbon) than glucose. With urea as nitrogen source, the RQ was higher compared to ammonium as nitrogen source, because the metabolism of 1 mol of urea releases 2 mol of ammonia and 1 mol of CO₂. The obtained results (Figure 3.3) clearly indicate that *S. cerevisiae* can use FA as carbon and energy source for growth and that the FA uptake rate is strongly dependent on the cultivation pH.

Furthermore the results obtained with urea and ammonium as nitrogen source were very similar, which shows that the uptake rate of FA was not dependent on the availability of protons released in the cytosol as a result of the metabolism of ammonium ions. This indicates that most probably only the H₂F species was taken up and metabolized, rather than HF⁻ or F²⁻ species.

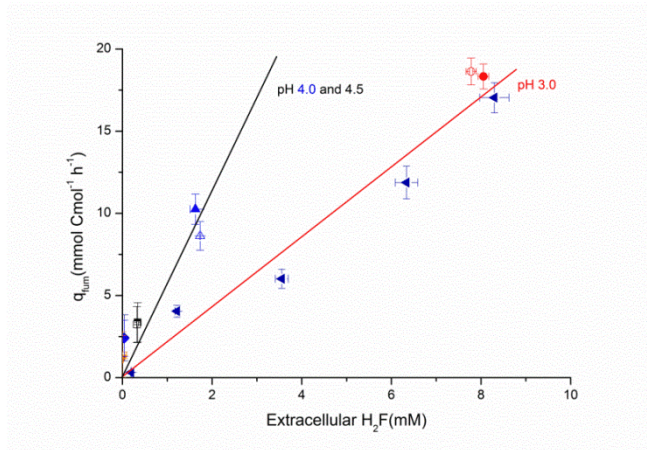


Figure 3.4. Biomass specific FA uptake rates during the steady states at different extracellular concentration of un-dissociated FA (H₂F) obtained by changing extracellular pH. (●: pH 3.0, ▲: pH 4.0, ■: pH 4.5, ◆: pH 5.0, ▼: pH 6.0). Open and closed symbols are for urea and ammonium as nitrogen source respectively; ◀: Data points obtained in a previous study done at pH 3.0 with different concentrations of FA in the feed (80)).

Kinetics of fumaric acid uptake

As shown above, the uptake rate of fumaric acid (FA) was strongly dependent on the cultivation pH and thus on the extracellular concentration of the lipophilic, fully undissociated species H_2F . From the relation between the biomass specific FA uptake and the concentration of the un-dissociated species the FA permeability coefficient can be calculated using the following equation:

$$q_{H_2F} = k \frac{6V_x}{d_x} C_{H_2F_{ex}} \quad (1)$$

wherein q_{H_2F} is the biomass specific uptake rate (Figure 3.4) of the un-dissociated FA in $mmol\ Cmol^{-1}\ s^{-1}$, k is the permeability coefficient in $m\ s^{-1}$, $C_{H_2F_{ex}}$ is the extracellular concentration of un-dissociated FA in $mmol\ m^{-3}$, V_x is the cell volume in $m^3\ Cmol^{-1}$ ($52.8 \times 10^{-6}\ m^3\ Cmol^{-1}$, (58)) and d_x is the cell diameter in m ($5 \times 10^{-6}\ m$, (58)).

From a plot of the biomass specific FA uptake rate against the concentration of un-dissociated acid (Figure 3.4) it can be seen that the FA permeability decreases at decreasing pH. We therefore calculated separate permeability coefficients for cultivation pH 4.0, 4.5, and pH 3.

The calculated permeability coefficients were $(0.89 \pm 0.13) \times 10^{-8}\ m\ s^{-1}$ for pH 3.0 and $(3.50 \pm 0.99) \times 10^{-8}\ m\ s^{-1}$ for pH 4.0 and 4.5. The permeability coefficients for pH 5.0 and 6.0 could not be calculated. Due to a negligible difference between the FA concentrations in inflow and outflow of the chemostat no reliable values of the FA uptake rate could be obtained. In previous study done at pH 3.0, the q_{fum} was also found to depend on the concentration of extracellular H_2F (80). These results are also shown in Figure 3.4 and completely agree with the results obtained in this experiment.

Futile cycling

In the production processes of organic acids at low pH, energy loss due to futile cycling of H^+ or un-dissociated weak organic acids is an important aspect to consider. In aerobic processes this leads to increased biomass specific oxygen uptake rate (q_{O_2}) and lower yields of biomass and/or product. Figure 3.5 shows the q_{O_2} values as a function of increasing biomass specific FA uptake rate q_{fum} (attained at increasing extracellular H_2F concentration) for both the ammonium and urea cultures. At pH 6.0 to 4.0 when mostly dissociated FA is present in high extracellular concentrations (between 40 to 60 mM, Figure 3.3B) the organism does not show an increased q_{O_2} . This shows that futile cycling of FA does not occur at pH 6.0 to 4.0. However, at pH 3.0 both the urea and the ammonium culture show a significantly increased O_2 consumption rate (Figure 3.5). The question is whether this increased q_{O_2} at low pH is due to the futile cycling of un-dissociated FA (H_2F) and/or futile cycling of H^+ . As can be seen from Figure 3.5 the cultures at pH 3.0 without the presence of FA in the feed ($q_{fum}=0$) have a nearly identical high q_{O_2} . This clearly shows that the increased q_{O_2} is due to H^+ cycling and not due to FA cycling. From the additional oxygen consumption rate of about $25 \text{ mmol Cmol}^{-1} \text{ h}^{-1}$, observed for both nitrogen sources (Figure 3.5), we can calculate a H^+ cycling rate of $62 \text{ mmol Cmol}^{-1} \text{ h}^{-1}$ (assuming P/O ratio of 1.23 and plasma membrane H^+ /ATPase stoichiometry of 1). Using equation 1, the permeability coefficient for proton influx of the *S. cerevisiae* cell membrane at pH 3.0 was estimated to be $2.71 \times 10^{-7} \text{ m s}^{-1}$.

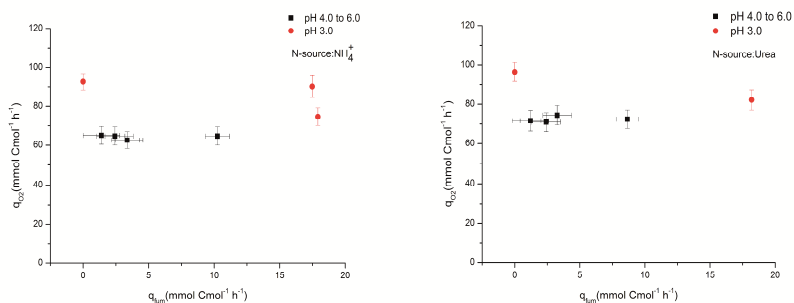


Figure 3.5. Steady state biomass specific oxygen uptake rate (q_{O_2}) observed at pH 4.0, 4.5, 5.0 and 6.0 (■) and at pH 3.0 (●) with NH_4^+ (Left side) and urea as nitrogen source (Right side) against the steady state biomass specific FA uptake rate (q_{fum})

Energy metabolism and N-source

Figure 3.5 shows that, irrespective of the FA uptake rate (pH 6.0 to 4.0 data), the specific oxygen consumption rate, q_{O_2} for the urea cultures was approximately $7 \text{ mmol O}_2 \text{ Cmol}^{-1} \text{ h}^{-1}$ higher than for the ammonium culture. This difference corresponds with the lower biomass yield for the urea cultures (Figure 3.3A). This result shows that the urea culture consumes more energy for biomass synthesis than the NH_4^+ culture.

Impact of FA metabolism on fluxes and metabolites levels

It is expected that changing fluxes relates to changes in intracellular metabolite levels (Supplementary material, Table 3.2S). The fluxes in central metabolism were calculated using the reconciled uptake and secretion rates (Supplementary material, Table 3.1S) as input for the metabolic network model. From the fluxes it was observed that the pentose phosphate pathway (PPP) flux (Data not shown) did not change, which is explained by the constant growth rate of 0.10 h^{-1} for all the steady states. The glycolytic flux decreased significantly at increasing FA uptake, leading to gluconeogenesis. The TCA cycle flux changed very little because q_{O_2} hardly changed (for pH 6.0 to 4.0). The flux through the pathway from FA to PEP strongly increased with the increased uptake of FA.

The metabolite levels were related to the flux changes at increased FA metabolism as follows:

-The levels of the upper glycolytic metabolites decreased while the levels of the lower glycolytic (oxidative part) metabolites increased, which is the expected response to a lower glycolytic flux (55).

-The metabolites in the oxidative part of the TCA cycle (citrate to succinate) did not change significantly from pH 6.0 to 4.0, which is in agreement with the absence of changes in the TCA cycle flux

-The major change (2 to 10 fold) occurs in the C4 metabolites (fumarate, malate, aspartate and oxaloacetate). This is due to FA uptake, which steeply increases the intracellular fumarate concentration and the concentration of the connected metabolites malate, aspartate and oxaloacetate. Apparently this high concentration is needed to provide the driving force for the gluconeogenesis pathway for fumarate (80).

It should be noted that the intracellular fumarate concentration could not be measured reliably at pH 4.0 and higher, even when an increased number of washing steps were applied (see Appendix 3.A). In contrast to this at pH 3.0, two washing steps appeared to be sufficient to remove the extracellular FA. The reason is probably that at pH 4.0 and higher, nearly all the FA is present in the anionic salt form, of which the solubility in cold methanol is poor which might result in precipitation as fumarate salt on the cold biomass filter cake.

From the flux and metabolite data we can make $Q(v)$ plots for near equilibrium reactions (55). In such a plot the mass action ratio (calculated from the metabolites measurement) is plotted against the reaction flux. For near equilibrium reactions the relationship is found to be linear (55) with the intercept on Y-axis representing the equilibrium ratio. Figure 3.6 shows the plot for the first step of fumarate metabolism which is the reversible fumarase reaction. The flux through the fumarase reaction almost doubles with the uptake of FA, which leads to a decrease in mass action ratio and therewith the thermodynamic driving force increases. From the plot an equilibrium constant

of 7.67 was estimated with ammonium as nitrogen source using the data points obtained at pH 3.0, which is significantly higher than the equilibrium ratio of 5.2 obtained by Canelas *et al.* (55) at a cultivation pH of 5.0. The calculated maximum flux through fumarase was approximately 50 $\text{mmol Cmol}^{-1} \text{h}^{-1}$ (Figure 6).

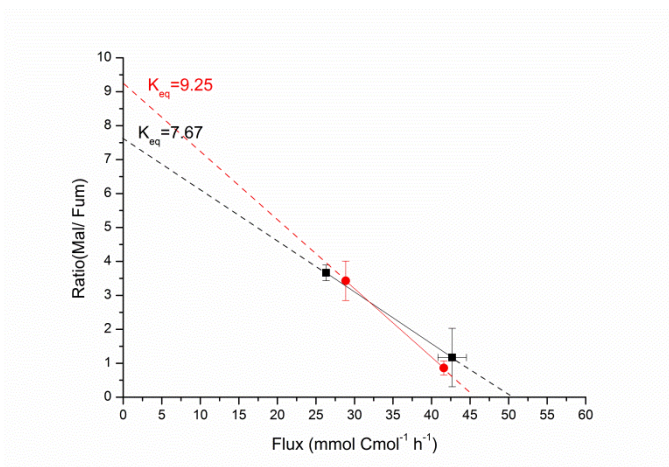


Figure 3.6 Mass action ratios (malate/fumarate) plotted against the fluxes through the fumarase reaction at pH 3.0 with ammonia (■) and urea (●) as nitrogen source. Dashed line (—, for NH_4^+ and - - -, for urea) intercept on Y-axis represents the equilibrium ratio and on the X-axis represents the maximum flux through the fumarase reaction.

For other reversible reactions (PGI, TPI, ENO and PGM) similar Q (v) plots were constructed (Appendix 3.B). The mass action ratios do not depend significantly on the fluxes, showing near equilibrium conditions. However the estimated equilibrium constants are 20-50% higher than in the study done by Canelas *et al.* (55).

Discussion

In this study an experimental design (chemostat cultivation in the presence of FA, using either ammonium or urea as nitrogen source which leads to different proton supply in the cytosol, Fig 1) was used to be able to discriminate between the FA species (H_2F , FA^- and F^{2-}) transported over the cell membrane. In addition the extracellular concentrations of these species were varied by controlling the cultivation pH at values between 6.0 and 3.0. The results show

that the absence of a cytosolic H^+ supply (in case of the urea cultivation) has no effect on the rate of FA uptake and metabolism. Moreover, there appeared to be a unique relation between the concentration of un-dissociated FA (H_2F) and the FA uptake rate. Both findings indicate that FA is imported by passive diffusion of the un-dissociated species (H_2F). This conclusion is further supported by comparing the FA uptake rate obtained in a previous study (80) where the FA supply varied at constant pH of 3.0, by changing the FA content of the chemostat feed medium. Figure 3.4 shows the corresponding biomass specific FA uptake (q_{fum}) data obtained at pH 3.0. The obtained linear relation between FA uptake and the concentration of un-dissociated FA confirms that this species passes the cell membrane through passive diffusion. The calculated H_2F permeability was found to decrease at decreasing pH (Figure 3.4, increased slope of pH 4.0 and 4.5). This is a well-known response of microorganisms to weak organic acid stress, where the membrane lipid composition is changed to decrease the acid permeability. Decrease in permeability with decreasing pH has also been reported for other organic acids, e.g. for succinic acid in *Hansenula anomala* yeast (81), malic acid in *Candida sphaerica* (82) and lactic acid in *Saccharomyces cerevisiae* (83).

The cultures carried out at pH 3.0 showed extra energy loss as observed by an increased oxygen consumption rate (q_{O_2}). This appears to be due to the futile cycling of H^+ . From the ATP balance a H^+ permeability parameter of $2.71 \times 10^{-7} \text{ m s}^{-1}$, was calculated, which is not so far from the reported value of $60 \times 10^{-7} \text{ m s}^{-1}$ for artificial liposomes (84). Moreover our value agrees very well with a previous reported value of $2.8 \times 10^{-7} \text{ m s}^{-1}$ for the same *S. cerevisiae* strain under aerobic, glucose limited conditions (25).

In a future production process of FA at pH 3.0, which must be carried out under aerobic conditions to ensure sufficient ATP generation (38), an active FA exporter is required which effectively exports the organic acid against a steep concentration gradient. Together with the observed rate of passive diffusion of H_2F into the cells this will result in a futile cycle of passive H_2F diffusion and its active export. Assuming that the fermentation process operates above the FA solubility (which facilitates downstream processing) it can be calculated (Appendix 3.C) that to supply the ATP dissipated in such a futile cycle an additional biomass specific glucose consumption rate of $6.8 \text{ mmol Cmol}^{-1} \text{ h}^{-1}$ is

required (Appendix 3.C). Furthermore an additional amount of energy is dissipated due to proton futile cycling at pH 3.0, which hardly occurs at pH 4.0 to 6.0. For H^+ futile cycling an extra oxygen consumption of $23 \text{ mmol Cmol}^{-1} \text{ h}^{-1}$ was measured at pH 3.0 and this extra oxygen consumption requires an extra catabolism of $3.8 \text{ mmol Cmol}^{-1} \text{ h}^{-1}$ of glucose. This leads in a FA fermentation process (pH 3.0, FA crystals), to an additional rate of $\sim 10.6 \text{ mmol Cmol}^{-1} \text{ h}^{-1}$ glucose ($\sim 3.8 + 6.8 \text{ mmol Cmol}^{-1} \text{ h}^{-1}$) of glucose consumption which must be aerobically catabolized, leading to a futile oxygen demand of $63.6 \text{ mmol O}_2 \text{ Cmol}^{-1} \text{ h}^{-1}$. This will seriously compromise the yield and productivity of FA production in a low pH aerobic FA process (Figure 3.7). These findings therefore show that it is relevant to evolve microorganisms that have a much lower proton and FA permeability. Figure 3.7 also shows that to minimize the contribution of futile cycling the engineered strain must have FA productivity above $200 \text{ mmol Cmol}^{-1} \text{ h}^{-1}$ FA.

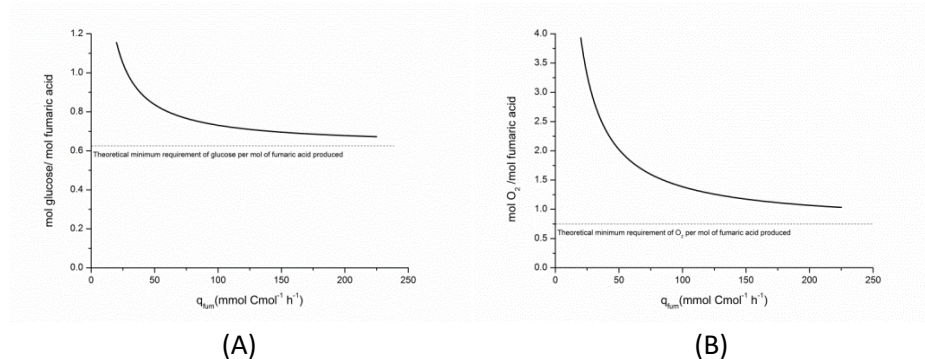


Figure 3.7. Effect of futile cycling of H_2F and H^+ (pH 3.0, 60 mM of extracellular FA)(A) Mol of glucose required per mol of fumaric acid produced plotted against the biomass specific fumaric acid production rate ($\text{mmol Cmol}^{-1} \text{ h}^{-1}$) (B) Mol of O_2 required per mol of fumaric acid produced against the biomass specific fumaric acid production rate ($\text{mmol Cmol}^{-1} \text{ h}^{-1}$). Dashed line (---) represents the theoretical minimum requirement of glucose and O_2 per mol of fumaric acid produced.

In our experiment at pH 3.0 there was no evidence of FA futile cycling, showing that a fumarate exporter was not expressed under these conditions. This is in stark contrast to our previous experiment at pH 3.0 (80) where extra ATP dissipation was observed due to FA futile cycling. In this experiment a higher FA uptake rate was achieved, by addition of 120 mM of FA to the chemostat

feed medium, leading to a much higher intracellular FA concentration of 24 $\mu\text{mol gDCW}^{-1}$ compared to 10 to 13 $\mu\text{mol gDCW}^{-1}$ in the present study. This suggests that a fumarate concentration close to 24 $\mu\text{mol gDCW}^{-1}$ induces a fumarate exporter. Given the situation that fumarate export has shown to be a major bottleneck, this observation offers a future opportunity to identify the much desired fumarate exporter.

Intracellular fluxes and metabolite concentrations significantly changed due to the co-metabolism of FA. The metabolism of FA (fluxes and intracellular metabolites levels) changed in a predictable way. As expected, the most significant changes (2-10 fold increase) occurred in the concentrations of FA linked C4 metabolites (malate, aspartate and oxaloacetate) which are apparently needed to create the driving force for FA based gluconeogenesis.

An unexpected and unexplained phenomenon is that, while in theory the uptake and assimilation of urea requires less ATP compared to ammonia, the cultures with urea as nitrogen consumed more ATP compared to the ammonia cultures. These observations agree with a recent study (85) where the expected ATP advantage by switching from NH_4^+ to urea as N-source was not observed.

Appendix 3.A. Influence of the extracellular fumaric acid on its intracellular measurements

Intracellular metabolites were measured during the steady states obtained at different pH and with high extracellular concentration of fumaric acid. During the experiment we observed that increasing the cultivation pH leads to a significant drop in fumaric acid uptake rate and unexpectedly it also did lead to increase in the intracellular concentration of fumarate (Table 3.2). This high intracellular concentration of fumarate could be due to the presence of high extracellular amounts of fumaric acid.

Therefore in order to check the influence of extracellular fumaric acid on its intracellular measurement we washed the intracellular sample with 1 to 4 of washing steps using methanol tubes (each tube containing 40 ml of 100% methanol stored at -40°C) as shown in Figure 3.A1. The concentration of other intracellular metabolites (data not shown) did not drop with increasing number of washing steps indicating no leakage of metabolites. We noticed that at pH 3.0 two to three washing steps were sufficient to remove extracellular fumaric acid. However, at pH higher than 3.0, the intracellular fumarate measured decreased gradually with increasing number of washing steps and never reached a steady value. This might be due to the low solubility of fumaric acid salts formed at higher pH in 100% methanol compared to the high solubility of un-dissociated fumaric acid at pH 3.0. There has been no study on the solubility of FA in methanol, but FA solubility has been studied in ethanol, where it was observed that ethanol has high solubility for fumaric acid while it has significantly reduced solubility for its sodium salts (86), which might also be the case with methanol. Therefore the intracellular fumaric acid measured at pH higher than 3.0 is likely to be influenced by the presence of extracellular FA. These data (pH 4.0 and higher) are therefore not reported.

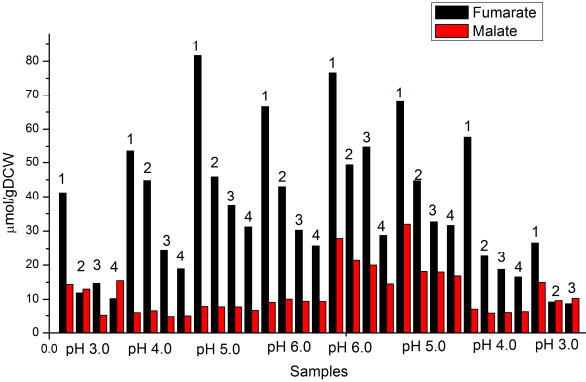


Figure 3.A1: Intracellular concentration of fumarate and malate with different number of washing steps (1,2,3 and 4) and at different pH (3.0, 4.0, 5.0 and 6.0)

Appendix 3.B. Equilibrium ratios of some of the reactions in the central carbon metabolism.

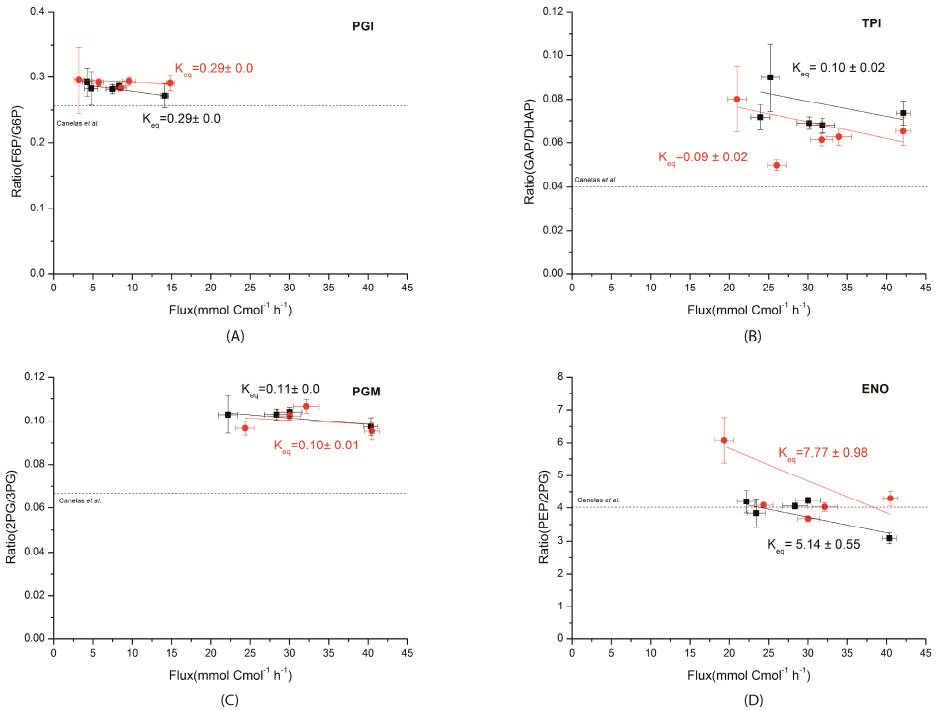


Figure 3.B1 Mass action ratios plotted against the intracellular fluxes obtained during the steady states with glucose limited chemostat using ammonium (■) and urea (●) as nitrogen source at pH of 3.0, 4.0, 5.0 and 6.0. A: PGI (B) TPI (C) PGM and (D) ENO. Dashed line (---) represents the equilibrium ratio obtained by Canelas *et al.* (55)

Appendix 3.C. Impact of H⁺ and FA futile cycling at low pH on FA production process

An industrial scale production process of FA will operate at its solubility limit (~ 60 mM FA) using the microorganism which can efficiently export FA. At low pH of 3.0, we can expect an extracellular concentration of upto 30 mM of undissociated FA (Figure 3.2A) which can passively diffuse into the cytoplasm. Using the permeability coefficient values calculated in this experiment, this amounts to the futile cycling rate of approximately 55 mmol FA Cmol⁻¹ h⁻¹, which requires an extra 110 mmol ATP Cmol⁻¹ h⁻¹ to export these protons (the influx of proton equals 55*2= 110 mmol H⁺ Cmol⁻¹ h⁻¹). In aerobic conditions, assuming that the catabolism of 1 mol of glucose produces 16 mol of ATP (87), then approximately 6.8 mmol Cmol⁻¹ h⁻¹ of glucose will be completely catabolised by the futile cycling of FA.

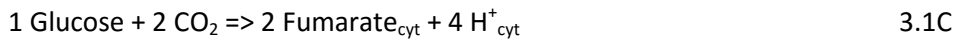
We also observed H⁺ cycling rate of 62 mmol Cmol⁻¹ h⁻¹ at pH 3.0 which requires additional 3.8 mmol Cmol⁻¹ h⁻¹ of glucose catabolism. Therefore approximately 10.6 mmol Cmol⁻¹ h⁻¹ (combining 6.8 and 3.8 mmol Cmol⁻¹ h⁻¹) of glucose will be aerobically catabolized to generate extra ATP required for the futile cycling of FA and H⁺. This leads to the consumption of 63.6 mmol Cmol⁻¹ h⁻¹ of oxygen (1 mol of glucose catabolism requires 6 mol of O₂). With the maximum oxygen uptake rate of 230 mmol Cmol⁻¹ h⁻¹ (88) observed in *S. cerevisiae*, almost 27% of the oxygen uptake will be used in the futile cycling of FA and protons, which is significant. This leaves 166.4 mmol Cmol⁻¹ h⁻¹ as a maximum O₂ rate utilised for fumarate production. The maximum FA production rate possible is 222 mmol Cmol⁻¹ h⁻¹ (222= 166.4/0.75; with 0.75 mol O₂ required per mol of FA produced, see reaction in eq. 3C) which requires the glucose uptake rate of 149.3 mmol Cmol⁻¹ h⁻¹ (138.7 mmol glucose Cmol⁻¹ h⁻¹ using 0.625 mol glucose required per mol of FA produced (eq. 3C) and additional 10.6 mmol Cmol⁻¹ h⁻¹ of glucose uptake for futile cycling). Note that we have neglected biomass formation. The yield of FA on glucose taking into account the futile cycling is 1.49 mol FA /mol gluc (222/ 149.3), where the yield in the absence of futile cycling is 1.60 mol FA /mol glucose. However, the maximum C4- acid production rate observed is about 20 mmol Cmol⁻¹ h⁻¹ which is 10 fold lower than the previous assumed rate. At this lower production rate the glucose uptake rate for fumarate production equals 12.5 mmol Cmol⁻¹ h⁻¹

($20 \times 0.625 \text{ mmol Cmol}^{-1} \text{ h}^{-1}$). Including H^+ and FA futile cycling this leads to a total glucose uptake rate of $23.1 \text{ mmol Cmol}^{-1} \text{ h}^{-1}$ ($12.5 \text{ mmol Cmol}^{-1} \text{ h}^{-1} + 10.6 \text{ mmol Cmol}^{-1} \text{ h}^{-1}$ catabolized for futile cycling), leading to a yield of 0.86 mol FA per mol glucose which is far lower than 1.60 mol FA /mol glucose in the absence of ATP dissipation due to H^+ and FA cycling. Figure 3.7 shows the relationship between the biomass specific FA production rate and the utilization of glucose and O_2 per mol of FA produced. It clearly shows that the yield of FA will be severely affected at the lower production rates (between ~ 20 to $75 \text{ mmol Cmol}^{-1} \text{ h}^{-1}$) and will asymptotically reach theoretical maximum (eq. 3C) with increasing production rates.

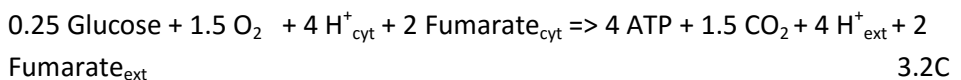
Therefore the selection of microorganisms with low permeability towards FA and proton will significantly improve the production process of FA at low pH.

Stoichiometry of aerobic FA production

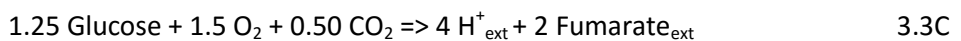
Stoichiometry of the FA production from ATP neutral reductive route of TCA cycle:



We assume the transport mechanism of fumarate via uniport and H^+ export by H^+ -ATPase. The required 4 ATP for H^+ export come from glucose catabolism (assuming generation of 16 ATP per mol of glucose consumed):



Overall stoichiometry of fumarate production:



From stoichiometry the minimal theoretical consumption of glucose and oxygen is 0.625 mol gluc / mol fumarate and 0.75 mol O_2 /mol fumarate taking into account the energy required to export FA via uniport mechanism and H^+

via H^+ -ATPase. The theoretical maximal yields are 1.60 mol FA/mol glucose and 1.33 mol FA per mol O_2 consumption.

Supplementary material

Table 3.1S. Biomass specific rates ($\text{mmol}\cdot\text{Cmol}^{-1}\cdot\text{h}^{-1}$) for CEN.PK 113-7D strain during the steady state at extracellular pH with ammonium (SS 1-4; SS 10-11) and urea (SS 5-9) as nitrogen source.

q-rates (mmol/C mol h)	pH 3.0 (0 mM fumaric acid in feed) (*SS:0)			pH 3.0 (with 60 mM fumaric acid in feed)(SS:1)			pH 4.0 (with 60 mM fumaric acid in feed)(SS:2)			pH 5.0 (with 60 mM fumaric acid in feed)(SS:3)						
	Unbalanced Value	Error	Balanced Value	Unbalanced Value	Error	Balanced Value	Unbalanced Value	Error	Balanced Value	Unbalanced Value	Error	Balanced Value				
qGlucose	-29.95	1.80	-30.41	0.80	-22.31	1.40	-22.44	1.10	-23.68	1.40	-21.96	1.00	-24.98	1.50	-25.15	1.40
qCO ₂	88.18	5.00	89.14	3.90	105.55	6.00	106.09	5.30	77.64	4.40	73.68	3.70	65.01	3.70	65.45	3.40
qO ₂	-96.55	20.00	-92.63	4.20	-93.09	16.00	-90.16	5.60	-76.82	17.00	-64.74	4.30	-71.87	17.00	-64.72	4.70
μ	106.32	2.40	106.35	2.40	106.53	2.40	106.54	2.40	105.16	2.40	105.00	2.30	107.05	2.40	107.07	2.40
qFumaric	0.00	0.00	0.00	0.00	-17.23	2.10	-17.48	0.92	-12.94	1.90	-9.96	0.92	-2.05	2.90	-2.43	1.40
qSuccinic	0.56	0.04	0.57	0.04	0.67	0.05	0.68	0.05	0.49	0.04	0.46	0.03	0.00	0.00	0.00	0.00
qMalic	0.09	0.01	0.10	0.01	0.16	0.01	0.16	0.01	0.08	0.01	0.07	0.01	0.00	0.00	0.00	0.00
qEthanol	-7.83	0.48	-7.92	0.36	-5.84	0.36	-5.87	0.31	-6.19	0.38	-5.83	0.31	-6.55	0.40	-6.58	0.37

*SS: Steady states as shown in Figure 3.2B

q-rates (mmol/C mol h)	pH 6.0 (with 60 mM fumaric acid in feed)(SS:4)			pH 3.0 (with 60 mM fumaric acid in feed)(SS:9)			pH 4.0 (with 60 mM fumaric acid in feed)(SS:8)			pH 4.5 (with 60 mM fumaric acid in feed)(SS:7)						
	Unbalanced		Balanced	Unbalanced		Balanced	Unbalanced		Balanced	Unbalanced		Balanced				
	Value	Error	Value	Error	Value	Error	Value	Error	Value	Error	Value	Error				
qGlucose	-25.19	1.50	-26.06	1.40	-19.44	1.20	-19.47	0.88	-21.59	1.30	-22.48	1.00	-24.75	1.50	-25.96	1.20
qCO ₂	62.36	3.50	63.91	3.30	105.92	6.00	106.32	5.20	84.58	4.80	86.97	4.30	80.70	4.60	83.33	4.10
qO ₂	-69.22	18.00	-65.10	4.60	-89.32	15.00	-82.19	5.20	-73.61	16.00	-72.40	4.70	-75.84	17.00	-74.44	4.90
mu	108.21	2.40	108.28	2.40	97.47	2.20	97.47	2.20	100.32	2.20	100.42	2.20	105.05	2.30	105.17	2.30
qFumaric	1.08	2.70	-1.39	1.40	-18.22	1.70	-18.19	0.80	-7.31	1.50	-8.65	0.87	-1.51	1.70	-3.26	1.10
qSuccinic	0.00	0.00	0.00	0.00	0.62	0.05	0.62	0.04	0.00	0.00	0.00	0.00	0.00	0.00	0.00	0.00
qMalic	0.57	0.04	0.58	0.04	0.10	0.01	0.10	0.01	0.05	0.00	0.05	0.00	0.00	0.00	0.00	0.00
qEthanol	-6.72	0.41	-6.90	0.38	-5.09	0.31	-5.10	0.26	-5.64	0.34	-5.82	0.30	-6.49	0.40	-6.72	0.36

q-rates (mmol/Cmol h)	pH 5.0 (with 60 mM fumaric acid in feed)(SS:6)				pH 6.0 (with 60 mM fumaric acid in feed)(SS:5)			
	Unbalanced		Balanced		Unbalanced		Balanced	
	Value	Error	Value	Error	Value	Error	Value	Error
qGlucose	-24.69	1.50	-25.65	1.30	-26.31	1.60	-26.98	1.40
qCO ₂	76.85	4.40	78.88	4.00	76.33	4.30	77.63	4.10
qO ₂	-72.70	18.00	-70.89	4.80	-72.88	18.00	-71.62	5.20
Mu	104.21	2.30	104.30	2.30	106.95	2.40	107.01	2.40
qFumaric	-0.84	1.90	-2.42	1.10	0.66	2.60	-1.21	1.40
qSuccinic	0.00	0.00	0.00	0.00	0.00	0.00	0.00	0.00
qMalic	0.00	0.00	0.00	0.00	0.66	0.08	0.67	0.08
qEthanol	-6.49	0.40	-6.67	0.36	-6.99	0.43	-7.13	0.40

		pH 3.0 (with 60 mM fumaric acid in feed)(SS:10)		pH 4.5 (with 60 mM fumaric acid in feed) (SS:11)					
		Unbalanced	Balanced	Unbalanced	Balanced				
(mmol/Cmol h)		Error	Error	Error	Error				
qGlucose		-18.23	1.10	-17.86	0.80	-22.82	1.40	-22.79	1.20
qCO ₂		92.95	5.30	91.72	4.40	64.41	3.70	64.46	3.30
qO ₂		-79.36	14.00	-74.71	4.50	-69.18	18.00	-62.65	4.30
mu		93.68	2.10	93.63	2.10	97.68	2.20	97.68	2.20
qFumaric		-18.67	1.70	-17.91	0.75	-3.56	2.20	-3.36	1.20
qSuccinic		0.56	0.04	0.55	0.04	0.00	0.00	0.00	0.00
qMalic		0.16	0.01	0.16	0.01	0.00	0.00	0.00	0.00
qEthanol		-4.77	0.29	-4.70	0.24	-5.98	0.36	-5.97	0.33

Table 3.2S Steady state intracellular concentrations of central carbon metabolites (in $\mu\text{mol/g DCW}$).

pH	3.0		4.0		5.0		6.0		6.0		4.0		3.0					
	Fum conc. (mM)	0 (SS:0)	60 (SS:1)	60 (SS:2)	60 (SS:3)	60 (SS:4)	60 (SS:5)	60 (SS:6)	60 (SS:8)	60 (SS:9)	Urea	Error	Urea	Error				
Nitrogen source	NH_4^+	Error	NH_4^+	Error	NH_4^+	Error	NH_4^+	Error	NH_4^+	Error	Urea	Error	Urea	Error				
G6P	8.73	0.30	7.03	0.42	6.62	0.31	5.86	0.10	5.04	0.06	4.90	0.02	5.77	0.02	0.06	0.06	4.63	0.44
F6P	2.38	0.14	1.99	0.13	1.94	0.11	1.65	0.03	1.44	0.02	1.44	0.01	1.64	0.02	1.69	0.02	1.38	0.15
6PG	0.56	0.01	0.90	0.02	0.86	0.04	0.93	0.02	1.31	0.03	1.20	0.03	0.91	0.01	0.79	0.03		
FBP	0.98	0.04	0.42	0.00	0.35	0.02	0.36	0.01	0.39	0.00	0.41	0.01	0.48	0.00	0.29	0.05		
GAP	0.04	0.00	0.04	0.00	0.03	0.00	0.03	0.00	0.03	0.00	0.03	0.00	0.03	0.00	0.02	0.00	0.03	0.00
G3P	0.06	0.01	0.06	0.01	0.08	0.01	0.10	0.01	0.15	0.01	0.13	0.02	0.10	0.01	0.06	0.01		
DHAP	0.60	0.04	0.42	0.07	0.48	0.03	0.43	0.01	0.45	0.00	0.42	0.02	0.46	0.01	0.47	0.02	0.43	0.05
3PG	3.99	0.11	5.77	0.32	8.26	0.51	7.84	0.15	7.44	0.10	6.80	0.15	7.31	0.06	7.40	0.22	4.17	0.24
2PG	0.39	0.01	0.59	0.04	0.85	0.05	0.81	0.01	0.77	0.01	0.72	0.01	0.75	0.01	0.71	0.01	0.43	0.04
PEP	1.20	0.05	2.27	0.20	3.57	0.22	3.27	0.05	3.27	0.06	2.92	0.07	2.75	0.04	2.92	0.03	2.76	0.18
Pyr	0.66	0.03	1.18	0.12	1.80	0.08	1.50	0.03	1.61	0.03	1.43	0.04	1.49	0.03	1.44	0.02	1.32	0.11
Cit	7.04	0.14	8.57	0.37	9.72	0.73	11.13	0.28	8.96	0.20	10.42	0.30	11.08	0.08	9.24	0.16	9.49	0.76
iso-Cit	0.17	0.00	0.12	0.01	0.31	0.04	0.55	0.02	0.41	0.01	0.49	0.02	0.52	0.01	0.31	0.01	0.13	0.02
α -KG	0.51	0.05	0.85	0.19	1.23	0.09	1.16	0.08	1.29	0.04	1.44	0.05	1.26	0.02	1.21	0.03	1.20	0.14
Succinate	0.82	0.10	2.39	0.60	1.27	0.06	0.96	0.09	1.12	0.04	1.20	0.09	1.23	0.13	1.66	0.02		
Fum	0.49	0.01	40.24 *	1.99	19.99 *	0.06	31.29 *	0.09	25.75 *	0.04	28.76 *	0.04	31.57 *	0.13	46.54 *	0.02	13.08	1.74
Mal	1.78	0.10	11.97	2.34	5.48	0.39	7.32	0.26	9.51	0.20	20.93	2.75	21.23	3.59	6.15	0.25	14.95	1.89
Asp	6.45	0.43	12.77	2.21	21.10	1.27	16.95	0.53	19.27	0.26	23.15	0.77	23.87	0.65	24.95	0.46	13.85	2.45
Oxa	0.00	0.00	0.10	0.01	0.10	0.02	0.15	0.03	0.11	0.05	0.16	0.04	0.14	0.02	0.08	0.01	0.09	0.02

*Intracellular fumarate values obtained at pH 4.0 and higher might be influenced by the presence of extracellular FA and are not reliable

Table 3.3S. Extracellular concentrations (mM) of secreted metabolites during the 12 steady states

Steady state no.	pH	N-source	Residual glucose	Error	Acetate	Error	Succinate	Error	Malate	Error
0*	3	NH4	0.10	0.01	0.10	0.04	1.55	0.10	0.13	0.01
1	3	NH4	0.18	0.00	0.28	0.01	2.51	0.11	0.30	0.01
2	4	NH4	0.09	0.00	0.87	0.01	1.69	0.08	0.13	0.01
3	5	NH4	0.20	0.04	0.87	0.02	N.D		N.D	
4	6	NH4	0.90	0.01	0.91	0.03	N.D		0.89	0.04
5	3	Urea	0.17	0.01	0.13	0.00	2.63	0.13	0.22	0.01
6	4	Urea	0.07	0.00	0.72	0.39	N.D		N.D	
7	4.5	Urea	0.20	0.01	1.05	0.01	N.D		N.D	
8	5	Urea	0.27	0.03	1.04	0.05	N.D		N.D	
9	6	Urea	0.79	0.05	1.00	0.04	N.D		1.00	0.11
10	3	NH4	0.17	0.01	N.D		2.54	0.13	0.37	0.02
11	4.5	NH4	0.15	0.01	N.D		N.D		N.D	

*Steady state obtained without FA in the feed.

Table 3.4S. Yields obtained at steady state 1 and 10 to check for evolution (in mmol /mmol glucose)

	SS:1		SS:10	
	Yield	Error	Yield	Error
Biomass	4.75	0.26	5.24	0.26
O2	4.02	0.32	4.18	0.31
CO2	4.73	0.33	5.14	0.34

Chapter 4

**Metabolic response of engineered C4- acids
producing *Saccharomyces cerevisiae* in high
CO₂ environments**

Abstract

In this study an engineered *Saccharomyces cerevisiae* strain overexpressing the cytosolic reductive part of the TCA cycle towards fumarate and a heterologous dicarboxylic acid transporter in the plasma membrane, was studied for its ability to produce fumarate, at pH of 3.0.

The engineered *S. cerevisiae* strain was cultivated in a glucose limited chemostat at a dilution rate of 0.10 h^{-1} , with a controlled pH of 3.0, under aerobic conditions. During the chemostat cultivation, the CO_2 concentration in the inlet gas was increased from the concentration in the air to 25% and 50% in order to increase the thermodynamic driving force towards the reductive branch of the TCA cycle and thereby to increase the secretion rate of fumaric acid. Surprisingly the strain designed for fumaric acid production produced mainly succinate and small amounts of fumarate (100 fold lower) and malate (10 fold lower).

At high CO_2 concentrations, the biomass specific succinic acid production rate increased from $2.3 \text{ mmol.Cmol}^{-1}.\text{h}^{-1}(\text{Air})$ to $18.7 \text{ mmol.Cmol}^{-1}.\text{h}^{-1}$ (at 50% CO_2). This succinate production was unexpected because no fumarate reductase activity was observed and fumarate was the end product of the reductive part of the TCA cycle in the cytosol. It appeared that the succinate production is caused by the combined cytosolic reductive and the mitochondrial (mit) oxidative part of the TCA cycle, with exchange of cytosolic (cyt) fumarate produced from the reductive part and the mitochondrial succinate produced from fumarate via the oxidative part. This mit/cyt exchange restricts the maximal q_{suc} in this engineered *S. cerevisiae* to $25 \text{ mmol succinate.Cmol}^{-1}.\text{h}^{-1}$ at near zero growth rate. A stoichiometry of 1.4 mol C4 acids (malate and succinate) per mol of glucose consumed was observed at a dilution rate of 0.10 h^{-1} . Futile cycling of succinic was observed and its membrane permeability coefficient was estimated on the basis of unaccounted ATP dissipation. Finally it was found that the succinic acid production rate increases with the intracellular concentration of HCO_3^- . The measured out/in ratios of succinate points towards its export by using the uniport mechanism.

Introduction

Dicarboxylic acids such as succinic, malic and fumaric acid, have applications in the food and polymer industry (89). The current process of dicarboxylic acids production involves their derivatization from hydrocarbons obtained from crude oil. To evade crude oil dependency, there is a keen interest to produce these dicarboxylic acids from renewable substrates using fermentation.

Rhizopus delemar (formerly known as *R. oryzae* (90)) is a natural producer of fumaric acid, its production is attributed to the higher affinity of fumarase enzyme towards malate rather than fumarate and also to the cytosolic route of fumaric acid formation in this organism (8–10). *R. delemar* can achieve a fumaric acid yield of up to 1.21 mol/mol glucose in aerobic batch cultures at a neutral pH (91). Apart from the metabolic pathway, efficient export of the acid from the cells is also a crucial step to achieve high yield and productivity of fumaric acid, however, until now no transport systems specific for the export of fumaric acid have been identified in *R. delemar* or in another organism. A disadvantage of using *Rhizopus spp.* in large scale industrial fermentation processes is its morphology, and its tendency to form large clumps, hampering the transfer of substrate and oxygen to the organism. In contrast, for *S. cerevisiae* we have the knowledge on its physiology and tools to genetically engineer this organism, it has unicellular morphology and its ability to grow at low pH facilitates the downstream processing of acids and reduces the production of waste salts (72). This study focusses on chemostat experiments with a *S. cerevisiae* strain engineered with the intention to produce fumaric acid.

Fumaric acid is an intermediate of the TCA cycle, which can be synthesized via the reductive and the oxidative branch of the TCA cycle. Synthesis via the reductive branch, that is via pyruvate carboxylase, malate dehydrogenase and fumarase, gives the theoretical yield (2 mol fumaric acid/mol glucose), but this route is ATP neutral. Therefore the production of fumaric acid in *S. cerevisiae* under anaerobic conditions solely via the reductive route is not feasible (38). Overexpression of the enzymes of the reductive TCA cycle branch has been done to improve the production of malic (17), fumaric (29) and succinic acid (24) under aerobic conditions. Taking into account the requirement of

additional ATP for fumaric acid export (especially at low cultivation pH) and cell maintenance (38), production of fumaric acid is feasible with the combination of flux through the oxidative and reductive branch of TCA cycle under aerobic conditions.

In aerobic conditions, the diversion of the carbon flux to the reductive route of the TCA cycle (Figure 4.1) can be enhanced by increasing the concentration of CO₂ in inlet gas, as CO₂ and bicarbonate are the substrates for PEP carboxykinase and pyruvate carboxylase reactions, both of which produce oxaloacetate which is further converted to fumarate. The improvement in dicarboxylic acids production in the presence of calcium carbonate in the media has been reported (7, 18, 92), which might be due to higher concentration of CO₂. In this study we aerobically cultivated an engineered *S. cerevisiae* (overexpressing the reductive TCA cycle enzymes to fumaric acid and a heterologous dicarboxylate transporter) at different concentrations of CO₂ supplied in the inlet gas. We also used previous results on the effect of increased CO₂ concentration on succinate production in chemostat experiment with another strain where the reductive pathway ends at succinate. We studied the stoichiometry and the kinetics of C4 acids formation as a function of the CO₂ concentration, along with the transport mechanism and kinetics of DCT-02 transporter.

Materials and methods

Strains used in this study: Suc 501 and Suc 958 strain

Saccharomyces cerevisiae strain Suc 501 is a succinic acid producer engineered to increase the capacity of the reductive part of the TCA cycle by overexpressing in the cytosol PEP carboxykinase (PCKa) from *Actinobacillus succinogenes*, pyruvate carboxylase (PYC2) from *Saccharomyces cerevisiae*, malate dehydrogenase (MDH3) from *Saccharomyces cerevisiae*, fumarase (FUMR) from *Rhizopus oryzae*, fumarate reductase from *Trypanosoma brucei* (FRDS) and a dicarboxylic acid transporter (DCT-02) from *Aspergillus niger* (see Figure 4.1B). Constitutive promoter of GPD (Glyceraldehyde 3-phosphate dehydrogenase) was used for the overexpression of all the genes. Furthermore

the alcohol dehydrogenase gene *ADH1* was deleted to reduce alcohol formation.

Strain Suc 958, intended to produce fumaric acid, was derived from Suc 501 strain by deleting the heterologous fumarate reductase gene. The homologous fumarate reductase gene is still present in Suc 958 but is expected to be non-functional under aerobic conditions (93)(94). Figure 4.1A shows the modifications done in the Suc 958 strain with FA as the end product of the reductive TCA route. The construction of the Suc 958 and Suc 501 strains is similar to what is described in the patent by DSM IP ASSETS B.V. (28). The genotypes of both strains are shown in Table 4.1.

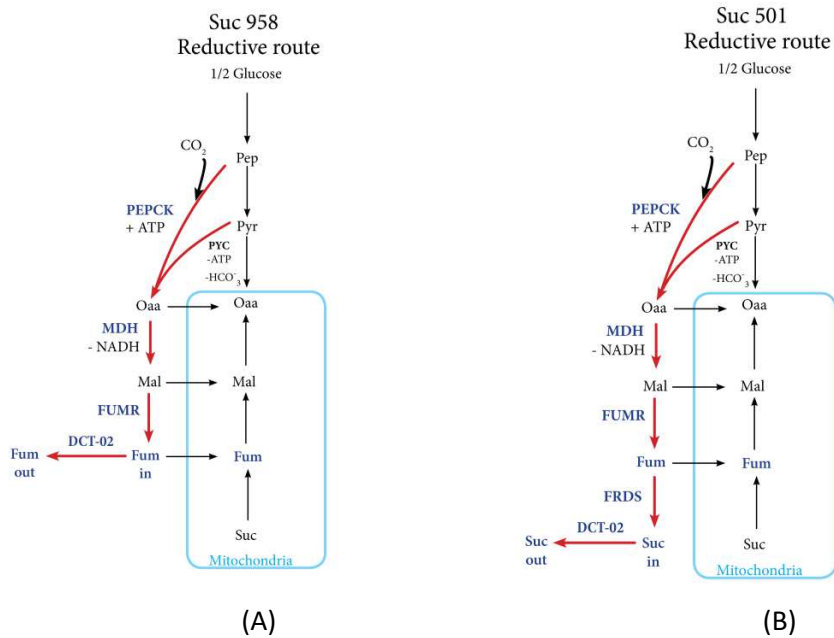


Figure 4.1 A) Biosynthesis of fumaric acid via the reductive route in Suc 958 through overexpression of PEPCK, MDH, FUMR and DCT-02. B) Biosynthesis of succinic acid via the reductive route in Suc 501 through the overexpression of PEPCK, MDH, FUMR, FRDS and DCT-02

Table 4.1 Genotype of the *S. cerevisiae* strains used in this study.

Strain	Genotype
CEN.PK 21-C	MATa; ura3-52; trp1-289; leu2-3,112; his3 D1; MAL2- 8C; SUC2
Suc 958	CEN.PK113-5D (matA, mal28c, suc2, ura3-52, sit2::[TPI1p-PCKa-PMA1t] sit4::[TDH3p-MDH3-TDH3t; ENO1p-DCT_02-ENO1t]; [TPI1p-FUMR-PMA1t] adh1::loxp; [PGK1p-PYC2-PGK1t]
Suc 501	CEN.PK113-5D (matA, mal28c, suc2, ura3-52, sit2::[TDH3p-FRDg-TDH3t;TPI1p-PCKa-PMA1t] sit4::[TDH3p-MDH3-TDH3t;ENO1p-DCT_02-ENO1t; lox72; TPI1p-FUMR-PMA1t]adh1::loxp;[PGK1p-PYC2-PGK1t;URA3p-URA3-URA3t]

Stock culture

Stock cultures of the engineered strains were grown at 30°C on a gyratory shaker at 200 rpm in 250 ml Erlenmeyer flasks with 100 ml of defined medium containing: 20 g.L⁻¹ glucose.H₂O, 5 g.L⁻¹ (NH₄)₂SO₄, 3 g.L⁻¹ KH₂PO₄, 0.5 g.L⁻¹ MgSO₄.7H₂O, 1ml.L⁻¹ trace mineral solution and 1ml.L⁻¹ vitamin solution. The compositions of the trace minerals and vitamin solutions were the same as described by Bruinenberg *et al.* (95). The growth media were filter sterilized using polyethersulfone (PES) membrane filters with a pore size of 0.20 μm (Millipore, Massachusetts, USA). Stock cultures were prepared by adding 30% (v/v) glycerol to the shake flask cultures during the exponential phase, and stored at -80° C in vials with 1 ml of culture.

Chemostat cultivation

The Suc 958 strain was grown under aerobic, glucose limited chemostat conditions in a 2L bioreactor (Applikon, The Netherlands) with a working volume of 1L. Chemostat cultivations were carried out on a minimal medium as described by Canelas *et al.* (45). The composition of the medium was: 8.25 g.L⁻¹ Glucose.H₂O, 0.30 g.L⁻¹ (NH₄)₂SO₄, 3.0 g.L⁻¹ NH₄H₂PO₄, 0.30 g.L⁻¹ KH₂PO₄, 0.50 g.L⁻¹ MgSO₄.7H₂O, 1ml.L⁻¹ trace mineral solution, 1ml.L⁻¹ vitamin solution, and 0.50 g.L⁻¹ ethanol. Ethanol was added to the feed medium to prevent metabolic oscillations.

The dilution rate in the chemostat was maintained at 0.10 h^{-1} , the temperature was controlled at $30 \text{ }^{\circ}\text{C}$, and the dissolved oxygen concentration (DO) was measured using an autoclavable Clark type DO sensor (Mettler-Toledo GmbH, Greifensee, Switzerland). The pH was controlled at 3.0 using an autoclavable pH sensor (type 465-50-S7, Mettler-Toledo, Urdorf, Switzerland) by adding 2M KOH and 2M H₂SO₄ using a Biostat Bplus controller (Sartorius BBI Systems, Melsungen, Germany). The stirrer speed was controlled at 800 rpm and the aeration rate was controlled at $0.3 \text{ L}\cdot\text{min}^{-1}$ using a mass flow controller (Brooks 5850 TR, Hatfield, PA, USA) while maintaining an overpressure of 0.30 bar. A combined paramagnetic/infrared off gas analyzer (NGA 2000, Rosemount, USA) was used to measure the CO₂ and O₂ fractions in the exhaust gas. At stable readings of the CO₂ and O₂ levels in the exhaust gas, it was assumed that a steady state was obtained. Steady states were sequentially achieved with different concentrations of carbon dioxide in the aeration gas. The first steady state was achieved with 100% air, afterwards, the inflow gas was changed to air/CO₂ mixtures containing 25% and 50% carbon dioxide, finally, the aeration gas was changed back to 100% air.

Aerobic shake flask cultivation in the absence of nitrogen source and glucose excess conditions

To test the C4 dicarboxylic acids production potential the engineered strains were incubated in aerobic shake flasks under nitrogen starved conditions at a high concentration of glucose. Prior to the transfer to nitrogen starved conditions the strains were cultivated in 250 ml Erlenmeyer flasks with 100 ml of minimal medium with the same composition as used for the stock cultures described earlier. Shake flask cultures were incubated overnight at 30°C on a gyratory shaker at 200 rpm. At the end of the exponential phase, the whole culture was centrifuged at 5000g for 10 minutes and washed with demineralized water and centrifuged again. The biomass pellet was re-suspended in a medium without nitrogen source containing: $100 \text{ g}\cdot\text{L}^{-1}$ glucose, $50 \text{ g}\cdot\text{L}^{-1}$ CaCO₃, $40 \text{ }\mu\text{g}\cdot\text{L}^{-1}$ biotin, $1 \text{ ml}\cdot\text{L}^{-1}$ trace element and $1 \text{ ml}\cdot\text{L}^{-1}$ vitamin solution. CaCO₃ was used as a buffering agent in order to maintain the pH between 6.0 and 6.5.

Analysis of intracellular and extracellular metabolites

Samples for quantification of extracellular metabolites were taken by rapidly withdrawing 2 ml of broth into a syringe containing stainless steel beads at -18°C to cool down the sample rapidly to 0°C , followed by immediate removal of the cells by filtration through PVDF syringe filters with a pore size of $0.45\ \mu\text{m}$ (Millex-HV, Millipore, USA). The procedure is described in detail by Mashego *et al.* (49). The concentrations of glucose, glycerol, acetate and ethanol were quantified through HPLC analysis using a Bio-Rad HPX-87H 300 column (7.8 mm). The column was eluted with phosphoric acid (1.5 mM in Milli-Q water) at a flow rate of $0.60\ \text{mL min}^{-1}$. Organic acids (malic, succinic, pyruvic and fumaric) were also measured using the Bio-Rad HPX-87H 300 column (7.8 mm) where the column was eluted with more concentrated phosphoric acid (45 mM in Milli Q water) in order to have a better separation of succinic and fumaric acid peaks.

For the measurement of intracellular metabolites, broth samples were withdrawn using the rapid sampling setup described by Lange *et al.*(47). Approximately 1.20 g of broth sample was withdrawn into 6 mL of quenching solution (100% methanol at -40°C) and immediately mixed and weighed. The quenched sample was then filtered through $0.45\ \mu\text{m}$ (PES, Pall, USA) filters and the biomass cake was washed two times with 40 ml of 100% methanol kept at -40°C to remove extracellular metabolites and other media components. For metabolite extraction from the cells, the filter containing the washed cell cake was immersed in 30 ml of a 75% (v/v) preheated (75°C) ethanol/water solution in a 50 ml falcon tube, and at the same time 120 μl of ^{13}C labelled cell extract was added as internal standard for all metabolites. Thereafter the tube was placed in a 95°C water bath for 3 min and then stored at -80°C until further processing. Subsequently the samples were evaporated to dryness using a Rapid-Vap (Labconco, USA) (48), and the residue was re-dissolved in 600 μl of milli-Q water and centrifuged at 10000g for 5 min to remove cell debris. After a second centrifugation step at 10000 g for 10 min, the cell extracts were stored at -80°C until quantification of the metabolites with GC-MS and LC-MS.

Enzymatic assay of fumarate reductase

The biomass from an overnight grown shake flask culture was centrifuged, washed, and re-suspended in potassium phosphate buffer (10 mM, pH 7.5, with 2 mM EDTA) and stored at -20°C. Before the assay, the culture was thawed, washed, and re-suspended in potassium phosphate buffer (100 mM, pH 7.5; with 2 mM MgCl₂ and 1 mM dithiothreitol).

For the preparation of cell extract, the cells were sonicated with a Fast Prep FP120 (Thermo Scientific) cell disruptor using 0.75 g glass beads (G8772; Sigma) per ml of cell suspension in four bursts (30s for each burst at speed 6, with 30s interval to allow for cooling). After sonication the cell lysate was centrifuged to remove cell debris (4°C, 20 min, 20000 g). The supernatant was used for the enzyme activity assay. The protein concentration of the cell extracts was determined using Lowry method.

Measurement of the activity of fumarate reductase was performed in a microtiter plate at a controlled temperature of 30°C. Total volume of the reaction mixture was 200 µl which contained 50 mM KH₂PO₄/K₂HPO₄ buffer (pH 7.5), 0.4 mM NADH and the cell extract. 20 mM of sodium fumarate was added to initiate the reaction. Fumarate reductase activity was measured by following the decrease of NADH by measuring the absorbance at 340 nm.

Flux analysis

Steady state biomass specific uptake and secretion rates were calculated from the fermenter mass balances for the extracellular metabolites. A data reconciliation method (50) was used to obtain the best estimates of the biomass specific rates within the measurement errors. Metabolic flux analysis was performed using a modified version of the stoichiometric model of *S. cerevisiae* as described by Lapujade *et al.* (51). In the stoichiometric model export of succinate and malate was assumed to occur via a uniport mechanism of the totally dissociated species, which was based on the results obtained in this study and from the studies done by Jamalzadeh *et al.* (25). The export of the produced H⁺ occurs via the plasma membrane H⁺-ATPase.

Results

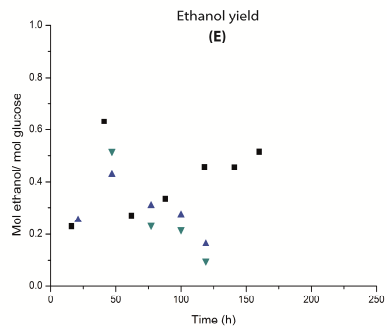
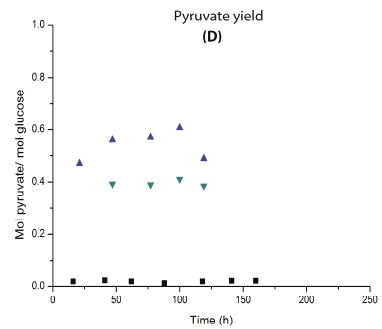
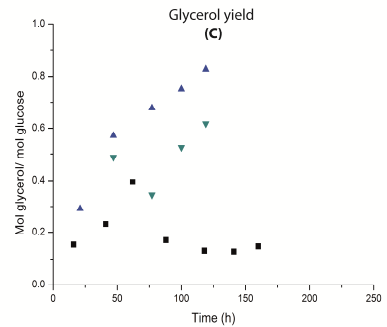
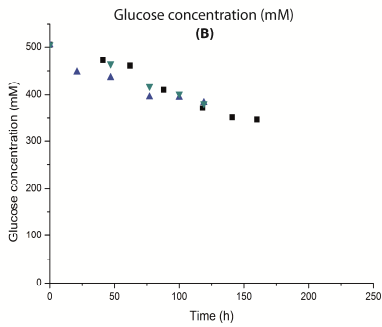
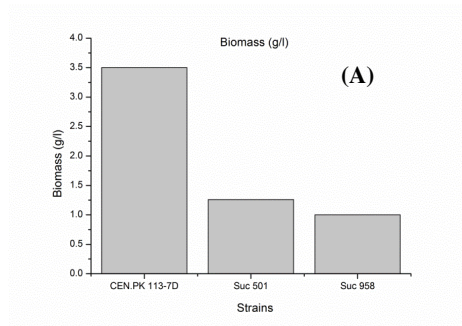
In this study we engineered the reductive branch of the TCA cycle in *S. cerevisiae* to produce either succinic or fumaric acid. In Suc 958 (Figure 4.1A) and Suc 501 strains (Figure 4.1B), the reductive branch of the TCA cycle was overexpressed along with a heterologous dicarboxylic acid transporter DCT-02 to improve the export of dicarboxylic acids. Suc 958 was derived from the succinate producing Suc 501, by deletion of heterologous FRDS with the expectation of fumaric acid production via the cytosolic reductive part of TCA cycle.

Organic acids production in the absence of nitrogen source in aerobic shake flasks

Suc 501, Suc 958 and CEN.PK 113-7D (reference wild type strain) were cultivated in aerobic shake flasks in the absence of a nitrogen source and in glucose excess condition (500 mM) to study the impact of the genetic modifications (compared to the CEN.PK 113-7D strain) on the production of fumaric acid and other metabolites.

Both mutant strains consumed glucose similar to wild type (Figure 4.2B). During the batch cultivation the pH varied between 6.0 and 6.5, showing that the calcium carbonate buffer was sufficient. The initial biomass concentrations are shown in Figure 4.2A. Both mutant strains showed hardly any fumaric acid production (Figure 4.2H). Both mutant strains behaved, with respect to secreted metabolites, very similar, but were different compared to the wild type much more glycerol and pyruvate, much less ethanol and high malate and, unexpected, considerable succinate (Figure 4.2). The deletion of fumarate reductase in the Suc 958, which was confirmed by an enzymatic assay (Table 4.2), did not lead to the expected fumarate production and the absence of succinate secretion. Unexpectedly, succinic acid was still produced in the absence of fumarate reductase.

Metabolic response of engineered C4-acids producing *S. cerevisiae* in high CO₂ environments



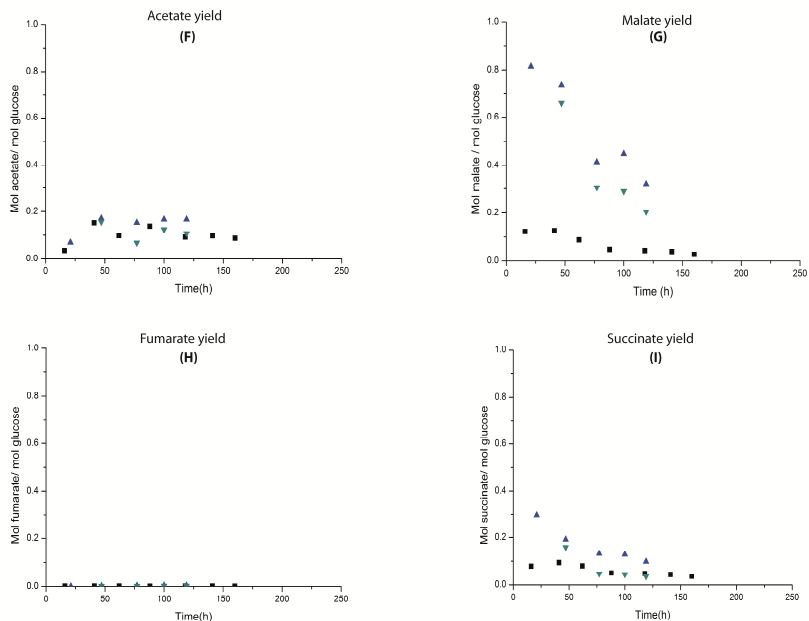


Figure 4.2 Metabolites production on glucose by Suc 501 (▼), Suc 958 (▲) and CEN.PK 113-7D (■) in aerobic glucose shake flasks in the absence of N-source. Concentrations of A) Biomass in g/L and B) extracellular glucose in mM. Yields (mol/ mol of glucose consumed) of C: Glycerol, D: Pyruvate, E: Ethanol, F: Acetate, G: Malate, H: Fumarate, I: Succinate.

Table 4.2. Fumarate reductase activity of CEN.PK113-7D, Suc 501 and Suc 958 strains in aerobic, glucose excess shake flask studies

Strain	Fumarate reductase activity ($\mu\text{mol}\cdot\text{min}^{-1}\cdot\text{mg protein}^{-1}$)
CEN.PK113-7D	0.0
SUC501	4.8 ± 2.8
SUC958	0.0

Kinetic/stoichiometric properties of the Suc 958 strain

General observations

Suc 958 was grown aerobically in a glucose limited chemostat culture at pH 3.0 with a dilution rate of 0.10 h^{-1} using different concentrations of CO₂ to study its impact on FA production. Different partial pressures of CO₂ were applied to increase the dissolved carbon dioxide concentration in order to thermodynamically and kinetically push the reductive route, specifically PEPCK and pyruvate carboxylase which require CO₂ and HCO₃⁻ as substrates respectively, producing oxaloacetate which is expected to increase the FA production. Figure 4.3A shows the off gas concentrations of carbon dioxide and oxygen. Because of mixed CO₂ /air gassing, the mole fraction of oxygen in the gas decreased with increasing CO₂ supply which resulted in a drop of dissolved oxygen concentration (Figure 4.3B) but there was no oxygen limitation as the dissolved oxygen level was always above 40%. Steady states were assumed to be achieved at stable off gas CO₂ and O₂ concentration measurements. In order to rule out adaptation of the culture after 250 h of cultivation in a glucose limited chemostat (76), the biomass specific conversion rates (Table 4.3) and the residual glucose concentration of the two air sparged steady states were compared (first and the last steady state, 0.82 mM and 0.52 mM respectively, Supplementary material, Table 4.S1) and no indications of adaptation were found.

The residual ethanol concentration was below the detection limit (0.10 mM) and the low concentration of residual glucose (Supplementary material, Table 4.S1) shows that in all the steady states the supplied glucose and ethanol were almost completely consumed.

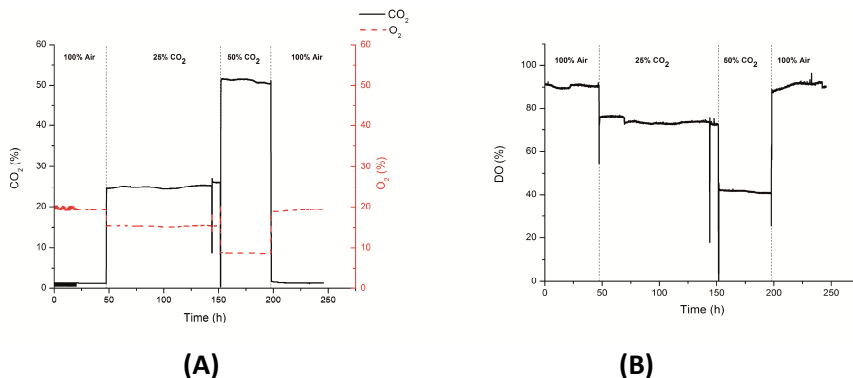


Figure 4.3 Suc 958: (A) Off gas measurement of CO₂ and O₂ during the chemostat cultivation of Suc 958 ($D=0.10\text{ h}^{-1}$, pH 3.0) at different CO₂ concentrations in the inlet gas. (B) Dissolved oxygen level at different CO₂ concentrations in the aeration gas

Remarkably, Suc 958, which was obtained by removing the heterologous fumarate reductase from Suc 501, produced significant amounts of succinic acid and small amounts of malic acid as the main products. FA production was negligible; its specific production rate (Table 4.3) was 200 times lower than the succinic acid production rate. The near absence of FA production agrees with the shake flasks study, showing that both under glucose excess and glucose limiting conditions negligible FA production occurred. The production of succinic acid in the absence of heterologous fumarate reductase activity (Table 4.2) in Suc 958 is unexpected, but was also noticed in the shake flask study. The effect of increased CO₂ partial pressure on the concentration of biomass, succinic, malic and fumaric acid is shown in Figure 4.4. The increased succinic acid production rate led to a decreased biomass level which is expected because the consumed glucose was diverted towards succinic acid rather than biomass formation.

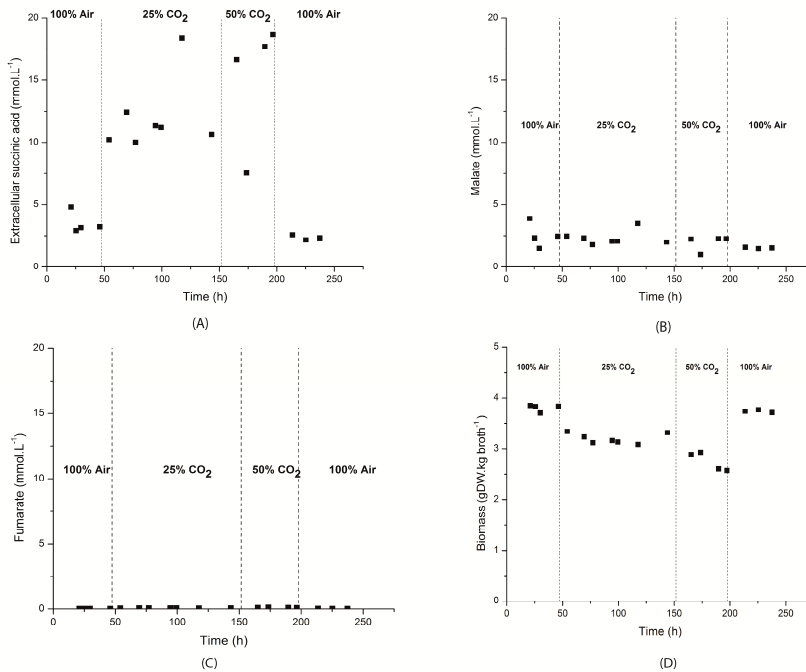


Figure 4.4 Suc 958: Steady state extracellular concentrations of succinic (A), malic (B), fumaric acid (C) and biomass (D) during the glucose limited chemostat cultivation ($D = 0.10 \text{ h}^{-1}$, pH 3.0) at different levels of CO₂ in the aeration gas.

Impact of increased partial pressure of CO₂ on the production rates of dicarboxylic acids

Table 4.3 shows the steady state biomass specific rates. The unbalanced rates are obtained from the fermenter compound balances. The balanced rates are obtained using data reconciliation, yielding the best estimates of the measured rates, within their standard errors, under the constraint that the elemental conservation relations are satisfied (50).

Figure 4.5 shows the biomass specific production rates of succinic acid (Figure 4.5A), malic acid (Figure 4.5B) glycerol and fumaric acid (Figure 4.5C), and pyruvic acid (Figure 4.5D) against the partial pressure of CO₂ ($p\text{CO}_2$) for Suc 501

and Suc 958. For Suc 958 clearly all the rates, except pyruvate do strongly increase with $p\text{CO}_2$ especially succinic acid. Zelle *et al.* (18) also noticed that, in a batch cultivation of a *S. cerevisiae* strain (engineered to overproduce malic acid), with high CO_2 partial pressure, the production rates of succinic and malic acid increased.

From a previous CO_2 study done with Suc 501 (25) performed under the same conditions but at a lower dilution rate of 0.05 h^{-1} , it was found that q_{suc} also increased with P_{CO_2} (Figure 4.5A), but the q_{suc} value was 2.5 times lower than what we measured for Suc 958. The reason for this difference is discussed in the section “Kinetic description of C4 carboxylic acids production”.

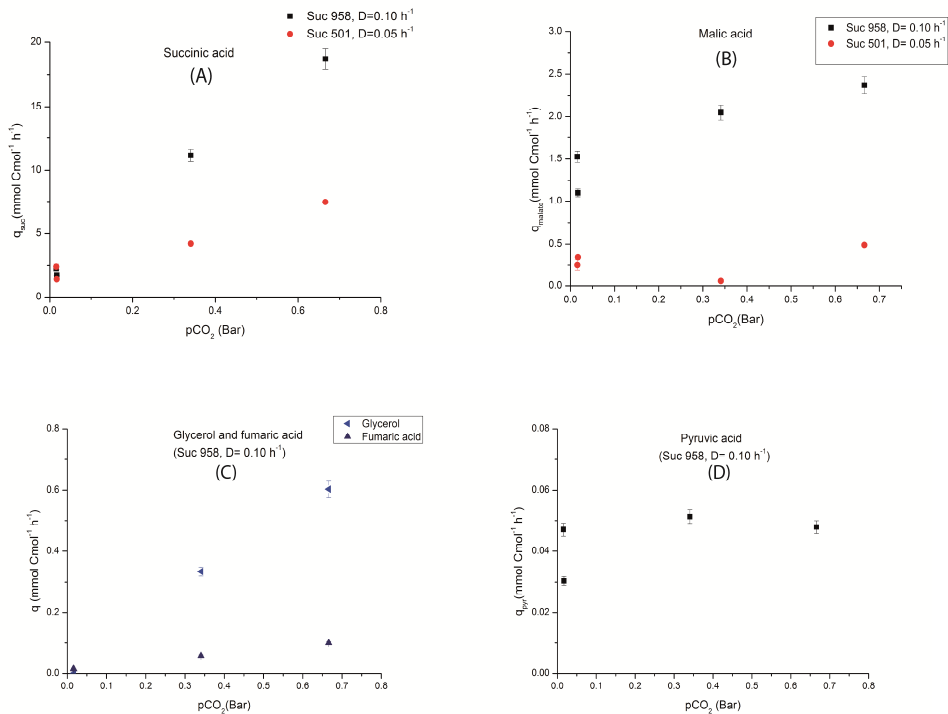


Figure 4.5 Impact of CO_2 partial pressure (at pH 3.0) on biomass specific production rates ($\text{mmol Cmol}^{-1} \text{ h}^{-1}$) of (A) succinic acid (q_{suc}) (B) malic acid (q_{mal}) in Suc 958 (■) and Suc 501 (●) strains. Suc 958 strain also secreted small amounts of (C) fumaric acid (q_{fumarate} , ▲) and glycerol (q_{glycerol} , ◀) (D) pyruvic acid (q_{pyruvate} , ■)

Table 4.3 Suc 958: Biomass specific rates (mmol.Cmol⁻¹.h⁻¹) at different CO₂ levels in the aeration gas (at pH 3.0)

Rates (mmol.Cmol ⁻¹ .h ⁻¹)	Phase I (Air)		Phase II (25% CO ₂)		Phase III (50% CO ₂)		Phase IV (Air)	
	Unbalanced	Balanced	Unbalanced	Balanced	Unbalanced	Balanced	Unbalanced	Balanced
Glucose	-29.2 ± 1.6	-27.9 ± 0.4	-36.1 ± 2.0	-35.5 ± 1.4	-42.0 ± 2.3	-40.4 ± 1.3	-29.5 ± 1.6	-27.8 ± 0.4
Ethanol	-7.8 ± 0.4	-7.7 ± 0.4	-9.7 ± 0.5	-9.7 ± 0.5	-11.3 ± 0.6	-11.2 ± 0.6	-7.8 ± 0.4	-7.8 ± 0.4
CO ₂	61.7 ± 1.4	62.0 ± 1.4	69.0 ± 32.0	71.2 ± 8.3	91.3 ± 100.0	70.5 ± 7.2	67.4 ± 1.6	67.3 ± 1.5
O ₂	-89.0 ± 20.0	-67.7 ± 1.6	-79.2 ± 18.0	-83.7 ± 8.4	-82.3 ± 14.0	-88.6 ± 7.3	-75.0 ± 20.0	-72.5 ± 1.7
Biomass	105.5 ± 1.1	105.5 ± 1.1	107.0 ± 1.1	107.0 ± 1.1	107.9 ± 1.1	107.9 ± 1.1	103.7 ± 1.1	103.6 ± 1.1
Succinate	2.3 ± 0.1	2.3 ± 0.1	11.1 ± 0.5	11.1 ± 0.5	18.6 ± 0.8	18.7 ± 0.8	1.7 ± 0.1	1.7 ± 0.1
Malate	1.5 ± 0.1	1.5 ± 0.1	2.1 ± 0.1	2.0 ± 0.1	2.4 ± 0.1	2.4 ± 0.1	1.1 ± 0.0	1.1 ± 0.0
Fumarate	0.016 ± 0.0	0.016 ± 0.0	0.06 ± 0.0	0.06 ± 0.0	0.10 ± 0.0	0.10 ± 0.0	0.014 ± 0.0	0.014 ± 0.0
Pyruvate	0.047 ± 0.0	0.047 ± 0.0	0.051 ± 0.0	0.051 ± 0.0	0.047 ± 0.0	0.047 ± 0.0	0.03 ± 0.0	0.03 ± 0.0
Glycerol	0.0 ± 0.0	0.0 ± 0.0	0.33 ± 0.01	0.33 ± 0.01	0.60 ± 0.02	0.60 ± 0.02	0.0 ± 0.0	0.0 ± 0.0
Carbon-recovery broth	95.7%	-	97.7%	-	103.9%	-	94.7%	-
y-recovery broth	106.7%	-	96.6%	-	94.3%	-	96.1%	-

Stoichiometry of C4 acids production

The obtained specific rates for growth, succinic, malic acid production and substrate consumption were combined in the Herbert-Pirt equation (equation 4.1) to obtain an experimental estimate of the stoichiometry of the product reaction for C4 acids (succinic and malic) in Suc 958. The biomass specific production rates of pyruvate and glycerol (< 1 % of the total amount of products formed) were neglected. The q_{C4} (equation 4.1) is the combined production rate of C4 acids (succinic, malic and very low amounts of fumaric acid), which is 89% succinic acid and 11% malic acid, based on the secretion rates obtained at 50% CO₂ (Table 4.3). The following Herbert pirt equation applies for aerobic growth and product formation:

$$-q_s = a \cdot \mu + b \cdot q_{C4} + m_s \quad (\text{eq 4.1})$$

q_s , q_{C4} ($q_{\text{succinate}} + q_{\text{malate}} + q_{\text{fumarate}}$) and μ are the biomass specific rates of the substrate carbon (of glucose and ethanol), C4 acids and growth respectively. a and b are the stoichiometric parameters in Cmol substrate consumed per Cmol biomass produced (for a) and Cmol substrate consumed per mol C4 acids produced (for b), m_s is the biomass specific substrate consumption rate for maintenance in Cmol substrate.(Cmol biomass)⁻¹.h⁻¹. The growth rate was kept at $0.106 \pm 0.001 \text{ h}^{-1}$ during the experiment and the maintenance coefficient was assumed constant (see appendix 4.C). This means that the term $a \cdot \mu + m_s$ can be assumed constant in these CO₂ experiments, where only q_{C4} , q_s , q_{O2} and q_{CO2} were varied. The above equation can thus be simplified to ($a' = a \cdot \mu + m_s$):

$$-q_s = a' + b \cdot q_{C4} \quad (\text{eq 4.2})$$

Note that q_s is the substrate consumption rate in mCmol.Cmol⁻¹.h⁻¹, where the feed contains 91.55% Cmol glucose and 8.45% Cmol ethanol. Equation 4.2 predicts that increased production of C4 acids leads to a linear increase in the uptake of substrate carbon, which is indeed observed (Figure 4.6). From the weighted regression of $-q_s$ and q_{C4} (Figure 4.6), b was estimated to be $4.66 \pm 0.33 \text{ Cmol substrate per mol of C4 acids produced}$ (Figure 4.6).

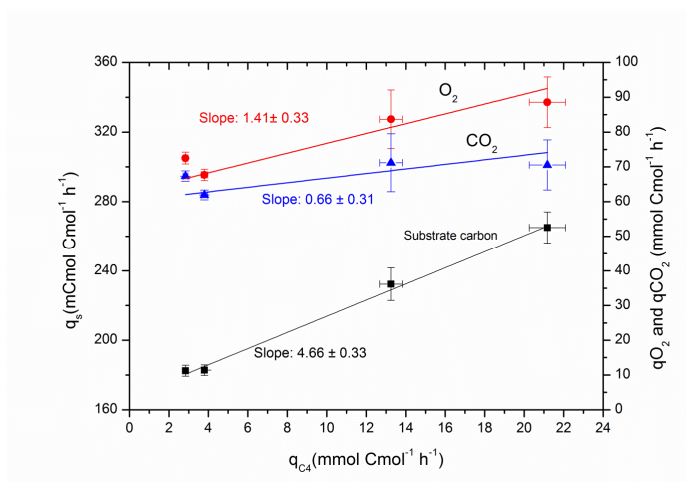
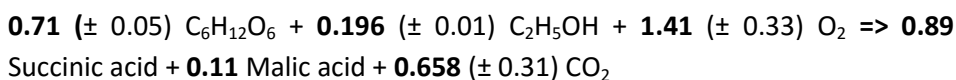


Figure 4.6 Suc 958: Steady state biomass specific rates (at pH 3.0) of substrate carbon (q_s , mCmol.Cmol⁻¹.h⁻¹, ■), O₂ (q_{O_2} , mmol.Cmol⁻¹.h⁻¹, ●) and CO₂ (q_{CO_2} , mmol.Cmol⁻¹.h⁻¹, ▲) against the biomass specific C4 acids production rates ($q_{\text{succinate}} + q_{\text{malate}} + q_{\text{fumarate}}$). The substrate carbon slope (black line) was calculated using weighed linear regression. Red (q_{O_2} data) and the blue line (q_{CO_2} data) represent the slope determined from the degree of reduction and carbon balance.

From the estimated glucose and ethanol carbon consumption of 4.66 mol carbon/mol C4 acids, the stoichiometry for the production of 1 mol of C4 acids from the glucose/ethanol mixture follows, using conservation calculation (carbon and degree of reduction balance):



The calculated O₂ consumption (slope: 1.41 ± 0.33 mol O₂ /mol C4 acids) and CO₂ production (slope: 0.658 ± 0.31 mol CO₂ /mol C4 acids) shown in Figure 4.6 agree with the experimental data. The above product reaction shows that the production of 1 mol of C4 acids (89% succinic, 11% malic) requires a consumption of 1.41 (± 0.33) mol O₂. Consumption of this amount of O₂ corresponds with the production of 3.47 ± 0.81 mol ATP per mol of C4 acids produced (see Appendix 4.B). This ATP produced might be associated with the export of the produced C4 acids. If we assume that the totally dissociated

succinic acid (Suc^{2-}) species is exported through a uniport mechanism (based on the total succinic acid out/in ratios, see Appendix 4.E), also 2H^+ must be exported via the H^+ -ATPase, which costs 2 ATP per mol of succinic acid secreted. This shows that there is an unaccounted ATP consumption of 1.47 ± 0.81 ($3.47 \text{ ATP produced} - 2 \text{ ATP consumed}$) mol ATP/ mol of succinic acid secreted. Appendix 4.C shows that futile cycling of succinic acid, which occurs significantly at pH 3.0, requires 0.15 mol O_2 or $(0.15 * 2.46) = 0.37$ mol ATP per mol of C4 acids secreted using the succinic acid permeability coefficient calculated for Suc 501 cultivated at a dilution rate of 0.05 h^{-1} (25). The unaccounted ATP consumption of 1.47 ± 0.81 could therefore be associated with the futile cycling of succinic acid with roughly four times the permeability value obtained with Suc 501. Suc 958 was cultivated at dilution rate of 0.10 h^{-1} and the growth rate difference could lead to these membrane and permeability changes.

Metabolic flux model

Surprisingly, overexpression of the reductive TCA branch in the cytosol towards fumaric acid did not result in the overproduction of fumaric acid. In contrast the strain produced significant amounts of succinic acid. Because Suc 958 did not contain a cytosolic fumarate reductase, succinic acid can only be produced in the mitochondria, which implies that there must be transport of cytosolic fumarate into the mitochondria. The mitochondrial fumarate is subsequently converted to succinic acid through the oxidative part of the TCA cycle and is transported back to the cytosol.

There are several possibilities to achieve an exchange of fumarate and succinate between mitochondria and cytosol (see Appendix 4.A). The straightforward option is the succinate-fumarate dicarboxylic acid exchange transporter SFC1 (96–99) which is reported to be present in the mitochondrial membrane of *S. cerevisiae*. This transporter is repressed by glucose and is functional with ethanol and acetate as carbon source (98), but its repression might be relieved at the low residual glucose concentration as in our glucose limited chemostat experiment. However, in the shake flask experiments at high extracellular glucose, glucose repression should have resulted in the

absence of SFC1p, but nevertheless succinic acid was still produced in significant amounts. It is therefore unlikely that the fumarate/succinate exchange occurred through SFC1p. Another possibility for the mitochondrial transport of succinic acid is $\text{Suc}^{2-}/\text{HPO}_4^{2-}$ exchanger DIC1, which is known to be present in *S. cerevisiae* (100), and can also transport fumaric acid. In addition there is a mitochondrial $\text{H}_2\text{PO}_4^{2-}/\text{OH}^-$ exchanger needed to balance phosphate; this exchanger is also well known in *S. cerevisiae* (101). It is shown in Appendix 4.A that the net stoichiometry of this combined mechanism is the same as for transport through SFC1p. For the reasons of simplicity we have used the stoichiometry of SFC1 transporter in the metabolic model.

The futile cycling of succinic acid, discussed before, was also incorporated in the metabolic model (see Appendix 4.C). With the metabolic network model we calculated the substrate carbon requirement, oxygen consumption and carbon-dioxide production rates as model output, using as model input the balanced experimental values (Table 4.3) of the growth rate and the, biomass specific production rates of succinate, ethanol, malate, glycerol and fumarate. Figure 4.7 shows the plots comparing the estimated and the experimentally obtained values, which are not significantly different and shows the reliability of the metabolic model.

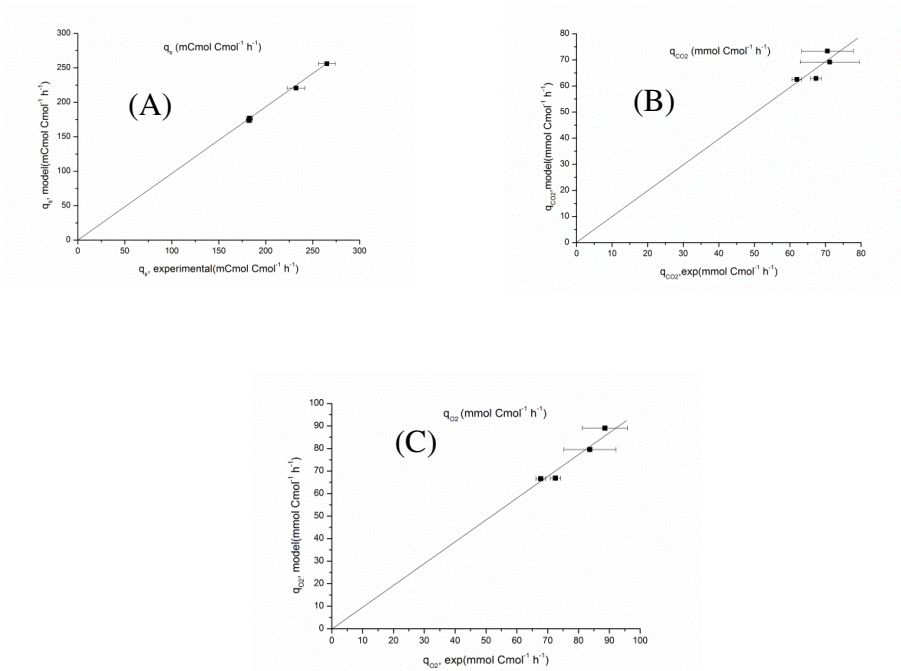


Figure 4.7. Suc 958: Steady state biomass specific rates obtained through metabolic network model compared with the experimental values for consumption of A) substrate carbon (q_s), B) CO₂ consumption (q_{CO_2}) and C) O₂ production (q_{O_2}).

Intracellular fluxes

Figure 4.8 shows the calculated fluxes for the four sequential steady states (Figure 4.3) to illustrate the impact of increased succinic acid secretion (q_{suc}) on the intracellular fluxes. As expected the glycolytic flux increased with increase in succinic acid secretion rate and the flux through PPP did not change significantly as the growth rate is always maintained at 0.10 h⁻¹. There is a significant increase (3.4 to 16.9 mmol Suc.Cmol⁻¹.h⁻¹) in the futile cycling rate of succinic acid (passive diffusion) at increasing succinic acid secretion rates and thus increased extracellular succinic acid concentration. For 50% CO₂, the futile cycling rate was 46% of the total secretion rate of succinic acid. Note that in Suc 501, cultivated at $\mu = 0.05$ h⁻¹, the futile cycling rate of succinic acid (maximal 7.0 mmol.Cmol⁻¹.h⁻¹ at 50% CO₂) is less, which might be due, as mentioned earlier, to a lower succinic acid permeability at lower growth rate.

The ATP for maintenance (with futile cycling excluded) is not significantly different in the 4 steady states, with an average of 71.3 mmol ATP.Cmol⁻¹.h⁻¹.

The most relevant flux change was observed for succinate dehydrogenase (SDH), the flux decreased with increasing q_{suc} . The reason for the decrease in SDH flux is the required exchange of cytosolic produced fumarate and mitochondrial produced succinate which leads to a stoichiometric coupling where 50% of the glucose which is converted to succinate is first converted to fumarate through the reductive route while the other 50% is converted to mitochondrial succinate through the oxidative route. These coupled reductive/oxidative pathways lead per mol of produced succinic acid to a production of 5 NADH and 2 ATP (Appendix 4.D). This shows that succinic acid production leads to excess electron production, therefore the rate of the TCA cycle must decrease at increasing succinate production. This implies that at a certain maximal succinic acid production rate, the rate through SDH reaction in the TCA cycle becomes zero. Using the metabolic model we calculated the decrease in the rate of SDH as a function of increasing succinic acid production rate (Figure 4.9A). The calculated maximal succinic acid production rate, which occurs at zero SDH flux is 37.6 mmol.Cmol⁻¹.h⁻¹. Further increase of q_{suc} would reverse the direction of SDH which is impossible because there is no source of FADH₂ and fumarate reductase is absent. At this maximum value of $q_{\text{suc,max}}$ all the energy needed for maintenance and growth is supplied by the product reaction (which produces 5 NADH and 2 ATP per mol succinic acid, Appendix 4.C). At a lower growth rate, less energy is needed and therefore $q_{\text{suc,max}}$ is expected to decrease with decreasing growth rate as predicted from the flux model (see Figure 4.9B). Industrial production of succinic acid is done at very low growth rate and Figure 4.9B shows that in Suc 958, $q_{\text{suc,max}}$ can never exceed ~ 25 mmol.Cmol⁻¹.h⁻¹ because of the stoichiometric coupling of reductive and oxidative route.

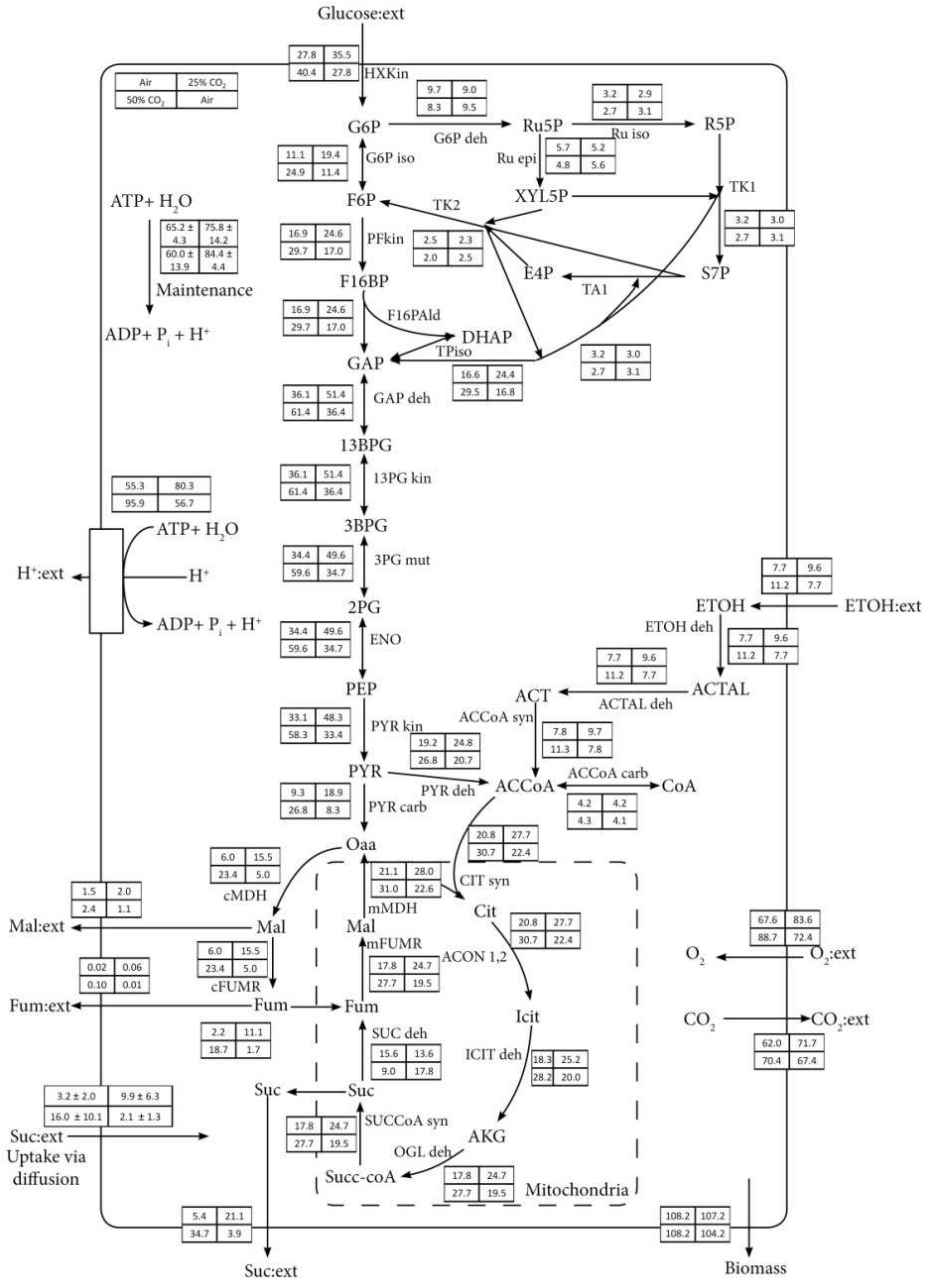


Figure 4.8. Suc98: Steady state intracellular fluxes at different CO₂ volume fractions in the sparged air

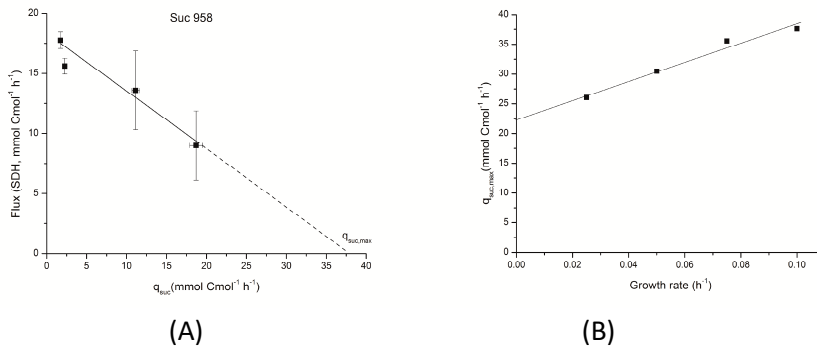


Figure 4.9. Suc 958: (A) Steady state intracellular fluxes ($D = 0.10 \text{ h}^{-1}$) through the succinate dehydrogenase reaction (SDH) against the succinic acid secretion rate (q_{suc}) (B) $q_{\text{suc,max}}$ predicted from the metabolic model at different growth rates.

Response of intracellular metabolites concentration in central carbon metabolism to increased succinic acid production rate

From the intracellular metabolite data of Suc 958 (Supplementary material, Table 4.S4) the following observations are made at the increased succinic acid production rate which occurs at higher CO₂ levels:

- There is no significant change in the intracellular metabolite levels of the pentose phosphate pathway (PPP) (6PG, Supplementary material, Table 4.S4) which was expected as the dilution rate was maintained at 0.10 h^{-1} , meaning that the NADPH requirement and therefore the PPP fluxes do not change (Figure 4.8).

- Glycolytic metabolites (3PG, 2PG, PEP, PYR, see supplementary material, Table 4.S4) of the lower oxidative part decrease which is a typical response to increased glycolytic flux (Figure 4.8).

- The increased GAP and decreased 3PG leads to increased cytosolic NADH/NAD ratio as observed by Canelas *et al.* (55) which in addition to the increased CO₂ pressure leads to increased thermodynamic force in the reductive route for C4 acids. The more reduced cytosol agrees with the increased glycerol production rate (Table 4.3).

-There is only a moderate change in most of the metabolites in the TCA cycle. Citrate and AKG decrease 2 and 1.2 fold respectively, malate and fumarate increased 1.2 and 1.5 fold with increased CO₂ partial pressure. The most significant change is the six fold increase in the intracellular succinate level from 2.25 μmol/g.DCW without CO₂ supply to 14.95 μmol/ g.DCW at a CO₂ level of 50%, which is clearly linked to the increased succinic acid production and secretion.

-The energy charge $[(ATP + 0.50 ADP) / (ATP + ADP + AMP)]$ did not change with the increase in secretion rate of succinic acid and is always above 0.90.

From the intracellular metabolite concentration data, mass action ratios were calculated (Supplementary material, Table 4.S2). The decrease in mass action ratios for the near equilibrium reactions (PGI, PGM, ENO and FMH) correlates as expected with increased intracellular fluxes. From the mass action ratios it follows that these reactions remained close to equilibrium which points to a high capacity of these enzymes, which was also noticed by Canelas *et al.* (55).

Kinetic description of the carboxylic acids production

In Suc 958, fumaric acid production occurs via the cytosolic reductive route (from pyruvate to fumarate) which is not secreted but is then converted to succinate via the mitochondrial oxidative route. Figure 4.5A shows that q_{suc} depends on the partial pressure of CO₂, but the secretion of succinic acid is 2 fold higher in Suc 958 than in Suc 501. Clearly the CO₂ level is an important factor in increasing the flux through the reductive route (Figure 4.8). The difference in q_{C4} between Suc 958 and Suc 501 at the same P_{CO_2} can have several explanations:

-It could be due to different intracellular metabolite levels in Suc 958 and Suc 501. Table 4.E1 (see Appendix 4.E) shows that intracellular pyruvate in Suc 958 is lower than in Suc 501, also PEP is not significantly different in both strains. Moreover the calculated NADH/NAD ratios (Appendix 4.E) are same for both strains. The intracellular fumarate level is higher in Suc 958 than in Suc 501, which excludes fumarate inhibition in Suc 501 as the reason for the lower flux.

These results show that in Suc 958 the substrate levels (pyruvate, PEP and NADH/NAD) are the same or lower and the product levels (Fumarate) are the same or higher than in Suc 501. It is therefore unlikely that differences in the metabolite levels can explain the flux differences.

-The flux through the reductive route is only dependent on P_{CO_2} (Figure 4.5A). The relation between CO₂ and q_{suc} in Figure 4.5A suggests a high affinity hyperbole for Suc 501 and a low affinity hyperbole for Suc 958 with two different V_{max} values for the PEPCK reaction which uses CO₂ as a co-substrate. Although the V_{max} for flux through the reductive route (q_{red}) can be different (Suc 958 at $\mu=0.10\text{ h}^{-1}$, and Suc 501 at $\mu = 0.05\text{ h}^{-1}$), different affinities are not likely.

-The flux depends on the intracellular HCO_3^- concentration (HCO_3^-) as the co-substrate of pyruvate carboxylase). It has been reported that at higher growth rate the cytosolic pH (pH_{in}) increases in *S. cerevisiae* (102). Assuming pH_{in} to be 7.0 for Suc 958 ($\mu=0.10\text{ h}^{-1}$) and 6.3 for Suc 501 ($\mu=0.05\text{ h}^{-1}$), we calculated the intracellular HCO_3^- concentration (Appendix 4.E). Figure 4.10 shows for both mutants the correlation between the calculated pyruvate carboxylase flux and the intracellular HCO_3^- concentration, and this appears to give a reasonable hyperbolic fit with $V_{max} = 30.2\text{ mmol.Cmol}^{-1}\text{ h}^{-1}$ and $K_{m,HCO_3^-} = 59.9\text{ mM}$ for the combined data of Suc 501 and Suc 958. Note that the estimate V_{max} is smaller than the maximum flux possible through the reductive route (at $\mu=0.10\text{ h}^{-1}$, Figure 4.9B).

The produced C4 acid must be secreted and the total succinic acid out/in ratios (Table 4.E4, Appendix 4.E) indicates that succinic acid export mechanism is a uniport mechanism of totally dissociated succinic acid (Suc^{2-}). The kinetics for a reversible uniporter of Suc^{2-} can be represented by the following equation:

$$q_{C4} = q_{C4}^{\max} \cdot \left(\frac{C_{suc,in}}{K_{m,suc,in} + C_{suc,in}} \right) \left(1 - \frac{(C_{suc,out} / C_{suc,in})}{K_{eq}} \right) \quad (\text{eq. 4.3})$$

$K_{m,suc,in}$ (in mM) is the affinity coefficient of the uniporter for the intracellular total succinic acid concentration, q_{C4}^{max} (in mmol.Cmol⁻¹.h⁻¹) is the biomass specific C4 acids secretion rate which also takes into account the futile cycling of succinic acid and K_{eq} is the theoretical total succinic acid out/in equilibrium ratio for uniport of Suc²⁻.

K_{eq} is expected to be different for Suc 501 and Suc 958 because of different pH_{in} . Assuming the same pmf of 150 mV and pH_{out} of 3.0 for Suc 501 and Suc 958, K_{eq} is 7.02 for Suc 958 with pH_{in} of 7.0 and K_{eq} is 150.9 for Suc 501 with pH_{in} of 6.30. The calculations of the out/in equilibrium ratios for dicarboxylic acids is explained in the study by Shah *et al.* (80).

This high K_{eq} of the Suc 501 strain does not lead to a proper fit for the transport kinetics of C4 acids. A unified fit with equation 4.3 for both strains is obtained when we assume that in Suc 501, due to lower growth rate, the pmf is lower than 150 mV. When in Suc 501 we assume the pmf of 106 mV and pH_{in} of 6.3 we obtain a lower K_{eq} of 5.22 for Suc 501. With $K_{m,suc,in}$ of 9.5 mM and $q_{C4,max}$ of 100 mmol.Cmol⁻¹.h⁻¹, the secretion rates for both Suc 958 and Suc 501 gives a good fit as shown in Figure 4.11. Note that q_{suc} values used in equation 3 are the succinic acid secretion rates including the futile cycling of succinic acid as discussed before.

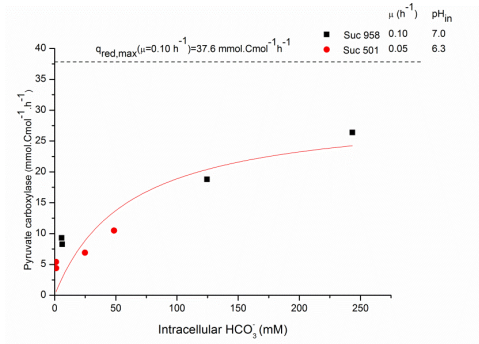


Figure 4.10. Pyruvate carboxylase kinetics: Steady state flux through pyruvate carboxylase against the intracellular concentration of HCO₃⁻ assuming the cytosolic pH of Suc 501 (●) and Suc 958 (■) as 6.3 and 7.0 respectively

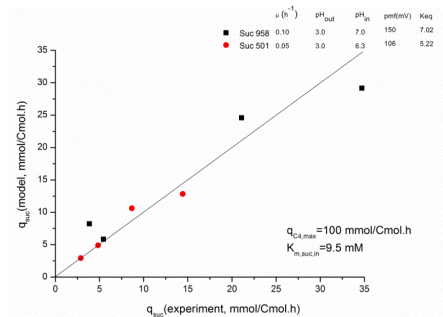


Figure 4.11. Succinic acid export kinetics: Comparison of the steady state biomass specific succinic acid secretion rate predicted (eq. 3) against the values obtained in experiment for Suc 958 (■) with pH_{in} of 7.0 and pmf of 150 mV and Suc 501 (●) with pH_{in} of 6.30 and pmf of 106 mV

Discussion

We studied the production of C4 acids in two metabolically engineered strains of *S. cerevisiae* in aerobic glucose limited chemostats at pH 3.0. From shake flasks results it was clear that the introduced heterologous dicarboxylic acid transporter (DCT-02) facilitated succinate and malate export in Suc 501 and Suc 958, but only a very low amount of fumarate was secreted. This initial

observation indicates that the DCT-02 transporter contributes towards the export of succinate and malate, but not fumarate.

In glucose limited chemostat cultivations of the Suc 958 strain, a high partial pressure of CO₂ was applied to increase the thermodynamic driving force of the reductive route of the TCA cycle towards C4 acid production. Surprisingly there was succinic, and hardly any fumaric acid produced. With increasing partial pressure of CO₂ there was a clear increase in the secretion rate of succinic acid. From the biomass specific steady state data we estimated the stoichiometry of C4 acids production, which showed that there was an additional consumption of 1.41 mol ATP per mol of C4 acids produced. This additional ATP consumption was most probably caused by futile cycling of the acids. The Suc 958 strain was cultivated at a pH of 3.0, at which most of the extracellular succinic acid is in the un-dissociated form which can passively diffuse into the cell (81). The subsequent export of the acids via the DCT-02 transporter results in an ATP dissipating futile cycle. The futile cycling rate of succinic acid was estimated from the ATP balance. The permeability coefficient of succinic acid was estimated to be $15.8 \times 10^{-6} \text{ m}\cdot\text{h}^{-1}$ in Suc 958 which is 3.8 fold higher than the permeability coefficient estimated in Suc 501 (25). This difference in the permeability coefficient could have been caused by the difference in the growth rate of the Suc 501 ($\mu=0.05 \text{ h}^{-1}$) and Suc 958 ($\mu=0.10 \text{ h}^{-1}$) strains, which is known to change the lipid composition of the membrane (103)(104) and thereby the permeability.

Surprisingly Suc 958, of which the heterologous cytosolic fumarate reductase was removed and which did not show any measurable fumarate reductase activity, was still able to produce succinic acid in significant amounts. In the absence of cytosolic fumarate reductase activity, the route of succinic acid formation must be via the oxidative branch of the TCA cycle, which implies that the mitochondrial formed succinate must be exported to the cytosol and subsequently secreted. There are only two reported mitochondrial transporters for succinate in *S. cerevisiae*, SFC1 (100) and DIC1(36). SFC1 is a succinate/fumarate exchanger, which is known to be repressed by glucose and is expressed during gluconeogenesis (51). Nevertheless succinic acid secretion was observed both in glucose excess shake flasks cultivations and in glucose limited chemostat cultures of Suc 958. Therefore the mitochondrial succinate

was most likely transported using the DIC1 mitochondrial transporter and subsequently exported to the extracellular space via the DCT-02 transporter.

The stoichiometry of succinic acid formation was shown to be a combination of reductive and oxidative pathway, mediated by the exchange of produced cytosolic fumarate (via reductive route) and produced mitochondrial succinate (via oxidative route).

Metabolic flux analysis revealed that in Suc 958 with increasing secretion rate of succinic acid there was a drop in the flux through the succinate dehydrogenase reaction which drives the TCA cycle. From the flux model we estimated the maximum succinic acid secretion rate ($q_{\text{suc,max}}$) of 37.6 mmol.Cmol⁻¹.h⁻¹ at the growth rate of 0.10 h⁻¹ in Suc 958, when the flux through SDH is zero. $q_{\text{suc,max}}$ drops with growth rate, and at near zero growth rate the $q_{\text{suc,max}}$ should not exceed 25 mmol.Cmol⁻¹.h⁻¹ in Suc 958. This analysis shows that the Suc 958 network for succinic acid production has both stoichiometric and kinetic limits.

The secretion rate of succinic acid (q_{suc}) in Suc 958 was more than 2 fold higher than Suc 501 at CO₂ partial pressure of 0.66 bar (Figure 4.5A). This indicates that apart from a high CO₂ concentration other factors contribute towards the succinic acid production. Differences in the intracellular metabolites levels were excluded as the cause for the differences in succinic acid secretion rate except the concentration of HCO₃⁻. Suc 958 and Suc 501 were cultivated at a different dilution rate (of 0.10 h⁻¹ and 0.05 h⁻¹ respectively) and it has been reported that cytosolic pH increases with increase in growth rate of *S. cerevisiae* (102). The difference in cytosolic pH, at the same CO₂ partial pressure leads to a significant difference in the intracellular concentration of HCO₃⁻ which is the co-substrate of the pyruvate carboxylase reaction. Figure 4.10 shows the change in pyruvate carboxylase flux against the intracellular concentration of HCO₃⁻ (see Appendix 4.E) assuming pH_{in} of 7.0 and 6.3 for Suc 958 ($\mu=0.10$ h⁻¹) and Suc 501 ($\mu=0.05$ h⁻¹). This difference of 0.70 units of the cytosolic pH assumed between Suc 501 and Suc 958 is significant, therefore in order to have a better understanding of the influence of the cytosolic HCO_3^-

concentration on the flux through the reductive route, the cytosolic pH should be measured in future experiments.

The total succinic acid out/in ratios measured for Suc 958 and Suc 501 indicates uniport of the totally dissociated succinic acid (Suc^{2-}) as the transport mechanism of DCT-02. We modelled the secretion rate of succinic acid using a reversible uniport (equation 3). Figure 4.11 shows that the model prediction of succinic acid secretion rate was close to the experimental values of both strains. To obtain this fit it was necessary to use a lower proton motive force (pmf of 106 mV) and pH_{in} (6.3) for Suc 501 which leads to lower equilibrium constant (Total succinic acid out/in ratio) in Suc 501. This shows that for the kinetics of C4 acids secretion, we have to take into account the changes in the cytosolic pH and pmf as a function of growth rate for better understanding of the factors influencing C4 acids secretion.

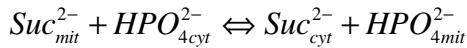
These kinetic results have major implications for the industrial production processes. The q_{C4} is pushed by high P_{CO_2} , but decreases at high extracellular concentration of C4 acids, especially at low pH_{out} , where the equilibrium out/in ratio is low. Moreover at low pH_{out} the high C4 acid extracellular concentration leads to futile cycling leading to a lower yield. At higher extracellular pH, futile cycling will have far less influence and the equilibrium out/in C4 acid ratio is much higher, promoting the secretion of C4 acids and increasing the C4 acid yield.

Acknowledgements

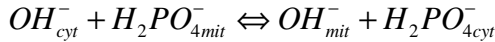
The research work is funded by BE-Basic foundation, Corbion Purac and DSM. We would like to thank Dr. Rene Verwaal and Dr. Sybe Hartmans from DSM B.V. (Delft, The Netherlands) for helpful discussions and for providing Suc 958 and Suc 501 strains.

Appendix 4.A. Mitochondrial transporters for dicarboxylic acids in *S. cerevisiae*

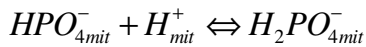
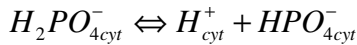
Succinate transport between mitochondria and cytosol can be achieved by different transporters. One such transporter is Dic1P (100). Dic1P transports succinate in exchange for hydrogen phosphate as shown in the following reactions:



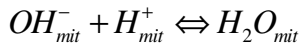
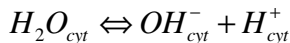
Dihydrogen phosphate is transported between the compartments in exchange of OH⁻ ions:



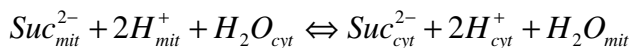
Dihydrogen phosphate in mitochondria and cytosol dissociates to hydrogen phosphate:



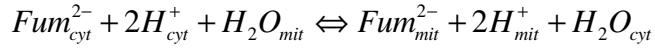
Also OH⁻ and H⁺ in cytosol and mitochondria react to H₂O:



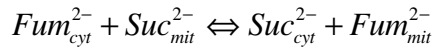
Summing up all the reactions mentioned above (2 transport reactions and 4 acid base equilibrium reactions), we get the overall stoichiometry of the transport of succinate between mitochondria and cytosol:



Dic1p can also exchange fumarate in the same way as succinate, leading to following reaction:



Because the cytosolic produced fumarate balances with the mitochondrial produced succinate, we can sum up both the reactions leading to:

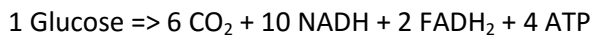


This is exactly the stoichiometry of the SFC1 dicarboxylic acid exchanger. Therefore using DIC1 or SFC 1 transporter in the metabolic model did not have any impact on the results obtained.

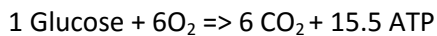
Appendix 4.B. ATP production from the catabolism of glucose/ethanol substrate mix used

In this experiment a mixture of glucose/ethanol (91.45 % Cmol of glucose and 8.45 % C-mol of ethanol) was used. This mixture is equivalent to the consumption of 0.276 mol of ethanol per 1 mol of glucose consumed, this ratio of glucose/ethanol consumption was maintained in all the steady states achieved with Suc 958. The following stoichiometric equations shows the ATP generated through the catabolism of glucose and ethanol.

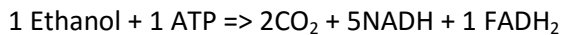
The catabolism of glucose proceeds as follows:



Using for O₂, P/NADH =1 and P/FADH₂ = 0.75, the net ATP production with the catabolism of glucose is:



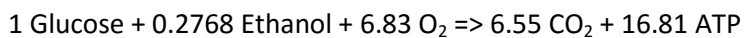
The catabolism of ethanol over acetate proceeds as follows:



This leads to the net ATP production from ethanol with O₂ to:



For the substrate mix, the catabolism of carbon can be summed up as follows:



Catabolism of 1 mol O₂ leads to (16.81/6.83)= 2.46 mol ATP/ mol O₂.

Appendix 4.C. The impact of futile cycling on the O₂ requirement

Figure 4.6 shows that there is an oxygen requirement of 1.41 ± 0.33 mol O₂/mol of C4 acids produced. From the material balance for C4 acids over the chemostat it follows that in chemostat experiments carried out at a constant dilution rate, an increase in the rate of product formation results in a proportional increase in the concentration of the product in the chemostat culture vessel:

$$C_{C4} = \frac{q_{C4} \cdot C_x}{D}$$

Thus in our chemostat experiments an increase in q_{C4} (due to increased P_{CO_2}) resulted in a proportional increase in the extracellular succinic acid concentration. During the 50% CO₂ experiment the concentration of extracellular un-dissociated succinic acid was 16 mM at pH 3.0. Using the permeability coefficient of 4×10^{-6} m h⁻¹ calculated by Jamalzadeh *et al.* in Suc 501 (25), the futile cycling rate of succinic acid can be estimated to be 4 mmol Cmol⁻¹ h⁻¹. This futile cycling (due to the export of 2H⁺ / mol C4 acids using H⁺ ATPase of 1 ATP/ mol H⁺) leads to 8 mmol ATP Cmol⁻¹ h⁻¹ consumption which requires an additional rate of O₂ consumption of $(8/(2.46)) = 3.25$ mol O₂ Cmol⁻¹ h⁻¹. The total biomass specific C4 acids secretion rate at 50% CO₂ was 21.17 mmol Cmol⁻¹ h⁻¹, therefore futile cycling increases the oxygen consumption per mol of secreted C4 acids by $(3.25/21.17) = 0.154$ mol O₂ per mol of C4 acids secreted. The experimentally observed oxygen consumption of 1.41 mol per mol of C4 acids produced (Figure 6) corresponds to an ATP requirement of $(1.41 \cdot 2.46) = 3.46$ mol ATP per mol secreted C4 acid. Because the production of C4 acids is ATP neutral, the measured ATP requirement must be associated with acid export. Assuming a uniport mechanism for export of the fully un-dissociated form, export of the acid requires 2 ATP (see above). This implies that there is an additional ATP consumption of $3.46 - 2 = 1.46$ mol ATP per mol of C4 acid produced. This additional ATP consumption and thereby extra O₂ consumption of $(1.46/(2.46)) = 0.59 (\pm 0.33)$ mol O₂/mol of C4 acids and can be explained by the futile cycling of succinic acid assuming its permeability to be $3.8 (\pm 2.14)$ fold higher than estimated in Suc 501.

The maintenance requirement taking into account the futile cycling of succinic acid, can be calculated using the three fold higher permeability coefficient of $3.8 \times 10^{-6} \text{ m h}^{-1}$ as follows:

$$m_{ATP} = m_{ATP,0} + 3.8 \left[8 \cdot \frac{q_{C4}}{21.17} \right] \quad 4.C1$$

$m_{ATP,0}$ is the maintenance in the absence of futile cycling of C4 acids which is estimated to be 71.33 mmol ATP.Cmol⁻¹.h⁻¹ (Figure 4.10). The maintenance including futile cycling in this experiment is dependent on q_{C4}

$$m_s = m_{s,0} + \delta q_{C4} \quad 4.C2$$

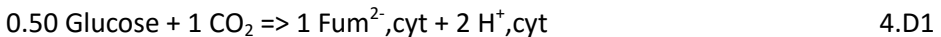
Where $m_{s,0}$ is the maintenance in the absence of the secretion of C4 acids, and δ is the futile cycling contribution of C4 acids to the maintenance. Combining eq. C2 with the Herbert-pirt equation gives:

$$q_s = (a\mu + m_{s,0}) + (b + \delta)q_{C4} \quad 4.C3$$

This shows that the slope between q_s and q_{C4} shown in Figure 6 is composed of the pathway part (b) and also futile cycling (δ).

Appendix 4.D. The cytosolic/mitochondrial fumarate/succinate exchange causes the stoichiometric coupling of the reductive and oxidative routes of C4 acid production

In the stoichiometric model fumarate is produced in the cytosol using the reductive pathway.



Cytosolic fumarate is exchanged to the mitochondria:



Succinate in the mitochondria is synthesized from mitochondrial fumarate and acetyl CoA synthesized from glycolysis and PDH:

Glycolysis: $0.50 \text{ Glucose} \Rightarrow 1 \text{ Pyr} + 1 \text{ NADH} + 1 \text{ ATP}$

PDH: $1 \text{ Pyr} \Rightarrow 1 \text{ AcCoA} + 1 \text{ CO}_2 + 1 \text{ NADH}$

Succinate in the mitochondria is synthesized via the oxidative route of the TCA cycle using acetyl CoA and Fum²⁻, mit:

MDH/ Fumarase: $1 \text{ Fum}^{2-}, \text{ mit} \Rightarrow 1 \text{ OAA} + 1 \text{ NADH}$

Citrate synthase: $1 \text{ OAA} + 1 \text{ AcCoA} \Rightarrow 1 \text{ Citrate}, \text{ mit}$

Oxidative TCA: $1 \text{ Citrate}, \text{ mit} \Rightarrow 2 \text{ CO}_2 + 2 \text{ NADH} + 1 \text{ Suc}^{2-}, \text{ mit} + 1 \text{ ATP}$

Summing up the reactions leads to the synthesis reaction of mitochondrial succinate from glucose and mitochondrial fumarate

$0.50 \text{ Glucose} + 1 \text{ Fum}^{2-}, \text{ mit} \Rightarrow 1 \text{ Suc}^{2-}, \text{ mit} + 2 \text{ ATP} + 3 \text{ CO}_2 + 5 \text{ NADH}$ 4.D3

Combining the above reactions (Reaction 4.D1, 4.D2 and 4.D3) leads to the succinate pathway reaction

$1 \text{ Glucose} \Rightarrow 1 \text{ Suc}^{2-}, \text{ cyt} + 2 \text{ CO}_2 + 5 \text{ NADH} + 2 \text{ ATP}$ 4.D4

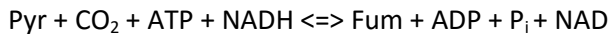
The result is the same as obtained from the oxidative route for succinic acid production, but now 50% of glucose carbon passes through the reductive route to form cytosolic fumarate and 50% passes through the oxidative route.

Appendix 4.E. Driving force towards cytosolic fumaric acid formation in Suc 501 and Suc 958

Figure 4.5A shows for Suc 501 and Suc 958 the correlation between q_{suc} and P_{CO_2} , and it appears that Suc 958 has approximately 2 fold higher q_{suc} . A possible explanation is that CO₂ is not the only contributor to the driving force of the reductive route. Therefore it is useful to define a measure of driving force towards cytosolic fumarate.

The reductive route starts with pyruvate carboxylase (PYC), PEP carboxykinase (PEPCK) or PEP carboxylase reactions.

Assuming that the pyruvate carboxylase (PYC) reaction is used for the reductive C4 route then the net reaction from pyruvate to fumarate is



For this route a measure of driving force (DF) can be defined by:

$$\text{DF}_{\text{PYC}} = \frac{[\text{PYR}]}{[\text{FUM}]} \frac{[\text{NADH}]}{[\text{NAD}]} \frac{[\text{ATP}]}{[\text{ADP.P}_i]} [P_{\text{CO}_2}] \quad 4.E1$$

Assuming PEP carboxykinase (PEPCK) is used then the net reaction from PEP to fumarate is



For this route a measure of driving force can be defined by:

$$\text{DF}_{\text{PEPCK}} = \frac{[\text{PEP}]}{[\text{FUM}]} \frac{[\text{NADH}]}{[\text{NAD}]} \frac{[\text{ADP.P}_i]}{[\text{ATP}]} [P_{\text{CO}_2}] \quad 4.E2$$

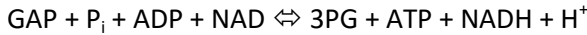
Assuming PEP carboxylase (PEPCx) is used then the net reaction from PEP to fumarate is



For this route a measure of driving force can be defined by:

$$DF_{PEPCx} = \frac{[PEP]}{[FUM]} \frac{[NADH]}{[NAD]} [P_{CO_2}] \quad 4.E3$$

We assume that the cytosolic NADH/NAD which is set by the combined GAPDH and PGK reaction (55).



From the combined reaction, the cytosolic NAD/NADH ratio can be calculated

$$K'_{GAPDH,PGK} = \frac{[NADH][H^+ / 10^{-7}]}{[NAD^+]} \frac{[ATP]}{[ADP.P_i]} \frac{[3PG]}{[GAP]}$$

This leads to the cytosolic redox ratio (NADH/NAD) of

$$\frac{[NADH]}{[NAD^+]} = K'_{GAPDH,PGK} \cdot 10^{7-pH} \frac{[GAP]}{[3PG]} \frac{[ADP.P_i]}{[ATP]} \quad 4.E4$$

The equilibrium constant $K'_{GAPDH,PGK}$ equals 113 M^{-1} as reported by Canelas *et al.* (55) at intracellular pH of 7.0. In Suc 501 intracellular GAP concentration was not measured therefore we introduced DHAP in eq. 4.E5. In Suc 958 strain, the equilibrium ratio of triose phosphate isomerase reaction (GAP/DHAP) was estimated to be 0.041, which is close to the equilibrium ratio of 0.039 estimated by Canelas *et al.* (55). In order to replace GAP by DHAP in eq. 4.E4, we multiplied eq. 4.E4 by the equilibrium constant of TPI reaction (0.041). This leads to

$$\frac{[NADH]}{[NAD^+]} = 4.63 \frac{[DHAP]}{[3PG]} \frac{[ADP.P_i]}{[ATP]}$$

4.E5

Replacing cytosolic NADH/NAD ratio by eq. 4.E5 in eq. 4.E1, 4.E2 and 4.E3 results in:

$$DF_{PYC} = 4.63 \cdot \frac{[PYR]}{[FUM]} \frac{[DHAP]}{[3PG]} \cdot [P_{CO_2}] \quad 4.E6$$

$$DF_{PEPCK} = 4.63 \cdot \frac{[PEP]}{[FUM]} \frac{[DHAP]}{[3PG]} \left[\frac{ADP \cdot P_i}{ATP} \right]^2 [P_{CO_2}] \quad 4.E7$$

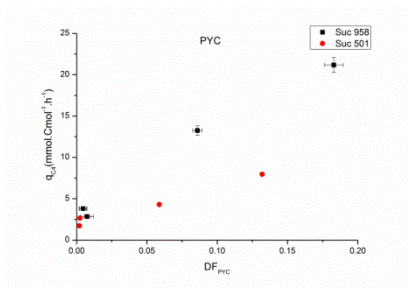
$$DF_{PEPCx} = 4.63 \cdot \frac{[PEP]}{[FUM]} \frac{[DHAP]}{[3PG]} \left[\frac{ADP \cdot P_i}{ATP} \right] [P_{CO_2}] \quad 4.E8$$

Intracellular ATP concentration and energy charge observed in Suc 501 (Table 4.E1) is much lower than expected indicating that the nucleotides measurement in Suc 501 are not reliable. Therefore for the calculation of DF_{PEPCK} and DF_{PEPCx} in Suc 501 we used the intracellular concentration of nucleotides (ATP and ADP) same as observed in Suc 958 strain. Intracellular concentration of inorganic phosphate (P_i) was assumed to be 25 mM (105).

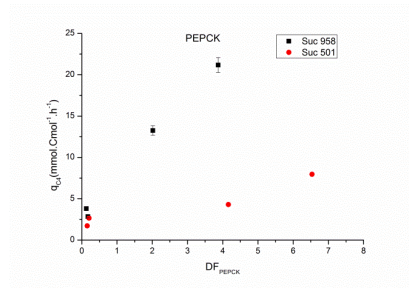
Figure 4.E1 shows the correlation between the secretion rate of C4 acids against the driving force of reductive route (via PYC, PEPCK or PEPCx) as obtained from eq. 4.E6, 4.E7 and 4.E8. Also we compared the ratios of the metabolites involved in DF_{PYC} (eq. 4.E6) (PYR/FUM, DHAP/3PG and NADH/NAD ratios) in order to understand the factors which increase the C4 q_{C4} production rate. None of these factors show the same behaviour for Suc 501 and Suc 958.

PEP/FUM ratio involved in the driving force using PEPCK and PEPCx reaction (eq. E7 and E8) dropped with increasing q_{C4} (Figure 4.E1) which was again compensated by increase in DHAP/3PG and P_{CO_2} . ATP/(ADP.Pi) ratio did not change significantly in all the steady states (Table 4.E1) and did not contribute towards the increase in the driving force.

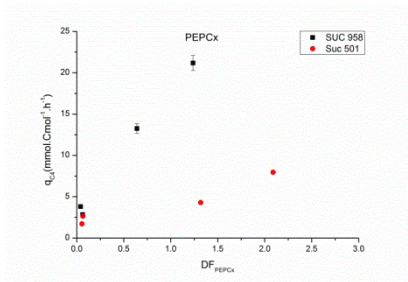
In summary, C4 production is increased by increasing NADH/NAD and DHAP/3PG ratio. However this does not explain the difference between Suc 501 and Suc 958 biomass specific C4 acids production rate. Therefore we also looked at the influence of the intracellular concentration of HCO_3^- on C4 acids production in the next section.



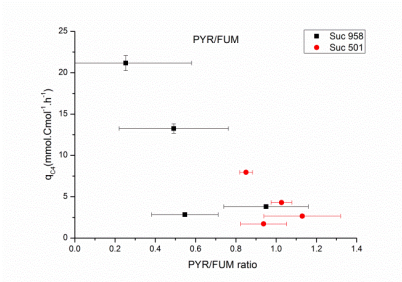
(a)



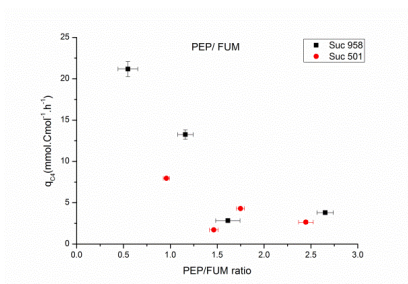
(b)



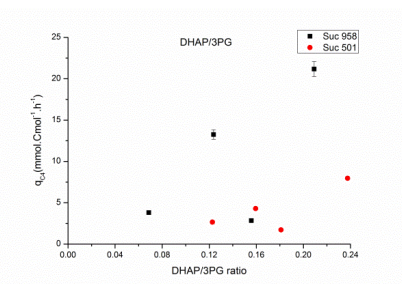
(c)



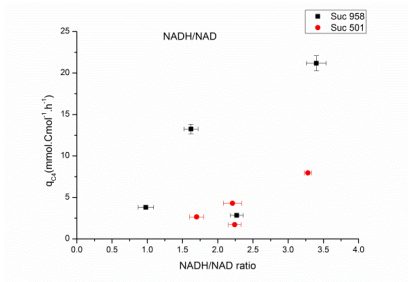
(d)



(e)



(f)



(g)

Figure4.E1. Steady state biomass specific C4 acids secretion (q_{C4}) against the driving force for the reductive route via (A) PYC (B) PEPCK and (C) PEPcX reactions. Q_{C4}

against D) PYR/FUM E) PEP/FUM ratios F) DHAP/3PG and G) cytosolic NADH/NAD ratios for Suc 958 (■) and Suc 501 (●).

Table 4.E1. Comparison of the intracellular and extracellular metabolites of Suc 958 and Suc 501 involved in the reductive pathway of TCA cycle

Strain		100% Air	Air/25% CO ₂	Air/50% CO ₂	100% Air
Suc 958	Succinate (EC, mM)	3.52 ± 0.44	10.97 ± 0.36	17.66 ± 0.58	2.36 ± 0.12
Suc 501	Succinate (EC, mM)	10.22 ± 0.66	18.52 ± 0.16	29.19 ± 0.23	6.37 ± 0.04
Suc 958	Pyruvate	1.06 ± 0.21	0.67 ± 0.17	0.34 ± 0.10	0.56 ± 0.09
Suc 501	Pyruvate	0.69 ± 0.12	0.73 ± 0.03	0.67 ± 0.02	0.83 ± 0.09
Suc 958	PEP	2.95 ± 0.14	1.58 ± 0.03	0.73 ± 0.02	1.64 ± 0.21
Suc 501	PEP	1.50 ± 0.02	1.24 ± 0.05	0.76 ± 0.02	1.30 ± 0.05
Suc 958	ATP	13.10 ± 0.20	13.46 ± 0.43	12.12 ± 0.41	14.85 ± 0.02
Suc 501	ATP	5.28 ± 0.27	5.13 ± 0.17	5.13 ± 0.06	5.15 ± 0.19
Suc 958	ADP	1.65 ± 0.03	1.70 ± 0.05	1.52 ± 0.03	1.67 ± 0.02
Suc 501	ADP	2.67 ± 0.19	2.70 ± 0.08	2.89 ± 0.09	3.5 ± 0.1
Suc 958	Energycharge	0.91 ± 0.02	0.92 ± 0.02	0.92 ± 0.03	0.93 ± 0.02
Suc 501	Energycharge	0.78 ± 0.09	0.78 ± 0.05	0.77 ± 0.03	0.74 ± 0.05
Suc 958	NADH/NAD ratio	0.98 ± 0.11	1.62 ± 0.10	3.40 ± 0.15	2.27 ± 0.09
Suc 501	NADH/NAD ratio	1.70 ± 0.10	2.21 ± 0.13	3.28 ± 0.05	2.24 ± 0.09
Suc	Malate	6.20 ± 0.53	7.87 ± 0.35	8.73 ± 0.60	5.37 ± 0.01

958					
Suc 501	Malate	3.48 ± 0.15	4.24 ± 0.11	4.68 ± 0.12	4.45 ± 0.08
Suc 958	Fumarate	1.11 ± 0.08	1.36 ± 0.11	1.33 ± 0.14	1.02 ± 0.00
Suc 501	Fumarate	0.61 ± 0.05	0.71 ± 0.01	0.79 ± 0.01	0.88 ± 0.01
Suc 958	Succinate	2.25 ± 0.38	10.36 ± 2.67	14.95 ± 2.22	2.44 ± 0.28
Suc 501	Succinate	5.10 ± 0.44	10.20 ± 0.81	15.64 ± 0.13	3.09 ± 0.18
Suc 958	Fumarase (Mal/Fum)	5.56 ± 0.18	5.77 ± 0.27	6.57 ± 0.18	5.28 ± 0.11
Suc 501	Fumarase (Mal/Fum)	5.67 ± 0.09	6.00 ± 0.03	5.90 ± 0.03	5.01 ± 0.03

Influence of the intracellular concentration of HCO_3^- on succinic acid secretion rates

Using Henry's law and partial pressure of CO_2 , the CO_2 concentration in the broth was calculated as shown in Table 4.E2.

Table 4.E2. Solubility of CO_2 at different partial pressures of CO_2 at 303K.

P_{CO_2} (Partial pressure) (in Bar)	CO_2 solubility(mM)
0.02	0.69
0.34	14.97
0.67	29.26
0.02	0.74

pK_1 of CO_2 dissociation was corrected for the ionic strength of cytoplasm which was assumed to be 0.25 M. The correction was done using Debye Huckel

equation. pK_1 is 6.35 at ionic strength of 0 and 6.08 at ionic strength of 0.25M.

It has been reported that the cytosolic pH of *S. cerevisiae* increases with increasing growth rate (102). At growth rate of 0.10 h⁻¹ cytosolic pH was assumed to be 7.0 and at a growth rate of 0.05 h⁻¹ cytosolic pH was assumed to be 6.30. With this difference in cytosolic pH there is a significant difference in the ratio of HCO₃⁻/CO₂. HCO₃⁻ is used as a substrate by pyruvate carboxylase and as shown in Table 4.E3 that in Suc 958 the intracellular concentration of HCO₃⁻ is much higher than Suc 501 due to cytosolic pH difference.

Table 4.E3. Cytosolic concentration of HCO₃⁻ in Suc 958 and Suc 501 with cytosolic pH of 7.0 and 6.3 respectively.

Steady state	CO ₂ (mM)	HCO ₃ ⁻ /CO ₂	HCO ₃ ⁻ /CO ₂	HCO ₃ ⁻	HCO ₃ ⁻
		ratio Suc 958 (pH 7.0)	ratio Suc 501 (pH 6.3)	(mM) Suc 958	(mM) Suc 501
Air	0.69	8.31	1.66	5.71	1.14
25% CO ₂	14.97	8.31	1.66	124.5	24.85
50% CO ₂	29.26	8.31	1.66	243.3	48.56
Air	0.74	8.31	1.66	6.1	1.23

Table 4.E4 compares the experimentally obtained out/in ratio of succinic acid estimated from the combined data obtained from Suc 501 and Suc 958. Suc out/in ratio varies significantly with the change in cytosolic pH and with change in proton motive force of the membrane as shown in Figure E2.

Table 4.E4: Thermodynamically calculated total acid ratios (out/in) at equilibrium for succinate using uniport mechanism for Suc^{2-} with $\text{pH}_{\text{out}} = 3.0$, and using different pH_{in} and pmf compared with the experimental ratios. The calculation of out/in ratios is described by Shah *et al.* (80).

Transported molecule	Uniport Equilibrium out/in ratio $\text{pH}_{\text{in}}=7.0$ $\text{pmf}=150\text{mV}$	Uniport Equilibrium out/in ratio $\text{pH}_{\text{in}}=6.3$ $\text{pmf}=150\text{mV}$	Uniport Equilibrium out/in ratio $\text{pH}_{\text{in}}=6.3$ $\text{pmf}=106\text{mV}$	Experimentally obtained ratios for Suc 958 strain ($D=0.10\text{h}^{-1}$)	Experimentally obtained ratios for Suc 501 strain ($D=0.05\text{h}^{-1}$)
Suc^{2-}	7.02	150.91	5.22	4.03 ± 0.31	4.03 ± 0.31

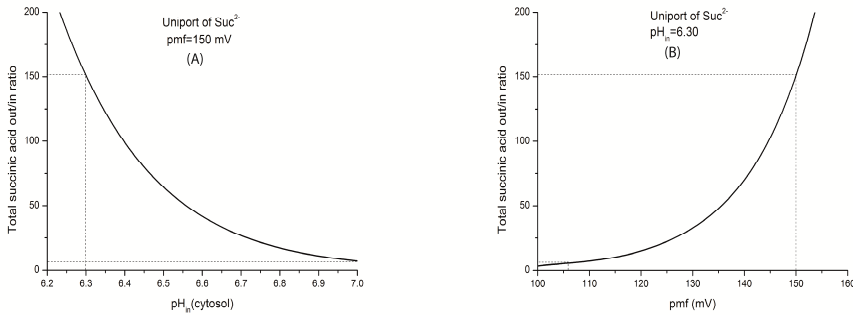


Figure 4.E2. (a) Change in total succinic acid out/in ratio against the cytosolic pH (pH_{in}) with pmf of 150 mV. (b) Change in total succinic acid out/in ratio against the pmf with pH_{in} of 7.0. Dashed lines (---) represents the values shown in Table 4.E4.

Supplementary Data:

Table 4.S1. Suc 958: Extracellular concentrations (mM) of secreted metabolites at different concentration of CO₂ in the inlet air, in aerobic glucose limited chemostat (D= 0.10 h⁻¹ and pH =3.0)

Time (h)	O ₂ (%)	Glucose	Glycerol	Fumarate	Succinate	Malate	Pyruvate
21.05	0.037	0.84	0.00	0.02	4.81	3.89	0.08
25.72	0.037	0.82	0.00	0.02	2.91	2.33	0.06
30.07	0.037	1.03	0.42	0.02	3.14	1.47	0.06
46.25	0.037	0.84	0.00	0.02	3.21	2.46	0.08
54.2	25	1.16	1.44	0.06	10.22	2.47	0.06
69.41	25	1.34	0.47	0.07	12.42	2.32	0.05
77.17	25	1.29	0.42	0.07	10.02	1.77	0.05
94.5	25	1.20	0.37	0.06	11.32	2.05	0.05
99.54	25	1.08	0.34	0.06	11.18	2.06	0.06
117.62	25	1.17	0.37	0.06	18.37	3.48	0.09
144	25	1.12	0.35	0.07	10.64	1.98	0.05
165.23	50	1.32	0.58	0.10	16.64	2.22	0.05
173.64	50	1.58	0.71	0.12	7.53	0.99	0.02
189.86	50	1.26	0.61	0.10	17.70	2.27	0.05
197.23	50	1.02	0.54	0.09	18.64	2.26	0.05
213.69	0.037	0.92	0.00	0.03	2.58	1.56	0.05
225.51	0.037	0.50	0.00	0.02	2.16	1.45	0.05
237.71	0.037	0.55	0.00	0.02	2.33	1.51	0.03

Table 4.S2. Suc steady state mass action ratios at different CO₂ concentration in the inlet gas compared with the corresponding intracellular flux observed through that reaction

	Air		25% CO ₂		50% CO ₂		Air	
	Ratio	Flux (mmol/Cmol h)	Ratio	Flux (mmol/Cmol h)	Ratio	Flux (mmol/Cmol h)	Ratio	Flux (mmol/Cmol h)
F6P/G6P (PGI)	0.29 ± 0.02	27.88	0.28 ± 0.02	35.5	0.25 ± 0.02	40.44	0.28 ± 0.02	27.82
G3P/DHAP (TPI)	0.12 ± 0.01	16.65	0.06 ± 0.01	24.41	0.06 ± 0.02	29.51	0.09 ± 0.01	16.81
2PG/3PG (PGM)	0.10 ± 0.01	34.39	0.10 ± 0.01	49.63	0.09 ± 0.00	59.57	0.10 ± 0.01	34.67
PEP/2PG (ENO)	4.29 ± 0.30	34.39	3.41 ± 0.12	49.63	2.71 ± 0.07	59.57	3.81 ± 0.64	34.67
MAL/FUM (FUMIR)	5.57 ± 0.62	16.60	5.78 ± 0.53	14.56	6.57 ± 0.81	9.94	5.28 ± 0.01	18.75
Fum/Succ (SDH)	0.49 ± 0.09	15.6	0.13 ± 0.04	13.59	0.09 ± 0.02	9.00	0.42 ± 0.05	17.76
Isocit/citrate (ACON)	0.02 ± 0.00	20.86	0.04 ± 0.00	27.77	0.06 ± 0.01	30.77	0.02 ± 0.00	22.44
AKG/Isocit (ICIT)	7.25 ± 1.29	18.36	7.14 ± 0.79	25.23	5.42 ± 0.85	28.21	7.97 ± 0.54	19.98

Table 4.S3. Suc 501: Intracellular metabolite levels (in $\mu\text{mol}/\text{g DCW}$) at different CO₂ supply regimes compared with the wild type strain, in a glucose limited chemostat ($D=0.05\text{ h}^{-1}$, $\text{pH}=3.0$)

Metabolite	Wild type 100% Air	Phase I 100% Air	Phase II Air/25% CO ₂	Phase III Air/50% CO ₂	Phase IV 100% Air
Glu_in	3.39 ± 0.19	1.90 ± 0.23	6.42 ± 0.13	2.90 ± 0.22	0.86 ± 0.11
G6P	5.46 ± 0.19	4.16 ± 0.05	3.65 ± 0.05	3.64 ± 0.05	4.00 ± 0.04
F6P	1.22 ± 0.07	0.86 ± 0.01	0.78 ± 0.07	0.81 ± 0.03	0.70 ± 0.03
FBP	0.28 ± 0.02	0.38 ± 0.02	0.41 ± 0.06	0.46 ± 0.01	0.44 ± 0.02
2PG	0.55 ± 0.01	0.41 ± 0.03	0.36 ± 0.01	0.263 ± 0.001	0.39 ± 0.01
3PG	4.6 ± 0.1	3.75 ± 0.29	3.63 ± 0.06	2.63 ± 0.01	3.65 ± 0.02
GAP	0.02 ± 0.01	0.061 ± 0.002	0.036 ± 0.002	0.037 ± 0.002	0.057 ± 0.002
DHAP	0.36 ± 0.04	0.3 ± 0.1	0.34 ± 0.02	0.356 ± 0.006	0.394 ± 0.013
PEP	1.49 ± 0.36	1.50 ± 0.02	1.24 ± 0.05	0.76 ± 0.02	1.30 ± 0.05
Pyruvate	0.44 ± 0.04	0.69 ± 0.12	0.73 ± 0.03	0.67 ± 0.02	0.83 ± 0.09
Citrate	16.9 ± 0.2	7.87 ± 0.61	3.60 ± 0.08	3.63 ± 0.06	9.27 ± 0.23
Isocitrate	0.26 ± 0.02	0.14 ± 0.03	0.105 ± 0.001	0.12 ± 0.01	0.14 ± 0.01
AKG	0.50 ± 0.07	1.10 ± 0.03	0.70 ± 0.01	0.57 ± 0.01	1.17 ± 0.02
Succinate	1.40 ± 0.25	5.09 ± 0.45	10.2 ± 0.8	15.64 ± 0.13	3.08 ± 0.18
Fumarate	1.89 ± 0.19	0.61 ± 0.05	0.71 ± 0.01	0.79 ± 0.01	0.88 ± 0.01
Malate	4.18 ± 0.31	3.48 ± 0.15	4.24 ± 0.11	4.68 ± 0.12	4.45 ± 0.08
Aspartate	8.9 ± 0.5	9.45 ± 2.40	14.39 ± 0.19	15.63 ± 0.49	13.51 ± 0.06
UDP-Glucose	3.42 ± 0.14	2.68 ± 0.09	2.98 ± 0.05	2.48 ± 0.09	2.53 ± 0.04
Trehalose	41.9 ± 2.9	84.3 ± 5.1	78.4 ± 1.5	63.2 ± 0.7	96.6 ± 0.17
T6P	0.12 ± 0.01	0.24 ± 0.01	0.24 ± 0.01	0.199 ± 0.004	0.260 ± 0.005
Manitol-6P	2.25 ± 0.07	1.24 ± 0.02	1.13 ± 0.02	1.141 ± 0.004	1.26 ± 0.03
6PG	0.36 ± 0.03	0.405 ± 0.001	0.52 ± 0.02	0.48 ± 0.01	0.334 ± 0.005
Rbu5P	0.133 ± 0.001	0.20 ± 0.03	0.189 ± 0.001	0.160 ± 0.004	0.190 ± 0.002
X5P	0.29 ± 0.01	0.48 ± 0.09	0.46 ± 0.01	0.376 ± 0.006	0.47 ± 0.02
R5P	0.35 ± 0.02	0.37 ± 0.03	0.322 ± 0.003	0.29 ± 0.01	0.335 ± 0.011
S7P	2.01 ± 0.02	2.7 ± 0.3	1.55 ± 0.10	1.11 ± 0.02	1.54 ± 0.04
E4P	0.043 ± 0.002	0.018 ± 0.002	0.024 ± 0.001	0.028 ± 0.001	0.023 ± 0.001
AMP	0.22 ± 0.03	0.50 ± 0.11	0.52 ± 0.04	0.57 ± 0.02	0.72 ± 0.01
ADP	1.51 ± 0.06	2.67 ± 0.19	2.70 ± 0.08	2.89 ± 0.09	3.5 ± 0.1
ATP	4.9 ± 0.2	5.28 ± 0.27	5.13 ± 0.17	5.13 ± 0.06	5.15 ± 0.19
NAD	1.45 ± 0.12	0.129 ± 0.004	0.129 ± 0.002	0.1270 ± 0.0001	0.1370 ± 0.0003
NADH	0.66 ± 0.06	0.75 ± 0.11	0.91 ± 0.02	0.99 ± 0.03	0.94 ± 0.03
CoA	0.075 ± 0.003	0.08 ± 0.01	0.11 ± 0.01	0.12 ± 0.01	0.082 ± 0.003
Acetyl-CoA	0.201 ± 0.005	0.34 ± 0.03	0.40 ± 0.02	0.46 ± 0.02	0.30 ± 0.01
Energy charge	0.85 ± 0.06	0.78 ± 0.09	0.77 ± 0.05	0.76 ± 0.03	0.73 ± 0.04

Table 4.S4. Suc 958: Intracellular metabolite levels (in $\mu\text{mol}/\text{g DCW}$) at different CO_2 supply regimes, in a glucose limited chemostat ($D=0.10\text{ h}^{-1}$, $\text{pH}=3.0$)

Metabolite	Wild type 100% Air	Phase I 100% Air	Phase II Air/25% CO_2	Phase III Air/50% CO_2	Phase IV 100% Air				
G6P	8.73	6.35	0.3	6.15	0.3	5.64	0.2	5.35	0.2
F6P	2.38	1.85	0.0	1.73	0.1	1.43	0.1	1.50	0.0
FBP	0.98	0.35	0.0	0.54	0.0	0.92	0.0	0.83	0.1
2PG	0.39	0.69	0.0	0.46	0.0	0.27	0.0	0.43	0.0
3PG	3.99	6.69	0.4	4.67	0.1	2.98	0.0	4.24	0.3
GAP	0.04	0.02	0.0	0.02	0.0	0.03	0.0	0.03	0.0
DHAP	0.60	0.46	0.0	0.58	0.0	0.62	0.0	0.66	0.0
PEP	1.20	2.95	0.1	1.58	0.0	0.73	0.0	1.64	0.2
Pyruvate	0.66	1.06	0.2	0.67	0.1	0.34	0.1	0.56	0.0
OAA	0.00	0.02 \pm	0.0	0.02 \pm	0.0	0.02 \pm	0.0	0.01 \pm	0.0
Citrate	7.04	7.88	0.2	3.56	0.0	3.07	0.3	7.44	0.0
Isocitrate	0.17	0.16	0.0	0.13	0.0	0.17	0.0	0.17	0.0
AKG	0.51	1.16	0.2	0.95	0.0	0.95	0.0	1.37	0.0
Succinate	0.82	2.25	0.3	10.36	2.6	14.95	2.2	2.44	0.2
Fumarate	0.49	1.11	0.0	1.36	0.1	1.33	0.1	1.02	0.0
Malate	1.78	6.20	0.5	7.87	0.3	8.73	0.6	5.37	0.0
Aspartate	6.45	18.1 \pm	1.8	21.15	1.9	16.97	1.1	18.03	0.6
UDP-glucose	N.M	4.03	0.2	4.29	0.2	3.62	0.0	3.78	0.1
Trehalose	N.M	N.M		N.M		N.M		N.M	
T6P	N.M	0.26	0.0	0.11	0.0	0.07	0.0	0.19	0.0
M6P	N.M	2.04	0.1	1.92	0.0	1.82	0.1	1.64	0.0
6PG	0.56	0.71	0.0	0.91	0.0	0.79	0.0	0.63	0.0
G1P	N.M	0.36	0.0	0.34	0.0	0.28	0.0	0.28	0.0
Glyox	N.M	0.06 \pm	0.0	0.08 \pm	0.0	0.05 \pm	0.0	0.05 \pm	0.0
AMP	N.M	0.48 \pm	0.0	0.37 \pm	0.0	0.43 \pm	0.0	0.38 \pm	0.1
ADP	N.M	1.65 \pm	0.0	1.70 \pm	0.0	1.52 \pm	0.0	1.67 \pm	0.0
ATP	N.M	13.10	0.2	13.46	0.4	12.12	0.4	14.85	0.0
CoA	N.M	0.79 \pm	0.0	1.26 \pm	0.0	1.04 \pm	0.0	1.15 \pm	0.2
AccoA	N.M	0.22 \pm	0.0	0.24 \pm	0.0	0.19 \pm	0.0	0.21 \pm	0.0
Energy charge	N.M	0.91 \pm	0.0	0.92 \pm	0.0	0.92 \pm	0.0	0.93	0.0

Chapter 5

Evolution of engineered *Saccharomyces cerevisiae* for the aerobic production of dicarboxylic acids

Abstract

The study explores an evolution approach to produce fumaric acid from engineered *S. cerevisiae*. Fumarase (FUM1) and glucose 6-phosphate dehydrogenase (ZWF1) genes were knocked out from *S. cerevisiae* in order to make fumaric acid as the energetically most favorable catabolic product in aerobic conditions and couple its ATP production to biomass formation. The study was done using two strains: Fum 114 (Δ FUM1, Δ ZWF1) and Fum 116 (Δ FUM1, Δ ZWF1, \uparrow DCT-02). The heterologous dicarboxylic acid transporter (DCT-02) in Fum 116 was used as a template protein which could evolve into a fumaric acid exporter. The evolution experiments were done in aerobic, glucose limited chemostats at a controlled dilution rate of 0.10 h^{-1} and at pH 5.0 for duration of 220 days. During evolution, as expected, biomass yield improved in Fum 114 (from 0.09 to 0.18 g.g^{-1} of glucose) and Fum 116 (from 0.12 to 0.17 g.g^{-1} of glucose) but no improvement in fumaric acid yield (0.008 to $0.01 \text{ mol.mol}^{-1}$ glucose in Fum 114; 0.005 to $0.009 \text{ mol.mol}^{-1}$ glucose in Fum 116) was observed. The gain in biomass yield of Fum 114 was attained by lowering ethanol secretion and improving acetate secretion rate. Unexpectedly, Fum 116 produced significant amounts of malic acid, with its export most probably facilitated by the DCT-02 transporter. Redox imbalance was observed in the metabolic network with ZWF1 and FUM1 knock-out, the network estimated much lower respiration rates (q_{O_2} and q_{CO_2}) than observed experimentally. This redox imbalance indicates a flux from fumarate to malate in the absence of FUM1. In order to solve the redox imbalance, the fumarase reaction was incorporated back into the metabolic network. The flux and metabolite analysis of the fumarate-malate reaction showed that the reaction is irreversible and the flux shows a linear relationship with the intracellular fumarate concentration. Also the reaction rate from fumarate to malate increased with time. This suggests that this reaction is performed by an unknown hydratase with low activity and low affinity for fumarate. The intracellular concentration of fumaric acid in Fum 114 and Fum 116 was at least 40 fold higher compared to the wild type CEN.PK 113-7D which indicates export as a major metabolic bottleneck in its production. Maintenance requirements of Fum 114 and Fum 116 were significantly higher due to the futile cycling of the secreted acetic acid. The permeability of acetic acid was estimated from the extra maintenance observed, and it was found that

permeability dropped significantly with evolution. The yield of malic acid in Fum 116 improved from 0.28 mol.mol⁻¹ glucose at the start to 0.43 mol.mol⁻¹ glucose at the end of the evolution experiment, with its export facilitated by DCT-02.

Introduction

Fumaric acid is an industrially relevant chemical with applications in the food and polymer industry (1)(4). Its current production process is dependent on the crude oil availability (2), eventually this process has to be replaced by a sustainable alternative route of production for example through a fermentation process using a renewable feedstock. In this study we have used *S. cerevisiae* to produce fumaric acid. *S. cerevisiae* is a well characterized organism which is used in many industrial scale fermentation processes to produce relevant chemicals. It is a well-studied organism with the ability to grow at low pH, which is preferred as the production of organic acid at low pH ($\text{pH} < \text{pK}$) reduces the downstream processing costs (12). The focus of this study is to evolve engineered *S. cerevisiae* into a fumaric acid producer.

In *S. cerevisiae* fumaric acid can be produced via the oxidative or the reductive part of the TCA cycle, and also through the glyoxylate route (Figure 5.1). Some studies have reported improved fumaric acid production by overexpressing the reductive part of the TCA cycle in *S. cerevisiae* (31), or with the simultaneous use of oxidative and reductive part in *S. cerevisiae* (32), by overexpressing the enzymes of the glyoxylate shunt in *E. coli* (106). Fumaric acid production has also been improved by engineering the urea and nucleotide cycle in *Torulopsis glabrata* (107) and *E. coli* (108). All these studies were done at pH 5.0 or higher, under aerobic conditions. The highest yield of fumaric acid obtained was $0.60 \text{ mol.mol glucose}^{-1}$ in an engineered *E. coli* strain (106). The yield of fumaric acid obtained from these engineered organisms is far below the theoretical maximum yield of $2 \text{ mol.mol glucose}^{-1}$. In these engineered strains the most likely metabolic bottleneck towards fumaric acid production would be its export. To improve the secretion rate of fumaric acid, SpMAE1 transporter from *Schizosaccharomyces pombe* was expressed in *Torulopsis glabrata* (107)(109), but apart from these, in none of the above mentioned engineered organisms a heterologous transporter was inserted to facilitate fumaric acid export. It has been reported that wild type and engineered *Rhizopus spp.* can produce fumaric acid at neutral pH with yields of $1 \text{ mol.mol glucose}^{-1}$ and $1.21 \text{ mol.mol glucose}^{-1}$ respectively (91) which suggests the presence of an efficient fumaric acid exporter. To produce fumaric acid from *S. cerevisiae*, an efficient export mechanism would be needed. However, no

information is available on the mechanism of fumaric acid export in *Rhizopus spp.* and the transporter protein(s) involved. In this study, evolution approach was used with engineered *S. cerevisiae* in order to select for the cells that can efficiently export fumaric acid.

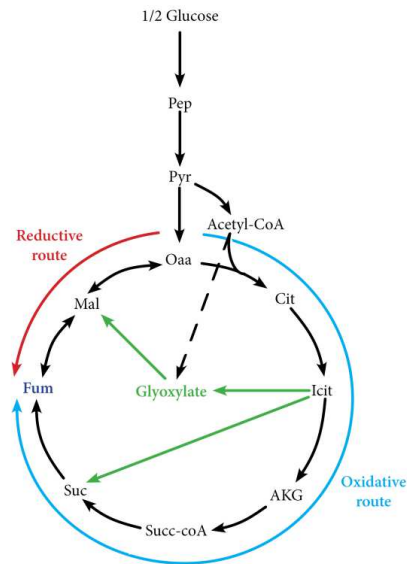


Figure5.1. Metabolic routes towards fumaric acid formation

Evolution approach

A genome scale model of *S. cerevisiae* (110) was used to find an optimal knock out strategy that couples fumaric acid production to biomass formation (25). Strains were engineered to make fumaric acid as a catabolic product with the knock-out of fumarase (FUM1) and glucose 6-phosphate dehydrogenase (ZWF1), as shown in Figure 5.2. The yield of ATP per mol glucose consumed with the secretion of a particular metabolite for Fum 114 and Fum 116 is shown in Table 5.1, with secretion of fumarate achieving the highest yield of ATP per mol glucose (with P/O ratio of 1.18 (52)). Thereby the strains producing fumaric acid will have higher biomass yield due to higher ATP yield per mol of glucose consumed. During the course of the evolution experiment we expect that the population of fumaric acid producing *S. cerevisiae* cells will

gradually increase and with that the productivity of fumaric acid. A heterologous dicarboxylic acid transporter DCT-02 from *Aspergillus niger* was also expressed in Fum 116 (27), although in a previous study it was clear that DCT-02 transporter was able to export succinate and malate but not fumarate (111). In this study the DCT-02 transporter was used as a template protein which is expected to evolve to improve its affinity and capacity to export fumarate.

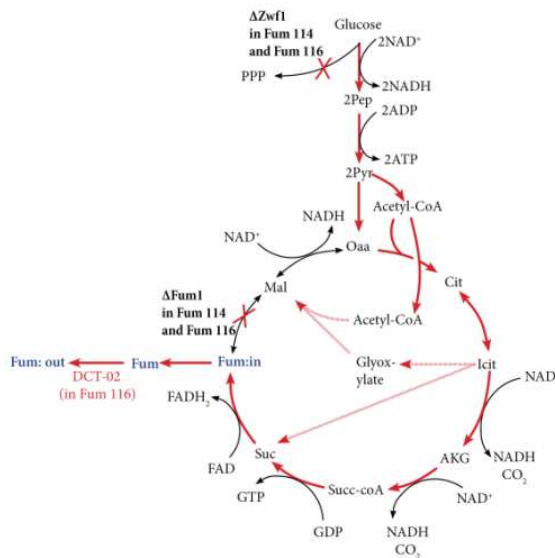


Figure 5.2. Evolution strategy: Disruption of FUM1 and ZWF1 genes in Fum 114 and Fum 116. Fum 116 also expresses the DCT-02 transporter in the cell membrane to facilitate dicarboxylic acids export from cytosol.

Table5.1. Production of ATP from the metabolism of glucose into different catabolic products in the engineered *S. cerevisiae* (Δ FUM1, Δ ZWF1) in aerobic conditions.

Pathway for ATP production	Catabolic reaction for the conversion of 1 mol of glucose to intracellular product and H ⁺	mol ATP produced/ mol of glucose catabolized	mol ATP / mol glucose catabolized considering the energy required in the export of metabolite and H ⁺
Pyruvate	-1 Glucose - O ₂ + 2 Pyruvate + 2H ⁺ + 4.36 ATP	4.36	2.36
Glycerol	-7/6 Glucose -1 H ₂ O + 2 Glycerol - 13/6 ATP + 1 CO ₂	-2.16	-2.16
Ethanol	-1 Glucose + 2 CO ₂ + 2 Ethanol + 2 ATP	2	2
Acetate	-1 Glucose -2 O ₂ + 2 Acetate + 2H ⁺ + 2 CO ₂ + 6.72 ATP	6.72	4.72
Malate (via reductive)	-1 Glucose + 2 Malate + 4H ⁺ - 2 CO ₂ + 0 ATP	0	-4
Malate and succinate (via glyoxylate pathway)	-1 Glucose - 5/3 O ₂ + 2/3 Malate + 2/3 Succinate + 8/3 H ⁺ + 5.26 ATP + 2/3 CO ₂	5.26	2.59
Citrate	-1 Glucose -1.5 O ₂ + Citrate + 3H ⁺ + 4.54 ATP	4.54	1.54
AKG	-1 Glucose -2 O ₂ + AKG + 2H ⁺ + 1 CO ₂ + 5.72 ATP	5.72	3.72
Succinate (via oxidative)	-1 Glucose -2.5 O ₂ + 1 Succinate + 2H ⁺ + 2 CO ₂ + 7.9 ATP	7.9	5.9
Fumarate (via oxidative)	-1 Glucose -3O₂ + 1 Fumarate + 2H⁺ + 2 CO₂ + 9.08 ATP	9.08	7.08

*Export of all organic acids was assumed to be via uniport mechanism of the fully dissociated form, and export of glycerol through permease

*P/O ratio of 1.18 (52)

*Export of H⁺ by H⁺/ATPase with a stoichiometry of 1

Materials and Methods

Strains

Saccharomyces cerevisiae CEN.PK 2_1C was used for genetic modifications. CEN.PK 2_1C (genotype MATa; ura3-52; trp1-289; leu2-3,112; his3 D1; MAL2-8C; SUC2) contains nutrient auxotrophy which facilitates genetic engineering using the selection markers for the transformed cells.

Fum 114 and Fum 116 were constructed from CEN.PK 2-1C. In Fum 114, ZWF1 gene which expresses glucose-6-phosphate dehydrogenase enzyme and FUM1 gene which expresses fumarase enzyme were disrupted. Fum 116 strain was derived from Fum 114; in addition to the two disrupted genes in Fum 114, Fum 116 also expresses a heterologous transporter DCT-02. Schematic representations of the genetic modifications in Fum 114 and Fum 116 are shown in Figure 5.1.

Strain construction

CEN.PK 2_1C was transformed using the lithium acetate method as described by Gietz *et al.* (112). The gene disruption method relies on the ability of *S. cerevisiae* for efficient and accurate homologous recombination with single stranded DNA of 20bp and greater. Using the methods and vectors (pUG6, pSH47) described by Guldener *et al.* (113) it allows for sequential gene disruptions by recovering the sensitivity of the selection marker, in this case the selection marker used was URA3 which eliminates the uracil auxotrophy in the transformed CEN.PK 2-1C.

Fum 116 was derived from Fum 114 by integrating a heterologous DCT-02 transporter gene into its genome. The procedure of integrating the DCT-02 gene in CEN.PK 21-C genome was same as described in the patent by DSM IP ASSETS B.V. (26).

Shake flask cultivation to assess dicarboxylic acids production

To check for C4 dicarboxylic acids production potential of Fum 114 and Fum 116, the strains were incubated in aerobic shake flasks under N-source starved conditions at a high concentration of glucose. Prior to the transfer to nitrogen starved media, strains were first cultivated for biomass formation in shake flasks with media containing 20 g.L⁻¹ glucose.H₂O, 5 g.L⁻¹ (NH₄)₂SO₄, 3 g.L⁻¹ KH₂PO₄, 0.5 g.L⁻¹ MgSO₄.7H₂O, 1ml.L⁻¹ trace mineral solution and 1ml.L⁻¹ vitamin solution. 0.015 g.L⁻¹ uracil, 0.5 g.L⁻¹ leucine, 0.0125 g.L⁻¹ histidine, 0.075 g.L⁻¹ tryptophan and 0.15 g.L⁻¹ methionine were also added to the media due to the auxotrophy of CEN.PK 2_1C (114). The shake flask cultures were incubated overnight at 30°C on a gyratory shaker at 200 rpm. After overnight growth, the whole culture was centrifuged at 5000g for 10 minutes and washed with demineralized water and centrifuged again. The biomass pellet was re-suspended in production medium without nitrogen source containing: 100 g.L⁻¹ glucose.H₂O, 50 g.L⁻¹ CaCO₃, 1 ml.L⁻¹ trace element and 1 ml.L⁻¹ vitamin solution. CaCO₃ was used as a buffering agent in order to maintain the pH between 6.0 and 6.5.

Media preparation and fermentation conditions for chemostat cultivations

The chemostat feeding medium for Fum 116 contained 8.25 g.L⁻¹ glucose.H₂O, 0.30 g.L⁻¹ (NH₄)₂SO₄, 3.0 g.L⁻¹ NH₄H₂PO₄, 0.30 g.L⁻¹ KH₂PO₄, 0.50 g.L⁻¹ MgSO₄.7H₂O, 1ml.L⁻¹ trace mineral solution, 1ml.L⁻¹ vitamin solution as described by Canelas *et al.* (45). Feed media also contained 0.015 g.L⁻¹ uracil, 0.5 g.L⁻¹ leucine, 0.0125 g.L⁻¹ histidine, 0.075 g.L⁻¹ tryptophan, and 0.15 g.L⁻¹ methionine in order to supplement the auxotrophy of CEN.PK2_1C. Feed media containing all the components were filter sterilized into an empty 50 L heat-sterilized vessel (at 110 °C for 20 min).

In chemostat cultivation of Fum 114 the feeding media contained 9.9 g.L⁻¹ of glucose.H₂O instead of 8.25 g.L⁻¹ glucose.H₂O used for Fum 116 and CEN.PK 113-7D. The feed medium of wild type CEN.PK 113-7D also contained 0.50 g.L⁻¹

of ethanol apart from glucose as a carbon source in order to prevent oscillations.

A 1 L fermenter (Applikon, The Netherlands) with 0.5 L working volume was used for chemostat cultivation. The steady state in the chemostat was maintained by controlling the volume in the fermenter with a level sensor. The exact mass of the broth was measured at the end of the chemostat by weighing the broth. The fermentation was performed at a stirrer speed of 800 rpm with overpressure of 0.30 Bar (in order to facilitate the rapid sampling procedure for intracellular metabolites) and aeration rate of 0.60 vvm. Temperature was controlled at 30°C and measured with a temperature probe. The pH was measured with pH-probe (Mettler-Toledo) and was maintained at 5.0 by adding 4M KOH. Dissolved oxygen (DO) was measured in situ through an oxygen probe (Mettler-Toledo), and was always above 80% air saturation. Oxygen and carbon dioxide concentrations in the off-gas were measured at-line with a combined paramagnetic/infrared analyzer (NGA 2000, Rosemount).

The chemostat phase was initiated by switching on the feeding at the end of batch phase, observed from a sudden drop of the CO₂ concentration in the off-gas. During the course of the evolution experiment, a dilution rate of 0.10 h⁻¹ was maintained by checking the weight of the effluent vessel intermittently.

The chemostat evolution experiments were carried out for approximately 200 days by replacing the medium vessel and providing fresh base solution for the pH control when required. Samples were taken intermittently to measure the dry weight, extracellular and intracellular metabolites.

Quantification of extracellular and intracellular metabolites

Filtrate samples for extracellular metabolites were taken by the cold filtration method (49). Glycerol, acetate and ethanol were quantified through HPLC analysis using a Bio-Rad HPX-87H 300 column (7.8 mm). The column was eluted with phosphoric acid (1.5 mM in Milli-Q water) at a flow rate of 0.60 mL.min⁻¹. Organic acids (malate, succinate, pyruvate and fumarate) were also measured using Bio-Rad HPX-87H 300 column (7.8 mm) where the column was

eluted with more concentrated phosphoric acid (45 mM in milli Q water) in order to have a better separation of the succinic and fumaric acid peaks.

During the cultivation of Fum 114, glucose concentration was measured using an enzymatic assay with R-Biofarm (Boehringer Mannheim, Germany) test kits and in Fum 116 cultivation the glucose concentration was measured using HPLC as described above.

For intracellular metabolites, a specialized rapid-sampling and quenching setup was used (47). To obtain biomass from the quenching solution, rapid filtration method was applied as described for *Penicillium chrysogenum* by Douma *et al.* (77), the only difference was that pure methanol was used as a quenching solution to prevent the leakage of metabolites in *S. cerevisiae* samples (45). Approximately 1 mL of broth was withdrawn and injected (in less than 0.8 s) into a pre weighed tube containing 5 mL pure methanol pre-cooled at -40 °C and the contents of the tube were quickly mixed by vortexing. The samples were weighed rapidly and thereafter filtered through a filter of pore size 0.45 µm (Pall) placed on the support disk of a filtering flask (connected to a vacuum pump) and washed with 40 mL of pure methanol (-40 °C). After washing, the filter with biomass cake was transferred to a 50 mL falcon tube (BD biosciences) containing 30 mL ethanol (75% v/v) solution (at 75°C) for metabolite extraction from the biomass. 120µL of 13C labelled internal standard solution (stored at 0°C) was added into the ethanol solution to enable IDMS based quantification of intracellular metabolites (115). The falcon tube was capped and vigorously shaken. The cap was then removed and the tube was placed in a water bath at 95°C for 3 minutes and thereafter stored at -80°C until further analysis. Samples taken from -80°C were concentrated by complete evaporation of the ethanol-water mixture under vacuum (48). The dried residue was re-suspended in 600 µL of demineralized water and centrifuged at 15000 g for 5 min at 4°C. The supernatant was centrifuged for the second time under same conditions and the supernatant obtained was stored at -80°C and later used for the quantification of intracellular metabolites. The intracellular metabolites were analyzed using GC-MS and LC-MS/MS (116)(117).

Calculation of the biomass specific rates, data reconciliation, and metabolic flux analysis

The biomass specific rates, e.g. growth rate, glucose and oxygen uptake rate, and the production rates of carbon dioxide and extracellular products such as fumaric acid, acetic acid, glycerol, and ethanol during the evolution experiment were calculated from their steady state compound balances. Reconciliation was done first using only element conservation to check for gaps in carbon and degree of reduction conservation. When such gaps were statistically not relevant, the reconciliation was performed with the metabolic network, leading also to calculated fluxes in the network reaction.

Metabolic network calculation was done using MNA PRO 3.0 software (118). The yeast aerobic metabolic network which was applied for flux analysis contained 150 reactions and 168 compounds in 3 compartments, the network was derived from the metabolic network developed by Lange *et al.* (52). The metabolic network did not contain FUM1 and ZWF1 catalyzed reactions for the flux analysis of Fum 114 and Fum 116 mutants. Flux analysis was also done with networks containing either FUM1 or ZWF1. Networks contained NAD and NADP dependent acetaldehyde dehydrogenase reactions in order to produce NADPH from acetaldehyde derived acetate after the knock-out of ZWF1. Metabolic networks described in the previous chapters, where ethanol was added in the chemostat feed, did not contain pyruvate decarboxylase reaction (PDC), but in the metabolic network for Fum 114 and Fum 116 mutants pyruvate decarboxylase reaction was added as ethanol was produced. The metabolic network also contains a glycerol export reaction via the uniport mechanism. Fum 116 expresses the DCT-02 transporter which facilitates the export of dicarboxylic acids via the uniport mechanism as observed in the previous studies. Fum 114 uses an unknown dicarboxylic acid transporter, its export mechanism was also assumed to be uniport. In the metabolic model the export of succinate (Suc^{2-}), fumarate (Fum^{2-}) and malate (Mal^{2-}) was via uniport, which was also included in the metabolic networks described in the previous chapters using the DCT-02 transporter. Mitochondrial transporters involved in the exchange of these dicarboxylic acids between cytosol and mitochondria present in the metabolic network are SFC1 (succinate-fumarate carrier), succinate/malate carrier and oxoglutarate/malate carrier.

Export of pyruvate (Pyr^-) and acetate (Ac^-) was also assumed to be via uniport mechanism. The produced protons were exported by H^+ -ATPase with the stoichiometry of 1 ATP per H^+ . P/NADH and P/FADH₂ ratio used was 1.23 and 0.98 respectively (52). The changes in the metabolic model are summarized in Table 5.2.

Table 5.2. List of reactions and transport mechanisms added (+) or removed (-) from the metabolic network.

Reactions	Fum 114	Fum 116
Fumarase	+/-*	+/-
Glucose 6-phosphate dehydrogenase	-	-
Glycerol export (uniport)	+	+
Acetate (-) export (uniport)	+	+
Pyruvate (-) export (uniport)	+	+
Dicarboxylic acids export [succinate(2-), malate(2-) and fumarate(2-)] (uniport)	+	+

*+/-: Metabolic network analysis was done with and without the incorporation of fumarase reaction. The reason for this is explained in the results and discussion section.

Results and discussion

Fum 114 (ΔFUM1 , ΔZWF1) and Fum 116 (ΔFUM1 , ΔZWF1 , $\text{DCT-02}\uparrow$) were constructed to link aerobic fumaric acid production with growth, based on energy coupling as discussed before. The physiology of the strains was first characterized in shake flasks experiments. Subsequently in-vitro evolution was carried out in an aerobic glucose limited chemostat (30°C, pH controlled at 5.0) at a dilution rate of 0.10 h^{-1} for duration of 220 days.

Shake flask study

Fum 114, Fum 116 and CEN.PK 113-7D (as a control) were cultivated in aerobic shake flasks in the absence of a N-source and in glucose excess condition (505 mM) to study the impact of the genetic modifications on the production of fumaric acid and other metabolites in the absence of growth. Calcium carbonate was used as a buffer to control the pH to around 6.5 and to have high partial pressure of CO₂. Figure 5.3 shows the results obtained from the duplicate shake flasks experiment.

Consumption of glucose and production of pyruvate, acetate, ethanol, glycerol, succinate, fumarate and malate was observed for all strains (Figure 5.2). During batch cultivation the pH varied between 6.0 and 6.5, showing that the calcium carbonate buffer sufficiently stabilized the pH. The initial biomass concentrations of the Fum 114, Fum 116 and CEN.PK 113-7D before transferring to the N-source absent media are shown in Figure 5.3A. All the strains hardly produced any fumarate (Figure 5.3I)

The presence of the DCT-02 transporter in Fum 116 did not make a difference in the C4 acids secretion, as both Fum 114 and Fum 116 strains showed very comparable secretion patterns for these acids. Both strains produced mainly the fermentative products: ethanol, glycerol, pyruvate, and acetate (Figure 5.3C, 3D, 3E and 3F) which can be understood because the TCA cycle is disrupted and the TCA cycle enzymes are known to be repressed by glucose (119). Remarkably the Fum 116 strain produced a significant amount of pyruvate compared to Fum 114 and CEN.PK 113-7D (Figure 5.3E). The final concentration of pyruvate was 220 mM in Fum 116 and 20 mM in Fum 114. This indicates that DCT-02 might also be a monocarboxylic acid transporter.

Evolution of engineered *S. cerevisiae* for the aerobic production of dicarboxylic acids

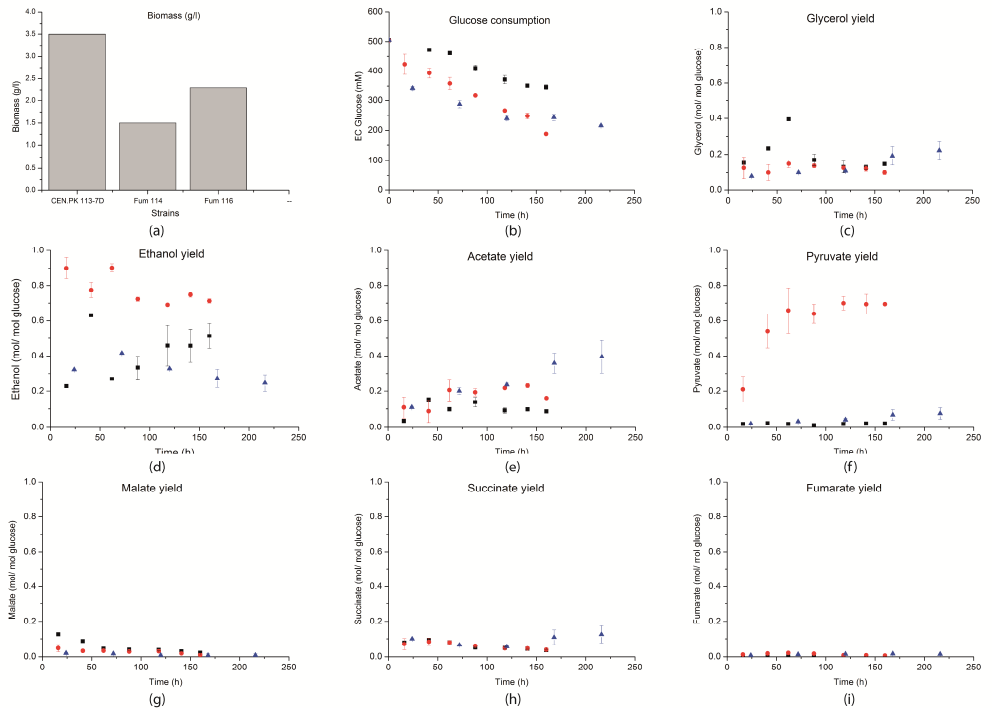


Figure 5.3. Metabolites production on glucose by Fum 114 (▲), Fum 116 (●) and CEN.PK 113-7D (■) in aerobic glucose shake flasks in the absence of N-source. Concentrations of A) Biomass (g/L) and B) extracellular glucose in mM. Yields (mol/mol of glucose consumed) of C) Ethanol, D) Glycerol, E) Pyruvate, F) Acetate, G) Malate, H) Succinate, I) Fumarate.

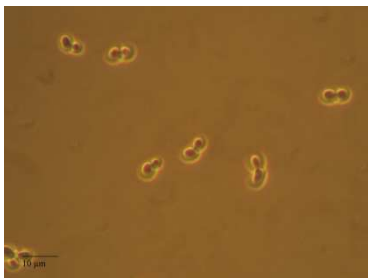
General observations during the aerobic chemostat evolution experiment

During the bioreactor batch growth phase, the maximum growth rate of Fum 114 and Fum 116, determined from the off gas CO_2 data, were 0.26 and 0.27 h^{-1} respectively (Figure 5.S5 and 5.S6, Supplementary material). These μ_{max} values are lower than that of the wild type CEN.PK 113-7D, which has a μ_{max} value of 0.34 h^{-1} (120). Extracellular metabolites were not measured during the batch cultivations. However, in shake flask cultivations in the presence of nitrogen source both Fum 114 and Fum 116 produced mainly ethanol with a yield of $1.4 \text{ mol ethanol/mol glucose consumed}$. This yield of ethanol in Fum 114 and Fum 116 is comparable to what is observed with CEN.PK 113-7D, which is expected

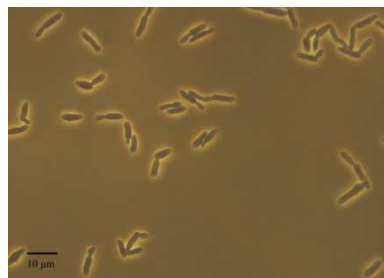
as in the glucose excess shake flask condition the TCA cycle enzymes are repressed which leads to a similar response of the wild type and the engineered strains.

The evolution experiment was partitioned into 3 phases. Phase I, from day 1 to 10, represents the initial phase of evolution. Phase II, a period of rapid evolution from day 10 to 80 where change in the secretion of metabolites is substantial. Finally phase III, a period of slow evolution, from day 80 to 220. During this phase fewer changes were observed in the profiles of the extracellular metabolite concentrations.

During the evolution experiments in glucose limited chemostats there was a decrease in the residual glucose concentration (Figure 5.5B and 5.6B) and a change in the morphology of Fum 116 from spherical to elongated cells (Figure 5.4). A drop in the residual glucose concentration and a change in cell morphology during long term aerobic glucose limited chemostat cultivation of wild type *S. cerevisiae* CEN.PK 113-7D was also reported by Mashego *et al.* (76).



(A)



(B)

Figure 5.4. A) Fum 116 cells during the batch phase of the evolution experiment B) Fum 116 cells in elongated form after 70 days of cultivation in the evolution experiment (Bar represents the length of 10 μm)

Extracellular metabolite levels during the course of the evolution experiment

During the course of the evolution experiment, the concentration of biomass and extracellular metabolites were measured regularly as shown in Figure 5.5 (Fum 114) and Figure 5.6 (Fum 116) with three phases (I, II and III) indicated.

The biomass concentration increased rapidly in phase I and II (Figure 5.5A and 5.6A) and did not change significantly thereafter in both Fum 114 and Fum 116 strains. The yield of biomass increased from 0.09 to 0.18 ($\text{g}\cdot\text{g}^{-1}$ of glucose) in Fum 114 and from 0.12 to 0.17 ($\text{g}\cdot\text{g}^{-1}$ of glucose) in Fum 116.

In Figures 5.5 and 5.6 certain outliers in the metabolite concentrations were identified which are indicated within a rectangle with dashed lines (--). For Fum 114, the glycerol data (Figure 5.5C) showed scatter: in phase I, glycerol concentration varied between 0.90 and 15.80 mM. The higher concentration of glycerol in phase I were marked as outliers because in aerobic conditions lower glycerol concentrations are expected. In phase III some of the glycerol data points close to zero were considered as outliers; in addition the data points with higher glycerol concentration had better carbon and degree of reduction balance. Data points with sudden absence of malate (Figure 5.5F) and sudden increase in succinate (Figure 5.5G) were also considered as outliers. For Fum 116, the malate and succinate data in phase III (Figure 5.6G and 5.6H) showed scatter. The lower malate concentration observed in 6 data points in phase III led to a gap in carbon balance (Figure 5.S5, supplementary material) and were therefore considered outliers. Data points with higher succinate and glycerol concentration were also considered as outliers and were not included to calculate the averaged values.

During the initial phase of the evolution experiment (phase 1), Fum 114 produced mainly ethanol and acetate. Thereafter the production of ethanol significantly decreased while the production of acetate and glycerol increased. The reason for this could be that the acetate production is energetically more favorable than ethanol production (see Table 5.1). Thus the increase of acetate and decrease of ethanol production could explain the rapid increase of the biomass concentration in Fum 114, as more ATP became available for cell growth. No further change in the secretion of the TCA cycle acids malate, fumarate and succinate was observed. This is most likely due to the absence of a dicarboxylic acid transporter in Fum 114. On the other hand, glycerol

production which consumes ATP (Table 5.1) increased gradually from phase I to III. This indicates increase in the redox stress in the cell with evolution.

Also in the evolution experiment with Fum 116, the ethanol production rate decreased significantly in phase I. This was, however, not accompanied by an increase in the production of acetate. Instead, the production of pyruvate increased (high yield of pyruvate was also noticed in shake flasks study). Glycerol concentration in Fum 116 was much lower than Fum 114 indicating much less redox stress than Fum 114. One of the main difference in Fum 114 and Fum 116 was high excretion rate in Fum 116 of malic (roughly twenty times in both phase I and phase II) and succinic acid. Production of malate in the reductive route re-oxidizes NADH which could be one of the reason for low glycerol production observed in Fum 116. High secretion rates of acetate and pyruvate in Fum 116 contributes towards ATP production. In contrast to this, production of malic acid via the reductive route consumes ATP (2 mol ATP/ per mol malate produced, see Table 5.1) while the production of succinate is via the oxidative route which produces ATP. In both the strains no significant evolution towards fumarate production was observed, which was unexpected because it is energetically the most favorable metabolite (Table 5.1).

These results of Fum 116 show that the DCT-02 transporter strongly stimulates the secretion of dicarboxylic acids, mainly malate and succinate. Fum 116 also secretes significant amount of pyruvate compared to Fum 114 as also noticed in the shake flask studies. This indicates that DCT-02 transporter might also facilitate pyruvate export in Fum 116, however, it should also be noted that wild type *S. cerevisiae* has the ability to secrete a high extracellular concentration of pyruvate (121). Also the evolution towards more energy yielding products seems to occur because ethanol secretion is replaced by acetate secretion in Fum 114 and Fum 116.

Fum 114

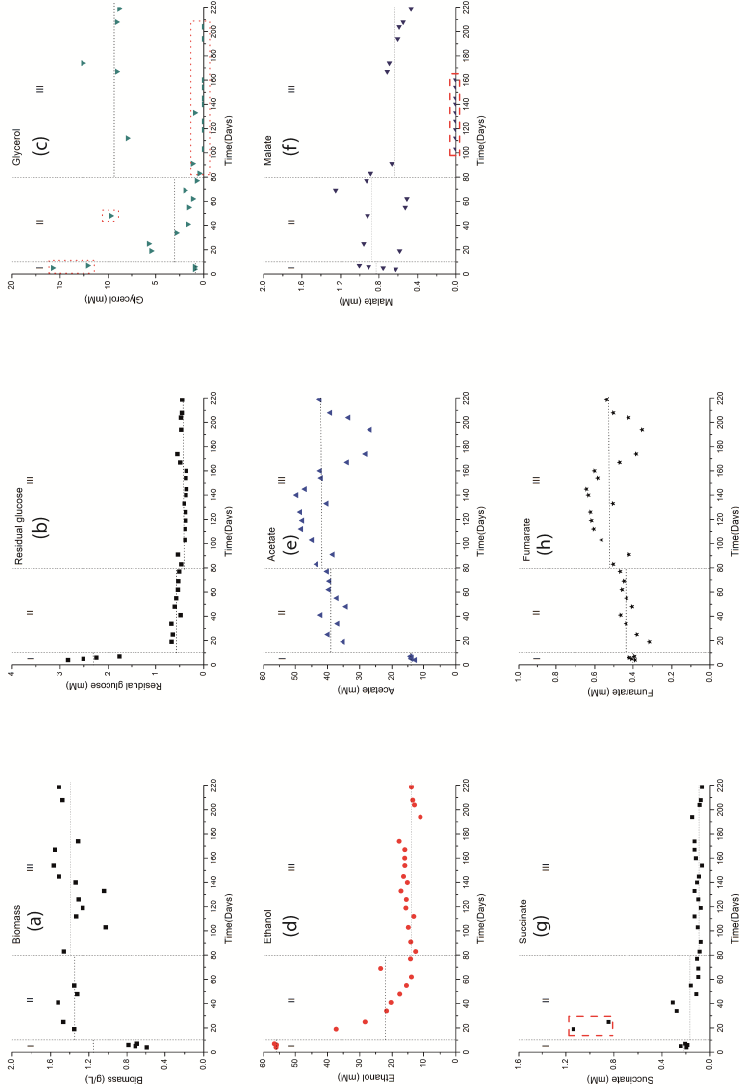


Figure 5.5. Profile of the concentrations (mM) of extracellular metabolites during evolution in Fum 114 a) Biomass (g/L) b) Residual glucose c) Glycerol d) Ethanol e) Acetate f) Malate g) Succinate h) Fumarate. The graphs are segmented into three phases, phase I from 1 to 10 days, phase II from 10 to 80 days and phase 3 from 80 to 220 days. Dashed lines (---) in each phase represents the average value taken for the calculation of biomass specific rates. Data points within a rectangle (- - -) are considered as outliers and have not been taken into account for calculating averages.

Fum 116

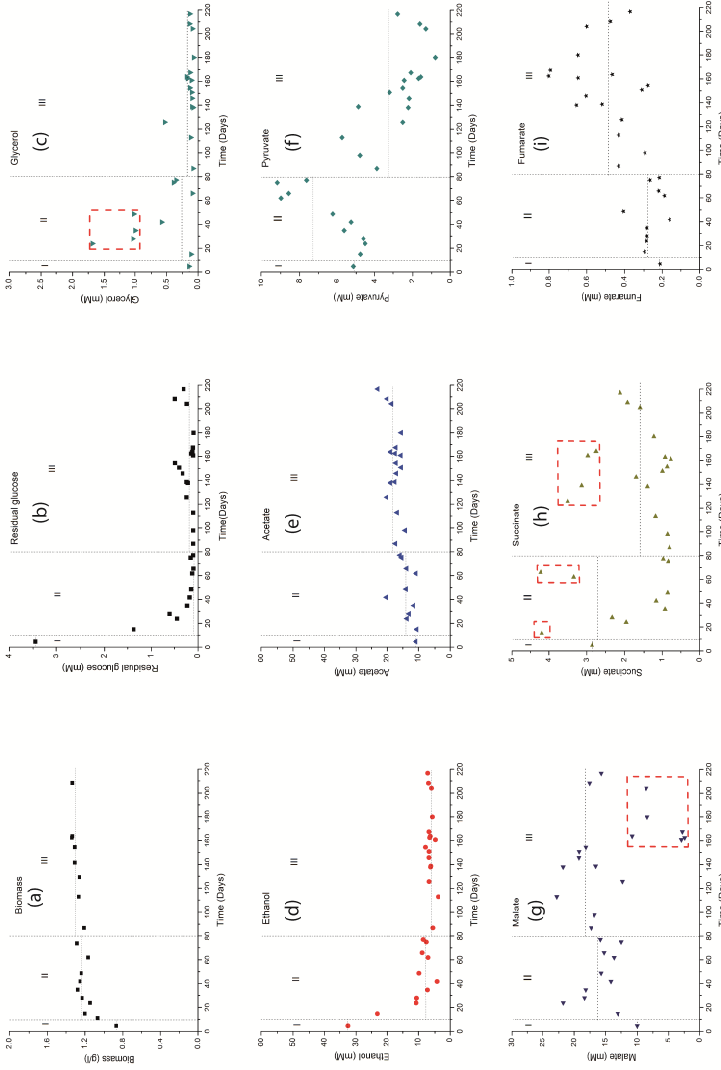


Figure 5.6. Profile of the concentrations (mM) of extracellular metabolites during evolution in Fum 116 a) Biomass (g/L) b) Residual glucose c) Glycerol d) Ethanol e) Acetate f) Pyruvate g) Malate h) Succinate i) Fumarate. The graphs are segmented into three phases, phase I from 1 to 10 days, phase II from 10 to 80 days and phase 3 from 80 to 220 days. Dashed line (---) in each phase represents the average value taken for the calculation of biomass specific rates. Data points within a rectangle (- - -) are considered as outliers and have not been taken into account for calculating averages.

Metabolic network model

Raw chemostat data of averaged concentrations and flow measurements were used (Supplementary material, Table 5.S3, Fum 114 and S9, Fum 116) with proper compound balances, in order to obtain non-reconciled compound rates and their standard errors (Table 5.S4, Fum 114 and S9, Fum 116). The carbon and degree of reduction (Υ) balances were close to 100%; therefore reconciliation using element conservation and experimental errors (Table 5.S3 and 5.S8) was performed (50). This reconciliation led to slight changes in calculated q -values and smaller errors. Biomass specific oxygen uptake rate (q_{O_2}) changed significantly, which was due to the large error in q_{O_2} due to very low oxygen depletion (Table 5.S4 and 5.S9) in the sparged air.

Non-reconciled rates were also reconciled using the metabolic network, but the network estimates much lower q_{O_2} and q_{CO_2} and smaller changes in other q rates (Table 5.S5 and 5.S10, significant changes marked in bold). This shows that the metabolic network could not accommodate the high oxygen consumption rate obtained using element conservation. Clearly in the vivo metabolic network releases much more NADH than is possible in the metabolic network used in this study which has blocked PPP and TCA cycle pathways.

This redox imbalance indicates that in both mutants there is an alternative pathway to generate NADH which is not incorporated into the metabolic network model or there is an alternative hydratase to convert fumarate to malate which allows the functioning of the TCA cycle and generation of NADH.

Although FUM1 and ZWF1 reactions were knocked out from Fum 114 and Fum 116, these reactions were incorporated back into the metabolic network to check if that solves the redox imbalance problem. First NADP-dependent glucose 6-phosphate dehydrogenase reaction (ZWF1) was incorporated into the metabolic network. The excess produced NADPH can in principle be converted into NADH by a transhydrogenase, but this is not present in *S. cerevisiae*. In its absence the metabolic model in *S. cerevisiae* does solve the NADPH redox imbalance problem by the formation of NADH from NADPH by operating the NADPH consuming acetaldehyde dehydrogenase reaction (ACTALdeh) in the reverse direction (from acetate using 2 ATP to acetyl coA to acetaldehyde) and NAD dependent ACTALdeh in the forward direction (from

acetaldehyde to acetate). Due to the extra ATP consumption (needed to convert acetate to acetyl-CoA), the maintenance obtained was negative which is implausible. Therefore incorporating ZWF1 results in a metabolic model gives improbable fluxes.

On the other hand, incorporating the fumarase reaction into the metabolic network increases the flux through the TCA cycle (Supplementary material, Table 5.S7 and 5.S12) which results into increased biomass specific rates especially of CO₂ and O₂, nearly identical to the rates obtained from the element conservation based reconciliation (Supplementary material, Table 5.S6 and 5.S11). Therefore the TCA cycle flux solves the redox imbalance problem due to the generation of NADH and production of CO₂. In Fum 114 and Fum 116, FUM1 reaction was knocked out, but an unknown hydratase could have evolved to convert fumarate to malate.

Intracellular fluxes and subsequent response of intracellular metabolites

Intracellular fluxes were obtained from the metabolic model (Δ ZWF1) containing fumarase reaction for phase I, II and III (Supplementary material, Table 5.S7 and 5.S12).

- With each consecutive phase there was increase in biomass concentration and as expected a drop in the glycolytic flux. The glucose uptake rate (q_s) correlates positively with C_s (Supplementary material, Figure 5.S5). Still the glycolytic flux in Fum 114 and Fum 116 was much higher than observed in CEN.PK 113-7D under similar condition (Table 5.3). The high glycolytic flux resulted in lower intracellular concentration of the metabolites in the oxidative lower part of the glycolysis pathway compared to wild type CEN.PK 113-7D (3PG, 2PG and PEP, see Table 5.3) as was also noticed by Visser *et al.* (122) and Canelas *et al.* (123).
- No flux towards the pentose phosphate pathway was observed with the knock-out of ZWF1 in the metabolic network. However, with no flux through the PPP, 6PG (higher in Fum 114 than in Fum 116) was still detected although its concentration was much lower than observed in CEN.PK 113-7D. Detection of small amounts of 6PG after ZWF1 knock-out in

S. cerevisiae is also reported by Nishino *et al.* (124) which could be due to the reversibility of 6-phosphogluconolactonase dehydrogenase reaction (125)(126).

- During evolution there was a shift from ethanol to acetate formation, this shift was more extensive in Fum 114 than in Fum 116. In Fum 116 significant rates of malate and pyruvate were observed. With this shift the flux through acetaldehyde dehydrogenase increased and the flux through alcohol dehydrogenase decreased in Fum 114. Extracellular concentration of acetate increased from phase I to phase III by 3 fold and 1.6 fold in Fum 114 and Fum 116 respectively. This resulted in a significant increase in the estimated futile cycling rate of acetic acid which also resulted in higher maintenance ATP requirement of Fum 114 and Fum 116 (discussed in next section).
- NADH/NAD ratios were also estimated to understand the redox state of the cell during evolution. The trend in the cytosolic NADH/NAD ratio can be estimated by the intracellular GAP/3PG ratio (Supplementary material, equation S.E1). During evolution, the NADH/NAD ratio in Fum 116 remained nearly constant (Supplementary material, Figure 5.S6) which also reflects in nearly constant glycerol production rates (Table 5.S9, Supplementary material) and intracellular concentration of G3P (Table 5.3). In Fum 114 there was a significant increase in GAP/3PG ratio and thereby the NADH/NAD ratio (Figure 5.S6), and also a significant increase in the glycerol production rate (Supplementary material, Table 5.S3) and intracellular G3P concentration (Table 5.3).
- Malic acid out/in ratios in Fum 116 (Supplementary material, Table 5.S1) supports the uniport mechanism of totally dissociated species of malic acid as the most likely export mechanism of DCT-02 (Supplementary material, Table 5.S2). This transport mechanism was also incorporated into the metabolic model. In a previous study done at pH 3.0, the malic acid out/in ratio observed with DCT-02 transporter was 0.29 ± 0.09 (111). This matches well with the equilibrium out/in ratio of 0.43 for uniport mechanism at pH 3.0. It is also clear that at pH 5.0 the equilibrium malate out/in ratio of

22.35 is about 50 times higher than observed at pH 3.0. Malic acid out/in ratios in Fum 116 at pH 5.0 increased from 2.30 in phase I to 19.07 in phase III of Fum 116 (Supplementary material, Table 5.S1). This ratio approaches the equilibrium ratio (22.35) while the secretion rate of malate did not change significantly. This indicates an increase in the flux capacity of the DCT-02 transporter towards malic acid during evolution. In Fum 114 at pH 5.0 the malate out/in ratio remained low (between 1.55 and 0.15) which is due to the absence of DCT-02 transporter

- Malic acid production rate in Fum 116 increased from 30.5 mmol/Cmol.h to 37.5 mmol/Cmol.h (Supplementary material, Table 5.S11), this is very high given the low CO₂ level (0.4 %). Suc 958 overexpressing reductive route of TCA cycle and DCT-02 transporter studied in chapter 4 had malate production rate of only 2.4 mmol/Cmol.h with 50% CO₂ in the inlet gas. The experiment with Suc 958 was done at pH 3.0 and the malate yield decreases rapidly with the drop in extracellular pH compared to succinic acid as observed by Zelle *et al.* (18). The reason for this high secretion of rate of malate in Fum 116 could be higher pH of 5.0 and DCT-02 transporter but the metabolic route of malic acid formation in Fum 116 should be further investigated.
- During the course of evolution no improvement in the secretion rate of succinate and fumarate was observed. Also their out/in ratios did not change significantly with evolution (Supplementary material, Table 5.S1) and remained far below their equilibrium values (Table 5.S2).
- The intracellular concentration of fumarate was 40 to 100 fold higher in both Fum 114 and Fum 116 than in the CEN.PK 113-7D strain. This clearly points towards the export of fumaric acid as a metabolic bottleneck. Along with high fumarate, high intracellular concentration of aspartate, malate, succinate and citrate was also observed in Fum 116 (Table 5.3).
- The calculated flux from fumarate to malate increased with time (phase I to III for Fum 114, and from phase II to III for Fum 116) and with increasing intracellular concentration of fumarate (Figure 5.7). This correlation suggests the possibility of an evolved hydratase enzyme with low affinity towards fumarate which could convert fumarate to malate after the knock-out of FUM1.

Table 5.3. Intracellular metabolites concentration for Fum 114 and Fum 116 before and after evolution

Metabolite [$\mu\text{mol.gDW}^{-1}$]	CEN.PK 113-7D	FUM114 (Phase I)	FUM114 (Phase III)	FUM116 (Phase II)	FUM116 (Phase III)
Residual glucose (mM)	0.12 \pm 0.02	2.34 \pm 0.23	0.45 \pm 0.02	0.13 \pm 0.03	0.22 \pm 0.04
Glucose uptake (mmol/Cmol.h)	26.8 \pm 0.3	190.7 \pm 7.7	81.2 \pm 2.7	86.1 \pm 2.8	82.8 \pm 2.7
G6P	5.62 \pm 0.26	3.84 \pm 0.24	4.75 \pm 0.19	5.60	3.08
F6P	1.66 \pm 0.07	0.60 \pm 0.03	0.945 \pm 0.039	1.40	0.72
6PG	0.93 \pm 0.01	ND	0.072 \pm 0.007	0.056	0.013
FBP	0.36 \pm 0.01	3.27 \pm 0.38	2.40 \pm 0.16	2.72	1.66
GAP	0.03 \pm 0.004	0.056*	0.048*	0.042	0.044
G3P	0.10 \pm 0.01	0.31 \pm 0.01	1.23 \pm 0.06	0.058	0.058
2PG	0.38 \pm 0.02	0.09*	0.05*	0.12	0.11
3PG	3.78 \pm 0.05	1.50*	0.85*	1.35	1.17
PEP	1.20 \pm 0.05	0.13 \pm 0.03	1.26 \pm 0.06	0.11	0.11
Pyruvate	1.50 \pm 0.03	5.28 \pm 0.38	3.56 \pm 0.12	1.49	2.43
Aspartate	6.45 \pm 0.43	N.M	N.M	16.06	12.00
Citrate	6.55 \pm 0.18	40.8 \pm 4.1	8.66 \pm 0.23	17.68	14.12
AKG	0.49 \pm 0.02	1.92 \pm 0.16	1.45 \pm 0.04	N.D	N.D
Succinate	0.82 \pm 0.10	7.41 \pm 0.45	5.8 \pm 0.56	2.50	3.42
Fumarate	0.49 \pm 0.01	42.9 \pm 3.0	19.8 \pm 0.2	36.08	30.11
Malate	1.78 \pm 0.10	0.80 \pm 0.10	5.84 \pm 0.21	8.83	1.74

* GAP concentration was estimated from FBP concentration in Fum 114. The correlation between FBP and GAP intracellular concentration was obtained by using different intracellular data points of Fum 116 ($\text{GAP} = 0.0309 * \text{FBP}^{0.5}$).

*: 2PG and 3PG concentrations in Fum 114 were estimated from the sum of both metabolites concentrations (2PG + 3PG) and using the equilibrium ratio of 2PG/3PG of 0.063 (55).

N.M: Not measured, N.D: Not detected

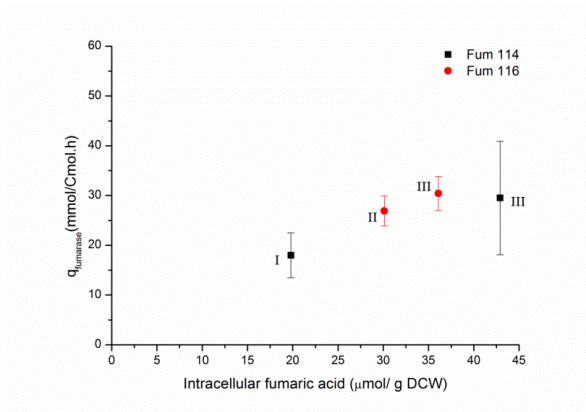


Figure 5.7. Shows the flux from fumarate to malate obtained from the metabolic network vs the intracellular concentration of fumarate. Fum 114 (■) shows the data points for phase I and III and Fum 116 (●) for phase II and III.

Futile cycling of acetic acid

The evolution experiment was carried out at pH 5.0, and a high extracellular concentration of acetic acid was observed for both Fum 114 and Fum 116. At pH 5.0, approximately 36% of the extracellular acetic acid is in un-dissociated form. This un-dissociated acetic acid could passively diffuse into the cell and dissociate (Ac^- and H^+). Ac^- is assumed to be exported by uniport and the H^+ by H^+ -ATPase consuming 1 ATP. This results in a futile cycling of acetic acid costing ATP. Other acids secreted by Fum 114 and Fum 116 (fumarate, succinate, malate and pyruvate) are in dissociated forms at pH 5.0 which do not passively diffuse into the cell and do not contribute towards futile cycling. Therefore the futile cycling rate of only acetic acid was estimated using the following equation:

$$q_{\text{HAC}} = k \frac{6V_x}{d_x} C_{\text{HAC}_{\text{ex}}} \quad \text{eq. 1}$$

where q_{HAC} is the biomass specific uptake rate of un-dissociated acetic acid via passive diffusion in $\text{mol Cmol}^{-1} \text{h}^{-1}$, k is the permeability coefficient of acetic acid (m.h^{-1}), $C_{\text{HAC}_{\text{ex}}}$ is the extracellular concentration of un-dissociated acetic acid in mol/m^3 , V_x is the cell volume ($52.8 \times 10^{-6} \text{ m}^3 \cdot \text{Cmol}^{-1}$, (58)) and d_x is the

cell diameter (5×10^{-6} m,(58)). The value of q_{HAC} can be found from the rate of extra ATP loss (1 ATP for 1 HAC) which is obtained from the ATP balance.

This shows higher maintenance for Fum 114 and Fum 116 strains compared to the maintenance of wild type CEN.PK 113-7D observed under the same cultivation conditions as Fum 114 and Fum 116. Assuming that the extra ATP production is used for futile cycling of acetic acid, the ATP balance gives the q_{HAC} and the permeability can be calculated. Figure 5.7 shows the permeability of acetic acid for both mutants at each phase. Maintenance of CEN.PK (58 mmol/Cmol h) used was obtained from the experiment done separately, which is the same as the maintenance of 60 mmol/Cmol h estimated using the ATP parameters (growth related maintenance of 170 mmol/Cmol and fixed maintenance of 43 mmol/Cmol h, which at $\mu = 0.10 \text{ h}^{-1}$ leads to ATP requirement of $0.1 \cdot 170 + 43 = 60 \text{ mmol/Cmol h}$) estimated by Lange *et al.* (52).

From Figure 5.8 it is clear that the permeability of acetic acid decreases with time. In the evolution experiment in phase I, permeability of acetic acid was $14.5 \pm 2.8 \times 10^{-4} \text{ m/h}$ and $5.7 \pm 1.7 \times 10^{-4} \text{ m/h}$ for Fum 114 and Fum 116 respectively. The permeability in phase III dropped to $1.65 \pm 0.35 \times 10^{-4}$ and $2.9 \pm 0.55 \times 10^{-4} \text{ m/h}$ for Fum 114 and Fum 116 respectively. The drop in permeability for acetic acid in *S. cerevisiae* with its prolonged exposure was also noticed by Jamalzadeh *et al.* (25), which is most likely due to the change in the plasma membrane composition of *S. cerevisiae*. Permeability of acetic acid reported in other studies is $2.6 \times 10^{-4} \text{ m/h}$ for CEN.PK 2_1C (25) and $4.56 \times 10^{-4} \text{ m/h}$ for CBS 8066 (127) in *S. cerevisiae* and $50.4 \times 10^{-4} \text{ m/h}$ in an artificial liposome (128), showing close agreement with our results.

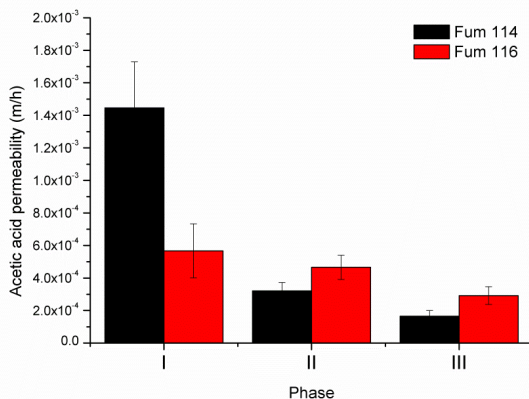


Figure 5.8. Acetic acid permeability estimated in three different phases of Fum 114 (black) and Fum 116 (red)

ATP production per mol consumed glucose

It was expected that the ATP-production per mol glucose would increase during evolution due to organic acid secretion. ATP production rate was calculated for each phase of Fum 114 and Fum 116 using the intracellular fluxes through ATP generating reactions in the metabolic network. As shown in Figure 5.9, with evolution there was indeed an increase in the yield of ATP produced per mol of glucose consumed. Figure 5.9 also shows the maximum yield of ATP when all the glucose is catabolised which is much higher than obtained in this experiment where significant amount of metabolites are secreted. Figure 5.9 also shows the amount of ATP utilised in the futile cycling of acetic acid which is significant enough to nullify the advantage of ATP gain through higher secretion rate of fumaric acid by evolved cells. To diminish the acetic acid uncoupling it is recommended to perform the future evolution experiments at pH 6.0 or to use a PDC negative mutant to avoid acetate formation (16).

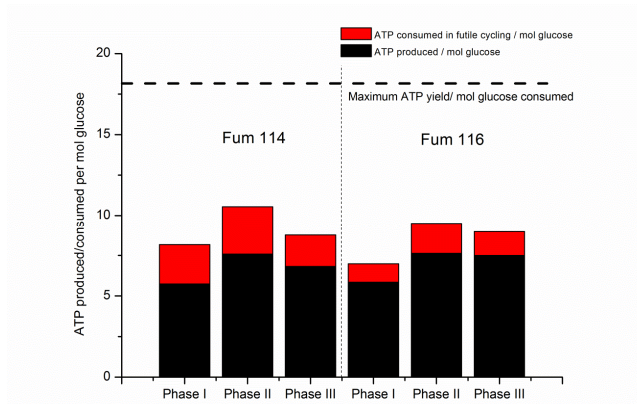


Figure 5.9. Shows ATP produced per mol of glucose consumed and ATP consumed in futile cycling per mol of glucose consumed. Dashed line (--) shows the maximum ATP yield obtained using the metabolic network.

Conclusions

In this study *S. cerevisiae* strains Fum 114 and Fum 116, engineered to produce fumaric acid, were evolved by coupling the ATP production obtained from oxidized metabolites secretion to the biomass formation. Fumaric acid is the catabolic product in Fum 114 and Fum 116 which gives the highest ATP yield compared to other metabolites.

During the course of evolution there was the expected improvement in the biomass concentration because of improved ATP production. However, the improved ATP production was not due to fumaric acid secretion, which did not occur at significant levels. Increased ATP production could be attributed to a change from ethanol secretion to acetate secretion in Fum 114 and acetate, pyruvate and malate secretion in Fum 116. The different behavior of Fum 116 is most likely due to DCT-02 transporter which is known to export malate but not fumarate. In both cultures, a significant amount of ATP was wasted in acetic acid futile cycling, but the permeability of acetic acid decreased with evolved time.

The intracellular concentration of fumaric acid remained 40 to 100 times higher in Fum 114 and Fum 116 compared to CEN.PK 113-7D during the course of evolution, indicating export as a bottleneck in fumaric acid production. Metabolic network analysis suggested that despite the knock-out of FUM1 there is a flux from fumarate to malate. Therefore, the fumarase reaction was incorporated back into the metabolic model to match the cellular respiration obtained from the metabolic network to that obtained in the experiment. The observed high intracellular concentration of fumarate, the irreversibility of the fumarate to malate reaction, the linear relation between the reaction rate and intracellular fumarate concentration and increase of the rate with time suggests that a non-specific enzyme present in *S. cerevisiae* evolved hydratase activity to convert fumarate to malate.

Unexpectedly Fum 116, expressing the DCT-02 transporter, produced, at low CO₂ level, malate with a high secretion rate of upto 37 mmol.Cmol⁻¹.h⁻¹. The route of malic acid is via the energy consuming reductive part of the TCA cycle with the incorporation of CO₂, however, with the unexpected presence of fumarate to malate conversion, malic acid production is also possible through the energy generating oxidative part. Further studies are required in Fum 116 to get insight into malic acid producing pathway.

Supplementary material

Table 5.S1. Out/in ratios of the organic acid during the course of evolution experiment with Fum 116 (with DCT-02) and Fum 114 (without DCT-02) at pH 5.0.

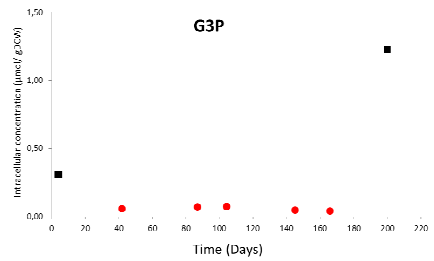
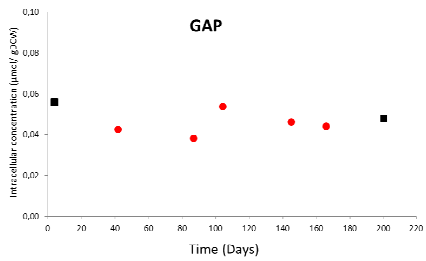
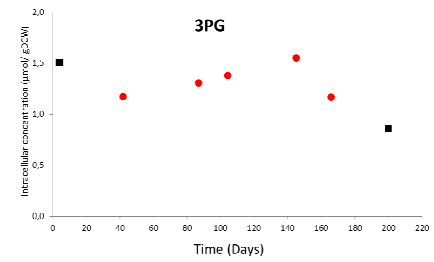
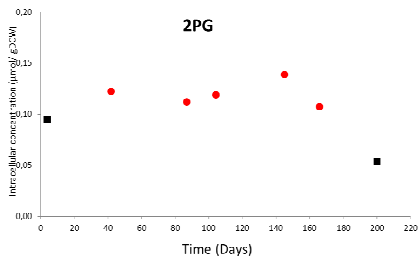
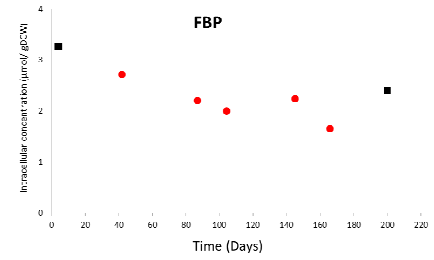
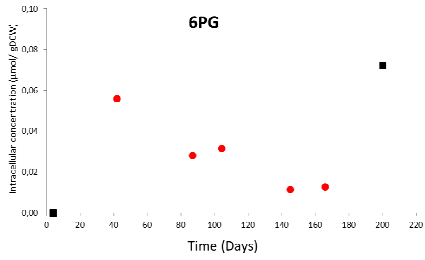
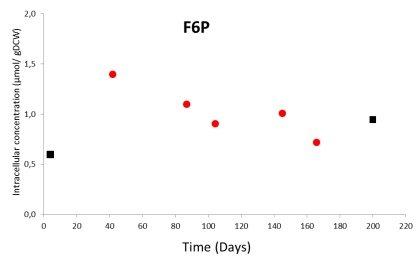
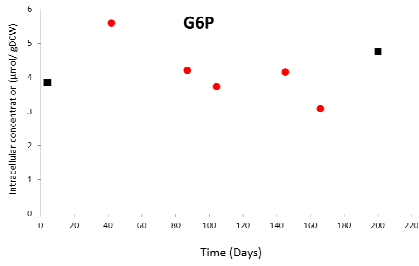
Fum 116				
Time (Days)	Malate (out/in)	Pyruvate (out/in)	Succinate (out/in)	Fumarate (out/in)
41.88	2.30	7.06	0.93	0.01
86.88	9.20	5.58	0.30	0.03
104.17	14.85	3.01	0.22	0.03
145.00	8.27	1.37	1.37	0.05
165.83	19.07	1.37	1.60	0.05
Fum 114				
Phase I	1.55			0.02
Phase III	0.15			0.05

Table 5.S2. Theoretical out/in equilibrium ratios of malate, succinate, fumarate, pyruvate and acetate were estimated assuming the intracellular pH of 7.0 and pmf of 150 mV and extracellular pH of 5.0 and 3.0. Estimation of the equilibrium ratios is explained in detail in Shah *et al.* (111).

	Total acid equilibrium out/in ratios for uniport mechanism (pH 5.0)	Total acid equilibrium out/in ratios for uniport mechanism (pH 3.0)
Malic acid (A^{2-})	22.35	0.43
Fumaric acid (A^{2-})	13.63	0.08
Succinic acid (A^{2-})	56.76	7.02
Pyruvic acid (A^-)	3.13	0.04
Acetic acid (A^-)	4.89	1.81

Profile of the intracellular metabolites in Fum 114 (■) and Fum 116 (●) during evolution

Chapter 5



Evolution of engineered *S. cerevisiae* for the aerobic production of dicarboxylic acids

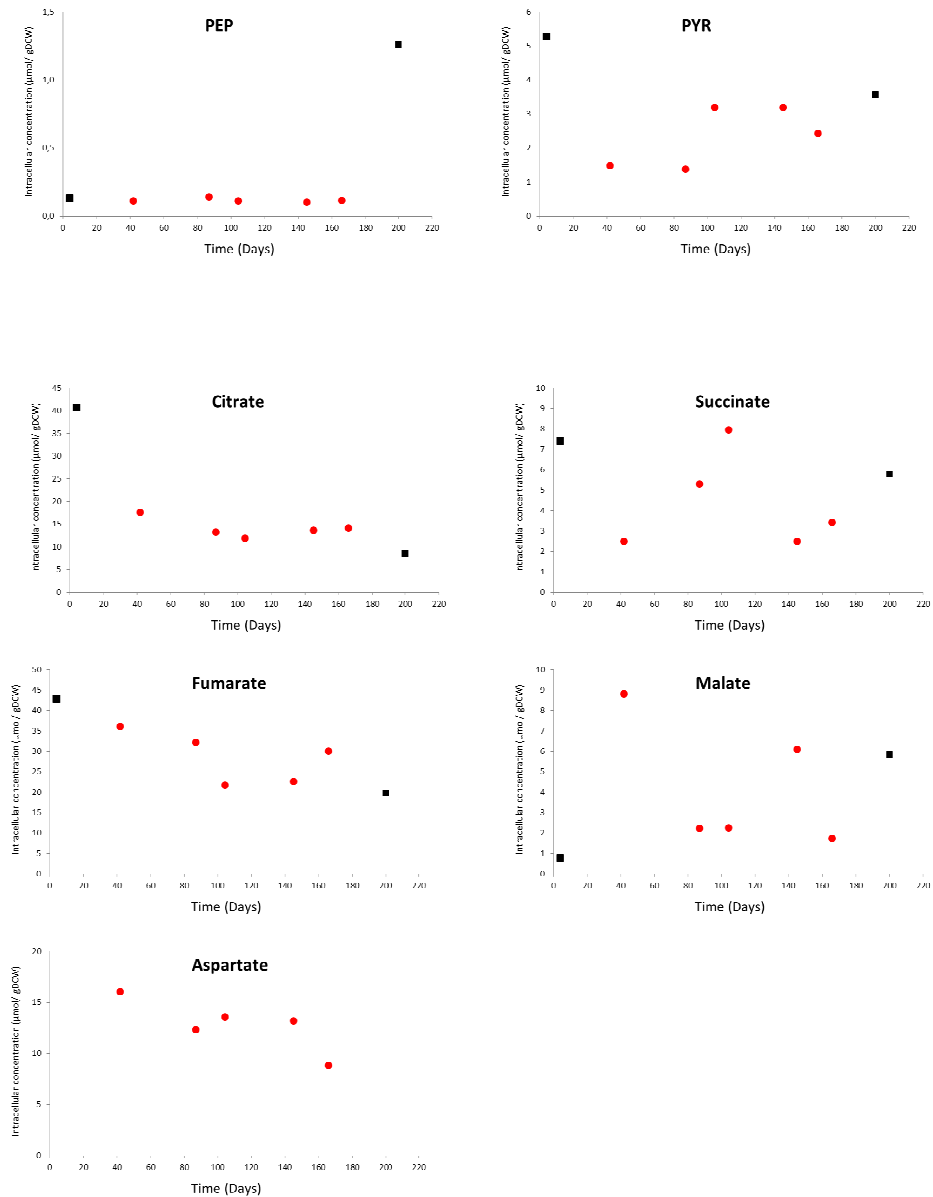


Figure 5.S1: Intracellular concentration of metabolites in central metabolism in Fum 114 (■) and Fum 116 (●) during the evolution experiment.

Off gas data during the evolution experiment of Fum 116

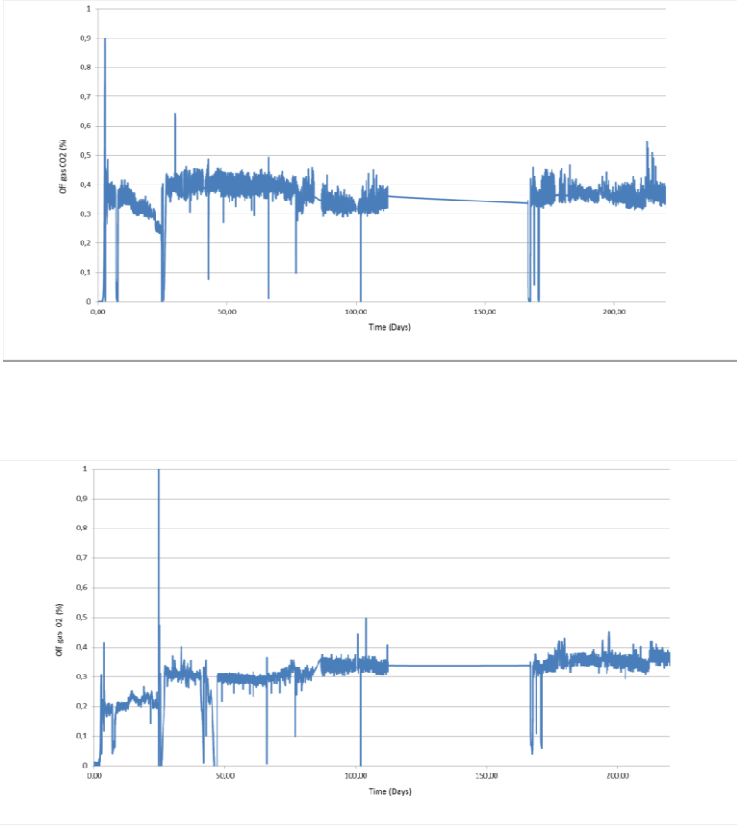


Figure 5.S2: Off gas CO₂ and O₂ data during the course of evolution experiment in Fum 116

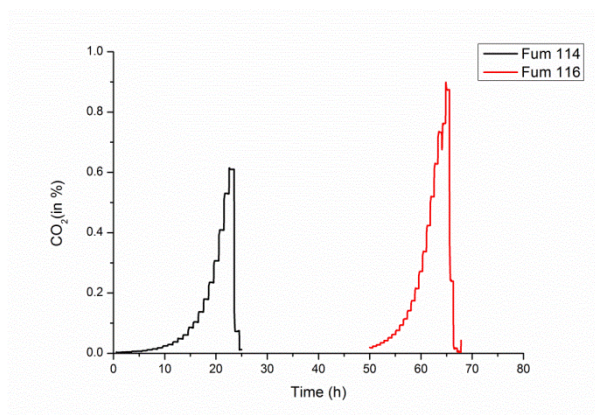


Figure 5.S3: Off gas CO₂ data during the batch phase of Fum 114 (-) and Fum 116 (-) strains.

Carbon and degree of reduction balance

Carbon and degree of reduction balance was done for Fum 114 (Figure 5.S5A) and Fum 116 (Figure 5.S5B). The utilization of amino acids was not considered for the balancing due to their negligible consumption as estimated from the biomass composition of *S. cerevisiae*. For example, leucine content in the biomass composition is 0.3 mmol/gDCW (129). This amounts to the utilization of 0.02 mmol/h (0.12 mCmol/h) of leucine in the chemostat when the biomass concentration is 1.34 g/L (biomass concentration during the end of evolution experiment with Fum 116) which is negligible when compared to the total carbon (glucose) utilized (~12.5 mCmol/h). Tryptophan, histidine and methionine content in the biomass composition was 0.028, 0.066 and 0.051 mmol/gDCW respectively (129) are even much lower than the leucine content. Due to this negligible contribution of amino acids towards biomass formation, the utilization of amino acids was not considered during calculation of carbon and degree of reduction balance.

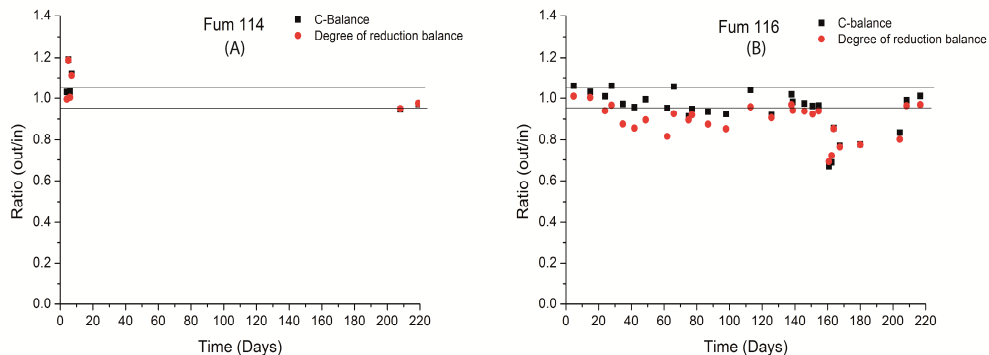


Figure 5.54. The plot shows the ratio of the amount of carbon and electrons going in over coming out against the time of the evolution experiment for A) Fum 114 and B) Fum 116. The two lines mark the ratios at 1.05 and 0.95.

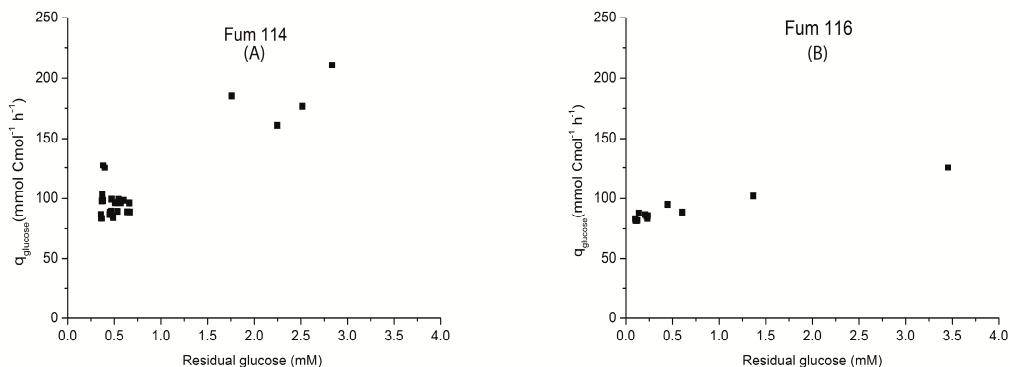


Figure 5.55. Biomass specific glucose uptake rate against the residual glucose concentration in A) Fum 114 and B) Fum 116.

NADH/NAD ratio:

Cytosolic NADH/NAD ratio can be estimated using the following equation:

$$\frac{[NADH]}{[NAD^+]} = K'_{GAPDH,PGK} \cdot 10^{7-pH} \frac{[GAP]}{[3PG]} \frac{[ADP.P_i]}{[ATP]} \quad (5S.E1)$$

The equilibrium constant $K'_{GAPDH,PGK}$ equals 113 M^{-1} as reported by Canelas *et al.* (55) at intracellular pH of 7.0. ADP and ATP concentration has not been measured in Fum 114 and Fum 116. Figure 5.S6 shows the trend in GAP/3PG ratio in Fum 114 and Fum 116 which is an indication of a change in NADH/NAD ratio. From the GAP/3PG ratio it seems that the NADH/NAD ratio did not change significantly during the course of evolution in Fum 116. On the contrary, in Fum 114 there was an increase in NADH/ NAD ratio during evolution indicating redox stress which also explains the increase in intracellular G3P concentration and biomass specific glycerol production rate.

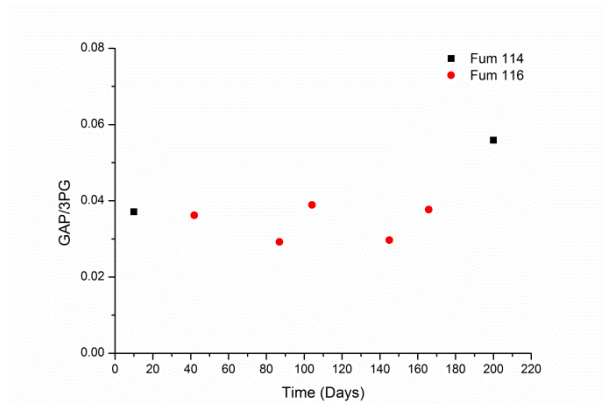


Figure 5.S6. GAP/3PG ratio observed during the evolution experiment in Fum 114 (■) and Fum 116 (●).

Assuming the intracellular concentration of ATP (10 mM), ADP (2 mM) and inorganic phosphate (20 mM). The cytosolic NADH/NAD ratio changed from 0.016 in the initial phase to 0.017 at the end of evolution experiment for Fum 116. For Fum 114 the NADH/ NAD ratio changed from 0.016 to 0.025.

Table 5.S3. Fum 114: Averaged raw data obtained in three different phases of the evolution experiment.

	Units	Phase I		Phase II		Phase III	
		Value	Error	Value	Error	Value	Error
<i>Fout</i>	Kg/h	0.0550	1%*	0.0510	1%	0.0475	1%
<i>V</i>	Kg	0.5000	2%	0.5000	2%	0.5000	2%
<i>Fgas,in</i>	mol/h	0.8009	1%	0.8009	1%	0.8009	1%
<i>Fadd</i>	Kg/h	0.0003	1%	0.0003	1%	0.0003	1%
<i>Cgluin</i>	mM	50.0000	2.5%	50.0000	2.5%	50.0000	2.5%
<i>Cglu</i>	mM	2.3400	0.2300	0.5480	0.0165	0.4500	0.0225
<i>Cetoh</i>	mM	56.1200	2.8060	21.3400	1.7593	13.7000	0.6850
<i>Cfum</i>	mM	0.4430	0.0222	0.4430	0.0110	0.5200	0.0260
<i>suc</i>	mM	0.2000	0.0100	0.3500	0.0175	0.1000	0.0050
<i>Mal</i>	mM	0.8264	0.0413	0.8264	0.1396	0.5100	0.0255
<i>Gly</i>	mM	0.920	0.020	3.4	1.689091	8.9700	0.4485
<i>Ace</i>	mM	13.6800	0.6840	38.1199	1.095656	40.8000	2.0400
<i>Pyr</i>	mM	0.0000	0.0000	0	0	0.0000	0.0000
<i>Cdw</i>	g/kg	0.690	0.035	1.39	0.0695	1.4900	0.0745
<i>CO2_in</i>	%	0.030	1%	0.020*	1%	0.030	1%
<i>O2_in</i>	%	20.946	0	20.946*	0	20.946	0
<i>CO2_out</i>	%	0.670	1%	0.700*	1%	0.570	1%
<i>O2_out</i>	%	20.676	1%	20.386*	1%	20.525	1%
<i>Mw</i>	-	26.400	5%	26.400	5%	26.4000	5%

*Some errors are fixed % of the net value

*Off gas data was not available for phase II therefore the values (%) used are in order to close the carbon and degree of reduction balances

Table 5.S4. Fum 114: Comparison of the non-reconciled and the reconciled q-rates obtained through element conservation in three phases of the evolution experiment. (All values are in mmol/Cmol h)

	Phase I				Phase II				Phase III			
	Non-reconciled		Element reconciled		Non-reconciled		Element reconciled		Non-reconciled		Element reconciled	
	Value	Error	Value	Error	Value	Error	Value	Error	Value	Error	Value	Error
qglu	-199.4	16.0	-188.1	13.0	-95.2	7.5	-95.3	6.3	-82.9	6.5	-79.8	4.8
qco2	394.1	30.0	386.4	29.0	207.3	16.0	207.3	15.0	153.5	12.0	150.3	10.0
qo2	-106.2	160.0	-143.5	15.0	-160.7	79.0	-160.9	12.0	-110.6	74.0	-117.7	8.6
μ	110.0	2.5	109.8	2.5	102.0	2.3	102.0	2.3	95.0	2.1	94.9	2.1
qfum	1.9	0.2	1.8	0.2	0.9	0.1	0.9	0.1	0.9	0.1	0.9	0.1
qsuc	0.8	0.1	0.8	0.1	0.7	0.1	0.7	0.1	0.2	0.0	0.2	0.0
qmal	3.5	0.3	3.4	0.3	1.6	0.3	1.6	0.3	0.9	0.1	0.8	0.1
qACE	57.6	5.1	56.9	5.0	73.8	5.9	73.9	5.7	68.7	6.1	68.2	6.0
qEthanol	236.2	21.0	241.7	21.0	41.3	4.6	41.4	4.6	23.1	2.1	22.7	2.0
qGly	3.9	0.3	3.8	0.3	6.6	3.3	6.6	3.0	15.1	1.4	14.8	1.3
C-balance	0.94				1.0				0.98			
Y-balance	0.90				1.0				0.96			

Table 5.S5. Fum 114: Comparison of the element reconciled q-rates with the metabolic network (Δ FUM1, Δ ZWF1) reconciled q-rates. (All values are in mmol/Cmol h).

	Phase I				Phase II				Phase III			
	Element reconciled		Metabolic network reconciled		Element reconciled		Metabolic network reconciled		Element reconciled		Metabolic network reconciled	
	Value	Error	Value	Error	Value	Error	Value	Error	Value	Error	Value	Error
qglu	-188.1	13.0	-190.5	7.7	-95.3	6.3	-90.3	3.4	-79.8	4.8	-78.9	2.7
qco2	386.4*	29.0	337.6	15.4	207.3	15.0	140.9	6.2	150.3	10.0	113.3	5.2
qo2	-143.5	15.0	-63.3	5.0	-160.9	12.0	-87.7	5.6	-117.7	8.6	-78.8	5.1
μ	109.8	2.5	112.9	2.5	102.0	2.3	102.2	2.3	94.9	2.1	95.2	2.1
qfum	1.8	0.2	0.6	0.1	0.9	0.1	0.9	0.1	0.9	0.1	0.9	0.1
qsuc	0.8	0.1	0.5	0.1	0.7	0.1	0.7	0.1	0.2	0.0	0.2	0.0
qmal	3.4	0.3	3.5	0.3	1.6	0.3	1.6	0.3	0.8	0.1	0.9	0.1
qACE	56.9	5.0	59.7	5.0	73.9	5.7	84.7	5.3	68.2	6.0	81.1	5.1
qEthan ol	241.7	21.0	271.6	15.3	41.4	4.6	47.8	4.3	22.7	2.0	24.5	2.1
qGly	3.8	0.3	3.9	0.3	6.6	3.0	7.0	3.2	14.8	1.3	15.2	1.4
qpyr	0	0	0.0	0.0	0	0	0.0	0.0	0.0	0.0	0.0	0.0

Table 5.S6. Fum 114: Comparison of the element reconciled q-rates with the metabolic network (Δ ZWF1) reconciled q-rates. (All values are in mmol/Cmol.h)

	Phase I				Phase II				Phase III			
	Element reconciled		Metabolic network reconciled		Element reconciled		Metabolic network reconciled		Element reconciled		Metabolic network reconciled	
	Value	Error	Value	Error	Value	Error	Value	Error	Value	Error	Value	Error
qglu	-188.1	13.0	-190.7	7.7	-95.3	6.3	-95.2	3.5	-79.8	4.8	-81.2	2.7
qco2	386.4	29.0	397.6	28.3	207.3	15.0	206.7	14.9	150.3	10.0	154.2	11.4
qo2	-143.5	15.0	-154.4	35.7	-160.9	12.0	-160.2	15.9	-117.7	8.6	-121.0	11.7
μ	109.8	2.5	110.0	2.5	102.0	2.3	102.0	2.3	94.9	2.1	95.0	2.1
qfum	1.8	0.2	1.9	0.2	0.9	0.1	0.9	0.1	0.9	0.1	0.9	0.1
qsuc	0.8	0.1	0.8	0.1	0.7	0.1	0.7	0.1	0.2	0.0	0.2	0.0
qmal	3.4	0.3	3.5	0.3	1.6	0.3	1.6	0.3	0.8	0.1	0.9	0.1
qACE	56.9	5.0	57.9	5.1	73.9	5.7	73.8	5.7	68.2	6.0	69.2	5.8
qEthanol	241.7	21.0	242.0	19.2	41.4	4.6	41.4	4.5	22.7	2.0	23.2	2.1
qGLY	3.8	0.3	3.9	0.3	6.6	3.0	6.6	3.2	14.8	1.3	15.1	1.4
qpyr	0	0	0.0	0.0	0	0	0.0	0.0	0.0	0.0	0.0	0.0

Table 5.S7. Fum 114: Intracellular fluxes obtained in three different phases using the metabolic network ($\Delta ZWF1$) (All values are in mmol/Cmol.h)

	CEN.PK 113-7D		Phase I		Phase II		Phase III	
	Value	Error	Value	Error	Value	Error	Value	Error
Glycolysis								
cHX kin	26.8	0.3	190.7	7.7	95.3	3.5	81.2	2.7
cG6P iso	17.0	0.3	183.4	7.7	88.6	3.5	74.9	2.7
cPF kin	13.1	0.3	182.6	7.7	87.8	3.5	74.3	2.7
cF16P ald	13.1	0.3	182.6	7.7	87.8	3.5	74.3	2.7
cGAP deh	31.1	0.6	360.4	15.4	168.2	6.6	132.6	5.3
c13PG kin	31.1	0.6	360.4	15.4	168.2	6.6	132.6	5.3
c3PG mut	29.2	0.6	358.6	15.4	166.5	6.6	131.0	5.3
cEnol	29.2	0.6	358.6	15.4	166.5	6.6	131.0	5.3
cPYR kin	27.9	0.6	357.2	15.4	165.3	6.6	129.9	5.3
Pyruvate branch point								
cPYR carboxylase	6.3	0.1	12.0	0.4	8.6	0.3	7.0	0.2
mPYR deh	17.6	0.5	34.2	12.0	31.4	5.7	20.9	4.5
cPYR decarboxylase	--	--	306.3	19.7	121.0	7.1	97.9	6.2
cACCoA carb	4.3	0.1	4.4	0.1	4.1	0.1	3.8	0.1
cACCoA syn	6.5	0.1	6.6	0.2	6.1	0.1	5.7	0.1
cACTAL deh (NAD)	6.4	0.8	35.8	5.1	53.3	5.8	50.1	5.9
cACTAL deh (NADP)	--	--	28.6	0.6	26.5	0.6	24.7	0.5
cETOH deh	-6.9	0.4	242.0	19.2	41.3	4.5	23.2	2.1
TCA cycle								
mCIT syn	17.6	0.5	34.2	12.0	31.4	5.7	20.9	4.5
mACON 1	17.6	0.5	34.2	12.0	31.4	5.7	20.9	4.5

Evolution of engineered *S. cerevisiae* for the aerobic production of dicarboxylic acids

mACON 2	17.6	0.5	34.2	12.0	31.4	5.7	20.9	4.5
mICIT deh_NAD	15.0	0.5	31.6	12.0	29.0	5.7	18.7	4.5
mICIT deh_NADP	2.6	0.1	2.6	0.1	2.4	0.1	2.3	0.0
mOGL deh	14.5	0.5	31.1	12.0	28.5	5.7	18.2	4.5
mSUC deh	14.5	0.5	30.3	12.0	27.8	5.7	18.0	4.5
Fumarase	15.5	0.5	29.5	12.0	27.9	5.7	18.0	4.5
Malate dehydrogenase	14.9	0.5	26.0	12.0	26.1	5.7	17.1	4.5
mNADH deh PO II	65.5	2.0	132.1	48.1	121.2	22.8	79.5	17.9
Uptake/secretion								
Glucose uptake	26.8	0.4	190.7	7.7	95.3	3.5	81.2	2.7
Ethanol	-6.9	0.4	242.0	19.2	41.3	4.5	23.2	2.1
CO ₂	63.4	1.8	397.6	28.3	207.2	14.9	154.2	11.4
O ₂ uptake	66.0	1.8	154.4	35.7	160.9	15.9	121.0	11.7
Acetate	0.0	0.0	57.9	5.1	73.8	5.7	69.2	5.8
Succinate	0.0	0.0	0.8	0.1	0.7	0.1	0.2	0.0
Malate	0.6	0.0	3.5	0.3	1.6	0.3	0.9	0.1
Pyruvate	0.0	0.0	0.0	0.0	0.0	0.0	0.0	0.0
eATPase	33.8	0.6	103.4	5.2	110.8	5.8	101.8	5.9
Glycerol	0.0	0.0	3.9	0.3	6.6	3.2	15.1	1.4
Fumarate	0.0	0.0	1.9	0.2	0.9	0.1	0.9	0.1
								0.0
Maintenance	58.0	5.8	520.3	91.9	342.5	45.3	216.1	33.7

Table 5.S8. Fum 116: Averaged raw data obtained in three phases of the evolution experiment.

	Units	Phase I		Phase II		Phase III	
		Value	Error	Value	Error	Value	Error
Fout	Kg/h	0.0510	1%	0.0510	1%	0.0510	1%
V	Kg	0.5000	2%	0.5000	2%	0.5000	2%
Fgas,in	mol/h	0.8009	1%	0.8009	1%	0.8009	1%
Fadd	Kg/h	0.0003	1%	0.0003	1%	0.0003	1%
Cgluin	mM	41.6667	2.5%	41.6667	2.5%	41.6667	2.5%
Cglu	mM	3.4540	0.1796	0.1243	0.0328	0.2202	0.0404
Cetoh	mM	32.4920	2.1120	7.6420	0.6684	6.3531	0.3136
Cfum	mM	0.2116	0.0106	0.2475	0.0307	0.4340	0.0370
suc	mM	2.8499	0.1425	1.2900	0.5328	1.2600	0.2801
mal	mM	10.0373	0.7528	15.0085	0.6867	17.9158	0.8697
gly	mM	0.1380	0.0102	0.2500	0.1524	0.1889	0.0454
ace	mM	10.8760	0.5438	14.5516	1.1819	17.9517	0.7261
pyr	mM	5.1442	0.2572	7.3518	0.6210	3.2984	0.4024
Cdw	g/Kg	0.8700	0.0435	1.2357	0.0618	1.3009	0.0650
CO2_in	%	0.036	1%	0.036	1%	0.023	1%
O2_in	%	20.946	0	20.946	0	20.946	0
CO2_out	%	0.386	1%	0.386	1%	0.353	1%
O2_out	%	20.749	1%	20.595	1%	20.605	1%
Mw	-	26.400	5%	26.400	5%	26.400	5%

Table 5.S9. Fum 116: Comparison of the non-reconciled and the reconciled q-rates obtained through element conservation in three phases of the evolution experiment. (All values are in mmol/Cmol h)

	Fum 116: Phase I						Phase II						Phase III					
	Non-reconciled			Element reconciled			Non-reconciled			Element reconciled			Non-reconciled			Element reconciled		
	Value	Error		Value	Error		Value	Error		Value	Error		Value	Error		Value	Error	
qglu	-117.52	9.30		-125.83	8.70		-89.99	7.00		-83.94	5.30		-85.28	6.70		-80.96	4.90	
qco2	170.47	13.00		175.52	13.00		119.78	9.00		115.03	8.00		107.26	8.00		103.98	7.20	
qo2	-76.21	130.00		-116.41	11.00		-120.04	89.00		-135.82	10.00		-111.61	85.00		-128.58	9.60	
mu	102.00	2.30		102.12	2.30		102.00	2.30		101.90	2.30		102.00	2.30		101.93	2.30	
qfum	0.66	0.06		0.68	0.06		0.54	0.08		0.52	0.07		0.90	0.10		0.87	0.10	
qsuc	8.82	0.79		9.07	0.80		2.81	1.20		3.10	1.10		2.61	0.61		2.60	0.59	
qmal	31.07	3.30		30.64	3.30		32.71	2.90		32.00	2.70		37.08	3.30		36.65	3.20	
qACE	33.66	3.00		34.43	3.10		31.71	3.50		31.38	3.40		37.16	3.10		36.24	2.90	
qEthanol	100.57	9.90		98.29	9.80		16.65	1.90		16.28	1.80		13.15	1.20		12.78	1.10	
qGly	0.43	0.05		0.44	0.05		0.54	0.33		0.55	0.32		0.39	0.10		0.38	0.10	
qPyr	15.92	1.40		16.34	1.40		16.02	1.80		15.76	1.70		6.83	0.97		6.73	0.94	
C-balance	1.06						0.95						0.96					
Y-balance	1.01						0.91						0.93					

Table 5.S10. Fum 1.16: Comparison of the element reconciled q-rates with the metabolic network (Δ FUM1, Δ ZWF1) reconciled q-rates. (All values are in mmol/Cmol h)

	Phase I			Phase II			Phase III					
	Element reconciled		Metabolic network reconciled	Element reconciled		Metabolic network reconciled	Element reconciled		Metabolic network reconciled			
	Value	Error		Value	Error		Value	Error				
qglu	-125.83	8.70	-123.90	4.21	-83.94	5.30	-77.83	2.64	-80.96	4.90	-71.72	2.34
qco2	175.52 *	13.00	144.10	7.92	115.03	8.00	55.05	4.64	103.98	7.20	48.89	4.14
qo2	-116.41	11.00	-69.10	3.57	-135.82	10.00	-68.69	4.14	-128.58	9.60	-64.27	3.17
mu	102.12	2.30	102.00	2.30	101.90	2.30	102.50	2.30	101.93	2.30	102.60	2.30
qfum	0.68	0.06	0.66	0.06	0.52	0.07	0.55	0.08	0.87	0.10	0.92	0.10
qsuc	9.07	0.80	8.97	0.79	3.10	1.10	5.49	1.16	2.60	0.59	3.41	0.60
qmal	30.64	3.30	28.97	3.16	32.00	2.70	27.03	2.72	36.65	3.20	28.80	2.99
qACE	34.43	3.10	34.74	2.94	31.38	3.40	43.10	3.22	36.24	2.90	47.44	2.85
qEthano l	98.29	9.80	112.20	7.43	16.28	1.80	19.99	1.86	12.78	1.10	14.68	1.19
qGLy	0.44	0.05	0.43	0.05	0.55	0.32	0.56	0.33	0.38	0.10	0.39	0.10
qPyr	16.34	1.40	15.85	1.40	15.76	1.70	16.43	1.79	6.73	0.94	6.97	0.97

*Bold values indicate significant differences between element and metabolic network reconciled rates

Table S.S11. Fum 1.16: Comparison of the element reconciled q-rates with the metabolic network (Δ ZWF1) reconciled q-rates. (All values are in mmol/Cmol.h)

	Phase I				Phase II				Phase III			
	Element reconciled		Metabolic network reconciled		Element reconciled		Metabolic network reconciled		Element reconciled		Metabolic network reconciled	
	Value	Error	Value	Error	Value	Error	Value	Error	Value	Error	Value	Error
qglu	-125.83	8.70	-123.7	4.2	-83.94	5.30	-86.1	2.8	-80.96	4.90	-82.8	2.7
qco2	175.52	13.00	168.1	12.7	115.03	8.00	120.6	8.8	103.98	7.20	107.7	7.8
qo2	-116.41	11.00	-108.4	16.5	-135.82	10.00	-142.2	9.3	-128.58	9.60	-132.8	8.4
mu	102.12	2.30	101.9	2.3	101.90	2.30	102.1	2.3	101.93	2.30	102.1	2.3
qfum	0.68	0.06	0.7	0.1	0.52	0.07	0.5	0.1	0.87	0.10	0.9	0.1
qsuc	9.07	0.80	8.8	0.8	3.10	1.10	2.9	1.2	2.60	0.59	2.6	0.6
qmal	30.64	3.30	30.5	3.2	32.00	2.70	33.1	2.8	36.65	3.20	37.5	3.1
qACE	34.43	3.10	33.5	3.0	31.38	3.40	32.0	3.5	36.24	2.90	37.4	3.1
qEthanol	98.29	9.80	98.4	9.4	16.28	1.80	16.8	1.9	12.78	1.10	13.2	1.2
qGLy	0.44	0.05	0.4	0.0	0.55	0.32	0.5	0.3	0.38	0.10	0.4	0.1
qPyr	16.34	1.40	15.9	1.4	15.76	1.70	16.1	1.8	6.73	0.94	6.8	1.0

Table 5.S12. Fum 116: Intracellular fluxes obtained in three different phases using the metabolic network (Δ ZWF1) (All values are in mmol/Cmol.h)

	Phase I		Phase II		Phase III	
Glycolysis	Value	Error	Value	Error	Value	Error
cHX kin	123.7	4.2	86.1	2.8	82.8	2.7
cG6P iso	117.0	4.2	79.3	2.8	76.0	2.6
cPF kin	116.3	4.2	78.6	2.8	75.3	2.6
cF16P ald	116.3	4.2	78.6	2.8	75.3	2.6
cGAP deh	231.3	8.4	155.8	5.6	149.3	5.3
c13PG kin	231.3	8.4	155.8	5.6	149.3	5.3
c3PG mut	229.6	8.4	154.1	5.6	147.6	5.3
cEnol	229.6	8.4	154.1	5.6	147.6	5.3
cPYR kin	228.3	8.4	152.9	5.6	146.4	5.3
Pyruvate branchpoint						
cPYR carboxylase	45.3	3.3	41.9	3.0	46.4	3.2
mPYR deh	25.0	5.6	35.8	3.4	32.3	3.0
cPYR decarboxylase	137.8	9.7	54.7	3.9	56.5	3.3
cACCoA carb	4.1	0.1	4.1	0.1	4.1	0.1
cACCoA syn	6.1	0.1	6.1	0.1	6.1	0.1
cACTAL deh (NAD)	13.0	3.0	11.6	3.5	16.9	3.1
cACTAL deh (NADP)	26.5	0.6	26.5	0.6	26.5	0.6
cETOH deh	98.4	9.4	16.8	1.9	13.2	1.2
TCA cycle						
mCIT syn	25.0	5.6	35.8	3.4	32.3	3.0
mACON 1	25.0	5.6	35.8	3.4	32.3	3.0
mACON 2	25.0	5.6	35.8	3.4	32.3	3.0
mICIT deh_NAD	22.6	5.6	33.3	3.4	29.9	3.0
mICIT deh_NADP	2.4	0.1	2.4	0.1	2.4	0.1
mOGL deh	22.1	5.6	32.9	3.4	29.4	3.0
mSUC deh	13.4	5.6	30.0	3.5	26.8	3.0

Evolution of engineered *S. cerevisiae* for the aerobic production of dicarboxylic acids

Fumarase	13.7	5.6	30.4	3.4	26.9	3.0
Malate dehydrogenase	-16.9	5.6	-2.7	3.4	-10.5	3.0
mNADH deh PO II	95.7	22.4	138.5	13.5	124.8	12.1
Uptake/secretion						
Glucose uptake	123.7	4.2	86.1	2.8	82.8	2.7
Ethanol	98.4	9.4	16.8	1.9	13.2	1.2
eCO ₂ <-cCO ₂	168.1	12.7	120.6	8.8	107.7	7.8
O ₂ uptake	108.4	16.5	142.2	9.3	132.8	8.4
Acetate	33.5	3.0	32.0	3.5	37.4	3.1
Succinate	8.8	0.8	2.9	1.2	2.6	0.6
Malate	30.5	3.2	33.1	2.8	37.5	3.1
Pyruvate	15.9	1.4	16.1	1.8	6.8	1.0
eATPase	159.9	7.3	152.0	7.0	156.9	7.0
Glycerol	0.4	0.0	0.5	0.3	0.4	0.1
Fumarate	0.7	0.1	0.5	0.1	0.9	0.1
Maintenance	199.0	41.5	219.9	25.8	180.3	22.9

Chapter 6

Metabolic engineering of *Saccharomyces cerevisiae* to produce dicarboxylic acids

Abstract

S. cerevisiae was engineered to divert the carbon flux towards fumaric acid formation. Enzymes involved in the reductive part of the TCA cycle were overexpressed in the cytosol and to facilitate the secretion of fumaric acid two heterologous transporters, SpMAE1 from *Schizosaccharomyces pombe* and DCT-02 from *Aspergillus niger* were tested. The engineered *S. cerevisiae* strains were cultivated in shake flasks under conditions of nitrogen starvation and glucose excess at near neutral pH, which was maintained by the addition of CaCO₃. CaCO₃ was also used for maintaining a high partial pressure of CO₂ to promote dicarboxylic acid production. The parent strains used for further strain construction in this study were CEN.PK2_1C (control strain), Fum 116 (Δ FUM1, Δ ZWF1, \uparrow DCT-02) and Fum 107 (Δ FRDS1, Δ OSM1). Fum 116 was engineered to produce fumaric acid via the oxidative branch of the TCA cycle while Fum 107 was constructed to produce fumaric acid via the reductive branch. In these strains the enzymes involved in the reductive branch of the TCA cycle (PEP carboxykinase, pyruvate carboxylase, malate dehydrogenase and fumarase) were overexpressed in different combinations. In addition the reductive TCA cycle genes from *Rhizopus delemar* were overexpressed in *S. cerevisiae*.

Overexpression of pyruvate carboxylase led to an increase of the yield of metabolites produced through the oxidative branch of the TCA cycle (succinate, fumarate and α -Ketoglutarate). The overexpression of fumarase and malate dehydrogenase in Fum 116 and Fum 107 resulted in an increased malic acid production, most likely via the reductive branch of the TCA cycle. The overexpression of the reductive pathway enzymes resulted in a significant increase in the yields of succinic and malic acid. In case of malic acid, the final yield in Fum 116 (\uparrow PEPCK, \uparrow FUMR, \uparrow MDH3) and Fum 107 (\uparrow RoFUM) were 0.20 and 0.35 mol acid/mol glucose consumed respectively. The yield of fumaric also improved, but was still much lower than the malic and succinic acid yields. The presence of the heterologous dicarboxylic acid transporters DCT-02 and SpMAE1 resulted in improved export of malic and succinic acid but did not have any effect on the export of fumaric acid.

Introduction

Metabolic engineering has been applied successfully to *Saccharomyces cerevisiae* to produce dicarboxylic acids. The applied metabolic engineering strategies primarily included the overexpression of enzymes involved in the TCA cycle (17, 24, 34), knock-out of the TCA cycle reactions to make the dicarboxylic acid of interest as the end product of either the reductive or the oxidative branch of the TCA cycle (21, 30). Some studies also focused on the expression of heterologous transporters to facilitate the export dicarboxylic acids (17, 21, 28, 34). In this study *S. cerevisiae* was engineered with the intention to divert the carbon flux towards fumaric acid and thereby improve the yield and productivity.

Rhizopus spp. is a natural producer of fumaric acid, which some studies have mentioned is due to the kinetic properties of the fumarase in this organism, which has a higher affinity for malate than for fumarate (8, 9, 11). The biosynthesis of fumaric acid in *Rhizopus* spp. occurs mainly in the cytosol, through the reductive branch of the TCA cycle (10). However, no information is available on the export mechanism of fumaric acid in *Rhizopus* spp. which most likely plays a pivotal role in achieving the high productivity of fumaric acid.

S. cerevisiae has been engineered to produce fumaric acid by overexpressing heterologous genes of the reductive TCA cycle from *Rhizopus* spp.. The highest yield of fumaric acid reported in *S. cerevisiae* so far is $0.51 \text{ mol. (mol glucose)}^{-1}$ with module based optimisation of the pathways consisting of a reductive module (RoPYC, RoMDH, RoFUM1 and plasma membrane dicarboxylic acid transporter SpMAE1), an oxidative module (KGD2, SUCLG2, SDH1 and SFC1) and a module to control the expression levels of glycerol 3-phosphate and pyruvate decarboxylase and thus the formation of glycerol and ethanol (34).

In this study heterologous genes from *R. delemar* were overexpressed in *S. cerevisiae* to improve the production of dicarboxylic acids. Two heterologous transporters SpMAE1 and DCT02 were also overexpressed to improve the secretion rate of dicarboxylic acids. Genetic modifications were carried out in the strains CEN.PK2_1C (control strain), Fum 116 (Δ Fum1, Δ Zwf1, \uparrow DCT-02) and Fum 107 (Δ osm1, Δ frds1).

Materials and methods

Strain storage and cultivation conditions

Strains used in this study are listed in Table 6.1. CEN.PK 21_C was used for genetic modifications due to its auxotrophy for tryptophan, leucine and uracil which allows to use the plasmids with different selection markers (tryptophan, leucine or uracil).

All strains were pre-grown in shake flasks with media containing 20 g.L⁻¹ glucose.H₂O, 5 g.L⁻¹ (NH₄)₂SO₄, 3 g.L⁻¹ KH₂PO₄, 0.5 g.L⁻¹ MgSO₄.7H₂O, 1ml.L⁻¹ trace mineral solution and 1ml.L⁻¹ vitamin solution. Due to the auxotrophies, the growth media also contained 0.15 g.L⁻¹ uracil, 0.125 g.L⁻¹ histidine, 0.5 g.L⁻¹ leucine, 0.075 g.L⁻¹ tryptophan and 0.15 g.L⁻¹ methionine, in addition to the media components mentioned above. Stock cultures were prepared from the shake flasks with the addition of 30% glycerol v/v and stored at -80 °C.

To overproduce dicarboxylic acids, the strains were first cultivated overnight at 30°C on a gyratory shaker at 200 rpm in shake flasks on the growth medium described above. After overnight cultivation, the culture was centrifuged and the pellet containing the biomass was re-suspended in a medium containing 100 g.L⁻¹ glucose.H₂O, 50 g.L⁻¹ CaCO₃, 40 µg.L⁻¹ biotin, 1 ml.L⁻¹ trace element and 1 ml.L⁻¹ vitamin solution. CaCO₃ was used as a buffering agent in order to maintain the pH between 6.0 and 6.5. The reason to add 40 µg.L⁻¹ of biotin was to ensure a sufficiently high activity of pyruvate carboxylase.

Plasmid construction and transformation

The plasmids used for the transformations are listed in Table 6.2. All plasmids used were single copy plasmids (pRS 414, pRS 415 and pRS 416), and the genes were expressed under the control of a strong constitutive promoter. The sequences of the genes RoPYC, RoMDH and RoFUM were codon optimised for *S. cerevisiae* and synthesized by GeneArt™. Each gene from GeneArt™ was obtained in a separate plasmid with a kanamycin marker. The plasmids were transformed into chemically competent *E. coli* obtained from Invitrogen™. The transformed cells were grown in LB media for plasmid amplification. The amplified plasmids were isolated using the QIAprep spin miniprep kit (QIAGEN) and digested with appropriate restriction enzymes (New England BioLabs)

(*XmaI* and *SacII* for RoFUM, *XhoI* and *SacI* for RoMDH, *XmaI* and *SacI* for RoPYC). The fragments of plasmids were separated on a 0.8 % agarose gel, the fragments containing *Rhizopus* spp. genes (RoFUM, RoMDH and RoPYC) were extracted using the QIA quick gel extraction kit (QIAGEN). The extracted RoFUM, RoMDH and RoPYC genes with sticky ends were ligated to the plasmids pRS 414, pRS 415 and pRS 416 respectively, which were also treated with the same set of restriction enzymes. Plasmids pGBS414PPK, pGBS415FUM3, pGBS416PYC2 and pRS416MAE1 were kindly provided by DSM B.V. (Delft, The Netherlands), the details of these plasmids are provided in a patent by DSM IP assets B.V. (28) and the reductive TCA cycle genes in these plasmids are shown in Table 6.2.

The plasmids listed in Table 6.2 were first transformed into *E. coli* for amplification and were thereafter transformed into *S. cerevisiae*. The transformation protocol was the same as described by Guldener *et al.* (113). After transformation, *S. cerevisiae* cells were plated on selective agar plates and the colonies obtained were re-streaked. Colony PCR was done to ensure that the cells were transformed with the intended plasmid. The primers used for the colony PCR are listed in Table 6.3.

Metabolite analyses

Samples for quantification of extracellular metabolites were taken by withdrawing 2 ml of broth from shake flasks into Eppendorf tubes, which were then rapidly centrifuged at 5000 g for 5 min to remove biomass and CaCO₃ from the samples. The supernatants was then transferred to new Eppendorf tubes and stored at -20°C until further analysis. Glucose, glycerol, acetate and ethanol were quantified through HPLC analysis using a Bio-Rad HPX-87H 300 column (7.8 mm). The column was eluted with phosphoric acid (1.5 mM in Milli-Q water) at a flow rate of 0.60 mL min⁻¹. Organic acids (malic, succinic, pyruvic and fumaric) were also quantified using the Bio-Rad HPX-87H 300 column (7.8 mm) where the column was eluted with more concentrated phosphoric acid (45 mM in Milli Q water) in order to achieve a better separation of succinic and fumaric acid.

Table 6.1. *S. cerevisiae* strains used in this study

Strain	Genotype
CEN.PK21_C	MATa; ura3-52; trp1-289; leu2-3,112; his3 D1; MAL2- 8C; SUC
CEN.PK21_C + RoPYC↑	MATa; ura3-52; trp1-289; leu2-3,112; his3 D1; MAL2- 8C; SUC {pGPD416RoPYC}
CEN.PK21_C + RoPYC↑ + RoFUM↑	MATa; ura3-52; trp1-289; leu2-3,112; his3 D1; MAL2- 8C; SUC {pGPD416RoPYC} {pGPD414RoFum}
CEN.PK21_C + SpMAE1↑	MATa; ura3-52; trp1-289; leu2-3,112; his3 D1; MAL2- 8C; SUC {pRS416SpMAE1}
Fum 116	CEN.PK 21_C, fum1::lox P zwf1::KanMX, <i>sit4</i> ::[<i>ENO1p-DCT_02-ENO1t</i>]
Fum 116 + RoPYC↑	CEN.PK 21_C, fum1::lox P zwf1::KanMX, <i>sit4</i> ::[<i>ENO1p-DCT_02-ENO1t</i>], {pGPD416RoPYC}
Fum 116 + FUM1 ↑ + MDH3↑	CEN.PK 21_C, fum1::lox P zwf1::KanMX, <i>sit4</i> ::[<i>ENO1p-DCT_02-ENO1t</i>], {pGBS415FUM3}
Fum 116 + PEPcK↑ + FUMR↑ + MDH3	CEN.PK 21_C, fum1::lox P zwf1::KanMX, <i>sit4</i> ::[<i>ENO1p-DCT_02-ENO1t</i>], {pGBS414PPK}
Fum 116 + SpMAE1↑	CEN.PK 21_C, fum1::lox P zwf1::KanMX, <i>sit4</i> ::[<i>ENO1p-DCT_02-ENO1t</i>], {pRS416SpMAE1}
Fum 107	MATA ura3-52 leu2-112 trp1-289 frds1::lox P osm1::KanMX (kindly provided by DSM B. V.)
Fum 107 + RoPYC↑	MATA ura3-52 leu2-112 trp1-289 frds1::lox P osm1::KanMX, {pGPD416RoPYC}
Fum 107 + RoMDH↑	MATA ura3-52 leu2-112 trp1-289 frds1::lox P osm1::KanMX, {pGPD415RoMDH}
Fum 107 + FUM1↑ + MDH3↑	MATA ura3-52 leu2-112 trp1-289 frds1::lox P osm1::KanMX, {pGBS415FUM3}

Table 6.2. Plasmids used for the transformations of *S. cerevisiae*

Plasmid	Comments
pGBS414PPK	pRS 414 plasmid with tryptophan marker for <i>S. cerevisiae</i> and ampicillin marker for <i>E. coli</i> , overexpression of PEP carboxykinase from <i>Mannheimia succiniciproducens</i> . P _{TEF}
pGBS415FUM3	pRS 415 plasmid with leucine marker for <i>S. cerevisiae</i> and ampicillin marker for <i>E. coli</i> , overexpression of fumarase (FUMR or FUM1) from <i>S. cerevisiae</i> under the control of TDH1 promoter and terminator, and malate dehydrogenase (MDH3) from <i>S. cerevisiae</i> under the control of TDH3 promoter and terminator
pGBS416PYC2	pRS 416 plasmid with uracil marker for <i>S. cerevisiae</i> and ampicillin marker for <i>E. coli</i> , expression of pyruvate carboxylase (PYC2) from <i>S. cerevisiae</i>
pRS416MAE1	pRS 416 plasmid with uracil marker for <i>S. cerevisiae</i> and ampicillin marker for <i>E. coli</i> , expression of heterologous dicarboxylic acid transporter SpMAE1 from <i>Schizosaccharomyces pombe</i>
pGPD414RoFUM	pRS 414 plasmid with tryptophan marker for <i>S. cerevisiae</i> and ampicillin marker for <i>E. coli</i> , overexpression of heterologous fumarase (RoFUM) from <i>Rhizopus oryzae</i> under the control of constitutive GPD promoter and CYC terminator
pGPD415RoMDH	pRS 415 plasmid with leucine marker for <i>S. cerevisiae</i> and ampicillin marker for <i>E. coli</i> , overexpression of heterologous malate dehydrogenase (RoMDH) from <i>Rhizopus oryzae</i> under the control of constitutive GPD promoter and CYC terminator
pGPD416RoPYC	pRS 416 plasmid with uracil marker for <i>S. cerevisiae</i> and ampicillin marker for <i>E. coli</i> , overexpression of heterologous pyruvate carboxylase (RoPYC) from <i>Rhizopus oryzae</i> under the control of constitutive GPD promoter and CYC terminator

Table 6.3: Primers used in this study

Amplification of gene	FW Primer	REV Primer
PEPcK	GGTTGTTACGCCAAGACCATC	GCAAGACACCGAAAGCATCAG
PYC2	TCGATGTCGCCATGAGATTTC	ACCAGCCATGTCCTTGATAC
MDH3	CCCAAACGCTCGTATCTTAG	TCCTTGACAGCAGTGTGAC
FUM1	AGGCTGCTGACGAAGTTATC	GCAAGTGGGTCTACCAATC
RoFUM	GGCTGCTGATGAAGTTATCG	AACAGCAGTACCACCTTGAG
RoPYC	GGCTGTAAAGTCCGGTATGG	CCACCTGGCATTTCGTGTTTC
RoMDH	TGCTGGTGGTATTGGTCAAC	TGGGTCAAAGCGTCCAATTC

Results and discussion:

The engineered *S. cerevisiae* strains were first cultivated in shake flasks on media containing glucose, nitrogen and the required supplements (leucine, tryptophan, uracil and methionine) to counter auxotrophy. After overnight cultivation, the cultures were centrifuged and the pellets containing the biomass were re-suspended in a medium containing glucose, CaCO₃ and biotin. Biotin was added for proper functioning of pyruvate carboxylase. The net glucose consumption varied significantly between the different *S. cerevisiae* strains. Therefore to better compare the results obtained for the different strains the yields of metabolites (mol produced per mol of glucose consumed) are presented in figures 6.1, 6.2 and 6.3.

Genetic modifications in CEN.PK2_1C

Overexpression of RoPYC in CEN.PK2_1C led to a 7 fold increase in the yield of succinic acid to a value of 0.21 mol/mol glucose (see Figure 6.1). The final concentration of succinic acid obtained was 12.7 mmol/L, while 61.1 mmol/L of glucose was consumed. This increase of the yield of succinic acid was most likely caused by an increase in the flux through the oxidative part of the TCA cycle through the overexpression of RoPYC. The combined overexpression of RoPYC and RoFUM resulted in a yield of succinic acid of 0.11 mol/mol glucose, which was lower than the yield obtained by the overexpression of RoPYC only, and a slight increase of the fumaric acid and α -ketoglutarate yields. The final concentration of succinic acid obtained was 32 mM with the net consumption of 282 ± 16 mM of glucose.

The expression of the *Schizosaccharomyces pombe* malate transporter SpMAE1 resulted in improved C4 acid secretion in CEN.PK 2_1C. It has indeed

been reported that this transporter exports malic (17), succinic (130) and fumaric acid (34, 107). In our study, SpMAE1 expression mainly improved the yield of succinic acid from 0.027 mol/mol glucose in CEN.PK 2_1C to 0.05 mol/mol glucose in CEN.PK2_1C SpMAE1 \uparrow . The concentration of fumaric acid in CEN.PK2_1C SpMAE1 \uparrow was 3.9 mM (yield 0.009 mol/mol glucose) compared to the absence of fumaric acid secretion in CEN.PK 2_1C. So the SpMAE1 transporter did facilitate the export of succinic and fumaric acid to some extent. However, in all strains the yield of fumaric acid on glucose was significantly lower than for malic and succinic acid.

The fermentative products ethanol, glycerol, acetate and pyruvate were produced in significant amounts. There was not much difference in the yields of fermentative products on glucose between the different strains, with the exception of CEN.PK2_1C RoPYC \uparrow RoFUM \uparrow for which the yields of all fermentative products were lower, which might be due to a higher flux through the TCA cycle.

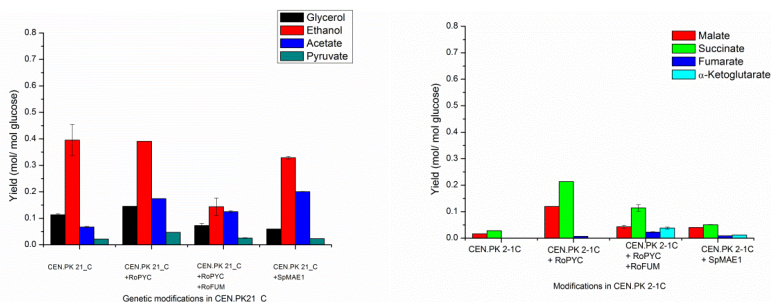


Figure 6.1. Measured yields of metabolites (mol/ mol glucose consumed) for different mutant strains derived from CEN.PK21_C.

Genetic modifications in Fum 116

Fum 116 was derived from CEN.PK2_1C with the knock-out of fumarase (FUM1) and glucose 6-phosphate dehydrogenase (ZWF1) and integration of the DCT-02 transporter in its genome. This strain was used as background for the overexpression of different combinations of enzymes of the reductive

branch of the TCA cycle. The SpMAE1 transporter was also overexpressed in this strain although the strain already contained the DCT-02 transporter. Fum 116 produced pyruvate as main product (Figure 6.2) and has therefore, with the overexpression of the reductive TCA pathway enzymes, has the potential to produce dicarboxylic acids.

Overexpression of pyruvate carboxylase

The overexpression of RoPYC led to a decrease of the pyruvate yield and an increase in the yield of metabolites in the oxidative part of the TCA cycle (α -ketoglutarate, succinate, fumarate and malate, see Figure 6.2). This was most probably caused by an increased flux through the TCA cycle, which also resulted in an increased yield of glycerol due to redox imbalance. Remarkably, the introduction of RoPYC resulted in a very significant decrease of the ethanol yield and a significant increase of the acetate yield.

Overexpression of SpMAE1

SpMAE1 was expressed in strain Fum 116 to examine whether it would facilitate the export of fumaric acid. Apart from SpMAE1, Fum 116 also contained the DCT-02 transporter, but as discussed in the previous chapters this transporter is able to export malic and succinic acid but not fumaric acid.

Fum 116 SpMAE1 \uparrow improved the yield of malic acid by 13 fold and the yield of succinic acid by 4 fold compared to the parent strain Fum 116 which contains only the DCT-02 transporter. This increase was significant, considering that no enzymes involved in the reductive route of the TCA cycle were overexpressed. This shows the higher affinity of SpMAE1 towards intracellular malate and succinate compared to the DCT-02 transporter.

Overexpression of fumarase and malate dehydrogenase

RoFUM and MDH3 were expressed in the cytosol to push fumaric acid formation via the reductive part of the TCA cycle. This resulted in a 20 fold increase in the yield of malic acid but no significant change in the yield of fumaric acid. RoFUM has been reported to have a higher affinity for malate compared to fumarate, which is believed to contribute to fumaric acid production in *R. oryzae* (8, 11, 91). However, in our study the expression of RoFUM did not improve the production rate of fumaric acid, which is most likely due to the bottleneck in the export of fumaric acid.

Overexpression of PEP carboxykinase, fumarase and malate dehydrogenase

PEPCK from *Mannheimia succiniciproducens* along with FUM1 and MDH3 were overexpressed. The intention was to improve the flux through the reductive part of the TCA cycle and thus produce fumaric acid. Also in this case no improvement in the yield and the final concentration of fumaric acid was observed. However, the yield of malic acid increased significantly to 0.32 mol/mol of glucose consumed. Malic acid was the most abundant dicarboxylic acid with final concentration of 53 mM.

The results obtained from the different modifications of Fum 116 clearly show that the overexpression of different combinations of genes involved in the TCA cycle clearly improved the yield of succinate and malate. But with export as one of the most likely bottlenecks in fumaric acid production, no significant improvement in the final yield and concentration of fumaric acid was observed.

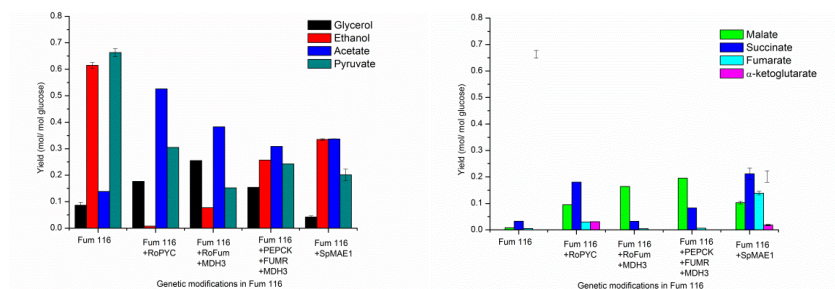


Figure 6.2: Yield of metabolites (mol/mol glucose consumed) obtained with different genetic modifications done in Fum 116

Genetic modifications in Fum 107

Fum 107 was derived from strain SUC501 which was engineered to produce succinic acid via the reductive route and also contained the DCT-02 transporter. By removing the heterologous fumarate reductase gene, fumaric acid should be the end product of the reductive part of the TCA cycle in this strain. Fum 107 produced significant amounts of malic acid with a yield of 0.25 mol/ mol glucose and final titre of upto 115 mM with the consumption of 379 mM of glucose. The reason for the significant malic acid secretion of this strain is not clear. However, a similar result was also obtained with *E. coli*, where the knockout of fumarate reductase also led to the secretion of malic acid with a yield of 0.53 mol/ mol glucose consumed (131), however, no explanation for the observed malic acid secretion was provided in this study.

Overexpression of pyruvate carboxylase

Overexpression of RoPYC led to a significant improvement in the yields of metabolites in the oxidative part of the TCA cycle (α -Ketoglutarate, succinate and fumarate) which was also observed if RoPYC was overexpressed in CEN.PK 21_C and Fum 116. Also the glycerol yield increased upon overexpression of RoPYC, which is probably due to a redox imbalance and oxygen limitation in shake flasks. The final concentration of succinic acid obtained was 24.6 mM (yield shown in Figure 6.3).

Overexpression of Malate dehydrogenase and fumarase

Overexpressing RoMDH, RoFUM or FUMR+MDH3 in FUM107 led to a further increase of the yield of malate but no significant changes in the yields of α -Ketoglutarate, succinate and fumarate. This is probably due to a higher flux through the reductive branch of the TCA cycle. The parent strain Fum 107 produced significant amounts of malic acid and was therefore thought to become a fumaric acid producer after overexpressing FUMR from *Rhizopus delemar*, however, no improvement in the fumaric acid yield was observed. The concentration of malic acid obtained with simultaneous overexpression of

RoFUM and MDH3 was 71.6 mM with the consumption of 235 mM of glucose (yields shown in Figure 6.3).

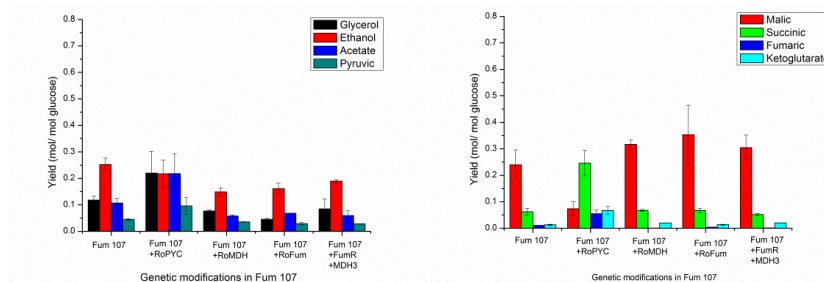


Figure 6.3. Yield of metabolites (mol/ mol glucose consumed) obtained with genetic modifications done in Fum 107

Conclusions

In this study the reductive TCA cycle genes were overexpressed in different combinations with the aim to improve fumaric acid production in *S. cerevisiae* CEN.PK2_1C (control strain), Fum 116 and Fum 107. Two heterologous dicarboxylic acid transporters DCT-02 and SpMAE1 were also expressed to improve the secretion of dicarboxylic acids. The genetically modified strains were cultivated under the conditions of glucose excess and nitrogen starvation, with the addition of calcium carbonate to maintain a near to neutral pH and to accomplish an elevated CO₂ level to facilitate the production of dicarboxylic acids via the reductive pathway.

The applied genetic engineering efforts in *S. cerevisiae* resulted in significant improvements in the yields of malate and succinate. Similar results have been described by other authors, as discussed in chapter 1. However, all engineered strains produced very low amounts of fumarate. Several different attempts have been undertaken to divert the carbon flux towards fumarate production but no substantial improvement in the yield was obtained.

S. cerevisiae lacks efficient exporters of dicarboxylic acids, therefore, two heterologous dicarboxylic acid transporters, SpMAE1 and DCT-02 were expressed to improve their secretion. The SpMAE1 transporter has been

reported to facilitate the secretion of fumaric acid (5), malic acid (17) and also succinic acid (17) in *S. cerevisiae*, and in the secretion of fumaric and malic acid in *Torulopsis glabarta* (107, 109, 132). However, in our study, the expression of the SpMAE1 transporter only improved the export of malate and succinate in CEN.PK2_1C and Fum 116.

Only one research group was successful in engineering *S. cerevisiae* to produce fumaric acid (30, 109, 133). This research group also expressed the reductive TCA cycle genes from *Rhizopus delemar* with or without the presence of a heterologous transporter in the cell membrane. They did not report the secretion of other dicarboxylic acids (e.g. malate and succinate). The results reported by this research group were not in the agreement with the results obtained by us. Apart from this research group there are no other published reports with engineered *S. cerevisiae* producing fumaric acid. We can't explain the reason for the contrast in result obtained by us and the other research group. Our results indicate that the export of fumaric acid might be one of the major bottlenecks in its production. This study lacks the measurements of enzymatic activities in the engineered strains and also the characterization of the engineered strains in a controlled environment using a bioreactor which could have provided a clear picture of the impact of different combinations of genetic modifications on dicarboxylic acids production.

Chapter 7

Outlook

In this chapter the challenges in the fumaric acid production with *S. cerevisiae* on the basis of the results obtained in this thesis are discussed. Recommendations to have better insights into the metabolism, production and transport of dicarboxylic acids in *S. cerevisiae* are also discussed.

Challenges in producing fumaric acid from *S. cerevisiae*

The production of fumaric acid from *S. cerevisiae* is preferred at low pH ($\text{pH} < \text{pK}$). However, at low pH the permeation of fumaric acid into *S. cerevisiae* is significant. In a fumaric acid producing strain this permeation of fumaric acid into the cell would contribute significantly towards its futile cycling and would considerably lower its yield and productivity and increase O_2 consumption. Futile cycling would be much lower in the production process of succinic and malic acid as their permeability is significantly lower compared to fumaric acid. Therefore it is relevant to consider evolving *S. cerevisiae* to reduce its permeability towards fumaric acid. Also the strategy of producing fumaric acid at low pH should be re-evaluated, as at low pH the process is feasible only in aerobic conditions and could also lead to significant futile cycling of fumaric acid. On the other hand at high pH, the fumaric acid production process can be carried out anaerobically (38) and at high pH the futile cycling rate will be negligible but the downstream processing costs will increase. Research is also focused on developing downstream process techniques which allows cost effective purification of acids at higher pH without the formation of gypsum (134). Therefore, cost analysis of the fumaric acid production process (fermentation and DSP) at different pH values should be done taking into account the impact of futile cycling and aeration requirements with associated yield losses.

Another important aspect to consider in the production of fumaric acid is its export from *S. cerevisiae*. *S. cerevisiae* is not a natural producer of dicarboxylic acids and lacks transporters that could achieve the desired high extracellular concentration of dicarboxylic acids. Heterologous DCT-02 and SpMAE1 transporters were expressed in *S. cerevisiae*; both the transporters were able to export succinate and malate but not fumarate. A search for the fumaric acid transporter in its natural producer *Rhizopus spp.* was carried out in Wageningen University using transcriptomics data. The potential transporter

identified from the transcriptomics data was expressed in *Aspergillus niger* and studied in a bioreactor, but the potential transporter was not a fumaric acid transporter (F. Lameiras, personal communication). In one of our experiments (Chapter 3) there were indications of fumaric acid futile cycling in the chemostat experiment at high residual fumaric acid concentration (~65 mM) along with its high intracellular concentration in *S. cerevisiae*. This could be a metabolic response of *S. cerevisiae* in order to avoid the intracellular accumulation of fumaric acid due to the high uptake rate via diffusion. *S. cerevisiae* expresses ABC transporters to prevent the intracellular accumulation of organic acids which could also export fumaric acid. Transcriptomics studies will help in identifying these fumaric acid transporters and the constitutive expression of these transporters could facilitate the export of fumaric acid.

Fumaric acid as a sole carbon source for *S. cerevisiae*

Fumaric acid taken up via diffusion was metabolized (gluconeogenesis) by *S. cerevisiae* via fumarate to malate, malate to oxaloacetate, and from oxaloacetate to PEP through PEP carboxykinase reaction, with glucose as co-substrate. However, *S. cerevisiae* was not able to utilize fumaric acid as the sole carbon source (experiment not discussed in thesis) at low pH of 3.0, in aerobic conditions. This was noticed when the chemostat feed containing glucose and 60 mM of fumaric acid was switched off with 20 mM of residual fumaric acid and 0.2 mM of residual glucose present in the fermentation. After switching off the chemostat feed, there was a rapid drop in the respiration activity of the cell which remained low and no consumption of the residual fumaric acid was observed for a period of up to 5 hrs. After 5 hrs a glucose pulse was given, and just after the pulse there was a rapid increase in the respiration activity of the cell. This ability of *S. cerevisiae* to switch rapidly between the metabolism and no metabolism of fumaric acid depending on the presence or the absence of residual glucose should be further investigated.

Role of mitochondrial dicarboxylic acid transporter in C4 acids production

The production rate of succinic acid in Suc 958 (which can only produce fumaric acid in the cytosol through the reductive part of the TCA cycle) with increase in the CO₂ partial pressure was unexpected (Chapter 4). This was most probably due to the import of cytosolic fumarate formed via the reductive route of the TCA cycle and the export of mitochondrial succinate formed via the oxidative route to cytosol and its subsequent export. From this study, it seems that such mitochondrial transporters play a pivotal role in the formation of succinic acid and also in the exchange of fluxes between the oxidative and reductive part of the TCA cycle. In order to understand the influence of such mitochondrial transporters on the productivity and the yield of C4 acids in engineered strains, a sequential knock-out study of mitochondrial transporters would provide insights into their role in C4 acids production and metabolism. Knocking out mitochondrial transporters would also limit the exchange between the flux through the reductive part of the TCA cycle and the oxidative part of the TCA cycle which would help in understanding the contribution of the reductive and the oxidative part of the TCA cycle towards the formation of a particular C4 acid.

Route of malic acid formation in Fum 116

S. cerevisiae was engineered to make fumaric acid as a catabolic product thereby coupling its formation to ATP generation and biomass formation. The DCT-02 transporter was used as a template protein in strain Fum 116 which through evolution could improve its ability to export fumaric acid. During aerobic evolution the ATP producing ability of the cell improved by replacing ethanol formation with acetate (Fum 114), malate (Fum 116) and pyruvate (Fum 116). However, in both strains there was no improvement in fumaric acid formation, on the contrary there was improvement in the production rate of malate (only in Fum 116). The route of malic acid secretion in Fum 116 is via the energy consuming reductive part of the TCA cycle. The intracellular concentration of fumaric acid in Fum 116 was at least 40 to 100 fold higher than in CEN.PK 113-7D strain indicating export as a major metabolic bottleneck in its production. Metabolic flux calculation indicated that there should be a

conversion from fumarate to malate in order to have a redox balance. Due to the high intracellular concentration of fumarate, which could not be exported, evolution of a hydratase might have occurred with low affinity towards fumarate that could convert fumarate to malate. To confirm, an enzymatic assay should be performed with high initial concentration of fumaric acid (~ 50 mM) using whole cell extract of Fum 116 cultivated in a glucose limited, aerobic chemostat.

Secretion of dicarboxylic acids

Secretion of malic acid in Fum 116 occurred at an exceptionally high biomass specific rate of 30 to 37 mmol/Cmol.h (at pH 5.0) facilitated by DCT-02 transporter and at low CO₂ level of 0.40 %. Suc 958 strain cultivated in high CO₂ environment at pH 3.0 secreted succinic acid (18.7 mmol/Cmol.h) and malic acid (2.4 mmol/Cmol.h) with 50% CO₂ in the aeration gas. It has been shown that high CO₂ environment contribute more towards succinate formation than malate (135). The high production rate of malic acid in Fum 116 at low CO₂ level is remarkable. One of the possibilities of this high rate of malic acid production by Fum 116 could be the high extracellular pH of 5.0 which promotes high out/in ratios of dicarboxylic acids and their secretion rates. Malic acid production rate of 37 mmol/Cmol.h has been observed in shake flask with pH between 6.5 and 7.5 by Zelle *et al.* (17) in an engineered *S. cerevisiae* (Δ PDC1, Δ PDC5, Δ PDC6, \uparrow PYC2, \uparrow MDH3, \uparrow SpMAE1). Extracellular pH also impacts the cytosolic pH which would impact the cytosolic concentration of CO₂ and HCO₃⁻ and also the out/in ratios of the dicarboxylic acids. Therefore it is relevant to measure the cytosolic pH and also the proton motive force (pmf) and their effect on the productivity of dicarboxylic acids. The cytosolic pH of *S. cerevisiae* grown in shake flasks with extracellular pH of 3.0 was estimated to be 6.43 ± 0.05 , the cytosolic pH was calculated using the equilibrium benzoic acid out/in ratios (68) (results not shown in thesis), however, the cytosolic pH was not measured during the chemostats experiments but it is expected to be lower at low extracellular pH of 3.0 compared to the extracellular pH of 5.0 (136). Our results clearly indicate that dicarboxylic acids production is more favorable at extracellular pH of 5.0 and higher.

Transport of mono-dissociated species of dicarboxylic acids

There are reports that indicate the transport of the mono-dissociated form of dicarboxylic acids in wild type yeast (81, 137, 138). At a cytosolic pH of 7.0 the fraction of mono-dissociated species of intracellular fumaric, malic and succinic acid are 0.004, 0.0127 and 0.0418 respectively. If indeed mono-dissociated species are exported then this could explain the secretion of fumaric acid in very low amounts by wild type *S. cerevisiae*. For e.g. Fum 114 which does not express any heterologous transporter secretes fumaric acid in very low amounts, this low secretion rate could be explained by intracellular accumulation of fumaric acid which increases the availability of its mono-dissociated species in the cytosol. The equilibrium ratio for the mono dissociated species of fumaric acid is 0.0001 and 0.14 for symport and uniport mechanism respectively (proton motive force of 180 mV, temperature 30°C and cytosolic pH_{out} 5.0, pH_{in} 7.0), and in our experiment fumaric acid out/in ratio was close to 0.03 (in Fum 114 and Fum 116), therefore the export of mono-dissociated fumaric acid is most likely via the uniport mechanism. Also in shake flasks experiment done in glucose excess concentration, CEN.PK 113-7D with modified metabolic pathway produces malate, succinate and fumarate in low amounts without any heterologous transporter but with an extracellular fumaric acid concentration at least 40 fold lower than malate and succinate concentration. This hypothesis of dicarboxylic acid transporter with uniport mechanism in wild type *S. cerevisiae* holds only if the transporter is only involved in the export of mono-dissociated form of dicarboxylic acids and not import because the uptake rate of fumaric acid at higher pH of 4.0 and 5.0 was much lower even when the extracellular concentration of mono-dissociated species was considerably higher.

Fumaric acid production from *S. cerevisiae*

Heterologous genes from *Rhizopus delemar* (RoFUM, RoMDH and RoPYC) were overexpressed in *S. cerevisiae* to improve the production rate of fumaric acid. But no significant improvement in the fumaric acid yield and productivity was obtained; instead there was significant improvement in succinic and malic acid

yield. Another research group also modified *S. cerevisiae* CEN.PK2_1C strain (30, 109, 133) (also used in our study) , they also overexpressed heterologous reductive pathway genes from *R. delemar* and were able to produce considerable amounts of fumaric acid with or without the presence of a heterologous transporter, also no other dicarboxylic acids (malate and succinate) were reported to be secreted as by-products. This is in complete contrast to our results. Apart from this research group there are no other published reports which engineered *S. cerevisiae* to produce fumaric acid. At the moment we do not have an explanation for this significant difference between the results obtained by us and the other research group. Our results indicate that the export of fumaric acid is a major metabolic bottleneck in its production from *S. cerevisiae*.

References

1. **Doscher CK, Kane JH, Cragwall G, Staebner WH.** 1941. Industrial Applications of Fumaric Acid. *Ind. Eng. Chem. Res.* **33**:315–319.
2. **Forgac JM.** 1999. Process of co-producing fumaric acid and maleic anhydride. 5929255. United states patent.
3. **Newton LW.** 1950. Method for the preparation of fumaric acid. United States of America.
4. **Werpy T, Petersen G.** 2004. Top Value Added Chemicals from Biomass US Department of energy.
5. **Rhodes RA, Moyer AJ, Smith ML, Kelley SE.** 1959. Production of fumaric acid by *Rhizopus arrhizus*. *Appl. Microbiol.* **7**:74–80.
6. **Kane JH, Finlay A, Amann PF.** 1943. Production of fumaric acid. 2327191. United states patent office.
7. **Kenealy W, Zaady E, du Preez JC, Stieglitz B, Goldberg I.** 1986. Biochemical Aspects of Fumaric Acid Accumulation by *Rhizopus arrhizus*. *Appl. Environ. Microbiol.* **52**:128–33.
8. **Song P, Li S, Ding Y, Xu Q, Huang H.** 2011. Expression and characterization of fumarase (FUMR) from *Rhizopus oryzae*. *Fungal Biol.* **115**:49–53.
9. **Friedberg D, Peleg Y, Monsonogo a, Maissi S, Battat E, Rokem JS, Goldberg I.** 1995. The *fumR* gene encoding fumarase in the filamentous fungus *Rhizopus oryzae*: cloning, structure and expression. *Gene* **163**:139–44.
10. **Peleg Y, Battat E, Scrutton MC, Goldberg I.** 1989. Isoenzyme pattern and subcellular localisation of enzymes involved in fumaric acid accumulation by *Rhizopus oryzae*. *Appl. Microbiol. Biotechnol.* **32**:334–339.

11. **Ding Y, Li S, Dou C, Yu Y, Huang H.** 2011. Production of fumaric acid by *Rhizopus oryzae*: role of carbon-nitrogen ratio. *Appl. Biochem. Biotechnol.* **164**:1461–7.
12. **Roa Engel CA, van Gulik WM, Marang L, van der Wielen L a M, Straathof AJJ.** 2011. Development of a low pH fermentation strategy for fumaric acid production by *Rhizopus oryzae*. *Enzyme Microb. Technol.* **48**:39–47.
13. **Nakayama S, Tabata K, Oba T, Kusumoto K, Mitsuiki S, Kadokura T, Nakazato A.** 2012. Characteristics of the high malic acid production mechanism in *Saccharomyces cerevisiae* sake yeast strain No . 28. *J. Biosci. Bioeng.* **114**:281–285.
14. **Pines O, Even-Ram S, Elnathan N, Battat E, Aharonov O, Gibson D, Goldberg I.** 1996. The cytosolic pathway of L-malic acid synthesis in *Saccharomyces cerevisiae*: the role of fumarase. *Appl Microbiol biotechnol* **46**:393–399.
15. **Neufeid RJ, Peleg Y, Rokem JS, Pinest O, Goldberg I.** 1991. Malic acid formation by immobilized *Saccharomyces cerevisiae* amplified for fumarase. *Enzyme Microb. Technol.* **13**:991–996.
16. **Winkler AA, Hulster AF de, van Dijken JP, Pronk JT.** 2008. Malic acid production in recombinant yeast. US 2008/0090273 A1. United states patent application publication.
17. **Zelle RM, de Hulster E, van Winden WA, de Waard P, Dijkema C, Winkler AA, Geertman J-MA, van Dijken JP, Pronk JT, van Maris AJA.** 2008. Malic acid production by *Saccharomyces cerevisiae*: engineering of pyruvate carboxylation, oxaloacetate reduction, and malate export. *Appl. Environ. Microbiol.* **74**:2766–77.
18. **Zelle RM, de Hulster E, Kloezen W, Pronk JT, van Maris AJA.** 2010. Key process conditions for production of C(4) dicarboxylic acids in bioreactor batch cultures of an engineered *Saccharomyces cerevisiae* strain. *Appl. Environ. Microbiol.* **76**:744–50.
19. **Viladevall L, Serrano R, Ruiz A, Domenech G, Giraldo J, Barceló A, Ariño J.** 2004. Characterization of the calcium-mediated response to

- alkaline stress in *Saccharomyces cerevisiae*. *J. Biol. Chem.* **279**:43614–43624.
20. **Liu L, Li Y, Zhu Y, Du G, Chen J.** 2007. Redistribution of carbon flux in *Torulopsis glabrata* by altering vitamin and calcium level. *Metab. Eng.* **9**:21–29.
 21. **Ito Y, Hirasawa T, Shimizu H.** 2014. Metabolic engineering of *Saccharomyces cerevisiae* to improve succinic acid production based on metabolic profiling. *Biosci. Biotechnol. Biochem.* **78**:151–159.
 22. **Otero JM, Cimini D, Patil KR, Poulsen SG, Olsson L, Nielsen J.** 2013. Industrial systems biology of *Saccharomyces cerevisiae* enables novel succinic acid cell factory. *PLoS One* **8**:1–10.
 23. **Raab AM, Gebhardt G, Bolotina N, Weuster-botz D, Lang C.** 2010. Metabolic engineering of *Saccharomyces cerevisiae* for the biotechnological production of succinic acid. *Metab. Eng.* **12**:518–525.
 24. **Yan D, Wang C, Zhou J, Liu Y, Yang M, Xing J.** 2014. Construction of reductive pathway in *Saccharomyces cerevisiae* for effective succinic acid fermentation at low pH value. *Bioresour. Technol.* **156**:232–2399.
 25. **Jamalzadeh E.** 2013. Transport of Dicarboxylic Acids in *Saccharomyces cerevisiae*. Technical University Delft.
 26. **Jansen MLA, Heijnen JJ, Verwaal R.** 2013. Process for preparing dicarboxylic acids employing fungal cells. WO 2013/004670 A1.
 27. **Jansen MLA, Graaf van de M, Verwaal R.** 2010. Dicarboxylic acid production process. WO 2010/ 118932 A1. World intellectual property organization.
 28. **Verwaal R, Wu L, Damveld R, Sagt CMJ.** 2009. Succinic acid production in a eukaryotic cell. W2009/065778.
 29. **Pines O, Shemesh S, Battat E.** 1997. Overexpression of cytosolic malate dehydrogenase (MDH2) causes overproduction of specific organic acids in *Saccharomyces cerevisiae*. *Appl Microbiol biotechnol* **48**:248–255.

30. **Xu G, Zou W, Chen X, Xu N, Liu L, Chen J.** 2012. Fumaric acid production in *Saccharomyces cerevisiae* by in silico aided metabolic engineering. *PLoS One* **7**:1–10.
31. **Xu G, Liu L, Chen J.** 2012. Reconstruction of cytosolic fumaric acid biosynthetic pathways in *Saccharomyces cerevisiae*. *Microb. Cell Fact.* **11**:24.
32. **Xu G, Chen X, Liu L, Jiang L.** 2013. Fumaric acid production in *Saccharomyces cerevisiae* by simultaneous use of oxidative and reductive routes. *Bioresour. Technol.* **148**:91–6.
33. **Xu G, Hua Q, Duan N, Liu L, Chen J.** 2012. Regulation of thiamine synthesis in *Saccharomyces cerevisiae* for improved pyruvate production 209–217.
34. **Chen X, Zhu P, Liu L.** 2015. Modular optimization of multi-gene pathways for fumarate production. *Metab. Eng.* **33**:76–85.
35. **Camarasa C, Bidard F, Bony M, Barre P, Dequin S.** 2001. Characterization of *Schizosaccharomyces pombe* Malate Permease by expression in *Saccharomyces cerevisiae*. *Appl. environ. microbiol.* **67**:4144–4151.
36. **Casal M, Paiva S, Queirós O, Soares-Silva I.** 2008. Transport of carboxylic acids in yeasts. *FEMS Microbiol. Rev.* **32**:974–94.
37. **Aliverdieva DA, Mamaev DV, Bondarenko DI, Sholtz KF.** 2006. Properties of yeast *Saccharomyces cerevisiae* plasma membrane dicarboxylate transporter. *Biochem.* **71**:1161–1169.
38. **Tayamaz Nikerel H, Jamalzadeh E, Borujeni AE, Verheijen PJT, van Gulik WM, Heijnen JJ.** 2013. A thermodynamic analysis of dicarboxylic acid production in microorganisms, p. 547–579. *In* *Biothermodynamics: the role of thermodynamics in biochemical engineering.*
39. **Piper P, Calderon CO, Hatzixanthis K, Mollapour M.** 2001. Weak acid adaptation : the stress response that confers yeasts with resistance to organic acid food preservatives. *Microbiology* **147**:2635–2642.

40. **Barnett JA, Kornberg HL.** 1960. The utilization by yeasts of acids of the tricarboxylic acid cycle. *J. Gen. Microbiol.* **23**:65–82.
41. **Bonnet JABAF, Koellmann CJW, Dekkers-de Kok HE, Roels JA.** 1984. The Growth of *Saccharomyces cerevisiae* CBS 426 on Mixtures of Glucose and Succinic Acid: A Model. *Biotechnol. Bioeng.* **26**:269–274.
42. **Xu Q, Li S, Huang H, Wen J.** 2012. Key technologies for the industrial production of fumaric acid by fermentation. *Biotechnol. Adv.* **30**:1685–96.
43. **Roa Engel CA, Straathof AJJ, Zijlmans TW, van Gulik WM, van der Wielen LAM.** 2008. Fumaric acid production by fermentation. *Appl. Microbiol. Biotechnol.* **78**:379–89.
44. **Cochrane VW.** 1948. Commercial production of acids by fungi. *Econ. Bot.* **2**:145–157.
45. **Canelas AB, ten Pierick A, Ras C, Seifar RM, van Dam JC, van Gulik WM, Heijnen JJ.** 2009. Quantitative evaluation of intracellular metabolite extraction techniques for yeast metabolomics. *Anal. Chem.* **81**:7379–89.
46. **Verduyn C, Postma E, Scheffers WA, van Dijken JP.** 1992. Effect of benzoic acid on metabolic fluxes in yeasts: a continuous-culture study on the regulation of respiration and alcoholic fermentation. *Yeast* **8**:501–17.
47. **Lange HC, Eman M, van Zuijlen G, Visser D, van Dam JC, Frank J, de Mattos MJ, Heijnen JJ.** 2001. Improved rapid sampling for in vivo kinetics of intracellular metabolites in *Saccharomyces cerevisiae*. *Biotechnol. Bioeng.* **75**:406–15.
48. **Mashego MR, Wu L, van Dam JC, Ras C, Vinke JL, van Winden WA, van Gulik WM, Heijnen JJ.** 2004. MIRACLE: mass isotopomer ratio analysis of U-13C-labeled extracts. A new method for accurate quantification of changes in concentrations of intracellular metabolites. *Biotechnol. Bioeng.* **85**:620–8.

49. **Mashego MR, van Gulik WM, Vinke JL, Heijnen JJ.** 2003. Critical evaluation of sampling techniques for residual glucose determination in carbon-limited chemostat culture of *Saccharomyces cerevisiae*. *Biotechnol. Bioeng.* **83**:395–9.
50. **Verheijen PJT.** 2010. Data Reconciliation and Error Detection, p. 8.1–8.13. *In* *The metabolic pathway engineering.*
51. **Daran-Lapujade P, Jansen ML a, Daran J-M, van Gulik W, de Winde JH, Pronk JT.** 2004. Role of transcriptional regulation in controlling fluxes in central carbon metabolism of *Saccharomyces cerevisiae*. A chemostat culture study. *J. Biol. Chem.* **279**:9125–38.
52. **Lange H christian.** 2002. Quantitative physiology of *S.cerevisiae* using metabolic network analysis. Technical University Delft.
53. **Kresnowati MTAP, Winden WA Van, Gulik WM Van, Heijnen JJ.** 2008. Dynamic In Vivo Metabolome Response of *Saccharomyces cerevisiae* to a Stepwise Perturbation of the ATP Requirement for Benzoate Export. *Biotechnology* **99**:421–441.
54. **Lawford HG, Rousseau JD.** 1994. The pH-Dependent Energetic Uncoupling of *Zymomonas* by Acetic Acid. *Appl. Biochem. Biotechnol.* **45**:437–448.
55. **Canelas AB, Ras C, ten Pierick A, van Gulik WM, Heijnen JJ.** 2011. An in vivo data-driven framework for classification and quantification of enzyme kinetics and determination of apparent thermodynamic data. *Metab. Eng.* **13**:294–306.
56. **Piper P, Mahé Y, Thompson S, Pandjaitan R, Holyoak C, Egner R, Mühlbauer M, Coote P, Kuchler K.** 1998. The pdr12 ABC transporter is required for the development of weak organic acid resistance in yeast. *EMBO J.* **17**:4257–65.
57. **Orij R, Postmus J, Ter Beek A, Brul S, Smits GJ.** 2009. In vivo measurement of cytosolic and mitochondrial pH using a pH-sensitive GFP derivative in *Saccharomyces cerevisiae* reveals a relation between intracellular pH and growth. *Microbiology* **155**:268–278.

58. **Kresnowati MTAP, Suarez-Mendez CM, van Winden WA, van Gulik WM, Heijnen JJ.** 2008. Quantitative physiological study of the fast dynamics in the intracellular pH of *Saccharomyces cerevisiae* in response to glucose and ethanol pulses. *Metab. Eng.* **10**:39–54.
59. **Escher BI, Berger C, Bramaz N, Kwon J-H, Richter M, Tsinman O, Avdeef A.** 2008. Membrane-water partitioning, membrane permeability, and baseline toxicity of the parasiticides ivermectin, albendazole, and morantel. *Environ. Toxicol. Chem.* **27**:909–18.
60. **Kresnowati MTAP, van Winden WA, van Gulik WM, Heijnen JJ.** 2008. Energetic and metabolic transient response of *Saccharomyces cerevisiae* to benzoic acid. *FEBS J.* **275**:5527–41.
61. **Douma RD, Deshmukh AT, de Jonge LP, de Jong BW, Seifar RM, Heijnen JJ, van Gulik WM.** 2011. Novel insights in transport mechanisms and kinetics of phenylacetic acid and penicillin-G in *Penicillium chrysogenum*. *Biotechnol. Prog.* **28**:337–48.
62. **Namdarit H, Cabelli VJ.** 1990. Glucose-Mediated Catabolite Repression of the Tricarboxylic Acid Cycle as an Explanation for Increased Acetic Acid Production in Suicidal *Aeromonas* Strains. *J. Bacteriol.* **172**:4721–4724.
63. **Mescam M, Vinnakota KC, Beard DA.** 2011. Identification of the catalytic mechanism and estimation of kinetic parameters for fumarase. *J. Biol. Chem.* **286**:21100–9.
64. **Gregori C, Schüller C, Frohner IE, Ammerer G, Kuchler K.** 2008. Weak organic acids trigger conformational changes of the yeast transcription factor War1 in vivo to elicit stress adaptation. *J. Biol. Chem.* **283**:25752–64.
65. **Causton HC, Ren B, Koh SS, Christopher T, Kanin E, Jennings EG, Lee I, Heather L, Lander ES, Young RA.** 2001. Remodeling of Yeast Genome Expression in Response to Environmental Changes. *Mol. Biol. Cell* **12**:323–337.
66. **Hatzixanthis K, Mollapour M, Seymour I, Bauer BE, Krapf G, Sch C, Kuchler K, Piper PW.** 2003. Moderately lipophilic carboxylate

compounds are the selective inducers of the *Saccharomyces cerevisiae* Pdr12p ATP-binding cassette transporter. *Yeast* **20**:575–585.

67. **Rogers PJ, Stewart PR.** 1974. Energetic Efficiency and Maintenance Energy Characteristics of *Saccharomyces cerevisiae* (Wild Type and Petite) and *Candida parapsilosis* Grown Aerobically and Micro-Aerobically in Continuous Culture. *Arch. Microbiol.* **99**:25–46.
68. **Kresnowati MTAP, Groothuizen MK, van Winden WA.** 2007. Measurement of Fast Dynamic Intracellular pH in *Saccharomyces cerevisiae* Using Benzoic Acid Pulse. *Biotechnology* **97**:86–98.
69. **Alberty RA.** 2006. Thermodynamic properties of weak acids involved in enzyme-catalyzed reactions. *J. Phys. Chem. B* **110**:5012–6.
70. **Gonzalez B, de Graaf A, Renaud M, Sahm H.** 2000. Dynamic in vivo (³¹P) nuclear magnetic resonance study of *Saccharomyces cerevisiae* in glucose-limited chemostat culture during the aerobic-anaerobic shift. *Yeast* **16**:483–97.
71. **Perrin D.** 1963. Buffers of low ionic strength for spectrophotometric pK determinations. *Aust. J. Chem.* **16**:572–8.
72. **Sandström AG, Almqvist H, Portugal-Nunes D, Neves D, Lidén G, Gorwa-Grauslund MF.** 2014. *Saccharomyces cerevisiae*: a potential host for carboxylic acid production from lignocellulosic feedstock? *Appl. Microbiol. Biotechnol.* 7299–7318.
73. **Castrillo JI, Miguel I DE, Ugalde UO.** 1995. Proton Production and Consumption Pathways in Yeast Metabolism. *Yeast* **11**:1353–1365.
74. **Roos W, Luckner M.** 1984. Relationships Between Proton Extrusion and Fluxes of Ammonium Ions and Organic Acids in *Penicillium cyclospium*. *J. Gen. Microbiol.* **130**:1007–1014.
75. **Cooper TG, Sumrada R.** 1975. Urea Transport in *Saccharomyces cerevisiae*. *J. Bacteriol.* **121**:571–576.
76. **Mashego MR, Jansen MLA, Vinke JL, van Gulik WM, Heijnen JJ.** 2005. Changes in the metabolome of *Saccharomyces cerevisiae* associated

with evolution in aerobic glucose-limited chemostats. *FEMS Yeast Res.* **5**:419–30.

77. **Douma RD, Jonge LP De, Jonker CTH, Seifar RM, Heijnen JJ, van Gulik WM.** 2010. Intracellular Metabolite Determination in the Presence of Extracellular Abundance: Application to the Penicillin Biosynthesis Pathway in *Penicillium chrysogenum* **107**:105–115.
78. **Ullmann RT, Andrade SLA, Ullmann GM.** 2012. Thermodynamics of Transport Through the Ammonium Transporter Amt-1 Investigated with Free Energy Calculations. *J. Phys. Chem.* **116**:9690–9703.
79. **Kleiner D.** 1981. The transport of NH₃ and NH₄⁺ across biological membranes. *Biochem. Biophys. acta* **639**:41–52.
80. **Shah MV, van Mastrigt O, Heijnen JJ, van Gulik WM.** 2016. Transport and metabolism of fumaric acid in *Saccharomyces cerevisiae* in aerobic glucose limited chemostat culture. *Yeast* 1–33.
81. **Corte-real M, Leao C.** 1990. Transport of Malic Acid and Other Dicarboxylic Acids in the Yeast *Hansenula anomala*. *appl. environ. microbiol.* **56**:1109–1113.
82. **Corte-real M, Leao C, van Uden N.** 1989. Transport of L (-) malic acid and other dicarboxylic acids in the yeast *Candida sphaerica*. *Appl Microbiol biotechnol* 551–555.
83. **Cassio F, Leao C, van Uden N.** 1987. Transport of Lactate and Other Short-Chain Monocarboxylates in the Yeast *Saccharomyces cerevisiae* **53**:509–513.
84. **Wrigglesworth JM, Cooper CE, Sharpe MA, Nichollst P.** 1990. The proteoliposomal steady state: Effect of size, capacitance and membrane permeability on cytochrome-oxidase-induced ion gradients. *Biochem. J.* **270**:109–118.
85. **Milne N, Luttik MAH, Rojas HFC, Wahl A, van Maris AJA, Pronk JT, Daran JM.** 2015. Functional expression of a heterologous nickel-dependent , ATP-independent urease in *Saccharomyces cerevisiae*. *Metab. Eng.* **30**:130–140.

86. **Roa Engel CA, ter Horst JH, Pieterse M, van der Wielen LAM, Straathof AJJ.** 2013. Solubility of Fumaric Acid and Its Monosodium Salt. *Ind. Eng. Chem. Res.* **52**:9454–9460.
87. **Verduyn C, Stouthamer AH, Scheffers WA, van Dijken JP.** 1991. A theoretical evaluation of growth yields of yeasts. *Antonie Van Leeuwenhoek* **59**:49–63.
88. **van Hoek P, Flikweert MT, van der Aart QJM, Steensma H, van Dijken JP, Pronk JT.** 1998. Effects of Pyruvate Decarboxylase Overproduction on Flux Distribution at the Pyruvate Branch Point in *Saccharomyces cerevisiae*. *Appl. Environ. Microbiol.* **64**:2133–2140.
89. **Zeikus JG, Jain MK, Elankovan P.** 1999. Biotechnology of succinic acid production and markets for derived industrial products. *Appl Microbiol biotechnol* **51**:545–552.
90. **Abe A, Oda Y, Asano K, Sone T.** 2007. *Rhizopus delemar* is the proper name for *Rhizopus oryzae* fumaric-malic acid producers. *Mycologia* **99**:714–722.
91. **Zhang B, Skory CD, Yang S.** 2012. Metabolic engineering of *Rhizopus oryzae* : Effects of overexpressing *pyc* and *pepc* genes on fumaric acid biosynthesis from glucose. *Metab. Eng.* **14**:512–520.
92. **Samuelov NS, Lamed R, Lowe S, Zeikus JG.** 1991. Influence of CO₂-HC0₃- Levels and pH on Growth , Succinate Production , and Enzyme Activities of *Anaerobiospirillum succiniciproducens*. *Appl. Environ. Microbiol.* **57**:3013–3019.
93. **Camarasa C, Faucet V, Dequin S.** 2007. Role in anaerobiosis of the isoenzymes for *Saccharomyces cerevisiae* fumarate reductase encoded by OSM1 and FRDS1. *Yeast* **24**:391–401.
94. **Enomoto K, Arikawa Y, Muratsubaki H.** 2002. Physiological role of soluble fumarate reductase in redox balancing during anaerobiosis in *Saccharomyces cerevisiae*. *FEMS Microbiol. Lett.* **215**:103–108.

95. **Bruinenberg PM, van Dijken JP, Scheffers WA.** 1983. An Enzymic Analysis of NADPH Production and Consumption in *Candida utilis*. *J. Gen. Microbiol.* **129**:965–971.
96. **Palmieri L, Lasorsa FM, Vozza A, Agrimi G, Fiermonte G, Runswick MJ, Walker JE, Palmieri F.** 2000. Identification and functions of new transporters in yeast mitochondria. *Biochem. Biophys. acta* **1459**:363–369.
97. **Bojunga N, Kotter P, Entian KD.** 1998. The succinate / fumarate transporter Acr1p of *Saccharomyces cerevisiae* is part of the gluconeogenic pathway and its expression is regulated by Cat8p. *Mol. Gen. Genet.* **260**:453–461.
98. **Fernandez M, Fernandez E, Rodicio R.** 1994. ACR1 , a gene encoding a protein related to mitochondrial carriers, is essential for acetyl-CoA synthetase activity in *Saccharomyces cerevisiae*. *Mol. Gen. Genet.* **242**:727–735.
99. **Palmieri L, Lasorsa FM, Palma A De, Palmieri F, Runswick MJ, Walker JE.** 1997. Identification of the yeast ACR 1 gene product as a succinate-fumarate transporter essential for growth on ethanol or acetate. *FEBS Lett.* **417**:114–118.
100. **Palmieri F, Agrimi G, Blanco E, Castegna A, Di MA, Iacobazzi V, Lasorsa FM, Marobbio CMT, Palmieri L, Scarcia P, Todisco S, Vozza A, Walker J.** 2006. Identification of mitochondrial carriers in *Saccharomyces cerevisiae* by transport assay of reconstituted recombinant proteins. *Biochem. Biophys. Acta* **1757**:1249–1262.
101. **Herick K, Kramer R, Luhring H.** 1997. Patch clamp investigation into the phosphate carrier from *Saccharomyces cerevisiae* mitochondria. *Biochem. Biophys. acta* **1321**:207–220.
102. **Orij R, Urbanus ML, Vizeacoumar FJ, Giaever G, Boone C, Nislow C, Brul S.** 2012. Genome-wide analysis of intracellular pH reveals quantitative control of cell division rate by pHc in *Saccharomyces cerevisiae*. *Genome Biol.* **13**:1–15.

103. **Hunter K, Rose AH.** 1972. Lipid composition of *Saccharomyces cerevisiae* as influenced by growth temperature. *Biochem. Biophys. acta* **260**:639–653.
104. **Arneborg N, Salskov-iversen AS, Mathiasen TE.** 1993. The effect of growth rate and other growth conditions on the lipid composition of *Escherichia coli*. *Appl. Microbiol. Biotechnol.* **39**:353–357.
105. **Auesukaree C, Homma T, Tochio H, Shirakawa M, Kaneko Y, Harashima S.** 2004. Intracellular Phosphate Serves as a Signal for the Regulation of the PHO Pathway in *Saccharomyces cerevisiae*. *J. Biol. Chem.* **279**:17289–17294.
106. **Song CW, Kim DI, Choi S, Jang JW, Lee SY.** 2013. Metabolic engineering of *Escherichia coli* for the production of fumaric acid. *Biotechnol. Bioeng.* **110**:2025–34.
107. **Chen X, Wu J, Song W, Zhang L, Wang H, Liu L.** 2015. Fumaric Acid Production by *Torulopsis glabrata*: Engineering the Urea Cycle and the Purine Nucleotide Cycle. *Biotechnol. Bioeng.* **112**:156–167.
108. **Zhang T, Wang Z, Deng L, Tan T, Wang F, Yan Y.** 2015. Pull-in urea cycle for the production of fumaric acid in *Escherichia coli*. *Appl Microbiol biotechnol* **99**:5033–5044.
109. **Chen X, Dong X, Wang Y, Zhao Z, Liu L.** 2015. Mitochondrial engineering of the TCA cycle for fumarate production. *Metab. Eng.* 1–12.
110. **Mo ML, Palsson BØ, Herrgård MJ.** 2009. Connecting extracellular metabolomic measurements to intracellular flux states in yeast. *BMC Syst. Biol.* **17**:1–17.
111. **Shah MV, van Mastrigt O, Heijnen JJ, van Gulik WM.** 2016. Transport and metabolism of fumaric acid in *Saccharomyces cerevisiae* in aerobic glucose limited chemostat culture. *Yeast* **33**:145–161.
112. **Gietz RD, Woods RA.** 1987. Transformation of Yeast by Lithium Acetate / Single-Stranded Carrier DNA / Polyethylene Glycol Method. *Methods Enzymol.* **350**:87–96.

113. **Güldener U, Heck S, Fielder T, Beinhauer J, Hegemann JH.** 1996. A new efficient gene disruption cassette for repeated use in budding yeast. *Nucleic Acids Res.* **24**:2519–24.
114. **Pronk JT.** 2002. Auxotrophic Yeast Strains in Fundamental and Applied Research. *Appl. environ. microbiol.* **68**:2095–2100.
115. **Wu L, Mashego MR, van Dam JC, Proell AM, Vinke JL, Ras C, van Winden WA, van Gulik WM, Heijnen JJ.** 2005. Quantitative analysis of the microbial metabolome by isotope dilution mass spectrometry using uniformly ¹³C-labeled cell extracts as internal standards. *Anal. Biochem.* **336**:164–171.
116. **Cipollina C, ten Pierick A, Canelas AB, Seifar RM, van Maris AJA, van Dam JC, Heijnen JJ.** 2009. A comprehensive method for the quantification of the non-oxidative pentose phosphate pathway intermediates in *Saccharomyces cerevisiae* by GC-IDMS. *J. Chromatogr. B* **877**:3231–3236.
117. **van Dam JC, Ras C, ten Pierick A.** 2011. Metabolic Profiling, p. 131–146. *In* *Methods in Molecular Biology*.
118. **van der Heijden RT, Heijnen JJ, Hellinga C, Romein B, Luyben KC.** 1994. Linear constraint relations in biochemical reaction systems: I. Classification of the calculability and the balanceability of conversion rates. *Biotechnol. Bioeng.* **43**:3–10.
119. **Heyland J, Fu J, Blank LM.** 2009. Correlation between TCA cycle flux and glucose uptake rate during respiration-fermentative growth of *Saccharomyces cerevisiae*. *Microbiology* **155**:3827–3837.
120. **Siew LT, Daran-Lapujade P, Luttik MAH, Walsh MC, Diderich JA, Krijger GC, van Gulik WM, Pronk JT, Daran JM.** 2007. Control of the glycolytic flux in *Saccharomyces cerevisiae* grown at low temperature: A multi-level analysis in anaerobic chemostat cultures. *J. Biol. Chem.* **282**:10243–10251.
121. **Oud B, Flores CL, Gancedo C, Zhang X, Trueheart J, Daran JM, Pronk JT, van Maris AJA.** 2012. An internal deletion in MTH1 enables growth on

- glucose of pyruvate-decarboxylase negative, non-fermentative *Saccharomyces cerevisiae*. *Microb. Cell Fact.* **11**:131.
122. **Visser D, van Zuylen GA, van Dam JC, Eman MR, Proll A, Ras C, Wu L, van Gulik WM, Heijnen JJ.** 2004. Analysis of in vivo kinetics of glycolysis in aerobic *Saccharomyces cerevisiae* by application of glucose and ethanol pulses. *Biotechnol. Bioeng.* **88**:157–167.
 123. **Canelas AB.** 2010. Towards quantitative metabolimics and in vivo kinetic modeling in *S. cerevisiae*. Technical University Delft.
 124. **Nishino S, Okahashi N, Matsuda F, Shimizu H.** 2015. Absolute quantitation of glycolytic intermediates reveals thermodynamic shifts in *Saccharomyces cerevisiae* strains lacking PFK1 or ZWF1 genes. *J. Biosci. Bioeng.* **120**:280–286.
 125. **Hanau S, Montin K, Cervellati C, Magnani M, Dallochio F.** 2010. 6-Phosphogluconate Dehydrogenase Mechanism. *J. Biol. Chem.* **285**:21366–21371.
 126. **Hard GEL, Roses A.** 1964. The Mechanism of Action of 6-Phosphogluconate Dehydrogenase. *Biochemistry* **3**:190–195.
 127. **Verduyn C.** 1992. Energetic aspects of metabolic fluxes in yeasts. Technical University Delft.
 128. **Walter A, Gutknecht J.** 1984. Monocarboxylic acid permeation through lipid bilayer membranes. *J. Membr. Biol.* **77**:255–64.
 129. **Forster J, Famili I, Palsson BO, Nielsen J.** 2003. Genome-Scale Reconstruction of the *Saccharomyces Cerevisiae* Metabolic Network. *Genome Res.* 244–253.
 130. **Verwaal R, Wu L, Damveld R, Maria C, Sagt J.** 2014. Succinic acid production in a eukaryotic cell. 14/044,722. United states patent application publication.
 131. **Zhang X, Wang X, Shanmugam KT, Ingram LO, Zhang X, Wang X, Shanmugam KT, Ingram LO.** 2011. I-Malate Production by Metabolically Engineered *Escherichia coli*. *Appl. Environ. Microbiol.* **77**.

132. **Chen X, Xu G, Xu N, Zou W, Zhu P.** 2013. Metabolic engineering of *Torulopsis glabrata* for malate production. *Metab. Eng.* **19**:10–16.
133. **Xu G, Chen X, Liu L, Jiang L.** 2013. Fumaric acid production in *Saccharomyces cerevisiae* by simultaneous use of oxidative and reductive routes. *Bioresour. Technol.*
134. **Jansen MLA, van Gulik WM.** 2014. Towards large scale fermentative production of succinic acid. *Curr. Opin. Biotechnol.* **30**:190–197.
135. **Zelle RM.** 2011. Metabolic engineering of *Saccharomyces cerevisiae* for C 4 -dicarboxylic acid production. *Outlook. Technical University Delft.*
136. **Rault A, Bouix M, Béal C.** 2009. Fermentation pH influences the physiological-state dynamics of *Lactobacillus bulgaricus* CFL1 during pH-controlled culture. *Appl. Environ. Microbiol.* **75**:4374–4381.
137. **Sousa MJ, Mota M, Leão C.** 1992. Transport of malic acid in the yeast *Schizosaccharomyces pombe*: evidence for a proton-dicarboxylate symport. *Yeast* **8**:1025–31.
138. **Jamalzadeh E, Verheijen PJT, Heijnen JJ, van Gulik WM.** 2011. pH-dependent Uptake of Fumaric Acid in *Saccharomyces cerevisiae* under Anaerobic Conditions. *Appl. Environ. Microbiol.* **78**:705–716.

List of publications

Shah MV, Badle SS, Ramachandran KB. (2013), Hyaluronic acid production and molecular weight improvement by redirection of carbon flux towards its biosynthesis pathway. *Biochemical Engineering Journal*, 80, 53-60.

Shah M V, van Mastrigt O, Heijnen JJ, van Gulik WM. (2016). Transport and metabolism of fumaric acid in *Saccharomyces cerevisiae* in aerobic glucose limited chemostat culture. *Yeast* 33:145–161.

Shah MV, Jamalzadeh E, Heijnen JJ, van Gulik WM. (2016), Effect of pH on fumaric acid permeability, uptake and futile cycling in *Saccharomyces cerevisiae* (*To be submitted*).

Shah MV, Heijnen JJ, van Gulik WM. (2016), Metabolic response of engineered C4-acids producing *Saccharomyces cerevisiae* in high CO₂ environment (*To be submitted*).

Shah MV, Heijnen JJ, van Gulik WM. (2016), Evolution of engineered *Saccharomyces cerevisiae* for the aerobic production of dicarboxylic acids (*To be submitted*).

Curriculum vitae

Mihir Vidyut Shah was born on 8th August, 1986 in Gujarat, India. He completed his high school from Maharaja Agarsen public school, Delhi in 2004. He obtained his Bachelors of Engineering in Biotechnology with honors in 2008 from Maharishi Dayanand University, Haryana. After Bachelors he went to Chennai in 2009 to pursue Masters from the Department of Biotechnology, Indian Institute of Technology Madras with specialization in the field of Bioprocess technology. His Masters research project was on improving the molecular weight of Hyaluronic acid biopolymer produced from *Streptococcus zooepidemicus*. In 2012 he started his Ph.D in Cell Systems Engineering group (formerly known as Bioprocess Technology group) in the Department of Biotechnology, Technical University Delft. Currently he is looking for a challenging opportunity in the field of fermentation technology and metabolic engineering.

Acknowledgements

The fruitful time spent at the Technical University Delft and in The Netherlands would not have been possible without the contribution of colleagues and friends. First I would like to thank my promoter Sef Heijnen and copromoter Walter van Gulik. Sef, thank you for giving me the opportunity to pursue Ph.D in your research group. I am very grateful for your enthusiasm, ideas and time in this research project and for patiently reviewing my Ph.D thesis. I learnt a lot from our countless meetings, revisions of manuscripts and from your comments and constructive criticism on my scientific work. It was a pleasure assisting you in the fermentation technology course. Walter, I enjoyed every bit of working with you, thank you for your support during Ph.D and for the valuable feedback in experiments and scientific writing. Thank you for translating the summary in Dutch and for shaping up this thesis.

Thank you Prof. F. Bruggeman, Prof. M. Casal, Prof. G.J. Witkamp, Prof. G. Eggink, Prof W. R. Hagen and Dr. S. Hartmans for accepting the invitation of being my doctoral defence committee members and for reviewing this thesis.

I thank Oscar van Mastrigt for doing his masters thesis and for his significant contribution in this project, his research work is a part of chapter 2 and 4. In regard to the genetic engineering work done in this thesis I would like to thank Erwin Suir (formerly at DSM N.V.), Rene Verwaal (DSM N.V.) and Esengul (formerly at EBT group, TU Delft). The project was funded by BE-BASIC foundation, therefore I would like to thank everyone involved in the BE-BASIC flagship meetings: Sybe, Peter, Leo, Richard, Adrie, Erik, Dorret, Laura, Jasper, Juan, Francisca and Kiira for their feedback. I especially thank Sybe and Rene from DSM N.V. for helpful discussions, involvement and collaboration in this project.

I thank all the current and former members of CSE for their camaraderie: Aljoscha, Peter, Amit, Anisha, Cristina, Manuel, Jinrui, Elaheh, Katelijne, Luisa, Eleni, Mariana, Leonor, Yaya, and Karel. Intracellular metabolites quantification forms an important part of this thesis, for that I am grateful to the analytical team members Reza, Cor, Patricia and Angie for their support and always

keeping the focus on the quality and reliability of the measurements. Thank you Johan for TOC measurements. Most of the experimental work was done in the fermentation lab, for that I would like to thank Dirk, Yi Song and Rob, as they were always there when something went wrong. Jenifer, thank you for all the administrative support, directly and indirectly you made my job easier. Camilo and Hugo it was a pleasure having you as my colleagues and friends, thank you for all the time we spent together in and outside the lab. Our trip to India and Canada (with Jinrui) was a memorable experience and we should plan another trip soon. Hugo, thank you for planning to come to my defence from U.K., I know you always make it on time. Thank you Francisca, apart from CSE we were also associates in the BE-BASIC flagship meetings and Biopro course in Denmark which I enjoyed. Robin and Geetha thank you very much for being my paranymphs. Robin, thank you for all the time well spent with beers, parties, travelling and in the lab, and for backing me up when needed. Geetha, thank you for all the support, will never forget your hacking skill.

I thank my officemates: Sushil, Joana, Renato and Arjan for all the refreshing discussions. Sushil, thank you very much for the support and friendship during my Ph.D, you were always there to help whenever needed. I would also like to thank the group members of IMB, EBT and BPE with whom I shared labs, gave presentations and in some way or other have helped me in the lab. Thank you Astrid, Janine and Apilena for your assistance in autoclaving and maintaining a stockpile of tubings needed for the fermentation lab.

I am also grateful to my colleagues, friends and teachers at the Indian institute of technology, Madras where I did my masters in Bioprocess Engineering and studying there inspired me to pursue Ph.D. I would also like to thank Geetha, Chayan, Dharmesh, Swasti, Akshay, Mohit, Kishor and Vijay for the fun time spent in Delft, without them I would have finished this thesis earlier. Finally, I thank my parents for their support, understanding and encouragement in all my endeavors.